Advanced analysis of polyphenols and phytosterols from grapes and grape byproducts

A thesis submitted for the degree of

Doctor of Philosophy

By

Siti Nur Nazathul Shima Binti Hashim

BSc.(Hons) (University Putra Malaysia)

Centre for Green Chemistry, School of Chemistry,

Faculty of Science, Monash University, Australia

February 2013

The following amendments have been made in accord with the suggestions and valued comments of the examiners.

p vi	line 3	:	delete "*trans*" and read "The *E* notation refers to the absolute stereochemistry around the double bonds"
p vi	line 4	:	delete "*cis*" and read "The *Z* notation refers to the absolute stereochemistry around the double bonds"
p viii	line 13	:	"MW" for "Mw"
p viii	line 24	:	delete "Wavelength number" and read "nanometer"
p ix	line 23	:	"Pi" for "Pie"
p xi	para 2, line 2	:	add "prepared" and read "… to be most effectively prepared using covalent ..."
p xi	para 2, line 4	:	"non-target" for "non target"
p 4	para 1, line 5	:	"100 mL" for "100 ml"
p 4	para 3, line 3	:	delete "10^7" and read "… energy generated by sound wave of 20 kHz - 1 MHz."
p 4	para 3, line 4	:	delete "a substantive" and read "… that produce a substantial increase in temperature ..."
p 5	para 2, line 7	:	delete "fewer equipment involved" and read "… and fewer laboratory glassware was used."
p 46	para 3	:	insert non-breaking spaces between number and unit and read "5.0×10^{-1} mM" and "3.9×10^{-5} mM"
p 47	para 1	:	delete "of" and read "The eluent B was 10 mM AcOH."
p 48	para 2	:	delete "known as" and read "2,2′-azobis(2-methylpropionitrile) (AIBN, 0.3 M)"
p 48	para 2	:	comment: "The resultant MIP material was washed several times with MeOH/AcOH (9:1, v/v) until the wash fraction was free from the template, as confirmed by RP-HPLC with detection at 210 nm."
p 48	para 3	:	insert non-breaking spaces between number and unit and read "63-90 µm" and "20 µm pore size"
p 49	para 1, line 4	:	delete "with" and read "... and eluted by the force of gravity."
p 49	para 1, line 12	:	delete "100 µL" and read "… eluent B (1 mL) which corresponded to a 10-fold concentration."
p 51	para 2, line 5	:	delete "conventional" and read "The concentration of mobile phase additive was expressed in mM instead of the percentage (%, v/v) value in order to enable direct comparisons of the effectiveness of the four acid modifiers."
p 51	para 4, line 3	:	add "to" and read "… mobile phase led to a high back-pressure …"
p 51	para 4, line 6	:	add "($w_{1/2}$ = 0.30)" and read "… combination of ACN with FA ($w_{1/2}$ = 0.30) …"
p 54	Fig 2.6	:	insert non-breaking spaces between number and unit and read "10 °C"
p 58	Fig 2.8	:	insert non-breaking spaces between number and unit and read "10 mM"
p 59	para 1, line 5	:	delete "complies" and read "... as well as complying with the Green Chemistry principles."
p 59	para 1, line 8	:	replace "run" and read "… to achieve equivalent separation conditions."
p 59	end of para 2	:	"… from an analytical RP-HPLC to a microLC method …" for "… from a microLC to an analytical RP-HPLC …"
p 63	para 2, line 4	:	replace "unspecifically" and read "non-specifically"
p 63	para 3, line 3	:	add "of which" and read "… the dimensions of which were 2.8 diameter …"
p 65	para 1, line 3	:	insert non-breaking spaces between number and unit and read "1.0 cm"
p 69	abstract, line 11	:	replace "in conjunction" and read "… (MISPE) coupled with capillary-reversed-phase …"
p 71	para 1, line 10	:	delete "manifold" and read "… because of its nutraceutical properties …"
p 72	para 2, line 2	:	insert non-breaking spaces between number and unit and read "5.0×10^{-1} mM"

The following amendments have been made in accord with the suggestions and valued comments of the examiners.

p 72	para 4, line 3	:	replace "Then the supernatant of red wine ..." and read "The red wine supernatant ..."
p 73	para 4, last line	:	replace "to" and read "... the adsorption of this compound onto the imprinted binding sites."
p 74	Fig 3.1	:	insert non-breaking spaces between number and unit and read "20 °C"
p 78	para 2, line 4	:	add "to" and read "... underwent fragmentation to give rise to two ..."
p 80	end of para 2	:	insert non-breaking spaces between number and unit and read "20.8 min"
p 93	para 2, line 6	:	replace "K^+" and read "K"
p 94	para 3, line 3	:	insert non-breaking spaces between number and unit and read "1.0×10^{-1} mM"
p 95	para 4, line 1,4	:	insert non-breaking spaces between number and unit and read "30 mL" and "20 min"
p 97	para 1, line 3	:	insert non-breaking spaces between number and unit and read "8.7 μg/g"
p 97	para 1, line 6	:	add "compared" and "the" and read "... reduction of (*E*)-resveratrol compared to the (*Z*)-isomer ..."
p 97	para 1, line 8	:	delete "was determined" and read "... the concentration of this compound to be ..."
p 97	para 1, line 9	:	delete "that" and read "... the method required 13 hours ..."
p 97	para 1, line 10	:	delete "concomitant" and read "... several separation steps prior to analysis ..."
p 98	Fig 4.2	:	insert non-breaking spaces between number and unit and read "10 mM" and "0-2 min"
p 99	Fig 4.3	:	insert non-breaking spaces between number and unit and read "10 mM" and "0-2 min"
p 100	end of para 2	:	insert non-breaking spaces between number and unit and read "5 g"
p 101	para 1, line 6	:	insert non-breaking spaces between number and unit and read "38.8 min"
p 107	Fig 4.5	:	insert non-breaking spaces between number and unit and read "10 mM", "0-2 min", "5 μm particle size" and "10 mM"
p 123	para 2, line 7,14	:	insert non-breaking spaces between number and unit and read "5 μm particle size" and "0.5 mL/min"
p 125	para 1, line 1	:	insert non-breaking spaces between number and unit and read "1.5 mL"
p 125	para 3, line 5	:	delete "at" and read "... operated in the low boiling point mode ..."
p 127	para 3, line 1	:	insert non-breaking spaces between number and unit and read "10 mmol"
p 127	para 3, line 8	:	add "a" and read "... followed by a mortar and pestle ..."
p 127	para 3, line 11	:	add "was" and "and", and read "The resultant polymer was expected to have 'memory cavities' and was sieved using two sieves ..."
p 128	para 1, line 3	:	add "with detection" and read "... was analysed by RP-HPLC with detection at the absorbance ..."
p 128	para 1, line 4	:	replace "detected" and read "... until no trace of stigmasterol was observed."
p 128	para 1, line 5	:	replace "using" and read "... dried overnight under vacuum at room temperature."
p 128	para 2, line 1		delete "the" and read "Scanning electron microscopy was performed ..."
p 131	para 1, line 2	:	insert non-breaking spaces between number and unit and read "210 nm"
p 131	Fig 5.5	:	dot points were removed from Figure 5.5. "... ergosterol each at a concentration of 0.1 mM." for "ergosterol at a concentration of 0.1 mM each."
p 132	para 3, line 3, 4, 5	:	replace "soluble", add "of" and "of", and read "... these sterols were found to be soluble in polar solvents up to 1.0 mM under 10 min of ultrasonification to enhance the mass transfer rate and solvent penetration of the sterol molecules."
p 139	para 2, line 11	:	insert non-breaking spaces between number and unit and read "65 °C"
p 140	end of para 3	:	add "with detection" and read "... the absence of stigmasterol in the wash fraction confirmed with RP-HPLC with detection at 210 nm."

The following amendments have been made in accord with the suggestions and valued comments of the examiners.

p 142	end of para 1	:	comment: There is evidence in the literature to justify the statement made: "It can be presumed that the monomer-template composite is accountable for the surface variations (*23*)." (Yu, L.; Yun, Y.; Zhang, W.; Wang, L., Preparation, recognition characteristics and properties for quercetin molecularly imprinted polymers. *Desalin. Water Treat.* 2011, 34, 309-314).
p 144	para 3, line 10	:	insert non-breaking spaces between number and unit and read "y = 804.5*x*"
p 145	Fig 5.14	:	insert non-breaking spaces between number and unit and read "20 mg"
p 151	para 1, line 8	:	insert non-breaking spaces between number and unit and read "MIP - NIP = 0.3 μmoles/g polymer"
p 155	para 2, line 6	:	"able" for "enable"
p 155	para 3, line 1	:	replace "The application of RP-ESI ion trap MS/MS ..." and read "The application of RPLC-ESI ion trap MS/MS ..."
p 155	end of para 5	:	insert non-breaking spaces between number and unit and read "(*E*)-resveratrol"
p 157	para 1, line 3	:	delete "winery" and read "The global wine industry is producing a large volume of waste."
p 157	para 1, line 4	:	insert comma after "(stems)" and read "... byproducts are generated during de-stemming (stems), and grape crushing ..."
p 158	end of para 4	:	insert non-breaking spaces between number and unit and read "5.0×10^{-1} mM" and "y = m*x* + b"
p 159	para 2, line 1	:	insert non-breaking spaces between number and unit and read "1.3×10^{-4} mM"
p 159	para 5, line 1	:	insert non-breaking spaces between number and unit and read "10 mM"
p 160	para 4, line 5	:	comment: "The sample mixture was stirred using a magnetic stirrer (IKA RCT Basic, Staufen, Germany) at a speed of two (40 rpm) ..."
p 161	para 1, line 5	:	comment: "The sample mixture was left in the dark for 30 min and stirred using a magnetic stirrer (IKA RCT Basic, Staufen, Germany) at a speed of two (40 rpm) in a round-bottom flask."
p 161	para 1, line 6	:	insert non-breaking spaces between number and unit and read "10 min"
p 161	para 2, line 3	:	comment: "A vacuum was used to remove the residual solvents and then the sample was dried in a vacuum oven for 1 hour."
p 161	para 2, line 11	:	comment: "The *n*-hexane fraction was evaporated to dryness under reduced pressure using a rotary evaporator (Buchi Rotavapor R-215, Flawil, Switzerland)."
p 162	para 2, line 4	:	insert non-breaking spaces between number and unit and read "4 × 2 mL"
p 163	para 2, line 5	:	"instruments" for "instrumentations"
p 165	Fig 6.3	:	insert non-breaking spaces between number and unit and read "0.3 mm × 150 mm"
p 173	para 1, line 3	:	delete "for" and read "Although, the MIP was reused many times ..."
p 173	para 1, line 6	:	add "was" and read "... in most cases more than 99% of (*E*)-resveratrol was achieved."
p 174	para 3, line 1	:	insert non-breaking spaces between number and unit and read "31.4 μg/g"
p 174	para 3, line 2	:	replace "Resveratrol is more produced in the epidermal ..." and read "Resveratrol is produced more in the epidermal ..."
p 176	Fig 6.9	:	insert non-breaking spaces between number and unit and read "0.3 mm × 150 mm" and "2-52 min"
p 179	para 3, line 1	:	"use" for "used"
p 180	para 2, line 4, 5	:	replace "to remove the", add "the" and insert comma after "94.7%", and read "The application of wash solvents enabled the removal of majority of the (*E*)-resveratrol approximately 10.8 μg/g (94.7%), from the NISPE cartridge."

The following amendments have been made in accord with the suggestions and valued comments of the examiners.

p 180	para 2, line 6	:	replace "to hold" and insert non-breaking spaces between number and unit and read "In contrast, the MIP was capable of holding a significant amount of (*E*)-resveratrol (10.4 μg/g) ..."
p 180	para 2, line 9	:	replace "than" and read "the MIP exhibited a greater selectivity for (*E*)-resveratrol compared to the NIP."
p 182	para 2, line 4	:	comment: There is evidence in the literature to justify the statement made "However, this oil is incompatible with the RP-HPLC system as many hydrophobic substances such as triglycerides are present in the sample (*52*)." (Rezanka, T.; Mares, P., Determination of plant triacylglycerols using capillary gas chromatography, high-performance liquid chromatography and mass spectrometry. *J. Chromatogr.* 1991, 542, 145-159).
p 183	para 3, para 4	:	insert non-breaking spaces between number and unit and read "5 h" and "1 h", delete "salt" and read "... sodium chloride was added ..."
p 186	Fig 6.13	:	insert non-breaking spaces between number and unit and read "5 μm particle size"
p 188	para 1, line 4	:	delete "that" and add Section's number, and read "... as described in Section 5.3.2, ..."
p 190	para 3, para 4	:	insert spacing between para 2 and para 3 (para 3 begins with "Campesteryl glucoside ..."). Insert spacing between para 3 and para 4 (para 4 starts with "The high fidelity of the MIP ...")
p 199	para 1, line 2	:	insert comma after "products" and read "... food and beverages products, and ..."
p 205	end of para 6	:	add "Further research will be aimed at developing new MIP-based-sensors with high sensitivity and rapid response times for the selective detection of bioactive polyphenols and phytosterols. Despite considerable improvements in the field of imprinting technology with various types of new polymers, imprinting formats and applications have been achieved, significant challenges regarding the mechanisms underlying the imprinting technique remain to be solved and many opportunities for these applications are still not fully exploited."

Table of Contents

Notice 1

……

Siti Nur Nazathul Shima Binti Hashim

Notice 2

I certify that I have made all reasonable efforts to secure copyright permissions for third-party content included in this thesis and have not knowingly added copyright content to my work without the owner's permission.

……

Siti Nur Nazathul Shima Binti Hashim

Declaration

To the best of my knowledge and belief this thesis contains no material which has been accepted for the award of any degree or diploma in any university, nor any material previously published or written by any other person except where reference is made.

……

Siti Nur Nazathul Shima Binti Hashim

Acknowledgements

This thesis was financed with a scholarship from the Ministry of Science, Technology and Innovation of Malaysia, with the consumables paid by the Green Chemistry Foundation.

It would however not have been possible without the competent, friendly and inspiring support of everyone I worked with at the Centre for Green Chemistry at Monash University.

Foremost, I am deeply indebted to my supervisor, Prof. Milton Hearn, who gave me the opportunity to work on this interesting project and for his continuous encouragement, motivation and inspiration.

Equally, I would like to express my sincere appreciation to my associate supervisor, Dr. Reinhard Boysen, for his superb scientific guidance and knowledgeable support for every aspect of my research. I was impressed by his incredible enthusiasm, his facilitation of fruitful co-operation with other researchers in the Centre, enjoyed many valuable discussions and appreciated his thorough proofreading of my entire thesis.

Special thanks I owe to Dr. Lachlan Schwarz for introducing me to molecularly imprinted polymer chemistry and for the preparation of the (*E*)-resveratrol-templated and stigmasterol-templated MIPs. Also I would like to thank Mr. Basil Danylec for synthesizing four non-commercial stigmasterol analogue standards that have been instrumental in assessing crucial questions of my thesis and for making time for many valuable discussions. To Dr. William Yang I am indebted for training me in the use of the LC-MS equipment. Many thanks go to Chadin Kulsing for his guidance with the preparation of SEM images and discussing with me some mathematical equations.

A heartfelt thank you goes also to Judy Stewart for helping with the administration, Tracy Warner for superb technical advice and Dr. Jamil Chowdhury for his immense knowledge in the field of polymers. Erika Winter was my advisor in all things grape and wine related and organised the fresh grapes and wine for my research.

It is my pleasure to also acknowledge all the present and past post-graduate students, especially Priscilla Johnston, Andras Komaromy, Duy Do Pham, Roshanak Sepherifer, Ahmed Al-Hussin, Gagan Kaur, Sepa Nanayakkara, Dr. Martin Petzold and Dr. Rudy Ciayadi that have made my time in the Centre for Green Chemistry enjoyable and memorable.

My time in Australia was also made special through the Malaysian Community in Melbourne through their support, encouragement and friendship.

Most importantly, I would like to thank my husband, Mohamad Tarmizi Ahmad, and my children, Sarah (10 y) and Danial (6 y). Their love and support gave me the strength during my candidature and I am grateful for their patience and understanding and coming to Australia with me. It has been a wonderful experience for us all.

Finally, I would like to thank my family all over the world to have supported me in this endeavour. Your love and friendship despite the distance have endured.

Also thanks go to my superiors at Department of Chemistry, Petaling Jaya in Malaysia for my secondment, trusting that my knowledge and skills gained during my PhD will help me in my future work to make the world a safer and better place.

List of publications and conferences

1. Shima N.N.S. Hashim, Lachlan J. Schwarz, Reinhard I. Boysen, Yuanzhong Yang, Basil Danylec and Milton T.W. Hearn, Rapid molecularly imprinted polymer solid-phase extraction for the analysis of resveratrol and other polyphenols in red wine, *submitted for publication* **(2013)**.

2. Shima N. N. S. Hashim, Lachlan J. Schwarz, Reinhard I. Boysen, Yuanzhong Yang, Basil Danylec and Milton T.W. Hearn, Development of new technologies for the solid-phase extraction of polyphenols, *poster presentation*, Gordon Green Chemistry Conference, 22nd - 27th July **2012**, Lucca, Italy.

3. Shima N. N. S. Hashim, Lachlan J. Schwarz, Reinhard I. Boysen, Yuanzhong Yang, Basil Danylec and Milton T.W. Hearn, The use of molecularly imprinted polymers for the enrichment of nutraceuticals from agricultural by-products: Innovative solutions for a green economy, *poster presentation*, 3rd Asia and Oceania Conference on Green and Sustainable Chemistry (AOC-3), 7th - 9th December **2011**, Melbourne Convention Centre, Melbourne, Australia.

4. Brenda K. Y. Leung, Basil Danylec, Lachlan J. Schwarz, Shima N. N. S. Hashim, Reinhard I. Boysen, Simon J. Harris and Milton T. W. Hearn, Molecular imprinted polymer base separation technologies for extraction of bioactive compounds, *poster presentation*, 3rd Asia and Oceania Conference on Green and Sustainable Chemistry (AOC-3), 7th - 9th December **2011**, Melbourne Convention Centre, Melbourne, Australia.

5. Shima N.N.S. Hashim, New method for the extraction and analysis of bioactives from red wine, *oral presentation*, Annual Green Chemistry Workshop, 17th - 19th November **2010**, Melbourne, Australia.

Abbreviations, Symbols and Units

%	Percentage
(*E*)-	The *E* notation refers to the absolute stereochemistry around the double bonds
(*Z*)-	The *Z* notation refers to the absolute stereochemistry around the double bonds
$[M-H]^-$	Precursor ion in the negative ionisation mode
$[M-H]^+$	Precursor ion in the positive ionisation mode
°C	Degree Celsius
µ	Micro
4-VP	4-vinylpyridine
Å	Ångström
ACN	Acetonitrile
AcOH	Acetic acid
A_f	Peak area of free analyte
A_i	Peak area of initial concentration
AIBN	2,2´-azobis(2-methylpropionitrile)
AuPt	Aurum platinum
BPC	Base peak chromatogram
C	Carbon
C_{18}	Octadecyl
C_4	Butyl
C_6H_5	Phenyl
C_8	Octyl
Caco-2	A continuous line of heterogeneous human epithelial colorectal adenocarcinoma cells
CC	Column chromatography
CE	Capillary electrophoresis
CEC	Capillary electrochromatography
$CHCl_3$	Chloroform
CID	Collision induced dissociation
cm	Centimetre
CO_2	Carbon dioxide
COO^-	Carboxylic

COX	Cyclooxygenase
DAD	Diode array detector
DM	Dry matter content
DMAAM	N,N´-dimethylacrylamide
DMSO	Dimethyl sulphoxide
DVB	Divinyl benzene
EGDMA	Ethylene glycol dimethacrylate
EGFR	Epidermal growth factor receptor
EIC	Extracted ion chromatogram
ESI	Electrospray ionisation
EtOH	Ethanol
F	Flow rate
FA	Formic acid
g	Gram
GC	Gas chromatography
h	Hour
H	Hydrogen
H_2O	Water
HCl	Hydrochloric acid
HFBA	Heptafluorobutyric acid
HPLC	High performance liquid chromatography
HRF	Heterocyclic ring fission
Hz	Hertz
i.e.	For example
ICC	Ion charge control
IF	Imprinting factor
IPA	*Iso*-propanol
k	Kilo
L	Litre
LC	Liquid chromatography
lc	Low concentration of target analyte
LDL	Low-density lipoprotein
LLE	Liquid-liquid extraction
LOD	Limit of detection
LOQ	Limit of quantitation
m	Meter

m	Milli
M	Molar
m/z	Mass-to-charge ratio
MAA	Methacrylic acid
MAE	Microwave-assisted extraction
MeOH	Methanol
min	Minute
MIP	Molecularly imprinted polymer
MISPE	Molecularly imprinted solid-phase extraction
MMP	Metalloprotease
mPa	Milli Pascal
MS	Mass spectrometry
MS/MS	Tandem mass spectrometry
MW	Molecular weight
MΩ	Megaohm
N	Nitrogen
n	Number of measurements
N_2O	Nitrous oxide
NADPH	Nicotinamide adenine dinucleotide phosphate
NaOH	Sodium hydroxide
NH_2	Amino
NH_3^+	Ammonium ion
NIP	Non-imprinted polymer
NISPE	Non-imprinted solid-phase extraction
nm	Nanometer
NMR	Nuclear magnetic resonance spectrometer
NP	Normal-phase
O	Oxygen
OH	Hydroxyl-group
PG	Prostaglandin
psi	Pounds per square inch
QM	Quinine methide fission cleavage
r	Internal column radius
RDA	Retro-Diels-Alder reaction
RP	Reversed-phase
rpm	Revolutions per minute

s	Second
S	Sulphur
SD	Standard deviation
SEM	Scanning electron microscope
SFE	Supercritical fluid extraction
SPE	Solid-phase extraction
TFA	Trifluoroacetic acid
TIC	Total ion chromatogram
TLC	Thin layer chromatography
t_R	Retention time
UAE	Ultrasound-assisted extraction
UV	Ultraviolet
V	Voltage
V	Volume of injection
v/v	Volume per volume
Vis	Visible
vs	Versus
$w_{1/2}$	Peak width at half height
α	Alpha
β	Beta
δ	Delta
ε	Epsilon
λ	Wavelength
π	Pi
σ	Sigma

Thesis Summary

In the food and nutraceutical industries, increasing emphasis is being placed on value-added products. This high worldwide demand for health-beneficial natural compounds can be met by intensifying the focus on using phytochemicals for enriching food. Epidemiological studies have shown that phytochemicals, including polyphenols and phytosterols, derived from vegetables and fruits are substantial sources of bioactive compounds that are beneficial to human health. The polyphenols phytoalexin (*E*)-resveratrol has attracted considerable interest because of its remarkable pharmacological activity in the prevention of various human illnesses such as cancer and cardiovascular disease. Several studies have shown that phytosterols such as stigmasterol are useful in the prevention of some cancers, including ovarian, prostate, breast and colon cancers, in addition to serving as a precursor in the manufacture of synthetic progesterone. However, the determination of polyphenols and phytosterols from plants has proven to be an extremely challenging analytical task, hindered by the complexity of the numerous chemicals in natural extracts that necessitates tedious separation methodologies.

In this thesis, a new method for the separation and enrichment of health-beneficial polyphenols and phytosterols using green chemical techniques adaptable to analysis and isolation is described. This method utilises new molecularly imprinted polymers (MIPs) in a solid-phase extraction (SPE) format, known as MISPE, for the selective extraction of valuable (*E*)-resveratrol and stigmasterol from grape pressings, which are an abundant waste product in the wine industry currently used for tartrate and alcohol extraction or compost.

MIPs are synthetic materials designed to have selectivity for specific molecular targets and are synthesized from self-assembled pre-polymerization complexes of functional monomers around a molecular template by either thermal- or photo-polymerisation, followed by a post-synthetic template removal. The resulting polymer possesses recognition sites complementary to the size, shape or/and functionality of the chemical or biological template (imprint) molecule.

A selectivity evaluation of the recognition sites in MIPs is normally performed in batch-binding and dynamic binding experiments using the templates and template analogues with a non-imprinted polymer as control, on the basis of the quantitative information derived from

liquid chromatography supernatants or eluates. This evaluation process is frequently limited by the requirement for sufficiently large quantities of the template analogues, which must be chemically synthesised if they are not commercially available. MIPs have many advantages including predetermined selectivity, reusability, low cost of preparation, and stability in highly acidic and basic conditions.

The MIPs for the selective capture of (*E*)-resveratrol was synthesised using the non-covalent imprinting technologies and the MIP for stigmasterol proved to be most effective prepared using covalent imprinting. For both systems, comprehensive dynamic binding evaluations in aqueous media were performed using non-target imprinted polymers (NIPs). The optimised (*E*)-resveratrol-templated MIP in the SPE format enabled the capture of the target compound with 99% recoveries and high enrichment factor (*IF*) from red wine (*IF* = 32), fresh grape pressing residue extract (*IF* = 43), aged grape pressing residue extract (*IF* = 18), and extracts of grape skins (*IF* = 72) and grape seeds (*IF* = 26). The stigmasterol-templated MIP achieved 96% recovery and 12-fold enrichment of the target compound from grape seed extract.

Finally a new method to enrich the health-beneficial resveratrol, procyanidin and epicatechin as well as stigmasterol and campesteryl glycoside from one single grape pressing feedstock with two MIPs and green chemistry methods was elaborated. Furthermore, a systematic separation methodology for the identification and quantification of polyphenols (twenty compounds) and phytosterols (eight compounds) was developed using reversed-phase high performance liquid chromatography (RP-HPLC) in combination with electrospray ionisation ion trap tandem mass spectrometry (ESI-MS/MS) using environmentally benign mobile phases.

This rapid and high-resolution method can be used for binding site characterisation, selectivity optimisation and monitoring of the performance of MIPs intended for solid-phase extraction of bioactive molecules and nutraceuticals from diverse complex mixtures. These investigations demonstrated the application of MISPE for the selective enrichment of health-beneficial compounds from wines and grape byproducts, providing a new, efficient, cost-effective and sustainable approach for utilisation of natural resources.

Chapter 1

Introduction, background and research objectives

Abstract

The increasing public awareness and concern about the safety of various food products, drugs and cosmetics are the key factor that has prompted the industry and scientific community to look for phytochemicals as 'green alternatives' to some synthetic chemicals that are commonly used in such products. In this chapter, the pros and cons of several strategies for extracting phytochemicals, including liquid-liquid extraction, ultrasound-assisted extraction, microwave-assisted extraction, supercritical fluid and solid-phase extraction are discussed. A relatively new solid-phase extraction (SPE) method is introduced involving molecularly imprinted polymers (MIPs). Taking advantage of principles of molecular recognition, molecularly imprinted solid-phase extraction (MISPE) allows the selective extraction of target compounds from complex feed-stocks through size and shape complementarities as well as spatially defined non-covalent and/or covalent interactions. MISPE modes and the use of analytical techniques commonly used in conjunction with MIP-based extraction of polyphenols and sterols, including liquid chromatography and gas chromatography, are reviewed and the potential of reversed-phase high-performance liquid chromatography (RP-HPLC) in combination with tandem electrospray ionisation mass spectrometry (ESI-MS/MS) for the analysis is discussed. This chapter further describes the chemistry and biochemistry of polyphenols and phytosterols, their classification, their occurrence in plants and grapes, their biological activities and implications on human health. The chapter concludes with a statement of project aims and an overview of the thesis.

Table of Contents

1.1 Introduction

The increasing public awareness and concern about the safety of various food products, drugs and cosmetics are the key factor that has prompted the industry and scientific community to look for 'green alternatives' to synthetic chemicals that are commonly used in such products. Epidemiological studies have shown that phytochemicals, including polyphenols and phytosterols, derived from native or cultivated plants such as vegetables and fruits are natural sources of bioactive compounds, which are beneficial for human health (*1-3*). Hence, there is much interest in the use of phytochemicals as nutraceuticals in the food, pharmaceutical, and cosmetic industries. In the agro-industry, valorisation of vegetable and fruit waste has received a great deal of attention since it is an effective and commercially viable means of extracting valuable phytochemicals. However, there is considerable diversity in the composition and concentration of phytochemicals in vegetables and fruits as well as in processed products or byproducts. Finding a suitable platform for the extraction of phytochemicals is imperative because such compounds can be used in food products to provide health and medical benefits. Therefore, this research is aimed at searching for economical, environmentally benign extraction and separation techniques to isolate beneficial bioactive compounds from their complex matrices.

1.2 Extraction techniques for phenolic/phytosterol analysis

The samples containing polyphenols and/or phytosterols must be collected and prepared according to suitable protocols. Samples are often dried, frozen or lyophilised before extraction to avoid the degradation of polyphenols because high moisture or water content aids enzymatic decomposition activities. Sample pretreatment can also be done by filtration and centrifugation. In many cases, such drying, or heating as well as exposing samples to light and oxygen during preparation and transportation may affect their phenolic composition. There are many ways of extracting polyphenols from biological samples as described below.

1.2.1 Liquid-liquid extraction

Various extraction methods are available for different types of samples. Solvent extractions are the most frequently employed techniques for the analysis of plant-originated-food samples. The conventional liquid-liquid extraction (LLE) methods normally involve

multi-stage extraction procedures and are very time consuming (*4, 5*). The substantial amount of solvent used in LLE not only increases operating costs but also causes additional environmental problems. Minuti *et al.* (*6*) performed a continuous liquid-liquid extraction using 100 mL of ethyl acetate to isolate 22 phenolic compounds including *trans*-resveratrol from 100 mL of red wine. The method achieved a satisfactory recovery for *trans*-resveratrol, however the procedure was solvent intense, tedious and took 16 hours.

1.2.2 Ultrasound, microwave and supercritical fluid extraction

Significant technological advances have resulted in the development of newer extraction techniques suitable for phytochemical analysis, including ultrasound-assisted extraction (UAE) (*7, 8*), microwave-assisted extraction (MAE) (*9, 10*) and supercritical fluid extraction (SFE) (*11, 12*).

UAE methods have the advantages of significantly reducing the extraction times and enhancing extraction yield of polyphenolics compared to the traditional methods (*5*). The ultrasound waves (energy generated by sound wave of 20 kHz – 1 MHz) generate gas bubbles in liquid media that produce substantial increase in temperature and pressure, when the bubbles suddenly burst (*13*). The resulting plant membrane disruption is attributed to intracellular cavitation and micro-mechanical shocks that disrupt cellular structural and functional components up to the point of cell lysis. Depending on wave intensity, exposure time, membrane characteristics and medium type, ultrasonics can induce mechanical, thermal and biochemical effects. It has a large range of applications in food analysis, however, the ultrasound tends to increase the temperature of the ultrasonic water bath and sample, which may cause pigment degradation in the phenolic extract. Without the use of a temperature control device, a temperature increase from 23 °C to 65 °C was observed during 90 min of ultrasonication (*14*). To prevent degradation, the temperature of an ultrasonic water bath must be controlled at room temperature or lower which is an energy intensive process.

MAE can dramatically reduce the extraction time and lower solvent consumption due to the high temperature generated. With this method, an additional optimisation for polyphenol analysis usually requires monitoring the microwave temperature and power, and assessment the suitability of the extraction solvent to comply with the microwave device (*15*). This extraction method was reported to cause the degradation of some thermally unstable polyphenol compounds (*16*).

SFE applications for plant-derived products have remained scarce due to the lipophilic nature of the supercritical carbon dioxide (CO_2). Many active substances in plants such as polyphenols, alkaloids and glycosidic compounds are poorly soluble in CO_2 and hence not extractable (*17*). To circumvent this problem, some polar supercritical fluids such as Freon-22 (chlorodifluoromethane) and nitrous oxide (N_2O) have been used. They however are detrimental chemicals to ozone depletion or can cause explosions, respectively (*18*). Likewise, supercritical water and superheated water have certain advantages such as a higher extraction ability for polar compounds, but the application is not suitable for thermally labile phenolic substances (*18*). In addition, this SFE technique is often limited for routine analysis because it requires specially designed instrumentation and is comparatively costly.

1.2.3 Solid-phase extraction

There is a large number of published studies describing the role of solid-phase extraction (SPE) to pre-concentrate and enrich target analytes and eliminate interfering components (*19-21*). The principle of SPE is similar to that of LLE and involves a partitioning of solutes between two phases. Instead of partitioning two immiscible liquid phases, in SPE the sample compounds are partitioned between a liquid phase and a solid sorbent phase. This technique is preferable compared to the LLE due to its simplicity, versatility, low consumption of organic solvent and fewer laboratory glassware was used. The general procedure of SPE involves loading a liquid sample onto a solid sorbent bed, washing to eliminate the matrix interferences, and finally eluting the target analyte.

The applicability of SPE is mainly determined by the sorbent employed, either silica-based or organic resin-based, with suitable physical and chemical properties, which is contained within an extraction cartridge. The main drawbacks of the conventional sorbents (*e.g.*, C_{18}, ion-exchange and size exclusion phases) are a lack of selectivity, which often leads to co-extraction of matrix components with the target analytes. As a consequence, fractionation is often required (*22*). Sun *et al.* (*23*) reported the application of SPE with silica C_{18} sorbent for the isolation of procyanidin, anthocyanidin and phenolic acids from wines. The entire fractionation and separation protocol demanded a high volume of environmentally challenging chemicals and was a laborious process.

1.2.4 Extraction with molecularly imprinted polymers

Molecularly imprinted polymers (MIP) are elegant means to extract target molecules from complex samples fulfilling the selectivity requirement together with the need for high-speed of analysis. The MIP imprinting technology produces synthetic functional polymers with predetermined molecular recognition sites for a target or class of target molecules through the use of a molecular template. The most widely used technique to prepare a MIPs is the monolith bulk polymerisation. Although there have been other synthetic protocols such as emulsion (*24*) and precipitation polymerisation (*25*), the simplicity, robustness, limited organic chemistry requirements and the fact that no specialised equipment is needed (*26*) are the main factors making the monolith bulk format still preferable.

MIPs have many outstanding advantages including predetermined selectivity, low cost of preparation, low chemical usage, chemical and thermal stability as well as reusability. The benefits of MIPs have been directed toward a plethora of applications including catalysis (*27, 28*), drug design and delivery (*29*), as sensors (*30*) and most commonly as separation materials for chromatography and solid-phase extraction (*31-34*). A MIP for class-selective extraction was developed for the detection of several target analogues of phenolic acids (*35*), anti-epidermal growth factor inhibitors (*36*) and anti-inflammatory drugs (*37*).

1.2.4.1 Classification of molecularly imprinted polymers

Molecular imprinting is typically classified into the non-covalent imprinting (the self-assembly approach) and covalent imprinting/semi-covalent imprinting (the pre-organisation approach) according to the interactions between functional monomer and target molecules in the pre-polymerisation mixture and during the rebinding process. In both MIP preparations, a non-imprinted polymer (NIP) is usually also synthesised using the same method as the MIP however without the template molecule. The NIP functions as a control in order to evaluate the selectivity of the MIP.

1.2.4.1.1 Non-covalent imprinting

The non-covalent imprinting approach, introduced by Arshady and Mosbach (*38*), is based on the formation of relatively weak non-covalent interactions (*i.e.*, hydrogen bonding, hydrophobic interactions and Van der Waals forces) between the template molecule and selected monomers before polymerisation **(Figure 1.1)**. During the imprinting process, the

functional monomers are self-assembled and arrange themselves around the template by non-covalent interactions. Subsequently the functional monomers are "frozen" into position by polymerisation with a high degree of cross-linking in the presence of a porogenic solvent. After template removal by solvent extraction, the generated binding sites ideally afford a complimentary spatial arrangement of the functional groups within the individual nano-cavities resulting in high selectivity and affinity for the template and closely related compounds. This imprinting approach is the most widespread method for the preparation of MIP due to straightforward, one-step synthesis procedures, the broad range of imprintable compounds (due to the chemical diversity of monomers able to interact with various templates that are commercially available) and reversible template re-binding based on non-covalent interactions (*39*).

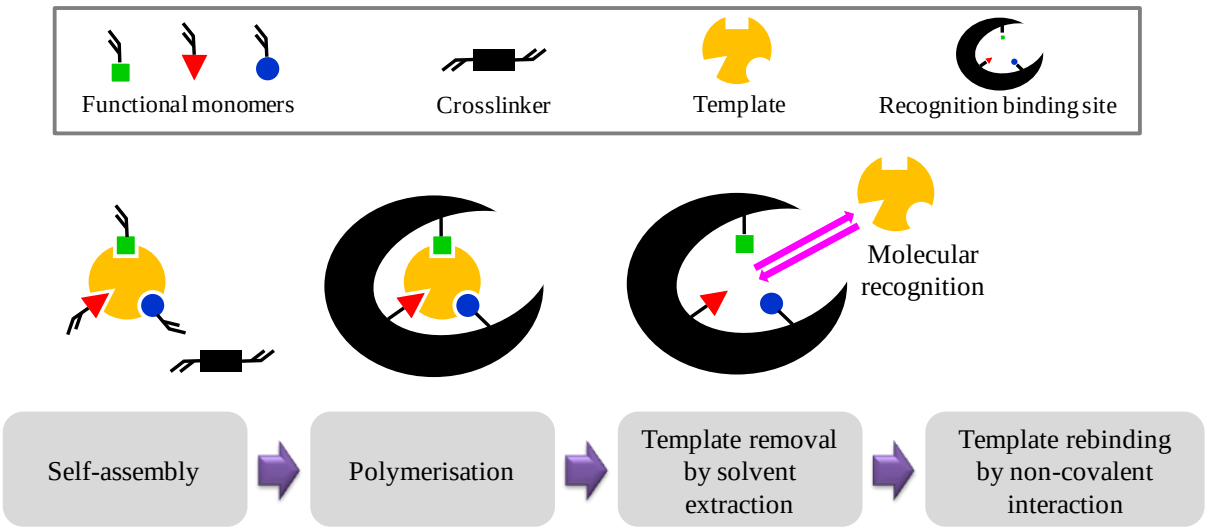

Figure 1.1: The synthesis of molecularly imprinted polymers (MIPs) using the non-covalent imprinting approach.

1.2.4.1.2 Covalent/semi-covalent imprinting

The covalent imprinting approach was first suggested by Wulff *et al.* (*40*, *41*). This approach involves the formation of reversible covalent bonds between the template and a monomer *via* chemical synthesis before polymerisation to form a cleavable monomer-template composite. After the template is removed from the polymer by chemical cleavage, the covalent bonds of the polymer-template composite are re-formed upon rebinding of the target analyte **(Figure 1.2)**. This imprinting approach results in a high stability of template-monomer interaction, which minimises the occurrence of non-specific binding sites. Due to the

difficulty of designing an appropriate cleavable monomer-template composite, this imprinting style is relatively restrictive.

An intermediate option is the semi-covalent approach (*42*). Semi-covalent imprinting is a hybrid method of covalent and non-covalent imprinting. The template is also covalently bound to a functional monomer prior to the polymerisation process, but the template rebinding by the formed MIP is based on the non-covalent interactions. The polymers prepared with the semi-covalent style have been claimed to improve homogeneity of the binding sites (*43*, *44*). Whitcombe *et al.* (*45*) introduced the semi-covalent approach with "sacrificial spacer" methodology to imprint cholesterol. They synthesised a 4-vinylphenyl carbonate ester as the covalently-template bound monomer, which was cleaved after the polymerisation was completed, resulting in a recognition site that could interact with the target molecule (cholesterol) through hydrogen bonding interactions.

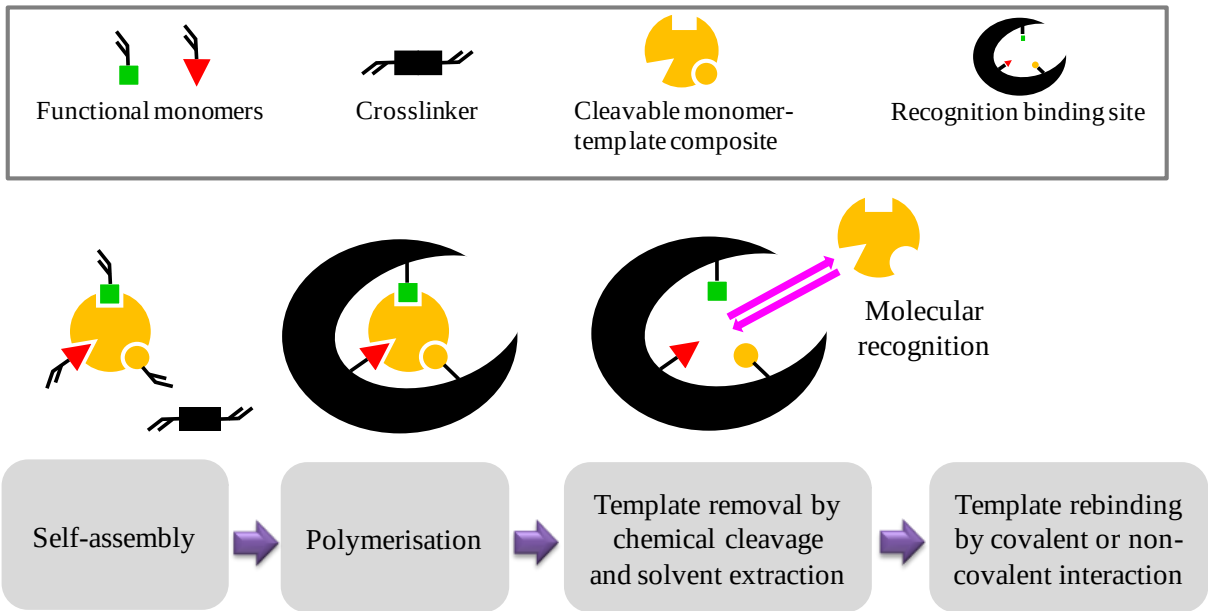

Figure 1.2: The synthesis of molecularly imprinted polymers (MIPs) using the covalent/semi-covalent imprinting approach.

1.2.5 Molecularly imprinted solid-phase extraction

The method using a molecularly imprinted polymer (MIP) for solid-phase extraction (SPE), so called MISPE, was first pioneered by Sellergren *et al.* (*46*) who successfully extracted the antimicrobial drug pentamidine from urine samples. Since then, the development of MISPE has exponentially expanded in affinity separation studies due to the high separation factors

obtained. The key benefits of MISPE include the rapid recovery of target analytes in high purity with a high enrichment factor and reduced consumption of organic solvents. This technique can revolutionise the conventional SPE technique by providing higher selectivity and reusable MIP materials. MISPE have been applied to polyphenols and sterols from complex biological samples and this technique was demonstrated in a number of proof-of-concept studies using different imprint molecules as exemplified in **Table 1.1** and **Table 1.2**.

Table 1.1: MISPE applications for the detection of polyphenols in various complex samples.

Template	MIP synthesis	Sample	Target analyte	MISPE mode	Analytical system	Ref.
(*E*)-Resveratrol	Non-covalent	Peanut press waste	(*E*)-Resveratrol	Off-line	HPLC-UV	(*47*)
(*E*)-Resveratrol	Non-covalent	*Polygonum cuspidatum*	(*E*)-Resveratrol	Off-line	HPLC-UV	(*48*)
(*E*)-Resveratrol	Core-shell microspheres	*Polygonum sachalinense*	(*E*)-Resveratrol	Off-line	HPLC-UV	(*49*)
(*E*)-Resveratrol	Non-covalent	*Polygonum cuspidatum*	(*E*)-Resveratrol, emodin	On-line	HPLC-UV	(*50*)
Caffeine	Non-covalent	Beverages	Caffeine	Off-line	HPLC-UV	(*51*)
Caffeine	Non-covalent	Green tea	Caffeine, catechin/ epicatechin derivatives	Off-line	HPLC-UV	(*52*)
(+)-Catechin	Non-covalent	Green tea	(+)-Catechin	Off-line	HPLC-UV	(*53*)
Catechin and caffeine	Non-covalent	Green tea	Catechin and caffeine	Off-line	HPLC-UV	(*54*)
Kaempferol	Non-covalent (microspheres)	Chinese medicine	Kaempherol	Off-line	HPLC-UV	(*55*)
Protocatechuic acid	Non-covalent	Plant material	*p*-hydroxybenzoic acid derivatives	Off-line	HPLC-UV	(*35*)
Quercetin	Non-covalent	Red wine	Quercetin	Off-line	HPLC-UV	(*56*)
Quercetin	Non-covalent	Plant material	Anti-EGFR inhibitors	Off-line	HPLC-UV	(*57*)
Quercetin	Non-covalent	Gingko leaves	Quercetin, kaempferol	Off-line	HPLC-UV	(*58*)
Quercetin	Non-covalent	Rat plasma	Quercetin	Off-line	HPLC-UV	(*59*)
Quercetin	Non-covalent	Tea, cocoa, grape residue	Catechin	Off-line	HPLC-UV	(*60*)
Quercetin	Non-covalent	Yellow onion	Quercetin	Off-line	HPLC-UV	(*61*)

Table 1.2: MISPE applications for the determination of sterols in a range of complex matrices.

Template	MIP synthesis	Sample	Target analyte	MISPE mode	Analytical system	Ref.
17β-estradiol	Non-covalent	Milk powder	17β-estradiol	Off-line	HPLC-UV	(*34*)
Cholesterol	Non-covalent	Cheese	Cholesterol	Off-line	HPLC-UV	(*62*)
Cholesterol	Non-covalent	Biological samples	Cholesterol	Off-line	GC-FID	(*33*)
Cholesterol	Non-covalent	Gastrointestinal fluid	Cholesterol	On-line	HPLC-UV	(*63*)
β-sitosterol	Magnetic bead	Mushroom, human blood serum, watermelon	β-sitosterol	Off-line	GC-MS	(*64*)
β-sitosterol	Non-covalent	Plant material	β-sitosterol	Off-line	HPLC-UV	(*65*)

1.2.5.1 MISPE modes

The MISPE method can be performed using the on-line, in-line or off-line mode.

1.2.5.1.1 On-line MISPE mode

A typical on-line mode involves the automation of the use of the MIP, which is packed into a small pre-column and placed in the loop of a six-port injection valve of LC system (*66*). During the extraction process, sample loading, washing and elution of target compounds was carried out initially in the MIP pre-column, with the eluted compounds subsequently analysed using an analytical column. Bjarnason *et al.* (*67*) reported the first application of an on-line MISPE procedure coupled to HPLC for the selective extraction of triazine herbicides in complex water samples. The lack of compatibility between the mobile phases used for solvent extraction to remove the target analytes from the MIP pre-column and that for the separation on an analytical column, made this approach less favourable.

1.2.5.1.2 In-line MISPE mode

The in-line MISPE style involves a direct attachment of the MISPE column to a chromatographic system. This approach was first described by Sellergren *et al.* (*46*) for the determination of pentamidine in urine. After loading a diluted urine sample (100 mL) onto the MISPE column, a wash procedure with a buffer solution (100 mL) was applied. Since a large volume of aqueous sample was loaded onto the MIP, a high degree of matrix interference was

observed, caused by hydrophobic interactions. In order to remove the non-specifically bound material, a large volume of washing solvent had to be applied prior to the elution steps.

1.2.5.1.3 Off-line MISPE mode

Most published studies of MISPE have used an off-line mode due to its simple procedure which is similar to the conventional off-line SPE method (*34*). The main advantages of this format is that the convenience of operation and the high recovery of the target analytes (*68*). For that reason, the present work only focussed on the off-line MISPE mode.

An off-line MISPE protocol typically involves packing a small amount of MIP (15-1000 mg) held in place by two frits into polypropylene cartridges. The method contains four basic steps, namely column conditioning, sample loading, wash and elution as illustrated in **Figure 1.3**.

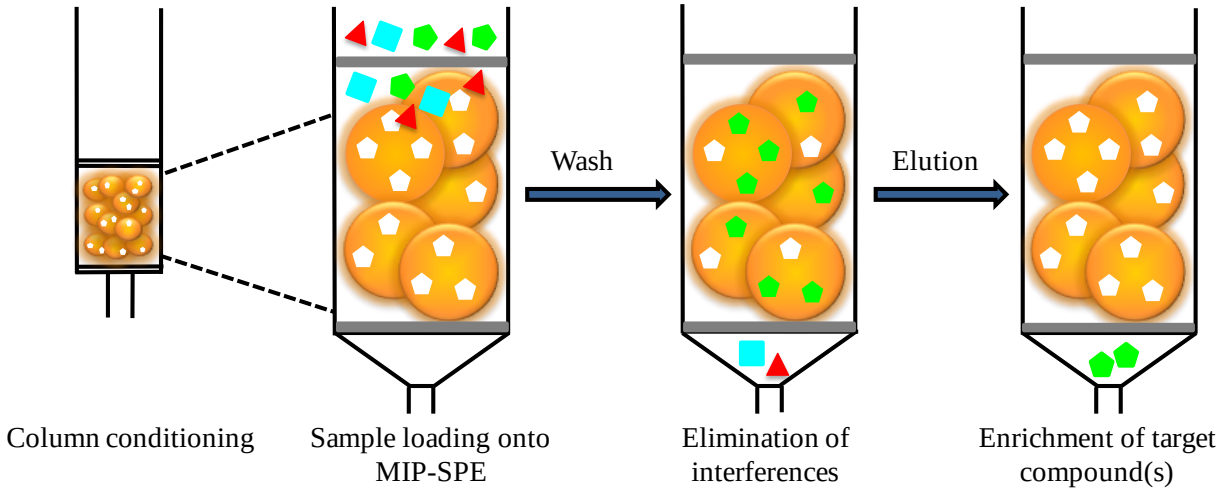

Figure 1.3: Steps of MISPE target compound enrichment.

The conditioning step is performed by passing a small volume of solvent through the SPE cartridge, so that the MIP sorbent bed can make effective surface contact with the target analyte present in the sample. Ideally, the conditioning solvents used should be the same as those used in the subsequent analytical chromatography. After the sample has been loaded, the analyte of interest is specifically retained by the porous polymer. Other interfering compounds could however also non-specifically adsorb onto the polymer. In order to achieve a selective extraction, a wash step with mixtures of organic solvents with a weak concentration of an acid is therefore introduced prior to the elution step. This wash stage must

be optimised in terms of pH, volume or composition of the washing solvent to exploit the MIP's ability to be highly selective in recognising the target molecule. This procedure should remove the interfering substances by suppressing the non-specific interactions between the MIP sorbent and the non-target molecules. In the elution step, a solvent with appropriate eluting properties is employed to release the target compound from the MIP binding sites. The importance hereby is the choice of eluent composition according to the interaction between target molecule and the binding sites within the porous polymer network. After completion of the MISPE protocol, the elution extract is analysed usually by chromatographic or spectroscopic techniques. The selectivity of the MIP to capture the target compound is evaluated against its control, the non-imprinted polymer (NIP). The MIP can be reused after some uncomplicated re-conditioning steps.

1.3 Chromatographic separation techniques for phytochemical analysis

The choice of the chromatographic separation technique plays a central role in determining phytochemicals either in the crude extract, partially crude extract prior to MISPE or after MISPE treatment. High performance liquid chromatography (HPLC), gas chromatography (GC), column chromatography (CC), thin layer chromatography (TLC), capillary electrophoresis (CE) and capillary electrochromatography (CEC) with various modes of detection including UV-Vis, mass spectrometry (MS), flame ionisation, evaporative light scattering and infrared are the most common analytical methods involved in natural product analysis.

1.3.1 High performance liquid chromatography

High performance liquid chromatography (HPLC) has become more popular for the analysis of phytochemicals (*69*) because there are no restrictions on sample volatility and derivatisation requirements in comparison to the GC technique. HPLC provides a high resolution and a rapid and reproducible separation. This technique has a wide range of chromatographic modes such as reversed-phase (*70*), normal-phase (*71*), aqueous normal phase (*72-74*), hydrophilic interaction chromatography (*75*), hydrophobic interaction (*70*), ion exchange (*76*), size exclusion (*77*) and affinity chromatography (*78*). The present work was directed at the separation of polyphenols and phytosterols, and was based on the

reversed-phase chromatographic mode. This technique is capable to handle compounds of a diverse polarity and varying molecular mass.

1.3.1.1 Reversed-phase HPLC

Reversed-phase HPLC (RP-HPLC) is a preferred technique for the analysis of phytochemicals due to several factors (i) a good resolution can be achieved under different chromatographic conditions; (ii) the chromatographic selectivity can be controlled through the changes in mobile phase properties; (iii) generally resulted in high recoveries and productivity; (iv) good reproducibility and repetitive separations over a long period of time due to the column stability and compatibility with various conditions of mobile phases (*79*) and (v) ease of use and robust instrumentation.

RP-HPLC separates the compounds on the basis of hydrophobicity. The separation depends on the hydrophobic interaction of the analyte with the immobilised ligands attached to the stationary phase. In general, an analyte with a larger hydrophobic surface area (with numerous C-H, C-C, S-S or other non-polar groups) displays a longer retention time because it increases the molecule's non-polar surface, which is non-interacting with water. In contrast, the presence of polar groups, such as OH, NH_2, COO^- or NH_3^+, reduce retention as they are well solvated in water. The most commonly used ligands are *n*-octadecyl (C_{18}), octyl (C_8), *n*-butyl (C_4), phenyl (C_6H_5) and amino (NH_2), each are imparting specific chromatographic characteristic to the column. The binding of the target analyte to the stationary phase is proportional to the contact surface area around the non-polar segment of the analyte molecule upon association with the non-polar surface of the immobilised *n*-alkyl ligand in the aqueous mobile phase conditions during the course of the analysis.

Several detectors are available for detection of analytes after chromatographic separation. The most commonly used is ultraviolet detection which relies upon the presence of an ultraviolet light absorbing chromophore (the functional group in the molecule responsible for the light absorption) in the analyte (*80*). It is applicable to a large number of compounds, as it can be rather sensitive, has a wide linear range and is relatively unaffected by temperature fluctuations and compatible with gradient elution. The diode array detector (DAD) allows the detection of the light absorbance at a number of wavelengths simultaneously and also allows the production of the absorbance spectra of the eluted components (*81*). Other common

detectors for HPLC systems include refraction index, fluorescence, electrochemical, radioactivity, evaporative light scattering and mass spectrometry (MS).

1.3.2 Liquid chromatography electrospray ionisation ion trap MS/MS

Mass spectrometry is an analytical technique that can provide information on the molecular mass, structure, and concentration of the target molecules after their desolvation and ionisation. The molecules of interest are first introduced into the ionisation source of the mass spectrometer, where they are first ionised to acquire positive or negative charges. The ions then travel through the mass analyser and arrive at different times at the detector according to their mass-to-charge *(m/z)* ratio. After the ions make contact with the detector, signals are generated and recorded by a computer system. The computer displays the signals graphically as a mass spectrum, showing the relative abundance of the signals separated according to their *m/z* ratio.

Tandem mass spectrometry is a powerful technique to identify low levels of target compounds in the presence of a high sample matrix background. In addition, this technique is very useful in the reliable identification of trace compounds and co-eluting peaks in complex matrices (*82*, *83*). In the case of unknown compounds present in the samples, tentative compound identification is usually performed by matching the precursor ion and the obtained product ion(s) with the theoretical molecular mass, fragmentation pathways and characteristic fragmentation behaviour using bioinformatics analysis tools and MS/MS data repositories as well as literature data.

1.3.2.1 Electrospray ionisation ion trap mass spectrometry

The possibility of generating gas-phase ions of macromolecules by spraying a solution from the tip of an electrically charged capillary was first reported by Dole and co-workers (*84*). Based on the ideas of Dole, Fenn (*85*) developed electrospray as a soft ionisation technique for mass spectrometry. Electrospray ionisation mass spectrometry has emerged as an important technique in natural product analysis. It provides a sensitive, robust and reliable tool for studying non-volatile and thermally labile biomolecules that are not amenable to analysis by other conventional techniques. Coupling ESI-MS with the HPLC has made this technique capable of analysing small and large molecules of various polarities in complex biological samples.

The electrospray ionisation generates ions by a potential different between a capillary and the inlet to the mass spectrometer. The electric field produces charged droplets in the form of a fine mist. Through the application of a drying gas or heat, the solvent evaporates and the size of the droplets decreases, eventually resulting in the production of desolvated ions (*86*). A characteristic of ESI is the formation of highly charged ions without fragmentation. This process reduces the *m/z* values to a range that can be easily measured by many different types of mass analysers. The true molecular mass of an ion can be calculated since more than one charge state is usually observed. Charge state and molecular mass can also be determined when the isotope forms of the molecular ion are resolved.

The ion trap mass analyser operates by trapping ions in a three-dimensional electric field. Ions created in external sources are focused into the ion trap using electrostatic lenses (88). An electrostatic ion gate pulses open and closed in order to inject ions into the ion trap. The pulsing of the ion gate makes this technique different from a quadrapole, where the ions continually enter the mass analyser. In ion traps, ions can be held for long time periods, giving an easy opportunity to fragment the ions. The ion trap is typically filled with helium. A small radio frequency field can be applied to the trap to cause the ions to move faster. As a result, the so-called precursor ions collide with the helium background gas causing fragmentation. After adding this collisional energy, the resultant product ions are scanned out of the ion trap in the normal way to determine their *m/z*. This process is called collision-induced dissociation (CID). In the ion trap analysis, multiple stage of ion dissociation (MS^n) can be performed to obtain detailed structural information from ions (89). For instance, an MS^3 experiment can be used to create structurally important fragment ions of a particular dissociation product from the ions produced in an MS^2 experiment.

1.4 The grape and wine industries in Australia

Australia is the seventh largest producer of wine in the world and this industry contributes to significant revenue to the country. According to the Australian Bureau of Statistics (*87*), the total production of grapes (based on fresh weight) was determined to be approximately 1.6 million tonnes across all Australian regions in 2010-2011. Winemaking produced about 120,000 tonnes of grape press residues of which 75% is transported to a company that extracts tartaric acid and distils residual alcohol out of the marc, and the remaining residue is then used for compost. South Australia contributed to the highest amount of grape production with

740,475 thousand tonnes, followed by New South Wales with 439,752 thousand tonnes and Victoria about 303,270 thousand tonnes. In 2011, 1.12 billion litres of wine were produced in Australia and more than 65% of that wine was exported internationally. In the last 10 years despite a high volume of export, the average price of the exported wine halved, due to large amounts of wine being shipped in bulk and bottled overseas.

In order to regain a high proportion of high quality bottled wines in wine exports, continual extensive research to improve wine quality over competitors is an important goal in the Australian wine industry. Therefore, several bodies, including the Australian Grape and Wine Research and Development Corporation, The Australian Wine Research Institute, the Commonwealth Scientific and Industrial Research Organisation (CSIRO) and universities, play a significant role to develop further research into wines not only having outstanding sensory characteristics but also being rich in health-beneficial compounds. The present research was undertaken to develop faster and greener methods to analyse health-beneficial compounds in wines and to develop new ways to extract polyphenolic components from grape waste-products using environmentally sustainable approaches.

1.5 Introduction to phytochemicals

Phytochemicals are widely distributed in plants, vegetables and fruits. These compounds encompass polyphenols, phytosterols, carotenoids, alkaloids, nitrogen containing compounds and organosulphur compounds (*88*). Due to the physiological functions of polyphenols and phytosterols in human well-being, including antioxidant activity and cancer prevention, this work focused only on these two types of bioactives.

1.5.1 Polyphenols

Polyphenols or phenolic compounds can be defined chemically as compounds having at least one aromatic ring with one or more hydroxyl-substituents, including their functional derivatives such as esters, methyl-esters, ethers and glycosides (*89*). To date, more than 8,000 types of polyphenols have been discovered in plants (*90, 91*). These compounds fall into various chemical classes and have a large number of structural variations, ranging from simple moieties consisting of a single aromatic ring to highly complex polymeric substances. The significant variations may occur due to the genetic factors, environmental conditions, growth and maturation stage of the plants.

Polyphenols play an important role in plant physiology and interactions with biotic and abiotic environments. Polyphenols are crucial for plant development, in particular for their nutrient uptake, protein synthesis, enzyme activity and photosynthesis (*92*). They also provide structural integrity and scaffolding support to plants and are also produced for their protection from infection by pathogens or from other stress factors.

In the human diet, polyphenols contribute to major visual and organoleptic characteristics of plant-derived foods and beverages, in particular colour and taste. For instance, chemical reactions of polyphenols are important in wine production because they are responsible for the colour and mouth-feel of wine.

1.5.1.1 Classification of polyphenols in grapes

Grapevines belong to the botanical family *Vitaceae* and the genus *Vitis*. *Vitis vinifera* is the main species cultivated for wine production. Grapes contain a significant amount of polyphenols. In general, polyphenolic compounds in grapes can be divided into two main groups, namely the non-flavonoids and flavonoids.

1.5.1.1.1 Non-flavonoids

The primary non-flavonoids in grapes are hydroxybenzoic and hydroxycinnamic acids and their derivatives, coumarins and stilbenes. They are stored primarily in the vacuoles of grape cells, and are easily extracted through crushing and fermenting. These compounds exist mainly as conjugates and are often bound to alcohols, sugars, polysaccharides or organic acids through an ester bond. Grapes and wines contain benzoic acid and cinnamic acid in the order of 100-200 mg/L (*93*). When wines are aged in new oak barrels, other compounds of the same family are absorbed into wine from the oak, namely guaiacol and syringol.

i) Stilbenes

Stilbenes are phenolics with a C_6-C_2-C_6 skeleton structure. The phytoalexin stilbenes are compounds produced by plants in response to attack by fungal, bacterial and viral pathogens, other stilbenes are elicited also by UV light. The stilbenes constitute an important class of non-flavonoid polyphenols which are found in the free, sugar-conjugated (glucoside) and oligomer forms. According to Soleas *et al.* (*94*), more than 30 types of stilbenes and stilbene glucosides have been found in the plant kingdom. Resveratrol-3-*O*-glucoside (also known as

piceid/polydatin) is the most abundant stilbene glucoside in plants (*95, 96*). Resveratrol was found in at least 72 types of plant species (*97*). The occurrence of resveratrol in grapevines was first detected by Langcake and Pryce (*98*). In that study, the leaf tissue was found to synthesise resveratrol in response to fungal infection or UV-light exposure. Creasy *et al.* (*99*) found that resveratrol can only be identified in the skins and seeds of the grapes, but not in the flesh. The concentrations of resveratrol in the grape skins and seeds are influenced by several factors including climate, ripening conditions and amount of fungal (*e.g. Botrytis cinerea*) infection. In addition, grape variety also affects resveratrol amounts with higher concentration reported in red grape compared to white grape cultivars (*100*).

Resveratrol occurs in free and analogue forms with two geometric isomers namely *trans*-(*E*) and *cis*-(*Z*) form. The (*E*)-form can undergo isomerisation to the (*Z*)-configuration when exposed to UV-irradiation. Resveratrol analogues including viniferin, pteostilbene, piceatannol and its glucosides have been identified in red wine (*95, 101*). Viniferin (an example of resveratrol oligomer) is present in epsilon-(ε) and delta-(δ) forms with (*E*)- and (*Z*)-molecular configurations. (*E*)-viniferin is a dimeric derivative of (*E*)-resveratrol. This compound is produced by the addition of a *meta*-hydroxyl-group and a neighbouring aryl CH of one resveratrol unit across the double bond of the second resveratrol (*102*). Viniferin is present naturally in *Vitis vinifera* grapes (*103*) and has been synthesised in the laboratory using a horseradish peroxidase reaction (*104*). Some examples of stilbenes and their derivatives which are present in the skins and seeds of the red grapes are shown in **Figure 1.4**.

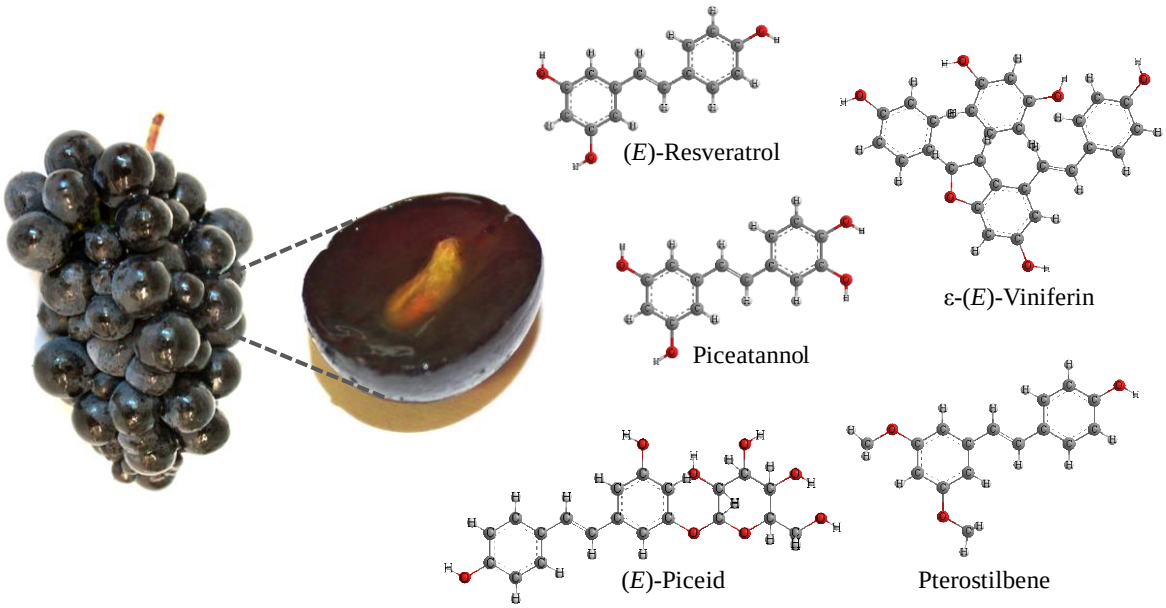

Figure 1.4: Examples of stilbenes in the skins and seeds of the red grape.

Health benefits of (E)-resveratrol in grapes

The notion that (*E*)-resveratrol (*trans*-3,4′,5-trihydroxystilbene) has benefits to improve human health has provoked ample research and efforts to extract it from a variety of plant sources. This section addresses the main therapeutic properties of (*E*)-resveratrol.

a) Antioxidant activity

The antioxidant activity of (*E*)-resveratrol is related to the number and location of hydroxyl (-OH) groups in the molecular structure that are able to scavenge free radicals (*105*). Stivala *et al.* (*106*) proposed that the 4′-OH group was responsible for undergoing free radical oxidation reactions. Caruso *et al.* (*102*) described the correlation of free radical scavenging ability of the hydroxyl-groups within (*E*)-resveratrol through a proton (H^+) transfer mechanism. The reaction took place predominantly at the 4′-OH group at the *para*-position in the B-ring rather than the 3,5-OH groups at the *meta*-positions in the A-ring. These findings were also supported by Cao *et al.* (*107*), who found that the 4′-OH group is the preferred reaction site for contributing to the free radical scavenging activity, based on a computational theoretical study of the resveratrol molecule.

The function of resveratrol as an antioxidant significantly prevents or delays oxidation stress-induced damage. This compound has been shown to inhibit oxidative-induced apoptosis in a variety of human cell lines, including retinal pigment epithelium cells (*108*) which minimises the prevalence of blindness in the elderly.

b) Cardiovascular protection

The cardiovascular function of (*E*)-resveratrol has been acknowledged since the findings of the phenomenon called the “French Paradox”, that linked moderate consumption of red wine to a lower incidence of cardiovascular disease amongst the French population (*109*). Resveratrol plays a significant role in cardiovascular protective effects, which is attributed to its ability to reduce platelet aggregation both *in vitro* and *in vivo* (*110*). The cardioprotective property of resveratrol involves the prevention of low-density lipoprotein (LDL) oxidation. This oxidation can cause fatty streaks to be deposited in coronary arteries, which could ultimately lead to the development of atherosclerosis (*111*).

c) Anti-inflammatory and anti-tumour effect

Inflammatory processes are mediated by the production of prostaglandin (PG). Resveratrol has been associated with the inhibition of prostaglandins in human peripheral blood leukocytes (*112*). This compound has been observed to inhibit the enzymatic activity of cyclooxygenase-2 (COX-2; the enzyme that catalyses PG synthesis) by inhibiting the expression of this enzyme *via* signal transduction pathways (*113*).

Resveratrol appears to show an anti-tumour effect by inducing apoptosis through modulation of various signalling pathways. Banerjee *et al. (114)* found that resveratrol reduced the incidence of carcinogen-induced mammary tumour through down-regulation of COX-2 and matrix metalloprotease-9 (MMP-9) expressions.

d) Estrogenic activity

Since (*E*)-resveratrol has structural similarity with estrogenic agents, several studies were performed to investigate the estrogenic potential of this compound. The results showed that (*E*)-resveratrol is a very potent antagonist to the binding of the sexual hormone estradiol to its receptors. These findings provide some beneficial effects in areas such as breast cancer (*115*). Basly and co-workers (*116*) investigated the biological activity of the two isomers of resveratrol on breast cancer cells. The study found that the (*E*)-resveratrol is a much stronger mixed estrogen receptor agonist than (*Z*)-resveratrol.

ii) Hydroxybenzoic acid and derivatives

Gallic acid is present in the flesh of white and red grapes. The latter was reported to contain higher amounts of gallic acid (*117*). The basic structures of hydroxybenzoic acids and derivatives are shown in **Figure 1.5**.

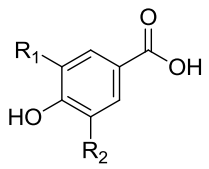

Hydroxybenzoic acids and derivatives	R_1	R_2
Gallic acid	OH	OH
Protocatechuic acid	OH	H
Syringic acid	OCH_3	OCH_3
Vanillic acid	OCH_3	H

Figure 1.5: Basic structures of hydroxybenzoic acids and derivatives.

iii) Hydroxycinnamic acid and derivatives

Hydroxycinnamic acids are the most notable subclass of non-flavonoids. *p*-Coumaric, ferulic and caffeic acids and their derivatives are some examples of hydroxycinnamic acids which are present in grapes **(Figure 1.6)**. Hydroxycinnamic acids are also found esterified to sugars, organic acids and choline, and combine with anthocyanin monoglucosides to form acylated anthocyanins. In grapes and wines, cinnamic acids are mainly esterified in particular with tartaric acid. They are highly oxidisable in grape juice and responsible of browning of unprotected white must.

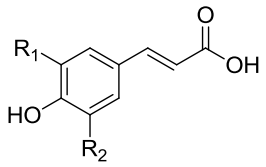

Hydroxycinnamic acids	R_1	R_2
p-Coumaric acid	H	H
Ferulic acid	OCH_3	H
Sinapinic acid	OCH_3	OCH_3
Caffeic acid	H	OH

Figure 1.6: Basic structures of hydroxycinnamic acids.

1.5.1.1.2 Flavonoids

The structure of flavonoids is comprised of fifteen carbon atoms (C_6-C_3-C_6) consisting of two aromatic A- and B-rings. These two aromatic rings are joined together by three carbons that are usually formed into an oxygenated heterocyclic entity. The main subclasses of flavonoids found in grapes are the flavonols, flavones, anthocyanins, flavanonols, flavanones and flavanols **(Figure 1.7)**. The various classes of flavonoids differ in the level of oxidation and pattern of substitution of the C-rings. The preferred glycosylation site is the C_3 position with the most common sugars attached to flavonoids being glucose, glucuronide, galactose, rhamnose and xylose. Many flavonoids have antioxidant activity as their conjugated π-electron systems, allow the donation of electrons or hydrogen atoms from the hydroxyl-group moieties to a free radical (*118*). However, the antioxidant efficacy depends on the structural features of flavonoids, including the number and position of the hydroxyl-group moieties on the phenolic rings, and delocalization of the unpaired electron within the molecular system.

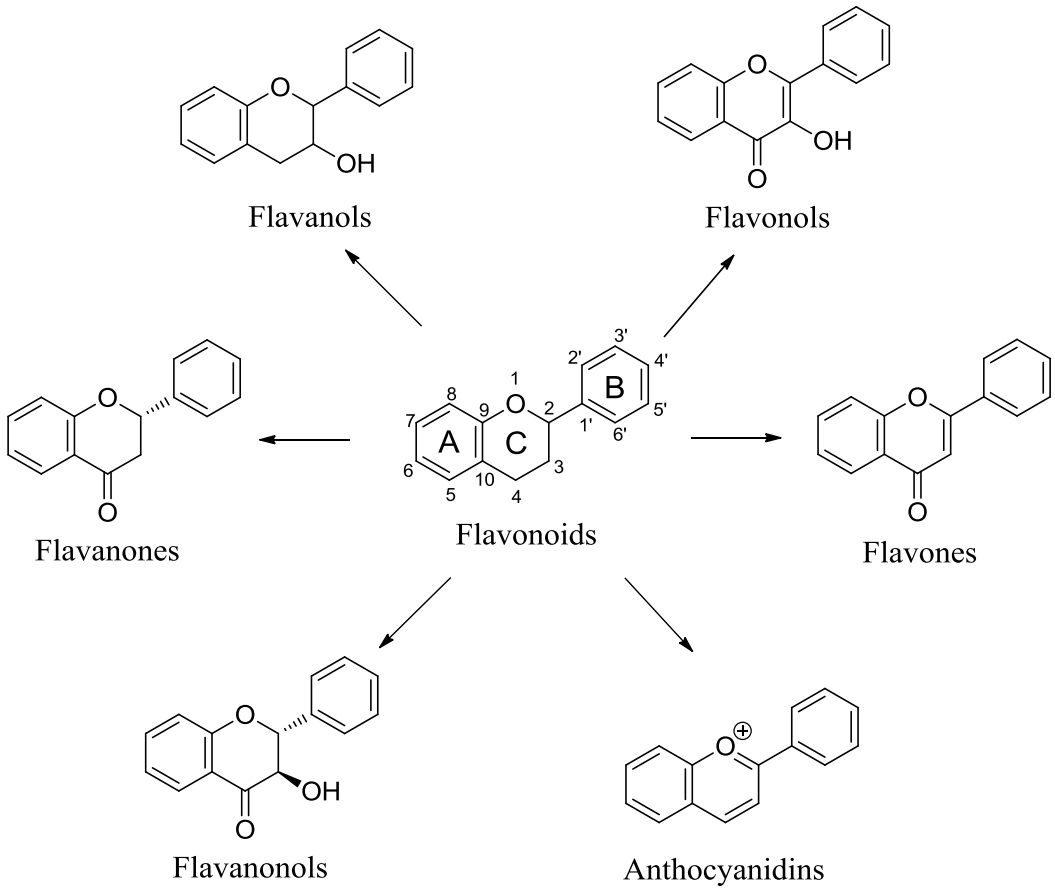

Figure 1.7: Basic structures of major flavonoids.

i) Flavanols

Flavanols are ubiquitous in various types of fruits and beverages, for instance grapes, red wine and tea (*119-121*). Their purpose is to act as an insect feeding deterrent and bactericide (*122*). Flavanol compounds have two chiral centres at the C_2 and C_3 positions of the C-ring. A predominant flavanol is (±)-catechin and its stereoisomer (±)-epicatechin. Based on the biosynthetic pathway of the flavonoids, (+)-catechin and (-)-epicatechin are predominantly synthesised in plant whilst (-)-catechin and (+)-epicatechin are very seldom present in nature (*123*). (+)-Catechin has a C_3 hydroxyl-group positioned in a plane opposite the B-ring, whereas (-)-epicatechin has both C_3 hydroxyl-groups positioned in the plane of the B-ring **(Figure 1.8)**. The concentrations of catechin/epicatechin in white wine were reported in a range of 5-10 mg/L whilst 76-115 mg/L were determined in red wine (*124*).

(+)-Catechin (-)-Epicatechin

Figure 1.8: The molecular structures of flavanols.

ii) Tannins

In general, tannins refer to a fraction of phenolic compounds whose fundamental characteristic is the capacity to precipitate proteins, in particular salivary proteins, which gives them an astringent character that can be easily recognized (*125*). Structurally, tannins possess 12-16 phenolic groups and 5-7 aromatic rings per 1000 units of relative molecular mass (*126*). This feature, together with their high molecular weight, clearly makes the tannins different in structure and properties from the low weight molecular phenolic acids and monomeric flavanols. Tannins are categorised into two groups, namely hydrolysable tannins and condensed tannins.

a) Hydrolysable tannins

Hydrolysable tannins have a simpler structure in comparison to condensed tannins. They exist as esters and can be degraded or hydrolysed. They contain a central core of polyhydric alcohol, which are esterified either partially or completely by phenolic acids. The phenolic acids are either gallic acid in gallotannins or other phenolic acid derived from the oxidation of galloyl residues in ellagitanins. After hydrolysis by acids, bases or certain enzymes, gallotannins yield glucose and gallic acid.

b) Condensed tannins

Proanthocyanidins, also known as condensed tannins, are very important compounds in winemaking. These compounds are more complex than hydrolysable tannins. They are polymers composed of subunits analogues of the flavanols based on catechin and epicatechin that are linked *via* interflavan bonds between C_4 and C_8 and less commonly between C_4 and C_6 linkages (both are called B-type procyanidin) as shown in **Figure 1.9**. The procyanidin can also be linked by an additional ether-bond between C_2-O-C_7 or C_2-O-C_5 linkage, called A-type

procyanidin. According to Santos-Buelga (*125*), procyanidin values from different varieties and vintages of red wines in a range of 0 to 500 mg/L.

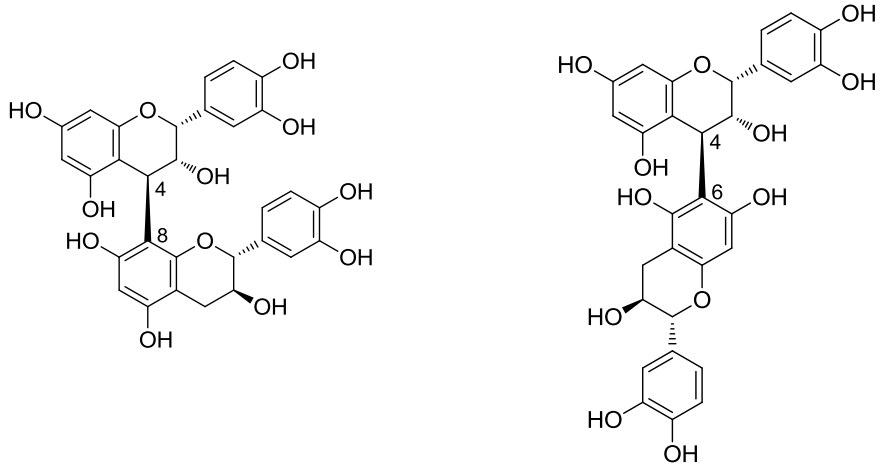

A **B**

Figure 1.9: Procyanidin B-type in **(A)** C_4-C_8 and **(B)** C_4-C_6 linkages.

Tannins are located in the seeds and skins of the grapes (*127*). These compounds play a prominent role in the composition and quality of wine contributing to astringency, colour and aging potential of red wine (*128*). Seed tannins are comprised of galloylated subunits. The polymers of seed tannins are present in an average length from 5 to 20 subunits. These types of tannins give a wine structure and body. When over-extracted to give higher concentrations, they however can impart excessive astringency to wine. Skin tannins contain epigallocatechin subunits (*129, 130*) with an average polymer length of 20 to more than 40 subunits (*131*). Skin tannins provide wine structure and stabilise its colour. They react with proteins in grapes (maturing), wine (aging) and in a human mouth eliciting a feeling of astringency (*122*).

c) Flavonols

Flavonols are found in wines and grape juices. They are localized in the grape skins. The flavonols have an important role in UV protection as their synthesis is up-regulated with high UV loads (*132*). Some common flavonol aglycones present in grapes are quercetin, myricetin, kaempferol, syringetin and laricitrin. They usually exist as flavonol glucoside forms which are typically bound to various sugars, including glucosides, glucuronides and galactosides (*133*). Conjugation mostly occurs at the C_3 position **(Figure 1.10)** but substitution can also take place at the 5, 7, 3′, 4′ and 5′ positions.

During white wine production, only small amounts of flavonol glucosides are extracted during the pressing of white grapes. In contrast, larger amounts of these compounds are obtained during the maceration and fermentation of red grapes (*134*). In wine, the majority of flavonols exist in the aglycone forms as their glycosidic bonds are hydrolysed by enzymes or acidic conditions during fermentation. The overall concentration of flavonols was reported in the range of 100 mg/L in red wine (*135*). Previous studies have shown that the flavonol profiles served as a biomarker to differentiate table grape cultivars (*136*). In a similar context, Andrade and co-workers (*137*) observed that the profile characterisation of flavonols helped to identify different types of red wines. With regards to the bioactivity of flavonols, the recent research has shown that quercetin possesses positive effects in the treatment of pancreatic cancer (*138*).

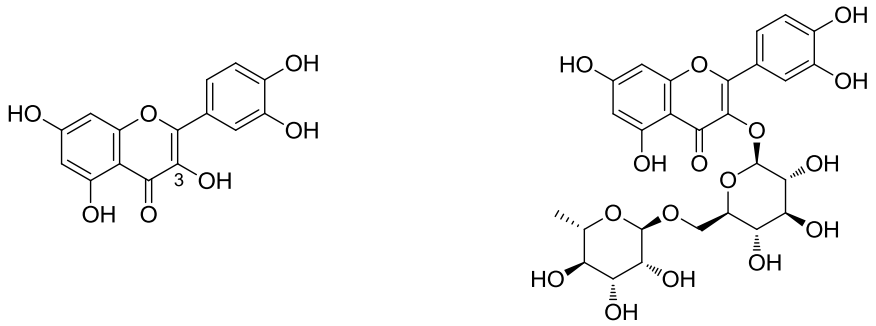

(A) Quercetin **(B)** Quercetin-3-*O*-rutinoside

Figure 1.10: Examples of important flavonol in **(A)** aglycone and **(B)** glycoside forms.

d) Flavanones and flavones

Naringenin is one of the examples of flavanones, which are predominantly found in citrus fruits such as oranges (*139*). This compound has been reported to be present in wine and associated with potential antioxidant capability (*140*). Flavonones possess similar structure as flavone flavonoids, except the flavonone structures lack a double bond at the position of C_2-C_3 in the C-ring. Flavone distribution appears to be limited to certain plant families, with the main flavones in the diet being apigenin and luteolin. Apigenin has been found in Italian red wine at a concentration of 0.2-3.1 mg/L (*141*). This compound is thought to prevent cancer as demonstrated by Shukla and co-workers (*142*). The molecular structures of naringenin and apigenin are shown in **Figure 1.11**.

A **B**

Figure 1.11: Molecular structures of **(A)** naringenin (flavanone), and **(B)** apigenin (flavone).

e) Flavanonols

Flavanonols have a saturated C-ring like flavanones, but these compounds are usually either hydroxylated or glycosylated at the C_3 position. Compounds from this subgroup are also known as 3-hydroxyflavanones or 2,3-dihydroflavonols. Taxifolin (dihydroquercetin) and astilbin (dihydroquercetin-3-*O*-rhamnoside) are the examples of flavanonols **(Figure 1.12)**. Astilbin is a bioactive and is thought to provide anti-microbial, antibacterial and cardiopreventive effects in humans (*143*). Astilbin was determined in Malbec (a grape variety planted predominantly in Argentina) wines with a concentration between 9.1 mg/L and 16.3 mg/L (*144*), which was consistent with the value obtained from previous findings of Vitrac and co-workers (*145*).

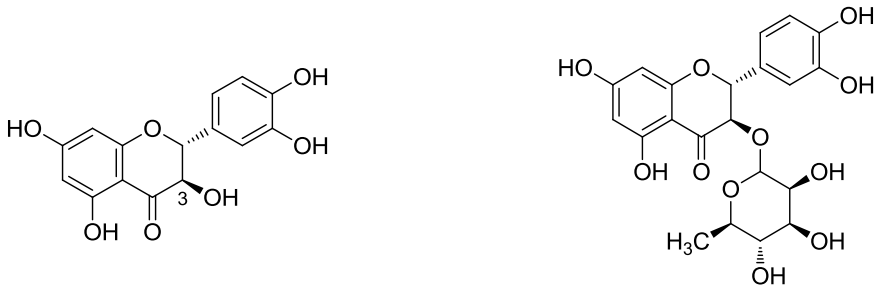

A **B**

Figure 1.12: Examples of flavanonols in wines **(A)** taxifolin and **(B)** (-)-astilbin.

f) Anthocyanins

Anthocyanidins, principally as their conjugated derivatives, known as anthocyanins, are plant pigments, responsible for the red, blue or violet colour of edible fruits like red grapes, plums and berries. The level of colour usually increases during fruit maturation. Anthocyanins mainly occur in the skins of the red grapes. They are not found in white grapes due to a

mutation of the gene that encodes colour formation later in the evolution of *Vitis*. Rosé wine made from red grapes contains less anthocyanin due to the removal of the skins before fermenting the wine. The concentration of anthocyanins ranges around 1 mg/g fresh weight in berries and between 100 mg/L (Pinot noir) to 500 mg/L (Shiraz) in red wine (*133*). During storage and ageing of red wine, anthocyanins can react with procyanidins to produce complex pigments (*146*). Free anthocyanins disappear with bottle ageing. This is evident by the colour change in a wine from the original sharp bright blue-red tone to red-orange, giving the wine a deeper hue (*147*).

Anthocyanins occur naturally as glycosides and the positive charge on the anthocyanin molecule makes this compound different from other flavonoids **(Figure 1.13)**. Several studies have investigated the relationship between the type of glycosylation of anthocyanins and characteristics of the grape variety. Although the glycosylation pattern in grapes are complex, it has been shown that glycosylation for *Vitis vinifera* cultivars appears exclusively at the C_3 position (*148*). In a similar area of study, Cheynier *et al.* (*149*) investigated that the Pinot noir grapes contain only anthocyanin-3-glucosides. However, this is not the case for non-*Vitis* or hybrid grapes where glycosylations commonly take place at the C_3 and C_5 positions (*150*). Therefore, Castia *et al.* (*151*) concluded that the anthocyanin profile was useful for chemotaxonomic studies to differentiate the red grape cultivars.

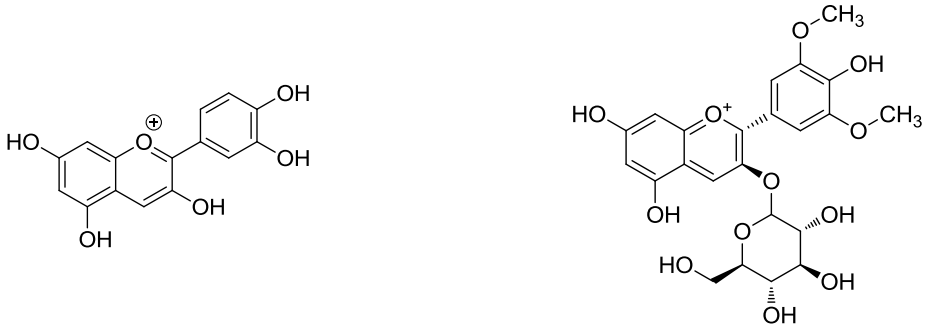

(A) Cyanidin **(B)** Malvidin-3-*O*-glucoside

Figure 1.13: **(A)** Free anthocyanidin and **(B)** anthocyanidin glucoside.

1.5.1.2 The need to develop a new method for polyphenol analysis

Resveratrol can be synthesised in the laboratory *via* the Heck reaction (*152*). The use of synthetic food additives in the food industry is often severely restricted. So, there is more interest in using natural resveratrol extracted from plant material like *Polygonum* weed or from grapes and grape byproducts.

Many chromatographic methods have been developed to identify individual compounds from plant extracts however the need for fast and high volume extraction of health-beneficial natural compounds from agricultural byproducts requires new methods. This study develops advanced "green" analytical techniques for the rapid and high-resolution analysis and capture of known health-beneficial substances in complex matrices of wine and grape byproducts using MISPE followed by capillary HPLC in combination with tandem electrospray ionisation MS. In contrast to previous MISPE separations of polyphenols from natural substances, this method allows the separation and capture of a target compound and the determination of its purity as well as the analysis of non-targeted substances. Moreover, this new approach allows the concomitant analysis of many health-beneficial substances. In another application area, the new methodology devised by this study can be used for monitoring of the performance of MIP based SPE tools for bioactive molecules from a diverse array of complex samples. The identification of polyphenol compounds before and after MISPE treatment afforded by microLC generates information on the selectivity of the MIP. The newly developed method will be designed according to the principles of Green Chemistry, aiming at an improved resource utilisation using environmentally benign methodologies.

1.5.2 Phytosterols

Plants are renewable sources of biologically active compounds. Vegetables and fruits contain substantial amounts of terpenoids particularly phytosterols (plant sterols). Phytosterols play significant roles in several areas including pharmaceuticals (production of therapeutic steroids), nutrition (anticancer properties) and cosmetics (ingredients for creams and lipsticks).

1.5.2.1 Classification of phytosterols

Sterols are biosynthetically derived from squalene and belong to the group of triterpenes that includes more than 4000 different compounds (*153*). In general, these compounds consist of an A-, B-, C- and D-ring structure systems (tetracyclic cyclopenta(α)phenanthrene), a hydrocarbon chain at C_{17} and an oxygen functional (usually a hydroxyl) group in the β-position at C_3. Phytosterols (plant sterols) have a structural resemblance to cholesterol (animal sterol) and ergosterol (fungi sterol).

Phytosterols have a double bond between C_5-C_6, but they are different from each other in the location of a double bond at C_{22}-C_{23} and the stereochemical orientation of the alkyl-group at C_{24}. They can represent themselves as free alcohols, esters with fatty acids, glycosides and acylated glycosides (*154*), but in edible oils they mainly exist as free and esterified forms. Saturated plant sterols are referred to as 'phytostanols', do not have a double bond at the position of C_5-C_6 in the B-ring. The examples of phytosterols in free, conjugated and saturated forms are illustrated in **Figure 1.14**. In plants, more than 200 types of phytosterols have been discovered, whereby the most abundant sterols are β-sitosterol, stigmasterol and campesterol (*153, 155*). Other relevant phytosterols found in plants in minor amounts are brassicasterol, sitostanol and campestanol (*154*).

1.5.2.2 Phytosterols in grape seeds

There is now a worldwide interest in the recovery and exploitation of bioactives from natural plant resources. Plant seeds contain many nutraceutical components, and one of underexploited seed is the grape seed. The majority of grape seeds are part of the waste generated during wine processing activities. The seeds from grape marc are usually utilised to gain grape seed oils or nutritional supplements containing polyphenols. However, less attention has been paid to the composition of phytosterols in those seed-based-products. Reports on the analysis of phytosterols in the grape seeds either in the extract or oil form is scarce, although these phytosterols are claimed to have important benefits such as reducing human cholesterol levels (*156*). The sterol content in grape seed oil was reported by Crews and co-workers (*157*) to consist of β-sitosterol, stigmasterol and campesterol. In that research, no brassicasterol was found. Brassicasterol has the most abundant occurrence in rapeseed oil. The phytosterol profile can also be used to detect product authenticity since they can be considered as a 'fingerprint' for the lipid composition of a product (*158*).

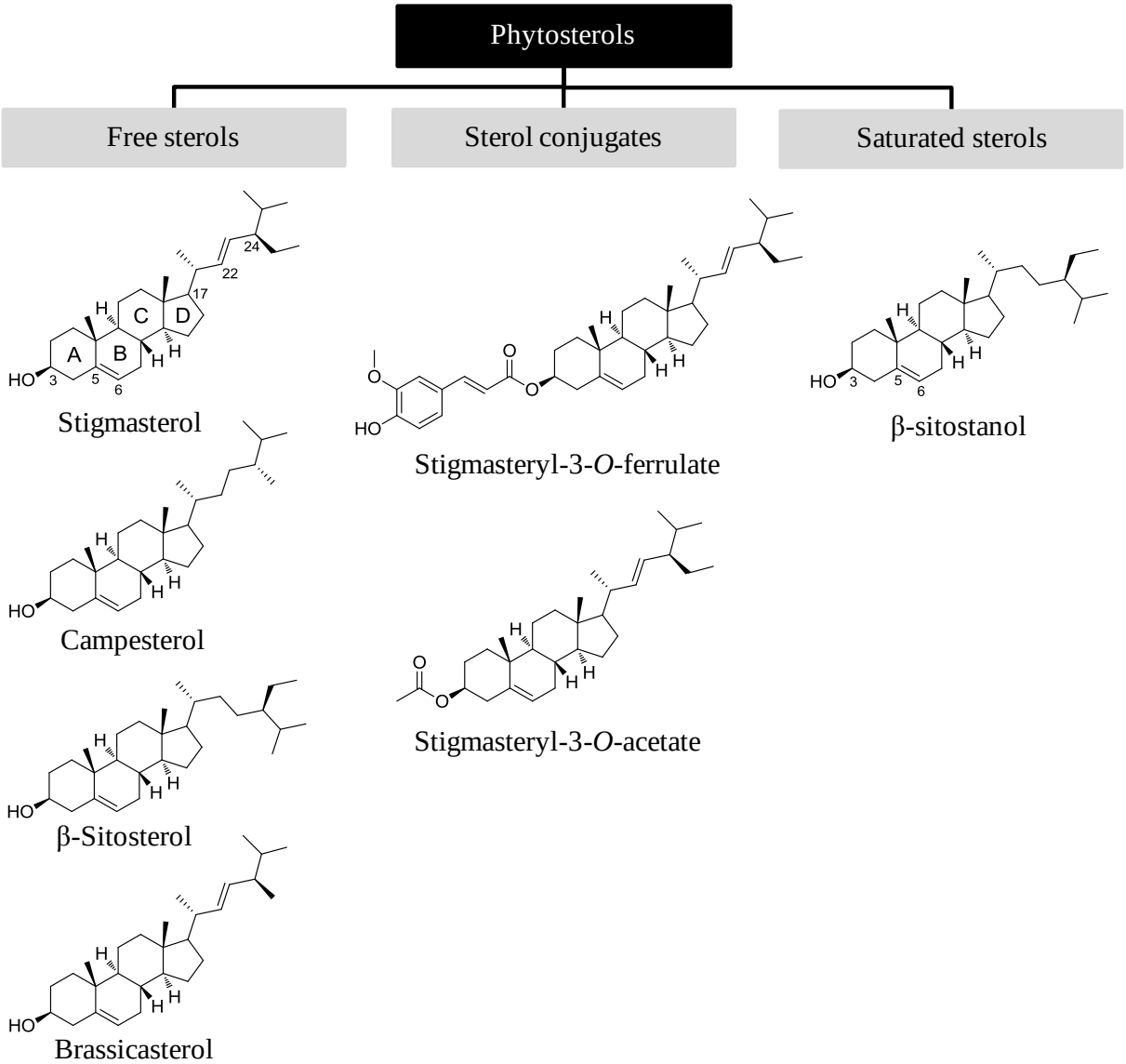

Figure 1.14: Major classification of phytosterols.

1.5.2.3 Bioactivity of phytosterols

The growing interest in the medical applications of phytosterols ensures that it is very important to obtain accurate quantitative data on their occurrence in foods. Phytosterols are known to possess various bioactive properties that play an important role for human health (*159*) such as anti-inflammatory, antibacterial, antifungal, antioxidant and anti-tumour activities (*160*, *161*). Recent investigation demonstrated that the involvement of sterols in plants innate immunity against bacterial infections by regulating nutrient efflux into the apoplast (*162*).

Phytosterols have been acknowledged for many years for reducing blood cholesterol levels as well as other beneficial health effects (*163*). The cholesterol lowering effects of phytosterols was reported from the studies on rabbits and chickens in the 1950s (*164*, *165*). Some years later, the first medical research of the beneficial effects of phytosterols was published (*166*). The estimated dietary intakes of phytosterols amongst different human populations were reported from 160 mg/day to 400 mg/day (*155*). Ingestion of these compounds in the human diet resulted in the reduction of plasma total cholesterol between 0.5% to 2.6% (*167*). Phytosterols also have been shown as an interesting approach in preventing coronary heart disease when combining them with statins (a drug that decreases the cholesterol metabolism) (*168*).

1.5.2.3.1 Stigmasterol

Amongst the phytosterols present in grape seed, stigmasterol is the main focus for this research. Several studies have shown that stigmasterol is useful in the prevention of certain chronic diseases including ovarian, prostate, breast and colon cancers (*169*). This compound is used as a precursor in the manufacture of synthetic progesterone (*170*). Stigmasterol is also the precursor of vitamin D_3 (*171*).

1.5.2.4 The need to develop a new method for sterol analysis

The use of MIP materials in the analysis of sterols has several challenges still unsolved especially in isolating the sterol target analytes from complex mixtures. The studies that have been done were often complicated and time-consuming procedures that used copious amount of environmentally problematic chemicals (*33*). In addition, the published MISPE method (*51*) was not able to collect other compounds or assess the efficiency of the binding of the target of interest in one step. Thus, the present study provides a novel design of stigmasterol imprinted polymers in the SPE format in conjunction with the latest modern LC techniques for the quantification and characterisation of the target compound and its analogues from grape seed extracts.

1.6 Aims of the project

A significant upsurge of interest in phytochemicals from vegetables, fruits and their byproducts as safe dietary components that have a considerable impact on human health led to this research with the aim to find an efficient way to extract and analyse two of the most important of these bioactive components. The herein described research provides new approaches to polyphenol and phytosterol analysis derived from grape complex samples.

Specifically, the objectives of the research are:

- Systematic development and optimisation of new chromatographic methods for polyphenol analysis using RP-HPLC as the main tool for (*E*)-resveratrol quantification in combination with ESI ion trap tandem mass spectrometry for polyphenolic characterisation according to the principles of Green Chemistry.
- Development of an effective protocol to monitor the performance of a MIP in an off-line SPE format to selectively enrich (*E*)-resveratrol and structurally related compounds from red wine samples.
- Evaluation of the efficacies of the MIP's imprinting effect to discriminate (*E*)-resveratrol in relation to (*Z*)-resveratrol at different stages of grape processing.
- Optimisation of binding sites characteristics of a novel MIP prepared by the covalent technique to capture stigmasterol from a mixture of sterol solutions.
- Development of efficient liquid chromatographic methods based on ethanol-water mixtures to simultaneously separate different types of sterols by RP-HPLC and LC-ESI ion trap MS/MS.
- Application of MISPE for the extraction and separation of (*E*)-resveratrol and other polyphenols from the extracts of grape skins and seeds.
- Novel application of stigmasterol MIP in the SPE format for the analysis of stigmasterol from grape seed residues.

1.7 Thesis overview

This thesis has been divided into seven chapters. **Chapter 1** begins by describing the mechanism of extraction and separation techniques involved with the analysis of phytochemicals derived from grape matrices. This chapter also addresses the classification, occurrence, functionality and bioactivity of polyphenols and phytosterols. **Chapter 2** provides key findings related to the systematic development of new chromatographic conditions with a Green Chemistry approach for the analysis of polyphenols using analytical RP-HPLC and LC-MS/MS. This chapter presents a generic procedure to use MISPE for polyphenol analysis using different types of grape samples. **Chapter 3** describes the application of MIP in the SPE format for the extraction, quantification and characterisation of (*E*)-resveratrol and structurally related polyphenols from red wine. **Chapter 4** adds the analysis of (*E*)-resveratrol and its analogues from grape pressing residues at different stages of grape waste storage. **Chapter 5** evaluates the optimisation of binding sites characteristics of a novel MIP prepared by the covalent approach to selectively enrich stigmasterol. **Chapter 6** presents a comprehensive evaluation of MISPE protocols for determining polyphenols and phytosterols from grape derived complex wastes. **Chapter 7** draws the conclusions and points to future research directions.

1.8 References

1. Cetin, A.; Sagdic, O., A concise review: antioxidant effects and bioactive constituents of grape. *Erciyes Tip Derg.* **2009**, *31*, 369-375.
2. Forester, S. C.; Waterhouse, A. L., Metabolites are key to understanding health effects of wine polyphenolics. *J. Nutr.* **2009**, *139*, 1824S-1831S.
3. Frankel, E. N., Food antioxidants and phytochemicals. Present and future perspectives. *Fett/Lipid.* **1999**, *101*, 450-455.
4. Nakatani, N.; Kayano, S. I.; Kikuzaki, H.; Sumino, K.; Katagiri, K.; Mitani, T., Identification, quantitative determination and antioxidative activities of chlorogenic acid isomers in prune (*Prunus domestica L.*). *J. Agric. Food Chem.* **2000**, *48*, 5512-5516.
5. Fernandez de Simon, B.; Perez Ilzarbe, J.; Hernandez, T.; Gomez Cordoves, C.; Estrella, I., HPLC study of the efficiency of extraction of phenolic compounds. *Chromatographia.* **1990**, *30*, 35-37.
6. Minuti, L.; Pellegrino, R. M.; Tesei, I., Simple extraction method and gas chromatography mass spectrometry in the selective ion monitoring mode for the determination of phenols in wine. *J. Chromatogr., A* **2006**, *1114*, 263-268.
7. Anastasiadi, M.; Pratsinis, H.; Kletsas, D.; Skaltsounis, A. L.; Haroutounian, S. A., Bioactive non-coloured polyphenols content of grapes, wines and vinification by-products: Evaluation of the antioxidant activities of their extracts. *Food Res. Int.* **2010**, *43*, 805-813.

8. Orozco-Solano, M.; Ruiz-Jimenez, J.; Luque, d. C. M. D., Ultrasound-assisted extraction and derivatization of sterols and fatty alcohols from olive leaves and drupes prior to determination by gas chromatography tandem mass spectrometry. *J. Chromatogr., A* **2010**, *1217*, 1227-1235.
9. Wang, L.; Qin, P.; Hu, Y., Study on the microwave-assisted extraction of polyphenols from tea. *Front. Chem. Eng. China* **2010**, *4*, 307-313.
10. Azadmard-Damirchi, S.; Habibi-Nodeh, F.; Hesari, J.; Nemati, M.; Achachlouei, B. F., Effect of pretreatment with microwaves on oxidative stability and nutraceuticals content of oil from rapeseed. *Food Chem.* **2010**, *121*, 1211-1215.
11. Nyam, K. L.; Tan, C. P.; Lai, O. M.; Long, K.; Man, Y. B. C., Optimization of supercritical fluid extraction of phytosterol from roselle seeds with a central composite design model. *Food Bioprod. Process.* **2010**, *88*, 239-246.
12. Pinelo, M.; Ruiz-Rodriguez, A.; Sineiro, J.; Senorans, F. J.; Reglero, G.; Nunez, M. J., Supercritical fluid and solid-liquid extraction of phenolic antioxidants from grape pomace: a comparative study. *Eur. Food Res. Technol.* **2007**, *226*, 199-205.
13. Paniwnyk, L.; Beaufoy, E.; Lorimer, J. P.; Mason, T. J., The extraction of rutin from flower buds of *Sophora japonica*. *Ultrason. Sonochem.* **2001**, *8*, 299-301.
14. Liu, F. F.; Ang, C. Y. W.; Heinze, T. M.; Rankin, J. D.; Beger, R. D.; Freeman, J. P.; Lay, J. O., Evaluation of major active components in St. John's Wort dietary supplements by high performance liquid chromatography with photodiode array detection and electrospray mass spectrometric confirmation. *J. Chromatogr., A* **2000**, *888*, 85-92.
15. Li, D. C.; Jiang, J. G., Optimization of the microwave assisted extraction conditions of tea polyphenols from green tea. *Int. J. Food Sci. Nutr.* **2010**, *61*, 837-845.
16. Font, N.; Hernandez, F.; Hogendoorn, E. A.; Baumann, R. A.; van Zoonen, P., Microwave assisted solvent extraction and reversed-phase liquid chromatography UV detection for screening soils for sulfonylurea herbicides. *J. Chromatogr., A* **1998**, *798*, 179-186.
17. Hamburger, M.; Baumann, D.; Adler, S., Supercritical carbon dioxide extraction of selected medicinal plants effects of high pressure and added ethanol on yield of extracted substances. *Phytochem. Anal.* **2004**, *15*, 46-54.
18. Lang, Q.; Wai, C. M., Supercritical fluid extraction in herbal and natural product studies - a practical review. *Talanta* **2001**, *53*, 771-782.
19. Dvorakova, M.; Hulin, P.; Karabin, M.; Dostalek, P., Determination of polyphenols in beer by an effective method based on solid-phase extraction and high performance liquid chromatography with diode array detection. *Czech J. Food Sci.* **2007**, *25*, 182-188.
20. Pinelo, M.; Laurie, V. F.; Waterhouse, A. L., A simple method to separate red wine non-polymeric and polymeric phenols by solid-phase extraction. *J. Agric. Food Chem.* **2006**, *54*, 2839-2844.
21. Toivo, J.; Piironen, V.; Kalo, P.; Varo, P., Gas chromatographic determination of major sterols in edible oils and fats using solid-phase extraction in sample preparation. *Chromatographia* **1998**, *48*, 745-750.
22. Palma, M.; Pineiro, Z.; Barroso, C. G., In line pressurized fluid extraction solid-phase extraction for determining phenolic compounds in grapes. *J. Chromatogr., A* **2002**, *968*, 1-6.
23. Sun, B.; Leandro, M. C.; de Freitas, V.; Spranger, M. I., Fractionation of red wine polyphenols by solid-phase extraction and liquid chromatography. *J. Chromatogr., A* **2006**, *1128*, 27-38.
24. Perez-Moral, N.; Mayes, A. G., Comparative study of imprinted polymer particles prepared by different polymerisation methods. *Anal. Chim. Acta* **2004**, *504*, 15-21.
25. Beltran, A.; Marce, R. M.; Cormack, P. A. G.; Borrull, F., Synthesis by precipitation polymerisation of molecularly imprinted polymer microspheres for the selective extraction of carbamazepine and oxcarbazepine from human urine. *J Chromatogr A* **2009**, *1216*, 2248-2253.

26. Beltran, A.; Borrull, F.; Cormack, P. A. G.; Marce, R. M., Molecularly-imprinted polymers: useful sorbents for selective extractions. *Trends Anal. Chem.* **2010**, *29*, 1363-1375.

27. Kirsch, N.; Hedin Dahlstroem, J.; Henschel, H.; Whitcombe, M. J.; Wikman, S.; Nicholls, I. A., Molecularly imprinted polymer catalysis of a Diels-Alder reaction. *J. Mol. Catal. B: Enzym.* **2009**, *58*, 110-117.

28. Hearn, M. T. W.; Chowdhury, J. M.; Boysen, R. I.; Banti, Y. B. Molecularly imprinted polymers with hydrolytic activity, methods for their production and uses thereof. WO2011014923A1, **2011**.

29. Roche, P. J. R.; Ng, S. M.; Narayanaswamy, R.; Goddard, N.; Page, K. M., Multiple surface plasmon resonance quantification of dextromethorphan using a molecularly imprinted β-cyclodextrin polymer: a potential probe for drug-drug interactions. *Sens. Actuators, B* **2009**, *139*, 22-29.

30. Fang, C.; Yi, C.; Wang, Y.; Cao, Y.; Liu, X., Electrochemical sensor based on molecular imprinting by photo-sensitive polymers. *Biosens. Bioelectron.* **2009**, *24*, 3164-3169.

31. Kitahara, K. I.; Yoshihama, I.; Hanada, T.; Kokuba, H.; Arai, S., Synthesis of monodispersed molecularly imprinted polymer particles for high performance liquid chromatographic separation of cholesterol using templating polymerization in porous silica gel bound with cholesterol molecules on its surface. *J. Chromatogr., A* **2011**, *1217*, 7249-7254.

32. Puoci, F.; Curcio, M.; Cirillo, G.; Iemma, F.; Spizzirri, U. G.; Picci, N., Molecularly imprinted solid-phase extraction for cholesterol determination in cheese products. *Food Chem.* **2007**, *106*, 836-842.

33. Shi, Y.; Zhang, J. H.; Shi, D.; Jiang, M.; Zhu, Y. X.; Mei, S. R.; Zhou, Y. K.; Dai, K.; Lu, B., Selective solid-phase extraction of cholesterol using molecularly imprinted polymers and its application in different biological samples. *J. Pharm. Biomed. Anal.* **2006**, *42*, 549-555.

34. Zhu, Q.; Wang, L.; Wu, S.; Joseph, W.; Gu, X.; Tang, J., Selectivity of molecularly imprinted solid-phase extraction for sterol compounds. *Food Chem.* **2009**, *113*, 608-615.

35. Karasova, G.; Lehotay, J.; Sadecka, J.; Skacani, I.; Lachova, M., Selective extraction of derivatives of *p*-hydroxybenzoic acid from plant material by using a molecularly imprinted polymer. *J. Sep. Sci.* **2005**, *28*, 2468-2476.

36. Zhu, L.; Chen, L.; Xu, X., Application of a molecularly imprinted polymer for the effective recognition of different anti-epidermal growth factor receptor inhibitors. *Anal. Chem.* **2003**, *75*, 6381-6387.

37. Caro, E.; Marce, R. M.; Cormack, P. A. G.; Sherrington, D. C.; Borrull, F., Selective enrichment of anti-inflammatory drugs from river water samples by solid-phase extraction with a molecularly imprinted polymer. *J. Sep. Sci.* **2005**, *28*, 2080-2085.

38. Arshady, R.; Mosbach, K., Synthesis of substrate selective polymers by host guest polymerization. *Macromol. Chem. Phys.* **1981**, *182*, 687-692.

39. Andersson, L. I., Molecular imprinting: developments and applications in the analytical chemistry field. *J. Chromatogr., B: Biomed. Sci. Appl.* **2000**, *745*, 3-13.

40. Wulff, G.; Heide, B.; Helfmeier, G., Enzyme analog built polymers. Molecular recognition through the exact placement of functional groups on rigid matrixes *via* a template approach. *J. Am. Chem. Soc.* **1986**, *108*, 1089-1091.

41. Wulff, G.; Vesper, W., Preparation of chromatographic sorbents with chiral cavities for racemic resolution. *J. Chromatogr.* **1978**, *167*, 171-186.

42. Sellergren, B.; Andersson, L., Molecular recognition in macroporous polymers prepared by a substrate analog imprinting strategy. *J. Org. Chem.* **1990**, *55*, 3381-3383.

43. Wang, X.; Wang, L.; He, X.; Zhang, Y.; Chen, L., A molecularly imprinted polymer-coated nanocomposite of magnetic nanoparticles for estrone recognition. *Talanta* **2009**, *78*, 327-332.

44. Qi, P.; Wang, J.; Wang, L.; Li, Y.; Jin, J.; Su, F.; Tian, Y.; Chen, J., Molecularly imprinted polymers synthesized *via* semi-covalent imprinting with sacrificial spacer for imprinting phenols. *Polymer.* **2010**, *51*, 5417-5423.

45. Whitcombe, M. J.; Rodriguez, M. E.; Villar, P.; Vulfson, E. N., A new method for the introduction of recognition site functionality into polymers prepared by molecular imprinting: synthesis and characterization of polymeric receptors for cholesterol. *J. Am. Chem. Soc.* **1995**, *117*, 7105-7111.

46. Sellergren, B., Direct drug determination by selective sample enrichment on an imprinted polymer. *Anal. Chem.* **1994**, *66*, 1578-1582.

47. Schwarz, L. J.; Danylec, B.; Yang, Y.; Harris, S. J.; Boysen, R. I.; Hearn, M. T. W., Enrichment of (*E*)-resveratrol from peanut byproduct with molecularly imprinted polymers. *J. Agric. Food Chem.* **2011**, *59*, 3539-3543.

48. Cao, H.; Xiao, J. B.; Xu, M., Evaluation of new selective molecularly imprinted polymers for the extraction of resveratrol from *Polygonum cuspidatum. Macromol. Res.* **2006**, *14*, 324-330.

49. Zhang, Z.; Liu, L.; Li, H.; Yao, S., Synthesis, characterization and evaluation of uniformly sized core-shell imprinted microspheres for the separation *trans*-resveratrol from giant knotweed. *Appl. Surf. Sci.* **2009**, *255*, 9327-9332.

50. Zhuang, X.; Dong, X.; Ma, S.; Zhang, T., Selective on-line extraction of *trans*-resveratrol and emodin from *Polygonum cuspidatum* using molecularly imprinted polymer. *J. Chromatogr. Sci.* **2008**, *46*, 739-742.

51. Theodoridis, G.; Manesiotis, P., Selective solid-phase extraction sorbent for caffeine made by molecular imprinting. *J. Chromatogr., A* **2002**, *948*, 163-169.

52. Jin, Y.; Row, K. H., Solid-phase extraction of caffeine and catechin compounds from green tea by caffeine molecular imprinted polymer. *Bull. Korean Chem. Soc.* **2007**, *28*, 276-280.

53. Blahova, E.; Lehotay, J.; Skacani, I., The use of molecularly imprinted polymer for selective extraction of (+)-catechin. *J. Liq. Chromatogr. Relat. Technol.* **2004**, *27*, 2715-2731.

54. Jin, Y.; Xuan, Y. H.; Jin, Y. S.; Row, K. H., Multi SPE of caffeine and catechin compounds from green tea by caffeine and (+)-catechin MIPs. *J. Liq. Chromatogr. Relat. Technol.* **2011**, *34*, 1604-1616.

55. Zhu, H.; Wang, Y.; Yuan, Y.; Zeng, H., Development and characterization of molecularly imprinted polymer microspheres for the selective detection of kaempferol in traditional Chinese medicines. *Anal. Methods* **2011**, *3*, 348-355.

56. Molinelli, A.; Weiss, R.; Mizaikoff, B., Advanced solid-phase extraction using molecularly imprinted polymers for the determination of quercetin in red wine. *J. Agric. Food Chem.* **2002**, *50*, 1804-1808.

57. Zhu, L.; Xu, X., Selective separation of active inhibitors of epidermal growth factor receptor from *Caragana jubata* by molecularly imprinted solid-phase extraction. *J. Chromatogr., A* **2003**, *991*, 151-158.

58. Xie, J.; Zhu, L.; Luo, H.; Zhou, L.; Li, C.; Xu, X., Direct extraction of specific pharmacophoric flavonoids from *Ginkgo* leaves using a molecularly imprinted polymer for quercetin. *J. Chromatogr., A* **2001**, *934*, 1-11.

59. Xie, J.; Chen, L.; Li, C.; Xu, X., Selective extraction of functional components derived from herb in plasma by using a molecularly imprinted polymer based on 2,2-bis(hydroxymethyl)butanol trimethacrylate. *J. Chromatogr., B: Anal. Technol. Biomed. Life Sci.* **2003**, *788*, 233-242.

60. Castro, L. M. d. M.; Cela, P. M. C.; Dopico, G. M. S.; Lopez, V. J. M.; Gonzalez, R. M. V.; Barral, L. L. F., Preparation, evaluation and characterization of quercetin molecularly imprinted polymer for preconcentration and clean-up of catechins. *Anal. Chim. Acta.* **2012**, *721*, 68-78.

61. Pakade, V.; Lindahl, S.; Chimuka, L.; Turner, C., Molecularly imprinted polymers targeting quercetin in high temperature aqueous solutions. *J. Chromatogr., A* **2012**, *1230*, 15-23.

62. Puoci, F.; Curcio, M.; Cirillo, G.; Iemma, F.; Spizzirri, U. G.; Picci, N., Molecularly imprinted solid-phase extraction for cholesterol determination in cheese products. *Food Chem.* **2007**, *106*, 836-842.

63. Sellergren, B.; Wieschemeyer, J.; Boos, K. S.; Seidel, D., Imprinted polymers for selective adsorption of cholesterol from gastrointestinal fluids. *Chem. Mater.* **1998**, *10*, 4037-4046.

64. Zhang, Z.; Tan, W.; Hu, Y.; Li, G., Simultaneous determination of trace sterols in complicated biological samples by gas chromatography mass spectrometry coupled with extraction using β-sitosterol magnetic molecularly imprinted polymer beads. *J. Chromatogr., A* **2011**, *1218*, 4275-4283.

65. Zhu, T.; Yoon, C.; Row, K., Solid-phase extraction of β-sitosterol from *Oldenlandia diffusa* using molecular imprinting polymer. *Chin. J. Chem.* **2011**, *29*, 1246-1250.

66. Martin Esteban, A., Molecularly imprinted polymers: new molecular recognition materials for selective solid-phase extraction of organic compounds. *Fresenius' J. Anal. Chem.* **2001**, *370*, 795-802.

67. Bjarnason, B.; Chimuka, L.; Ramstroem, O., Online solid-phase extraction of triazine herbicides using a molecularly imprinted polymer for selective sample enrichment. *Anal. Chem.* **1999**, *71*, 2152-2156.

68. Sellergren, B.; Esteban, A. M., The use of molecularly imprinted polymers for sampling and sample preparation. *Handbook of Sample Preparation.* **2010**, 445-473.

69. Boysen, R. I.; Hearn, M. T. W., Modern methods in natural product chemistry: high-performance chromatography separation methods, in: Comprehensive Natural Products Chemistry II, Chemistry and Biology. *Elsevier, Oxford* **2010**, *9*, 5-49.

70. Hearn, M. T. W., Reversed-phase and hydrophobic interaction chromatography of proteins and peptides. *Chromatogr. Sci. Ser.* **2002**, *87*, 99-245.

71. Shoji, T.; Masumoto, S.; Moriichi, N.; Kobori, M.; Kanda, T.; Shinmoto, H.; Tsushida, T., Procyanidin trimers to pentamers fractionated from apple inhibit melanogenesis in B16 mouse melanoma cells. *J. Agric. Food Chem.* **2005**, *53*, 6105-6111.

72. Boysen, R. I.; Yang, Y.; Chowdhury, J.; Matyska, M. T.; Pesek, J. J.; Hearn, M. T. W., Simultaneous separation of hydrophobic and hydrophilic peptides with a silica hydride stationary phase using aqueous normal phase conditions. *J. Chromatogr., A* **2011**, *1218*, 8021-8026.

73. Pesek, J. J.; Matyska, M. T.; Boysen, R. I.; Yang, Y.; Hearn, M. T. W., Aqueous normal-phase chromatography using silica-hydride-based stationary phases. *Trends Anal. Chem.* **2013**, *42*, 64-73.

74. Pesek, J. J.; Matyska, M. T.; Hearn, M. T. W.; Boysen, R. I., Aqueous normal-phase retention of nucleotides on silica hydride columns. *J. Chromatogr., A* **2009**, *1216*, 1140-1146.

75. Yang, Y.; Boysen, R. I.; Hearn, M. T. W., Hydrophilic interaction chromatography coupled to electrospray mass spectrometry for the separation of peptides and protein digests. *J. Chromatogr., A* **2009**, *1216*, 5518-5524.

76. Fan, T.; Jing, Z.; Fan, X.; Yu, M.; Jiang, G., Purification and characterization of phenol oxidase from brine shrimp *Artemia sinica*. *Acta Biochim. Biophys. Sin.* **2011**, *43*, 722-728.

77. D'Orazio, V.; Senesi, N., Spectroscopic properties of humic acids isolated from the rhizosphere and bulk soil compartments and fractionated by size-exclusion chromatography. *Soil Biol. Biochem.* **2009**, *41*, 1775-1781.

78. Mountford, S. J.; Campi, E. M.; Robinson, A. J.; Hearn, M. T. W., Synthesis of *N*-heterocyclic ligands for use in affinity and mixed mode chromatography. *Tetrahedron.* **2011**, *67*, 471-485.

79. Aguilar, M. I.; Hearn, M. T. W., High-resolution reversed-phase high-performance liquid chromatography of peptides and proteins. *Methods Enzymol*. **1996**, *270*, 3-26.

80. Scott, R. P. W., Liquid chromatography detectors. *Chromatogr. Sci. Ser.* **1998**, *78*, 531-558.

81. Huber, L.; Schuster, R., Environmental applications of diode array detection in HPLC. *Chromatogr. Sci. Ser.* **1993**, *62*, 325-350.

82. Wolfender, J. L., HPLC in natural product analysis: The detection issue. *Planta Medica.* **2009**, *75*, 719-734.

83. Flamini, R., Mass spectrometry in grape and wine chemistry. Part I: polyphenols. *Mass Spectrom. Rev.* **2003**, *22*, 218-250.

84. Dole, M.; Hines, R. L.; Mack, L. L.; Mobley, R. C.; Ferguson, L. D.; Alice, M. B., Gas phase macroions. *Macromolecules* **1968**, *1*, 96-97.

85. Fenn, J. B., Ion formation from charged droplets: roles of geometry, energy, and time. *J. Am. Soc. Mass Spectrom.* **1993**, *4*, 524-535.

86. Fenn, J. B.; Mann, M.; Meng, C. K.; Wong, S. F.; Whitehouse, C. M., Electrospray ionization for mass spectrometry of large biomolecules. *Science* **1989**, *246*, 64-71.

87. Wine and grape industry. *Statistical database available online* www.abs.gov.au **2011**.

88. Palaniswamy, S.; Mayilvanan, M.; Dharamani, A. S., Classification of functional groups of a phytochemical, gymnemic acid, using fuzzy logic. *Rasayan J. Chem.* **2009**, *2*, 475-487.

89. Harborne, J. B., Methods in plant biochemistry, Vol. 1: plant phenolics. *Academic Press New York and London*. **1989**, p 552.

90. Pandey, K. B.; Rizvi, S. I., Plant polyphenols as dietary antioxidants in human health and disease. *Oxid. Med. Cell Longev.* **2009**, *2*, 270-278.

91. Tsao, R., Chemistry and biochemistry of dietary polyphenols. *Nutrients* **2010**, *2*, 1231-1246.

92. Mazid, M.; Khan, T. A.; Mohammad, F., Role of secondary metabolites in defense mechanisms of plants. *Biol. Med.* **2011**, *3*, 232-249.

93. Kennedy, J. F.; Kaczmarek, A.; Glories, Y.; Maujean, A.; Dubourdieu, D., Handbook of Enology, The chemistry of wine stabilization and treatments. **2007**, Vol. 2, Second Edition.

94. Soleas, G. J.; Diamandis, E. P.; Goldberg, D. M., Resveratrol: a molecule whose time has come? and gone? *Clin. Biochem.* **1997**, *30*, 91-113.

95. Vitrac, X.; Bornet, A.; Vanderlinde, R.; Valls, J.; Richard, T.; Delaunay, J. C.; Merillon, J. M.; Teissedre, P. L., Determination of stilbenes (δ-viniferin, *trans*-astringin, *trans*-piceid, *cis*- and *trans*-resveratrol, ε-viniferin) in Brazilian wines. *J. Agric. Food Chem.* **2005**, *53*, 5664-5669.

96. Moreno, A.; Castro, M.; Falque, E., Evolution of *trans*- and *cis*-resveratrol content in red grapes (*Vitis vinifera* L. cv Mencia, Albarello and Merenzao) during ripening. *Eur. Food Res. Technol.* **2008**, *227*, 667-674.

97. Dercks, W.; Creasy, L. L., The significance of stilbene phytoalexins in the Plasmopara viticola-grapevine interaction. *Physiol. Mol. Plant Pathol.* **1989**, *34*, 189-202.

98. Langcake, P.; Pryce, R. J., A new class of phytoalexins from grapevines. *Experientia* **1977**, *33*, 151-152.

99. Creasy, L. L.; Creasy, M. T., Grape chemistry and the significance of resveratrol: an overview. *Pharm. Biol. (Lisse, Neth.)* **1998**, *36*, 8-13.

100. Siemann, E. H.; Creasy, L. L., Concentration of the phytoalexin resveratrol in wine. *Am. J. Enol. Vitic.* **1992**, *43*, 49-52.

101. Zghonda, N.; Yoshida, S.; Araki, M.; Kusunoki, M.; Mliki, A.; Ghorbel, A.; Miyazaki, H., Greater effectiveness of ε-viniferin in red wine than its monomer resveratrol for inhibiting vascular smooth muscle cell proliferation and migration. *Biosci., Biotechnol., Biochem.* **2011**, *75*, 1259-1267.

102. Caruso, F.; Tanski, J.; Villegas-Estrada, A.; Rossi, M., Structural basis for antioxidant activity of *trans*-resveratrol: ab initio calculations and crystal and molecular structure. *J Agric Food Chem* **2004**, *52*, 7279-7285.

103. Privat, C.; Telo, J. P.; Bernardes-Genisson, V.; Vieira, A.; Souchard, J. P.; Nepveu, F., Antioxidant properties of *trans-epsilon*-viniferin as compared to stilbene derivatives in aqueous and non-aqueous media. *J. Agric. Food Chem.* **2002**, *50*, 1213-1217.

104. Langcake, P.; Pryce, R. J., Oxidative dimerization of 4-hydroxystilbenes in vitro: production of a grapevine phytoalexin mimic. *J. Chem. Soc., Chem. Commun.* **1977**, 208-210.

105. Mikulski, D.; Szelag, M.; Molski, M.; Gorniak, R., Quantum-chemical study on the antioxidation mechanisms of *trans*-resveratrol reactions with free radicals in the gas phase, water and ethanol environment. *J. Mol. Struct.* **2010**, *951*, 37-48.

106. Stivala, L. A.; Savio, M.; Carafoli, F.; Perucca, P.; Bianchi, L.; Maga, G.; Forti, L.; Pagnoni, U. M.; Albini, A.; Prosperi, E.; Vannini, V., Specific structural determinants are responsible for the antioxidant activity and the cell cycle effects of resveratrol. *J. Biol. Chem.* **2001**, *276*, 22586-22594.

107. Cao, H.; Pan, X.; Li, C.; Zhou, C.; Deng, F.; Li, T., Density functional theory calculations for resveratrol. *Bioorg. Med. Chem. Lett.* **2003**, *13*, 1869-1871.

108. King, R. E.; Kent, K. D.; Bomser, J. A., Resveratrol reduces oxidation and proliferation of human retinal pigment epithelial cells *via* extracellular signal-regulated kinase inhibition. *Chem. Biol. Interact.* **2005**, *151*, 143-149.

109. Constant, J., Alcohol, ischemic heart disease, and the French paradox. *Clin. Cardiol.* **1997**, *20*, 420-424.

110. Wang, Z.; Huang, Y.; Zou, J.; Cao, K.; Xu, Y.; Wu, J. M., Effects of red wine and wine polyphenol resveratrol on platelet aggregation *in vivo* and *in vitro*. *Int. J. Mol. Med.* **2002**, *9*, 77-79.

111. Wu, J. M.; Hsieh, T. C.; Wang, Z., Cardioprotection by resveratrol: a review of effects/targets in cultured cells and animal tissues. *Am. J. Cardiovasc. Dis.* **2011**, *1*, 38-47.

112. Richard, N.; Porath, D.; Radspieler, A.; Schwager, J., Effects of resveratrol, piceatannol, tri-acetoxystilbene, and genistein on the inflammatory response of human peripheral blood leukocytes. *Mol. Nutr. Food Res.* **2005**, *49*, 431-442.

113. Kundu, J. K.; Shin, Y. K.; Surh, Y. J., Resveratrol modulates phorbol ester-induced pro-inflammatory signal transduction pathways in mouse skin *in vivo*: NF-κB and AP-1 as prime targets. *Biochem. Pharmacol.* **2006**, *72*, 1506-1515.

114. Banerjee, S.; Bueso-Ramos, C.; Aggarwal, B. B., Suppression of 7,12-dimethylbenz(a)anthracene-induced mammary carcinogenesis in rats by resveratrol: role of nuclear factor-κB, cyclooxygenase 2, and matrix metalloprotease 9. *Cancer Res.* **2002**, *62*, 4945-4954.

115. Gehm, B. D.; Levenson, A. S.; Liu, H.; Lee, E.-J.; Amundsen, B. M.; Cushman, M.; Jordan, V. C.; Jameson, J. L., Estrogenic effects of resveratrol in breast cancer cells expressing mutant and wild-type estrogen receptors: role of AF-1 and AF-2. *J. Steroid Biochem. Mol. Biol.* **2004**, *88*, 223-234.

116. Basly, J. P.; Marre-Fournier, F.; Le Bail, J. C.; Habrioux, G.; Chulia, A. J., Estrogenic/antiestrogenic and scavenging properties of *(E)*- and *(Z)*-resveratrol. *Life Sci.* **2000**, *66*, 769-777.

117. Paixao, N.; Perestrelo, R.; Marques, J. C.; Camara, J. S., Relationship between antioxidant capacity and total phenolic content of red, rose and white wines. *Food Chem.* **2007**, *105*, 204-214.

118. Amic, D.; Davidovic Amic, D.; Beslo, D.; Trinajstic, N., Structure radical scavenging activity relationships of flavonoids. *Croat. Chem. Acta* **2003**, *76*, 55-61.

119. Balentine, D. A.; Wiseman, S. A.; Bouwens, L. C. M., The chemistry of tea flavonoids. *Crit. Rev. Food Sci. Nutr.* **1997**, *37*, 693-704.

120. Mattivi, F.; Zulian, C.; Nicolini, G.; Valenti, L., Wine, biodiversity, technology, and antioxidants. *Ann. N. Y. Acad. Sci.* **2002**, *957*, 37-56.

121. Miura, Y.; Chiba, T.; Tomita, I.; Koizumi, H.; Miura, S.; Umegaki, K.; Hara, Y.; Ikeda, M.; Tomita, T., Tea catechins prevent the development of atherosclerosis in apoprotein E-deficient mice. *J. Nutr.* **2001**, *131*, 27-32.

122. Parr, A. J.; Bolwell, G. P., Phenols in the plant and in man. The potential for possible nutritional enhancement of the diet by modifying the phenols content or profile. *J. Sci. Food Agric.* **2000**, *80*, 985-1012.

123. Rockenbach, I. I.; Jungfer, E.; Ritter, C.; Santiago-Schuebel, B.; Thiele, B.; Fett, R.; Galensa, R., Characterization of flavan-3-ols in seeds of grape pomace by CE, HPLC-DAD-MS^n and LC-ESI-FTICR-MS. *Food Res. Int.* **2012**, *48*, 848-855.

124. Carando, S.; Teissedre, P. L.; Pascual-Martinez, L.; Cabanis, J. C., Levels of flavan-3-ols in French wines. *J. Agric. Food Chem.* **1999**, *47*, 4161-4166.

125. Santos-Buelga, C.; Scalbert, A., Proanthocyanidins and tannin-like compounds - nature, occurrence, dietary intake and effects on nutrition and health. *J. Sci. Food Agric.* **2000**, *80*, 1094-1117.

126. Haslam, E., Practical polyphenolics: from structure to molecular recognition and physiological action. *Cambridge Univ. Press.* **1998**, p 422.

127. Joutei, K. A.; Glories, Y.; Mercier, M., Localization of tannins in grape berry skins. *Vitis* **1994**, *33*, 133-138.

128. Glories, Y., Anthocyanins and tannins from wine: organoleptic properties. *Prog. Clin. Biol. Res.* **1988**, *280*, 123-134.

129. Downey, M. O.; Harvey, J. S.; Robinson, S. P., Analysis of tannins in seeds and skins of Shiraz grapes throughout berry development. *Aust. J. Grape Wine Res.* **2003**, *9*, 15-27.

130. Kennedy, J. A.; Taylor, A. W., Analysis of proanthocyanidins by high performance gel permeation chromatography. *J. Chromatogr., A* **2003**, *995*, 99-107.

131. Kennedy, J. A.; Troup, G. J.; Pilbrow, J. R.; Hutton, D. R.; Hewitt, D.; Hunter, C. R.; Ristic, R.; Iland, P. G.; Jones, G. P., Development of seed polyphenols in berries from *Vitis vinifera* L. cv. Shiraz. *Aust. J. Grape Wine Res.* **2000**, *6*, 244-254.

132. Price, S. F.; Breen, P. J.; Valladao, M.; Watson, B. T., Cluster sun exposure and quercetin in Pinot noir grapes and wine. *Am. J. Enol. Vitic.* **1995**, *46*, 187-194.

133. McDonald, M. S.; Hughes, M.; Burns, J.; Lean, M. E. J.; Matthews, D.; Crozier, A., Survey of free and conjugated myricetin and quercetin content of red wines of different geographical origins. *J. Agric. Food Chem.* **1998**, *46*, 368-375.

134. Cheynier, V.; Rigaud, J., HPLC separation and characterization of flavonols in the skins of *Vitis vinifera* var. Cinsault. *Am. J. Enol. Vitic.* **1986**, *37*, 248-252.

135. Fukumoto, L. R.; Mazza, G., Assessing antioxidant and prooxidant activities of phenolic compounds. *J. Agric. Food Chem.* **2000**, *48*, 3597-3604.

136. Cantos, E.; Espin, J. C.; Tomas-Barberan, F. A., Varietal differences among the polyphenol profiles of seven table grape cultivars studied by LC-DAD-MS/MS. *J. Agric. Food Chem.* **2002**, *50*, 5691-5696.

137. Andrade, P. B.; Mendes, G.; Falco, V.; Valentao, P.; Seabra, R. M., Preliminary study of flavonols in port wine grape varieties. *Food Chem.* **2001**, *73*, 397-399.

138. Zhou, W.; Kallifatidis, G.; Baumann, B.; Rausch, V.; Mattern, J.; Gladkich, J.; Giese, N.; Moldenhauer, G.; Wirth, T.; Buchler, M. W.; Salnikov, A. V.; Herr, I., Dietary polyphenol quercetin targets pancreatic cancer stem cells. *Int. J. Oncol.* **2010**, *37*, 551-561.

139. Bredsdorff, L.; Nielsen, I. L. F.; Rasmussen, S. E.; Cornett, C.; Barron, D.; Bouisset, F.; Offord, E.; Williamson, G., Absorption, conjugation and excretion of the flavanones, naringenin and hesperetin from α-rhamnosidase treated orange juice in human subjects. *Br. J. Nutr.* **2010**, *103*, 1602-1609.

140. Matejkova, S.; Gut, I., Effects of several wine polyphenols on lipid peroxidation and oxygen activation in rat liver microsomes. *Adv. Exp. Med. Biol.* **2001**, *500*, 275-278.

141. Gambelli, L.; Santaroni, G. P., Polyphenols content in some Italian red wines of different geographical origins. *J. Food Compos. Anal.* **2004**, *17*, 613-618.

142. Shukla, S.; Gupta, S., Apigenin: A promising molecule for cancer prevention. *Pharm. Res.* **2010**, *27*, 962-978.

143. Landrault, N.; Larronde, F.; Delaunay, J. C.; Castagnino, C.; Vercauteren, J.; Merillon, J. M.; Gasc, F.; Cros, G.; Teissedre, P. L., Levels of stilbene oligomers and astilbin in French varietal wines and in grapes during noble rot development. *J. Agric. Food Chem.* **2002**, *50*, 2046-2052.

144. Fanzone, M.; Pena-Neira, A.; Jofre, V.; Assof, M.; Zamora, F., Phenolic characterization of Malbec wines from Mendoza province (Argentina). *J. Agric. Food Chem.* **2010**, *58*, 2388-2397.

145. Vitrac, X.; Monti, J. P.; Vercauteren, J.; Deffieux, G.; Merillon, J. M., Direct liquid chromatographic analysis of resveratrol derivatives and flavanonols in wines with absorbance and fluorescence detection. *Anal. Chim. Acta* **2002**, *458*, 103-110.

146. Clifford, M. N., Anthocyanins - nature, occurrence and dietary burden. *J. Sci. Food Agric.* **2000**, *80*, 1063-1072.

147. Frank, T.; Netzel, M.; Strass, G.; Bitsch, R.; Bitsch, I., Bioavailability of anthocyanidin-3-glucosides following consumption of red wine and red grape juice. *Can. J. Physiol. Pharmacol.* **2003**, *81*, 423-435.

148. Flamini, R., Some advances in the knowledge of grape, wine and distillates chemistry as achieved by mass spectrometry. *J. Mass Spectrom.* **2005**, *40*, 705-713.

149. Cheynier, V., Polyphenols in foods are more complex than often thought. *Am. J. Clin. Nutr.* **2005**, *81*, 223S-229S.

150. Mazzuca, P.; Ferranti, P.; Picariello, G.; Chianese, L.; Addeo, F., Mass spectrometry in the study of anthocyanins and their derivatives: differentiation of *Vitis vinifera* and hybrid grapes by liquid chromatography electrospray ionization mass spectrometry and tandem mass spectrometry. *J. Mass. Spectrom.* **2005**, *40*, 83-90.

151. Castia, T.; Franco, M. A.; Mattivi, F.; Muggiolu, G.; Sferlazzo, G.; Versini, G., Characterization of grapes cultivated in Sardinia: chemometric methods applied to the anthocyanic fraction. *Sci. Aliments* **1992**, *12*, 239-255.

152. Guiso, M.; Marra, C.; Farina, A., A new efficient resveratrol synthesis. *Tetrahedron Lett.* **2002**, *43*, 597-598.

153. Moreau, R. A.; Whitaker, B. D.; Hicks, K. B., Phytosterols, phytostanols, and their conjugates in foods: structural diversity, quantitative analysis, and health promoting uses. *Prog. Lipid Res.* **2002**, *41*, 457-500.

154. Phillips, K. M.; Ruggio, D. M.; Toivo, J. I.; Swank, M. A.; Simpkins, A. H., Free and esterified sterol composition of edible oils and fats. *J. Food Compos. Anal.* **2002**, *15*, 123-142.

155. Berger, A.; Jones, P. J. H.; Abu Mweis, S. S., Plant sterols: Factors affecting their efficacy and safety as functional food ingredients. *Lipids Health Dis.* **2004**, *3*, 5-24.

156. Racette, S. B.; Spearie, C. A.; Phillips, K. M.; Lin, X.; Ma, L.; Ostlund, R. E., Jr., Phytosterol deficient and high phytosterol diets developed for controlled feeding studies. *J. Am. Diet. Assoc.* **2009**, *109*, 2043-2051.

157. Crews, C.; Hough, P.; Godward, J.; Brereton, P.; Lees, M.; Guiet, S.; Winkelmann, W., Quantitation of the main constituents of some authentic grape seed oils of different origin. *J. Agric. Food Chem.* **2006**, *54*, 6261-6265.

158. Piironen, V.; Lindsay, D. G.; Miettinen, T. A.; Toivo, J.; Lampi, A. M., Plant sterols: biosynthesis, biological function and their importance to human nutrition. *J. Sci. Food Agric.* **2000**, *80*, 939-966.

159. Normen, L.; Bryngelsson, S.; Johnsson, M.; Evheden, P.; Ellegard, L.; Brants, H.; Andersson, H.; Dutta, P., The phytosterol content of some cereal foods commonly consumed in Sweden and in the Netherlands. *J. Food Compos. Anal.* **2002**, *15*, 693-704.

160. Stuchlik, M.; Zak, S., Vegetable lipids as components of functional foods. *Biomed. Pap.* **2002**, *146*, 3-10.

161. Awad, A. B.; Downie, A. C.; Fink, C. S., Inhibition of growth and stimulation of apoptosis by β-sitosterol treatment of MDA-MB-231 human breast cancer cells in culture. *Int. J. Mol. Med.* **2000**, *5*, 541-545.

162. Wang, K.; Senthil-Kumar, M.; Ryu, C. M.; Kang, L.; Mysore, K. S., Phytosterols play a key role in plant innate immunity against bacterial pathogens by regulating nutrient efflux into the apoplast. *Plant Physiol.* **2012**, *158*, 1789-1802.

163. Quilez, J.; Garcia Lorda, P.; Salas Salvado, J., Potential uses and benefits of phytosterols in diet: present situation and future directions. *Clin. Nutr.* **2003**, *22*, 343-351.

164. Peterson, D. W.; Robbins, R.; Shneour, E. A.; Myers, W. D., Effect of soybean sterols in the diet on plasma and liver cholesterol in chicks. *Proc. Soc. Exp. Biol. Med.* **1951**, *78*, 143-147.

165. Pollak, O. J., Successful prevention of experimental hypercholesteremia and cholesterol atherosclerosis in the rabbit. *Circulation* **1953**, *7*, 696-701.

166. Dempsey, M. E.; Farquhar, J. W.; Smith, R. E., The effect of β-sitosterol on the serum lipids of young men with arteriosclerotic heart disease. *Circulation* **1956**, *14*, 77-82.

167. Jones, P. J. H.; Macdougall, D. E.; Ntanios, F.; Vanstone, C. A., Dietary phytosterols as cholesterol lowering agents in humans. *Can. J. Physiol. Pharmacol.* **1997**, *75*, 217-227.

168. Blair, S. N.; Capuzzi, D. M.; Gottlieb, S. O.; Nguyen, T.; Morgan, J. M.; Cater, N. B., Incremental reduction of serum total cholesterol and low-density lipoprotein cholesterol with the addition of plant stanol ester containing spread to statin therapy. *Am. J. Cardiol.* **2000**, *86*, 46-52.

169. Touillaud, M. S.; Pillow, P. C.; Jakovljevic, J.; Bondy, M. L.; Singletary, S. E.; Li, D.; Chang, S., Effect of dietary intake of phytoestrogens on estrogen receptor status in premenopausal women with breast cancer. *Nutr. Cancer* **2005**, *51*, 162-169.

170. Sundararaman, P.; Djerassi, C., A convenient synthesis of progesterone from stigmasterol. *J. Org. Chem.* **1977**, *42*, 3633-3634.

171. Kametani, T.; Furuyama, H., Synthesis of vitamin D_3 and related compounds. *Med. Res. Rev.* **1987**, *7*, 147-171.

Chapter 2

Chromatographic optimisation and method development for the analysis of polyphenols

Abstract

This chapter presents a new method to separate a set of important standard polyphenols under the application of benign chemicals and tools according to the principles of Green Chemistry, as it employed a mixture of ethanol-water and a low concentration of formic acid at ambient temperature for the reversed-phase high performance liquid chromatographic (RP-HPLC) analysis. A down-scale of the analytical procedure to a capillary liquid chromatography method and hyphenation with electrospray ionisation ion trap mass spectrometry (LC-ESI ion trap MS/MS) was performed with minimal solvent usage and waste. LC-ESI ion trap MS/MS was shown to be effective in the negative ionisation mode for the peak identity confirmation of the polyphenols. The tandem mass spectrometric identification was demonstrated for (*E*)-resveratrol as an example. The application of a newly developed molecularly imprinted polymer (MIP) in solid-phase extraction (SPE) format was optimised in terms of cartridge conditioning, sample loading, wash and elution conditions with suitable benign solvents for the selective enrichment of (*E*)-resveratrol. The comparison of MIP and control non-imprinted polymer (NIP) demonstrated that the MIP contained effective imprinting sites for (*E*)-resveratrol.

Table of Contents

2.1 Introduction

The importance of polyphenols for human health and well-being has driven the establishment of comprehensive databases on polyphenol composition in foods and in turn a demand for analytical methodologies for their identification and quantification. Due to the structural diversity and a multitude of occurrences of these compounds in food sources or medicinal plants, the efficient and selective extraction of specific target molecules from complex biological matrices represents a challenge to the analytical community.

Reversed-phase high performance liquid chromatography (RP-HPLC) with diode array detection (DAD) is the technique most often used to analyse polyphenols (*1*). In regards to achieving an optimal chromatographic separation, the column selection, column temperature, mobile phase composition, mobile phase additive concentration and elution program (either gradient or isocratic mode) is important and often guided by separation efficiencies alone, and not by considerations of new standards of environmental safety.

The main objective of this study was to optimise the chromatographic parameters for the development of a new green separation methodology in RP-HPLC, in conjunction with electrospray ionisation tandem mass spectrometric (ESI-MS/MS) for the separation of polyphenols of health-beneficial significance. The established separation method will then be applied to monitor the performance of new molecularly imprinted polymers (MIPs) incorporated in a solid-phase extraction (SPE) format for the enrichment of (*E*)-resveratrol derived from wine **(Chapter 3)** and grape wastes **(Chapter 4** and **6)**.

2.2 Materials and Methods

2.2.1 Reagents

Gallic acid, caffeic acid, *p*-coumaric acid, ferulic acid, chlorogenic acid, (±)-catechin, rutin, morin and quercetin were purchased from Sigma-Aldrich (Sydney, Australia). (*E*)-Resveratrol (99.8% purity) was purchased from AK Scientific (Union City, California, USA). HPLC grade of acetonitrile (ACN), methanol (MeOH), ethanol (EtOH), *iso*-propanol (IPA) and dimethylsulphoxide (DMSO) were purchased from Merck (Melbourne, Australia). Reagent grade formic acid (FA) and glacial acetic acid (AcOH) were purchased from Ajax Finechem

(Melbourne, Australia). Trifluoroacetic acid (TFA) and heptafluorobutyric acid (HFBA) were obtained from Sigma Aldrich (Sydney, Australia). Water was purified by a water purification system (Pall Corp., Melbourne, Australia) to a resistivity of 18.2 MΩ.cm.

2.2.2 Standards

A mixture of ten polyphenol standards containing gallic acid, caffeic acid, *p*-coumaric acid, ferulic acid, (±)-catechin, chlorogenic acid, rutin, morin, quercetin and (*E*)-resveratrol were prepared at a concentration of 0.01 mM or 0.10 mM (for each polyphenol component) using stock solutions. Stock solutions of (±)-catechin and (*E*)-resveratrol were both prepared in ACN at a concentration of 5.0 mM. Gallic acid, *p*-coumaric acid, chlorogenic acid, ferulic acid, rutin, morin and quercetin standard stock solutions were all prepared in DMSO at a concentration of 10.0 mM. The caffeic acid stock solution was prepared by dissolving the standard in a mixture of ACN/DMSO (2:1, v/v) at a concentration of 2.5 mM.

An eight-point calibration curve for (*E*)-resveratrol was prepared by serial dilution of the (*E*)-resveratrol stock solution with EtOH covering a concentration range of 2.4×10^{-4} to 5.0×10^{-1} mM. The standard calibration curve of (*E*)-resveratrol was established by plotting the chromatographic peak area *versus* concentration. The peak area was linearly proportional to a concentration ($y = mx + b$). In this equation, y is the peak area obtained from the HPLC chromatogram, x is the concentration of an (*E*)-resveratrol standard (mM), m is a response factor between the peak area and b is the intersection near to the origin (~0.0). The equation for the resulting calibration curve was $y = 15693x$ with a correlation factor (R^2) of 0.9. The limit of detection (LOD) (multiplying the standard deviation (SD) by 3) and the limit of quantitation (LOQ) (10 times the SD) for (*E*)-resveratrol were determined to be 3.9×10^{-5} mM and 1.3×10^{-4} mM, respectively.

2.2.3 Instrumentation

2.2.3.1 RP-HPLC analysis

RP-HPLC analysis was performed using an Agilent HPLC 1100 series (Agilent Technologies, Waldbronn, Germany) equipped with ChemStation software (B.02.01 SR1), a degasser, a binary gradient pump, an auto-sampler with a 900 µL sample loop, a thermostated column

compartment and a 80 Hz full spectra ultra-fast UV-DAD. Separation was performed with a double end-capped Zorbax Eclipse XDB C_{18} column (4.6 mm × 150 mm, 5 µm particle size) (Agilent Technologies, Melbourne, Australia) at 20 °C. The UV-DAD was set to 200-600 nm at a spectral acquisition rate of 2 nm scans per step with simultaneous monitoring at 280 nm, 320 nm and 370 nm. Compounds in the sample were identified based on their respective reference standards by comparison of the retention times and UV/Vis spectra. The mobile phase consisted of eluent A was 10 mM AcOH, FA, TFA or HFBA in water, respectively. The eluent B was 10 mM AcOH, FA, TFA or HFBA in ACN, MeOH, EtOH/H_2O (4:1, v/v) or IPA/H_2O (4:1, v/v). The phenolic compounds were analysed using a linear gradient of eluent B: 0-2 min: 10% (v/v), 2-52 min: 10-70% (v/v), 52-53 min: 10% (v/v). The total run time was 53 min and the injection volume was 5 µL at a flow rate of 0.5 mL/min. All mobile phases were filtered through polypropylene membrane filters (0.2 µm pore size, 47 mm diameter) purchased from Pall Corp. (Melbourne, Australia) and were degassed in an ultrasonic bath (Elmasonic, Singen, Germany) for 30 minutes.

2.2.3.2 LC-ESI ion trap MS/MS analysis

Identification of polyphenols in the sample mixture was carried out on an Agilent 1100 capillary LC system (Agilent Technologies, Palo Alto, CA, USA) coupled to an ion trap MS system (Agilent 1100 Series LC/MSD-SL). The RP-HPLC separation was performed at 20 °C using a Zorbax XDB capillary C_{18} column (0.3 mm × 150 mm, 3.5 µm particle size) from Agilent Technologies (Melbourne, Australia). The gradient elution conditions employed in this system were the same as in the earlier RP-HPLC analysis **(Section 2.2.3.1)**. The column was equilibrated with 10% (v/v) B for 10 min prior to an injection. The injection volume was 0.1 µL at a flow rate of 2 µL/min. The mass detection was performed in the full scan mode in the *m/z* range from 100 to 1200 using the negative ionisation mode. The capillary voltage was set to 3.5 kV. Nitrogen was used as the nebulising gas at a pressure of 10 psi. The drying gas flow rate was set to 5 L/min at 300 °C. The target mass, compound stability and trap drive level were set to *m/z* 600, 80% and 100%, respectively. The ion accumulation time was automatically adjusted *via* the Ion Charge Control (ICC) feature of the instrument. The ICC target was 30,000 units and the maximal accumulation time was 300 ms. For MS/MS analysis, helium was used as the gas for collision induced dissociation (CID). The instrument was operated using the “smart fragmentation” mode which allowed the fragmentation

amplitude to be varied from 30-200% of the default 1.0 V. The instrument automatically changed from MS to MS/MS when the intensity of particular ion surpassed the threshold of 5,000 units. Active exclusion was carried out after two spectra for 1 min. The number of precursor ion selection was set to 2. All data acquisition and processing were conducted with an Agilent ChemStation (version 4.2) and MSD Trap Control software.

2.2.4 Molecularly imprinted polymer preparation

The resveratrol imprinted polymers (MIPs) and the control non-imprinted polymers (NIPs) were synthesised by Dr. Lachlan Schwarz (Centre for Green Chemistry, Monash University, Melbourne Australia) using the non-covalent approach (*2, 3*). During the imprinting process, an (*E*)-resveratrol (template, 1 M), 4-vinylpyridine (4-VP, 3 M) as functional monomer, ethylene glycol dimethacrylate (EGDMA, 15 M) as crosslinker and 2,2′-azobis(2-methylpropionitrile) (AIBN, 0.3 M) as free radical initiator were dissolved in a porogen mixture of ACN/EtOH (5:1, v/v) in a thick-walled glass tube. The resulting mixture was sealed and purged with nitrogen gas for 2 min and then sonicated for 20 min. The glass tube was then placed in a 50 °C water bath for 18 h, followed by a thermal annealing treatment at 60 °C for 24 h. The resultant bulk polymer was crushed, ground into powder and sieved to produce a particle size distribution of 63-90 µm. The resultant MIP material was washed several times with MeOH/AcOH (9:1, v/v) until the wash fraction was free from the template, as confirmed by RP-HPLC with detection at 210 nm. The remaining MIP material was dried in a vacuum oven at 40 °C overnight. The NIP was prepared under the same experimental conditions as the MIP, in the absence of the template.

2.2.5 Molecularly imprinted solid-phase extraction protocol

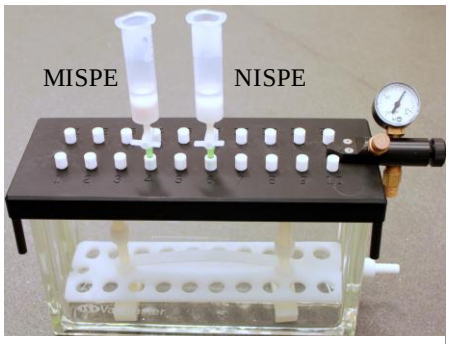

Figure 2.1: Molecularly imprinted polymers in the solid-phase extraction (MISPE) and control NISPE cartridges.

Approximately 1.0 gram of the MIP (particle size 63-90 µm) and NIP (particle size 63-90 µm) were slurry packed into polypropylene SPE cartridges (2.0 cm in diameter and 8.7 cm in length) using 30 mL of EtOH. These MISPE and NISPE cartridges were subsequently capped at the top and bottom with fritted polypropylene disks (20 µm pore size) and the setup can be seen in

Figure 2.1. Vacuum was not used in this MIPSE protocol in order to give a better contact and equilibrium time between the target analyte and imprinted binding sites. Both cartridges were then conditioned by rinsing (in sequence) with EtOH/AcOH (9:1, v/v, 15 mL), EtOH (15 mL) and EtOH/H_2O (15:85, v/v, 15 mL). The flow rate of each cartridge was adjusted to about 2 drops per second and eluted by the force of gravity. MISPE and NISPE cartridges were loaded with (*E*)-resveratrol standard solution in EtOH/H_2O (15:85, v/v) at a concentration of 0.1 mM (5 mL). Each column was subsequently washed with EtOH/H_2O (4:1, v/v) containing 1% (v/v) AcOH (4 × 5 mL) to remove components bound to the MIP or NIP through either weak or non-specific interactions. The bound material was eluted from the respective cartridges using EtOH/AcOH (9:1, v/v) (10 × 5 mL), and aliquots (1 mL) of each elution fraction were combined, evaporated to dryness using a Genevac EZ-2 vacuum evaporator (Pacific Laboratory Products, Melbourne, Australia) and re-constituted in the mobile phase eluent B (1 mL) which corresponded to a 10-fold concentration. The MISPE and NISPE cartridges were then reconditioned with H_2O (15 mL), followed by EtOH (15 mL) and finally with EtOH/H_2O (15:85, v/v, 15 mL) for repeated use. In the case of a complex biological sample, a wash step with 0.1 mM NaOH in water was added to render the MIP re-usable.

2.3 Results and Discussion

2.3.1 Chromatographic optimisation and method development

The optimisation and method development for the analysis of polyphenols were evaluated based on several experimental variables, which are considered to be the most important prerequisites to grant a good separation. To the best of my knowledge, this is the first time an entire experimental process was designed for polyphenolic compounds with environmentally benign solvents in accordance to the principles of Green Chemistry **(Figure 2.2)**.

2.3.1.1 Selection of a reversed-phase column

A number of publications on RP-HPLC techniques for polyphenols analysis reported the use of a single endcapped silica packing material with a particle size range from 3 to 10 µm in stainless steel columns (*4*, *5*). Usually these columns have a typical length of 15 cm or 25 cm and a standard internal diameter of 4.6 mm (*6*, *7*). In this work, the reversed-phase C_{18} double

end-capped column (4.6 mm × 150 mm, 5 µm particle size) was chosen because this type of column has a capability to reduce secondary interaction effects of silanols hence minimised peak tailing. Additionally, this column is stable at acidic, basic and/or neutral conditions over a pH range of 2-9.

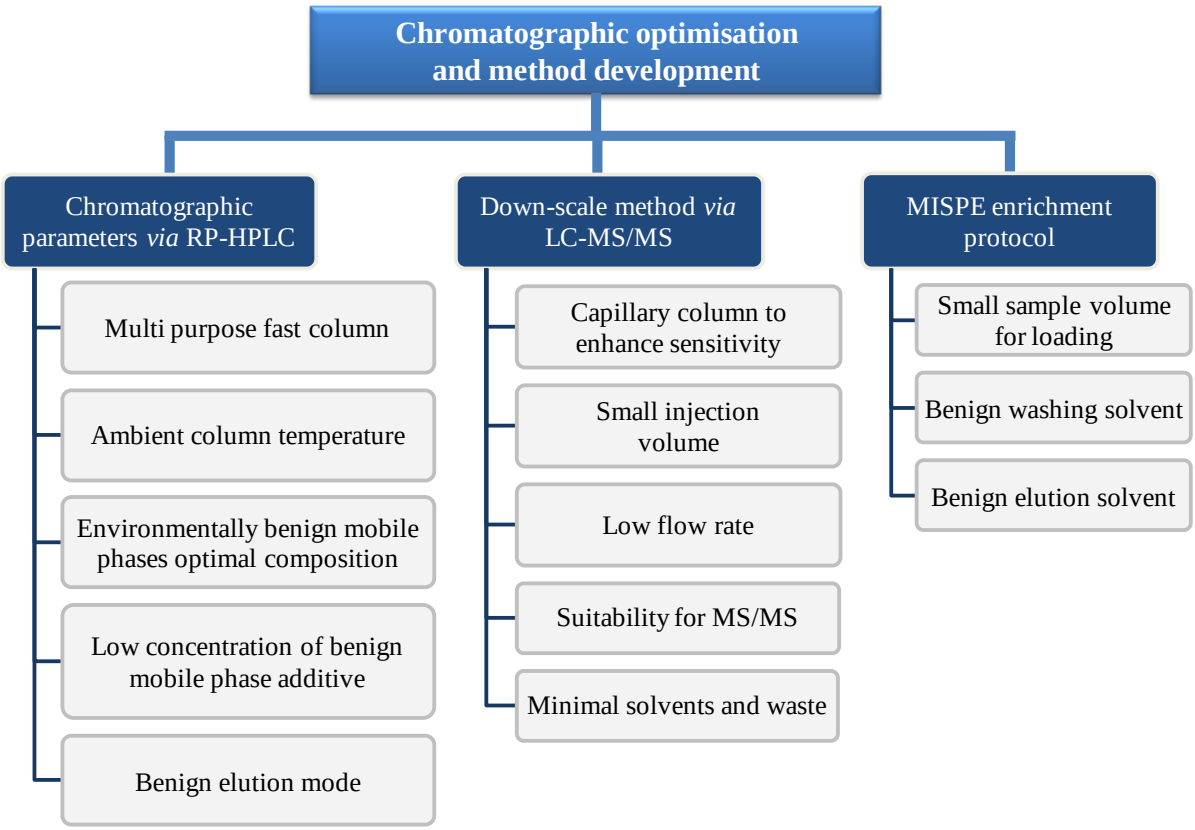

Figure 2.2: Chromatographic optimisation and method development for the analysis of polyphenols in accordance to the principle of Green Chemistry.

2.3.1.2 Effect of mobile phase and mobile phase additive

Since the mobile phase composition has a profound effect upon the spacing (selectivity) of chromatographic peaks, the most effort in the development of the analytical method focused on this criterion. In a series of preliminary experiments, a gradient elution mode was found preferable. Therefore, two types of mobile phases were applied for this mode. Eluent A (aqueous phase) consisted of water and mobile phase additives including acetic acid (AcOH), formic acid (FA), trifluoroacetic acid (TFA) or heptafluorobutyric acid (HFBA). These mobile phase additives were also employed in eluent B (organic phase) which used ACN, MeOH, EtOH or IPA as organic solvents. In order to enhance miscibility of eluent A and eluent B in the mixing chamber, EtOH or IPA was mixed with water at a ratio of 4 to

1 volume/volume. The polyphenol separations were evaluated by the peak shape and peak width obtained from RP-HPLC. For this purpose, a polyphenolic test mixture composed of ten standards including gallic acid, (±)-catechin, chlorogenic acid, caffeic acid, ferulic acid, *p*-coumaric acid, rutin, (*E*)-resveratrol, morin and quercetin was employed. The peaks were monitored simultaneously at 280 nm, 320 nm and 370 nm with a DAD detector.

Different types of mobile phase additives (AcOH, FA, TFA or HFBA) were used in a range of 5 mM - 25 mM to investigate their effect on the separation performance of polyphenolic compounds in the reversed-phase HPLC system. The low concentrations of mobile phase additives were applied to maintain a certain pH in the mobile phase and to assist the ionisation of polyphenols. The concentration of mobile phase additive was expressed in mM instead of the percentage (%, v/v) value in order to enable direct comparisons of the effectiveness of the four acid modifiers. Initially, 10 mM was chosen to separate simultaneously the ten polyphenols from the test mixture. Further investigations on the effect of mobile phase additives at different concentrations will be described later in **Section 2.3.1.3**.

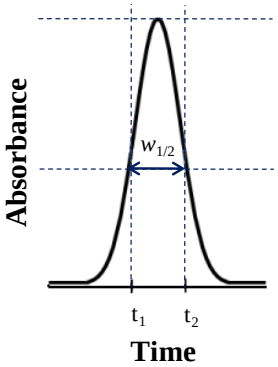

Figure 2.3: Peak width at half height.

Various mobile phases and different types of mobile phase additives were used to investigate the peak efficiency of caffeic acid based on the measurement of the peak width at half height ($w_{1/2}$). The $w_{1/2}$ is the distance measurement between each side of peak at half height (*8*) and is generally employed to assess the quality of the chromatographic operating conditions **(Figure 2.3)**. A smaller value of $w_{1/2}$ indicates a better peak shape. The $w_{1/2}$ was measured on the peak of caffeic acid ***(d)*** due to its consistent symmetric peak shape under all conditions.

Figure 2.4 shows the combination of mobile phases and mobile phase additives used in this study. The results showed that IPA/H_2O (4:1, v/v) with HFBA is the best match based on the smallest value of $w_{1/2}$ (0.26) obtained. However, the usage of IPA as a mobile phase led to a high back-pressure in RP-HPLC systems because of its high viscosity (2.86 centipoise) whilst HFBA is a relatively expensive and toxic fluorinated acid. The second best option based on the $w_{1/2}$ measurements was the combination of ACN with FA ($w_{1/2}$ = 0.30) or ACN with AcOH ($w_{1/2}$ = 0.30). Despite the popularity of ACN as an organic mobile phase modifier in reversed-phase chromatography, this solvent has several disadvantages including being toxic, costly and susceptible to supply shortage. The mixture of EtOH/H_2O (4:1, v/v) with FA or

EtOH/H_2O (4:1, v/v) with TFA gave similar results with regard to the $w_{1/2}$ ($w_{1/2}$ = 0.32), respectively. TFA is well suited for reversed-phase HPLC applications as it improves peak shape and resolution but it has negative effects on MS detection. Its high surface tension prevents efficient spray-formation, which consequently suppresses the ionisation and reduces the MS signal (*9*, *10*). Based on these considerations, a combination of EtOH/H_2O (4:1, v/v) with FA was chosen as they were compatible with MS/MS and their use was in accordance with the principles of Green Chemistry.

The elution behaviours of eight polyphenols in different types of mobile phases with 10 mM FA can be seen in **Figure 2.5**. Early eluting peaks were observed (following the increasing elution order) with **(A)** IPA/H_2O (4:1, v/v) < **(B)** ACN < **(C)** EtOH/H_2O (4:1, v/v) < **(D)** methanol. (*E*)-Resveratrol ***(h)*** was found to co-elute with morin ***(i)*** when ACN was employed whilst when using MeOH, (*E*)-resveratrol ***(h)*** overlapped with rutin ***(g)***. Separation of polyphenols in ACN resulted in peak fronting for rutin ***(g)*** whilst in IPA/H_2O (4:1, v/v) ferulic acid ***(e)*** was found unresolved. When MeOH was employed as a mobile phase, long analysis times and late eluting peaks were observed. From these investigations, EtOH/H_2O (4:1, v/v) and 10 mM FA was selected as a successful environmentally benign combination of mobile phase and mobile phase additive for the further optimisation of polyphenol separation protocols.

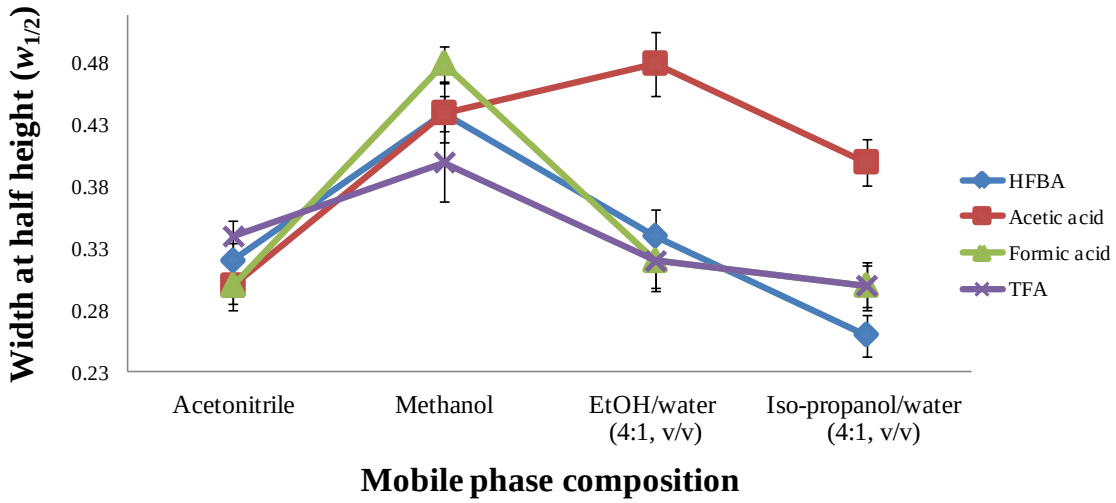

Figure 2.4: Influence of different types of mobile phases as eluent B (acetonitrile, methanol, EtOH/H_2O (4:1, v/v) or *iso*-propanol/H_2O (4:1, v/v)) with HFBA, acetic acid, formic acid or TFA (10 mM concentration each) as mobile phase additives on peak width at half height, $w_{1/2}$ of caffeic acid. LC gradient: 0-2 min to 10% (v/v) B, 2-52 min to 70% (v/v) B, 52-53 min to 10% (v/v) B; flow rate: 0.5 mL/min; 5 µL injection. Measurements were determined in duplicate (n = 2). Error bars indicate the standard error expressed by the formula $Error=\sigma/\sqrt{n}$, where σ is the standard deviation and n is the number of measurements.

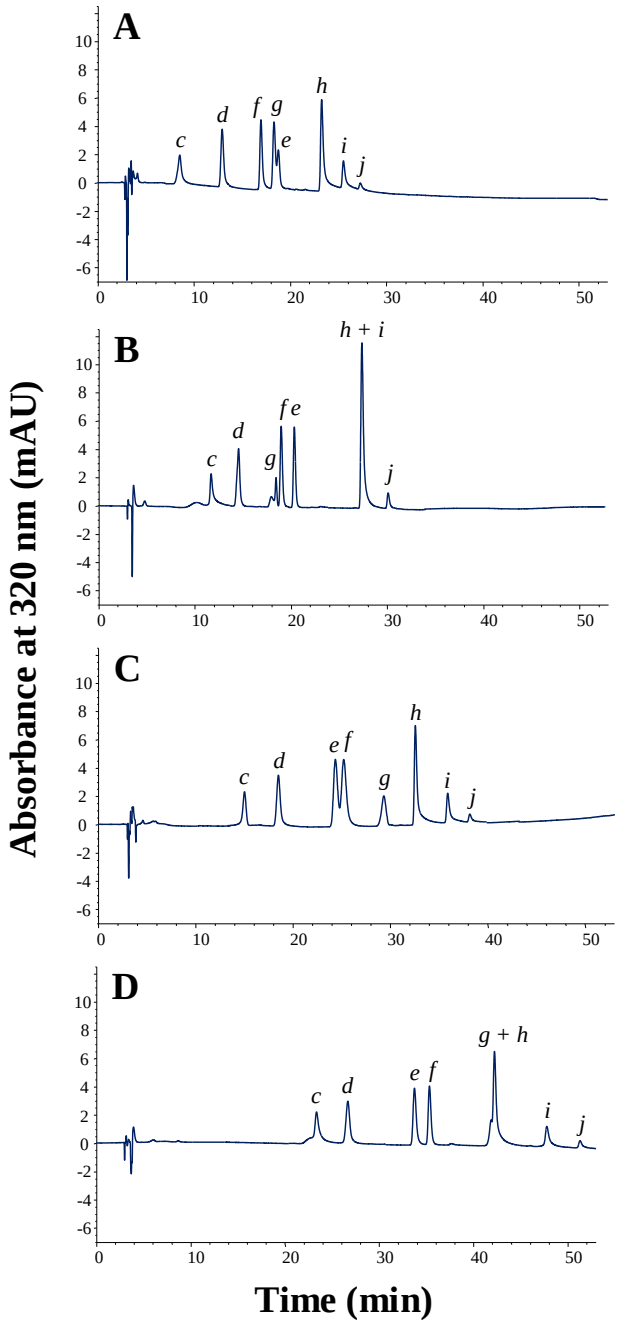

Figure 2.5: Effect of four types of mobile phases including **(A)** *iso*-propanol/water (4:1, v/v); **(B)** acetonitrile; **(C)** ethanol/water (4:1, v/v) or **(D)** methanol with 10 mM formic acid on RP-HPLC retention behaviour of a mixture of eight polyphenol standards consisted of ***(c)*** chlorogenic acid, ***(d)*** caffeic acid, ***(e)*** ferulic acid, ***(f)*** *p*-coumaric acid, ***(g)*** rutin, ***(h)*** (*E*)-resveratrol, ***(i)*** morin and ***(j)*** quercetin at a concentration of 0.01 mM for each component by RP-HPLC. The chromatograms were obtained after RP-HPLC separation on a Zorbax Eclipse XDB C_{18} column (4.6 mm × 150 mm, 5 µm particle size) at 20 °C. LC conditions: eluent A: 10 mM of formic acid in water, eluent B: IPA/H_2O (4:1, v/v), ACN, EtOH/H_2O (4:1, v/v) or MeOH with 10 mM of formic acid in; gradient: 0-2 min to 10% (v/v) B, 2-52 min to 70% (v/v) B, 52-53 min to 10% (v/v) B; flow rate: 0.5 mL/min; 5 µL injection. All the chromatograms were monitored at the wavelength of 320 nm using a DAD detector.

2.3.1.3 Impact of concentrations of the mobile phase additive and column temperatures

Based on the experiments in **Section 2.3.1.2**, formic acid (FA) was selected as the most suitable mobile phase additive for the method development of polyphenols separations. Instead of 10 mM in the preliminary work, five concentrations of FA (5 mM, 10 mM, 15 mM, 20 mM and 25 mM) in eluent B consisting of EtOH/H_2O (4:1, v/v) were employed at different temperatures to assess separation performance of the chromatographic system for a polyphenol mixture. The measurement was based on the $w_{1/2}$ of caffeic acid ***(d)***. The common trend for all formic acid concentrations showed an increase of the $w_{1/2}$ as the temperature was elevated to 50 °C - 60 °C **(Figure 2.6)**.

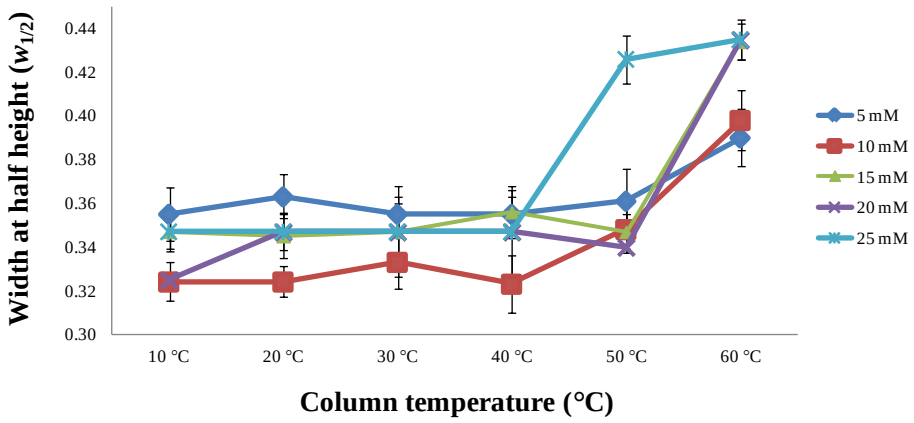

Figure 2.6: Effect of different concentrations of mobile phase additive on a Zorbax Eclipse XDB C_{18} column (4.6 mm × 150 mm, 5 µm particle size) at various column temperatures (10 °C, 20 °C, 30 °C, 40 °C, 50 °C and 60 °C) towards peak width at half height, $w_{1/2}$ of caffeic acid. LC conditions: eluent A: 10 mM of formic acid in water, eluent B: 5 mM to 25 mM of formic acid in EtOH/H_2O (4:1, v/v), gradient: 0-2 min to 10% (v/v) B, 2-52 min to 70% (v/v) B, 52-53 min to 10% (v/v) B; flow rate: 0.5 mL/min; 5 µL injection. Measurements were determined in duplicate (n = 2). Error bars indicate the standard error.

The lowest values of the $w_{1/2}$ were observed at a concentration of 10 mM FA at 10 °C, 20 °C and 40 °C ($w_{1/2}$ = 0.32, respectively). The highest values of $w_{1/2}$ were monitored for temperatures above 40 °C with 25 mM FA. In chromatographic separations, the peak efficiency often improves as the temperature increases due to the lower mobile phase viscosity (*11*). However, in the current case, an increase in the $w_{1/2}$-values for caffeic acid was observed for temperatures above 40 °C for all mobile phase additive concentrations. One possible reason for this increase in peak width at elevated temperatures might be associated with the decomposition of caffeic acid and a co-elution of this compound with its degradation product(s). Recent investigations have shown that caffeic acid is subject to decomposition in

organic solvents (*e.g.* MeOH and EtOH) at temperatures from 25 °C to 65 °C (*12*). Another possible reason for the increase in peak width may be the occurrence of *trans*/*cis*-isomerisation. In a previous study, Borges *et al.* (*13*) reported that caffeic acid predominantly occurs in nature in a *trans*-configuration which can be converted to the *cis*-form when exposed to sunlight or ultraviolet light. Therefore, 10 mM FA proved to be a suitable concentration for the mobile phase additive at column operation temperatures of ≤ 40 °C.

The effect of different temperatures from 10 °C to 60 °C on retention was also investigated. **Figure 2.7** only shows the chromatograms from 20 °C, 40 °C and 60 °C. As the temperature was increased by 10 °C in each separation (gradient unchanged), the polyphenol separations shifted toward lower retention times. The higher temperature resulted in faster compound elution but led to peak splitting, in particular for chlorogenic acid ***(c)*** and rutin ***(g)***. According to the column specification datasheet from the supplier, the maximum operating temperature is 60 °C. However to maintain a long column lifetime, the best operating temperature was suggested to be ≤ 40 °C. A high temperature was not considered beneficial for this work as it might deteriorate the non-polar bonded stationary phase of the column and might contribute to the degradation of polyphenolic compounds during the analysis. Hence, the optimal column temperature was demonstrated to be 20 °C (ambient temperature) whereby a baseline separation of polyphenols was observed. Moreover, this is the most energy-saving thus green temperature for a RP-HPLC separation.

2.3.1.4 Gradient mode

A simple linear gradient consisting of eluent A with 10 mM aqueous FA and eluent B consisting of 10 mM FA in EtOH/H_2O (4:1, v/v) was chosen for this work instead of a multi-stage gradient. The linear gradient was preferred due to greater reproducibility cycle by cycle and because of the nature of complex biological samples that contain a variable and/or unknown composition of substances of interest with a wide retention range. For a polyphenol sample, the linear gradient can perform better separations due to the continual increase of the elution strength throughout the gradient period, whilst a segmented gradient has the disadvantage of inconvenient complexity (*14*). In this work, a gradient program for eluent B: 0-2 min: 10% (v/v), 2-52 min: 10%-70% (v/v), 52-53 min: 10% (v/v) was employed. The linear gradient elution started with a very hydrophilic solvent (90% (v/v) aqueous) in order to

improve the separation of the earliest eluting very polar polyphenols (for example gallic acid). Then the solvent strength was increased gradually in order to separate flavonoid glycosides (*e.g.*, rutin) and eventually the aglycones (*e.g.*, quercetin). In this study, most polyphenols were eluted from the C_{18} reversed-phase column by 60% (v/v) eluent B. However, the gradient was extended to 70% (v/v) eluent B to ensure a complete elution of all substances from the column.

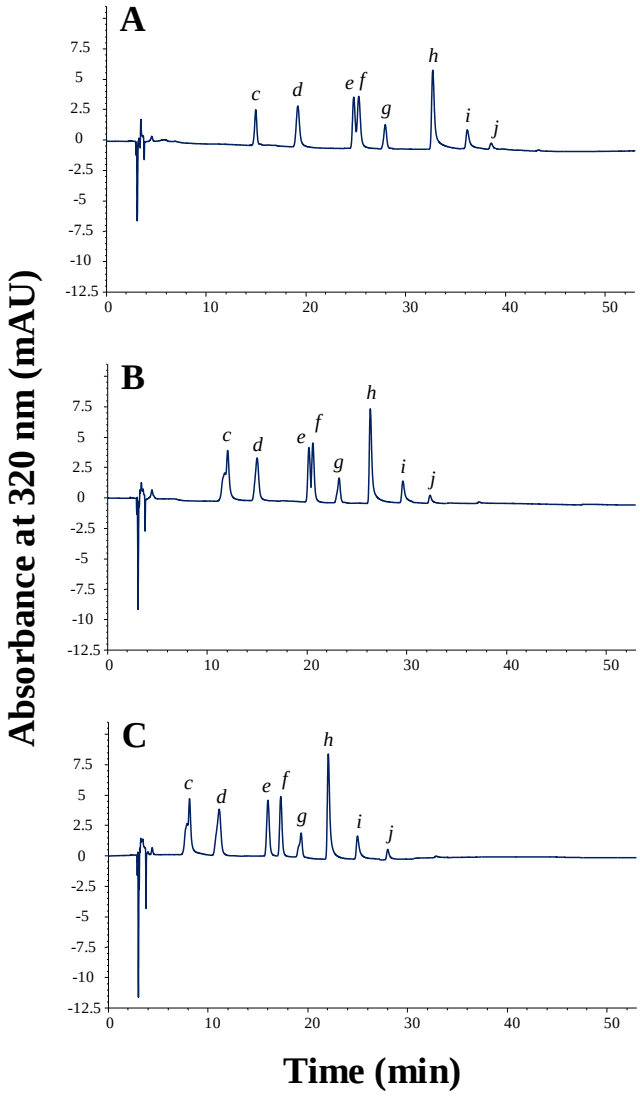

Figure 2.7: Impact of temperatures at **(A)** 20 °C, **(B)** 40 °C and **(C)** 60 °C on a mixture of eight polyphenol standards consisted of ***(c)*** chlorogenic acid, ***(d)*** caffeic acid, ***(e)*** ferulic acid, ***(f)*** *p*-coumaric acid, ***(g)*** rutin, ***(h)*** (*E*)-resveratrol, ***(i)*** morin and ***(j)*** quercetin (concentration of 0.01 mM for each component), measured by RP-HPLC. The chromatograms were obtained after RP-HPLC separation on a Zorbax Eclipse XDB C_{18} column (4.6 mm × 150 mm, 5 µm particle size). LC conditions: eluent A: 10 mM of formic acid in water, eluent B: 10 mM of formic acid in EtOH/H_2O (4:1, v/v); gradient: 0-2 min to 10% (v/v) B, 2-52 min to 70% (v/v) B, 52-53 min to 10% (v/v) B; flow rate: 0.5 mL/min; 5 µL injection. All the chromatograms were monitored at the wavelength of 320 nm using a DAD detector.

2.3.1.5 Concomitant detection of several polyphenol compounds

The experiments in this chapter **(Section 2.3.1.1 - 2.3.1.4)** demonstrated a successful separation method for ten polyphenols including the non-flavonoids and flavonoids (commonly found in grapes or other fruits), developed using a chromatographic optimisation methodology with environmentally benign chemicals. The various wavelengths used for the detection of the polyphenols are shown in **Table 2.1**. Component ***a*** and ***b*** were observed to give a higher absorbance at 280 nm. Component ***c***, ***d***, ***e***, ***f*** and ***h*** were shown to be best detected at the wavelength of 320 nm whilst component ***g***, ***i*** and ***j*** were better identified at the wavelength of 370 nm. In this work, the optimisation method for the separation of polyphenols was performed at the wavelength of 320 nm which corresponds to the maximum absorbance of (*E*)-resveratrol due to the polarised aromatic π-π electron interactions in the molecular structure (*15*). It is noteworthy to mention that eight components ***(c***, ***d***, ***e***, ***f***, ***g***, ***h***, ***i*** and ***j)*** could be identified at 320 nm using the herein developed RP-HPLC method. (*E*)-resveratrol ***(h)*** was well resolved under the linear gradient elution conditions with a retention time (t_R) of 32.7 min **(Figure 2.8)**.

Table 2.1: Polyphenol standards detected at various wavelengths with a DAD detector.

Component	Compound name	λ (nm)
a	Gallic acid	280
b	Catechin	280
c	Chlorogenic acid	320
d	Caffeic acid	320
e	Ferulic acid	320
f	*p*-Coumaric acid	320
g	Rutin	370
h	(*E*)-Resveratrol	320
i	Morin	370
j	Quercetin	370

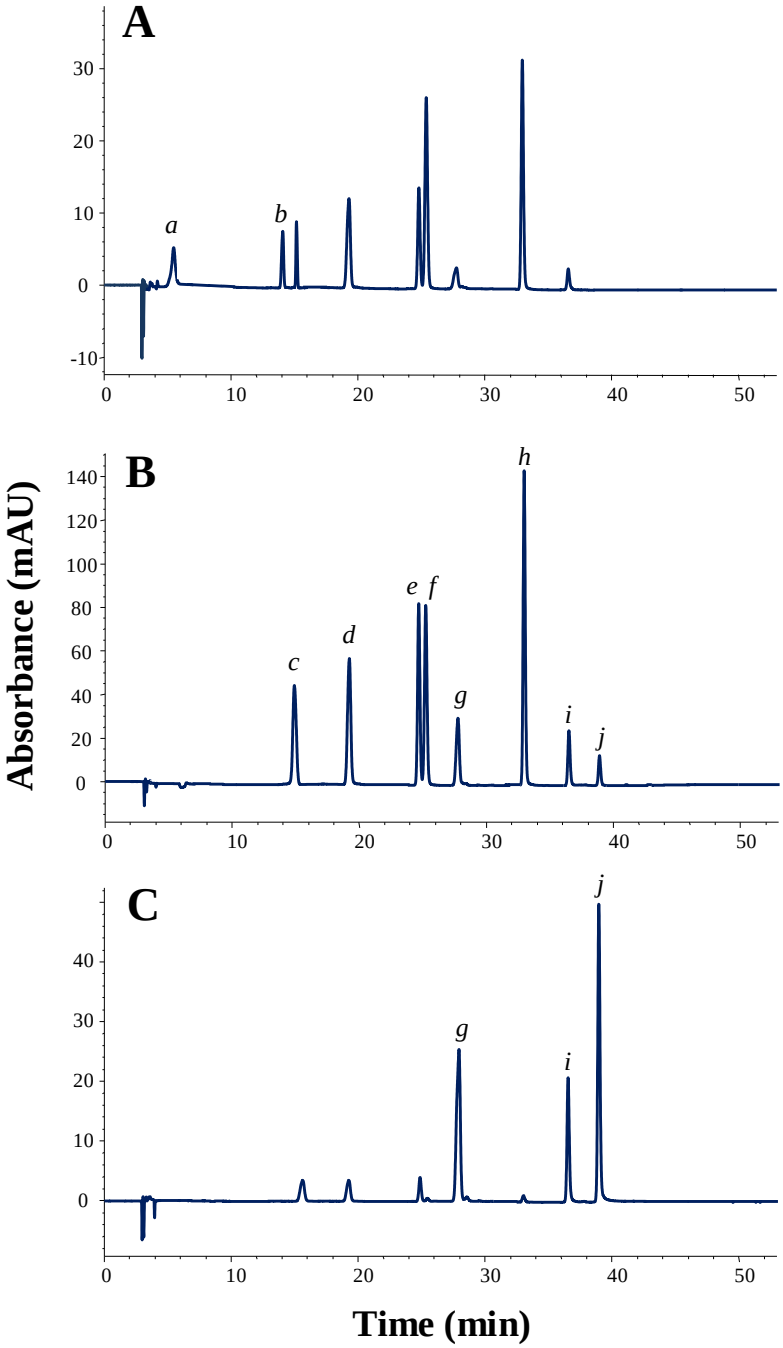

Figure 2.8: RP-HPLC chromatograms of a mixture of ten polyphenol standards monitored at the wavelength of **(A)** 280 nm, **(B)** 320 nm and **(C)** 370 nm consisting of ***(a)*** gallic acid, ***(b)*** (±)-catechin, ***(c)*** chlorogenic acid, ***(d)*** caffeic acid, ***(e)*** ferulic acid ***(f)*** *p*-coumaric acid, ***(g)*** rutin, ***(h)*** (*E*)-resveratrol, ***(i)*** morin and ***(j)*** quercetin at a concentration of 0.1 mM for each component, obtained with a Zorbax Eclipse XDB C_{18} column (4.6 mm × 150 mm, 5 µm particle size) at 20 °C. LC conditions: eluent A: 10 mM of formic acid in water, eluent B: 10 mM of formic acid in EtOH/H_2O (4:1, v/v); gradient: 0-2 min to 10% (v/v) B, 2-52 min to 70% (v/v) B, 52-53 min to 10% (v/v) B; flow rate: 0.5 mL/min; 5 µL injection.

2.3.2 Down-scaled method for LC-ESI ion trap MS/MS

2.3.2.1 MicroLC

The chromatographic conditions for LC-ESI ion trap MS/MS were established by applying a 'down-scaled' microLC method. By scaling down the chromatographic column dimensions using the same column chemistries, less solvent is needed to generate equivalent chromatographic separation compared to analytical LC. This approach can save time in method development and materials, as well as complying with the Green Chemistry principles. When the method was transferred from the analytical scale to micro-scale versions, the chromatographic conditions required some adjustments, especially for the injection volume and flow rate, to achieve equivalent separation conditions. Details about the column dimensions for an analytical LC and a microLC are shown in **Table 2.2**.

Table 2.2: Column dimensions of an analytical LC and microLC.

Column dimension	Analytical LC	MicroLC
Stationary phase	RP-C_{18}	RP-C_{18}
Length (mm)	150	150
Pore size (Å)	80	80
Surface area (m^2/g)	180	180
Internal diameter (mm)	4.6	0.3
Particle size (µm)	5.0	3.5

2.3.2.1.1 Adjusting the injection volume

The injection volumes were adapted to the column's internal diameter. Previously, 5 µL was chosen as the optimum volume for sample injection in the analytical RP-HPLC system, whereby the sample volume was kept as small as possible to avoid loss of resolution due to volume overloading. In order to determine an appropriate injection volume in microLC, **Equation 2.1** was used (*16*). Although the calculated injection volume using that equation was determined to be $V_{injection}$ = 0.02 µL, the minimum injection volume for this instrument was 0.1 µL. Thus, $V_{injection}$ = 0.1 µL was used for sample injection. The down-scale approach from an analytical RP-HPLC to a microLC method resulted in a reduction of the sample injection volume by a factor of 50.

$$V_{micro} = \left[\frac{r_{micro}}{r_{analytical}}\right]^2 \times V_{analytical}\ , \qquad \textbf{Equation 2.1}$$

$$V_{micro} = \left[\frac{0.15\ \text{mm}}{2.3\ \text{mm}}\right]^2 \times 5\ \mu L = 0.02\ \mu L\ ,$$

where V is the volume of injection (µL) and r is the internal column radius (mm) of the analytical or micro column.

2.3.2.1.2 Adjusting the flow rate

In the RP-HPLC method used previously, the flow rate of 0.5 mL/min provided the best resolution and most reproducible results for a 150 mm long analytical column. When down-scaling the method from an analytical LC to a microLC with the same column length, the flow rate must be adjusted to maintain comparable linear velocity through a capillary column with smaller internal diameter. The flow rate is defined as the volume of mobile phase which travels over a certain period of time (*8*). Based on the formula as described in **Equation 2.2** (*16*), the flow rates was determined to be 2 µL/min. In this case, the flow rate in the microLC method was decreased by a factor of 250 compared to that of the RP-HPLC method.

$$F_{micro} = \left[\frac{r_{micro}}{r_{analytical}}\right]^2 \times F_{analytical} \times C_L\ , \qquad \textbf{Equation 2.2}$$

$$F_{micro} = \left[\frac{0.15\ \text{mm}}{2.3\ \text{mm}}\right]^2 \times 0.5\ mL/min \times \left[\frac{150\ mm}{150\ mm}\right] = 2.13 \times 10^{-3} mL/\text{min} = 2.13\ \mu L/min,$$

where F is the flow rate (mL/min), r is the column internal diameter or column radius (mm) of the analytical or micro column and C_L is the column length ratio.

2.3.2.2 LC-MS/MS ionisation mode

The identification and characterisation of polyphenols was performed using LC-ESI ion trap MS/MS either in the positive or in the negative ionisation mode. The ten polyphenols were better identified using the negative ionisation mode **(Figure 2.9-A)** with more structurally informative results compared to the positive ionisation mode. The polyphenols are weakly acidic compounds, suggesting that their dissociation is easier than their protonation. This was clearly shown when the positive ionisation mode **(Figure 2.9-B)** was used, whereby caffeic

acid ***(4)*** was not fully ionised, *p*-coumaric acid ***(6)*** was not resolved properly, rutin ***(7)*** showed severe peak tailing and (*E*)-resveratrol ***(8)*** exhibited poor baseline separation.

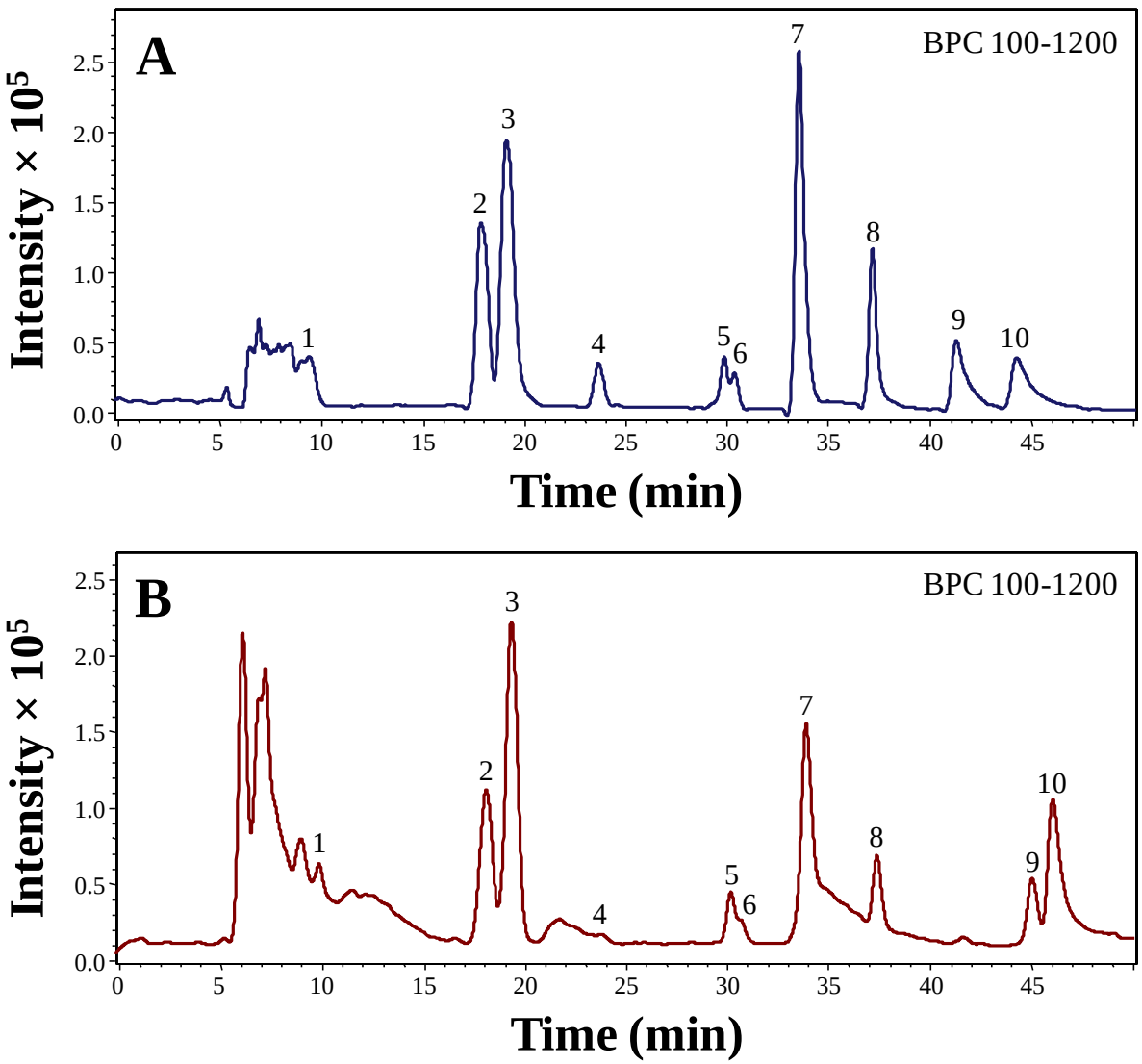

Figure 2.9: Base peak chromatograms (BPC) of a mixture of ten polyphenol standards containing ***(1)*** gallic acid, ***(2)*** (±)-catechin, ***(3)*** chlorogenic acid, ***(4)*** caffeic acid, ***(5)*** ferulic acid, ***(6)*** *p*-coumaric acid ***(7)*** rutin, ***(8)*** (*E*)-resveratrol, ***(9)*** morin and ***(10)*** quercetin. The chromatograms were obtained after LC-ESI ion trap MS/MS separation on a Zorbax XDB C_{18} capillary column (0.3 mm × 150 mm, 3.5 µm particle size) in the *m/z* range of 100-1200 using the **(A)** negative ionisation mode or **(B)** positive ionisation mode at 20 °C. LC conditions: eluent A: 10 mM of formic acid in water, eluent B: 10 mM of formic acid in EtOH/H_2O (4:1, v/v), gradient: 0-2 min to 10% (v/v) B, 2-52 min to 70% (v/v) B, 52-53 min to 10% (v/v) B; flow rate: 2 µL/min; 0.1 µL injection.

2.3.2.3 MS/MS of (E)-resveratrol

(*E*)-resveratrol ***(compound 8)*** was detected by LC-ESI ion trap MS/MS in the negative ionisation mode to give a precursor ion $[M-H]^-$ at *m/z* 226.7 **(Figure 2.10)**. This precursor ion then lost a CHCOH group (42 mass units) through deprotonation on the phenol ring by hydrogen rearrangement in the MS to yield a product ion at *m/z* 185.4. This diradical anion is believed to then undergo successive structural rearrangement to generate the stable anion (*m/z* 185.4). The latter underwent fragmentation to form two product ions at *m/z* 157.0 and 142.7 due to the loss of CO (28 mass units) and C_2H_2O (42 mass units), respectively (*17*).

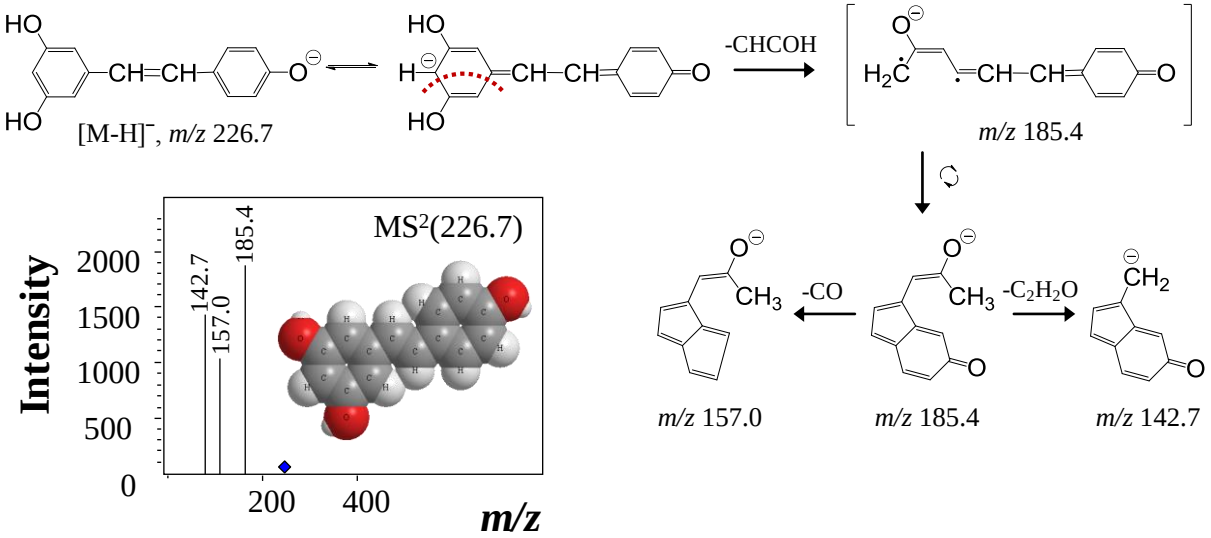

Figure 2.10: MS/MS fragmentation spectrum for (*E*)-resveratrol obtained with LC-ESI ion trap MS/MS in the negative ionisation mode, its space fill model and proposed fragmentation pathway. The diamond (♦) symbol shows the position of the residual precursor ion.

2.3.3 MISPE as a method of polyphenol enrichment

2.3.3.1 Development and optimisation

There have been a number of publications previously related to the use and optimisation of MISPE for polyphenols analysis in biological or food samples. For instance, Molinelli *et al.* (*18*) described the MISPE experimental protocols for the extraction of quercetin from red wine using ACN as a wash solvent and a very high percentage of AcOH (15%, v/v) in MeOH as an eluting solvent. Blahova *et al.* (*19*) reported a MISPE method for the selective extraction

of catechin in green tea using a mixture of ACN/H_2O in the wash steps followed by eluting steps with pure MeOH. Although the high extraction recoveries were achieved in both examples, the use of toxic and harmful solvents remained an environmental concern. Thus, this work aimed to develop a benign extraction protocol to capture (*E*)-resveratrol *via* MISPE technique with a high recovery using a greener solvent.

2.3.3.1.1 MISPE protocol

The first part of the MISPE work in the off-line mode was devoted to the development of an extraction procedure for (*E*)-resveratrol in four steps: (i) conditioning of the MIP sorbent in the SPE cartridge, (ii) sample loading, (iii) optimisation of the wash step to remove the components non-specifically bound to the cartridge and (iii) optimisation of the elution step in order to quantitatively recover (*E*)-resveratrol from the MISPE cartridge.

The MIP was produced in the Centre for Green Chemistry as described previously in **Section 2.2.4**. The MIP or NIP stationary phase (1.0 g) was packed into a large SPE cartridge, the dimensions of which were 2.8 cm in diameter × 13.5 cm in length, resulting in sorbent bed height of 0.5 cm. Vacuum was not applied in the MISPE process, the solvent dripped through the MIP cartridges under gravity flow to allow sufficient reaction time between the target analyte and the MIP cavities in the polymer network. In order to mimic the conditions of a wine sample (with typical alcohol content between 10% (v/v) and 15% (v/v)) a mixture containing EtOH/H_2O (15:85, v/v) was applied to both, the MIP and NIP cartridge. This conditioning step is necessary to wet the MIP and to provide an effective contact surface of the MIP particles to maximise the binding interactions with subsequently applied aqueous sample containing the target analyte.

The MISPE procedure was initially tested with an (*E*)-resveratrol standard solution at a concentration of 0.1 mM (5 mL) with several types of loading solvents including MeOH, ACN and EtOH in order to optimise the sample loading conditions. However, when using these neat solvents for sample loading, small amounts of the target analytes were detected in the MIP breakthrough fractions. Therefore, sample loading with neat solvents was not preferable. When the (*E*)-resveratrol standard (110.2 µg) was dissolved in a mixture of EtOH/H_2O (15:85, v/v) at a concentration of 0.1 mM (5 mL) and passed through the MISPE cartridge, the target compound was not observed in the breakthrough fraction which demonstrated that the MIP cartridge was not overloaded with excessive amount of

(*E*)-resveratrol as well as capable to absorb the target compound. The removal of non-selectively bound compounds was then investigated using EtOH at 50% (v/v) and 80% (v/v) in water with 1% (v/v) AcOH as wash solvents. The acetic acid functions as a hydrogen bond disruptor to remove non-specifically bound or entrapped (*E*)-resveratrol from NISPE cartridge. When using 50% (v/v) EtOH in water with 1% (v/v) AcOH **(Figure 2.11-A)**, almost similar amounts of (*E*)-resveratrol were removed from the MISPE and NISPE cartridges after wash and elution stages with EtOH/AcOH (9:1, v/v) were applied. Therefore, the MISPE protocol needed further optimisation to selectively retain (*E*)-resveratrol in the MIP cartridge but enable removal of non-specifically bound (*E*)-resveratrol from the NIP during the wash stage.

To solve the problem, increasing the EtOH proportion to 80% (v/v) in water with 1% (v/v) AcOH **(Figure 2.11-B)** was implemented. Most of the non-selectively bound compound was removed from the NISPE cartridge during the wash stage whilst (*E*)-resveratrol was successfully retained in the MISPE cartridge (75.5 µg/g polymer) prior to the elution step. The elution was successfully performed with EtOH/AcOH (9:1, v/v) and resulted in a selective recognition of (*E*)-resveratrol (MIP-NIP = 65.4 µg/g polymer). The recovery of (*E*)-resveratrol from MIP was 98.5% whilst 95.8% from NISPE cartridge.

Thereafter, to be able to re-use the MISPE cartridge, a conditioning step with EtOH/AcOH (9:1, v/v) followed by the application of pure EtOH was performed to eliminate the possibility of any component being trapped in the polymer from previous extractions.

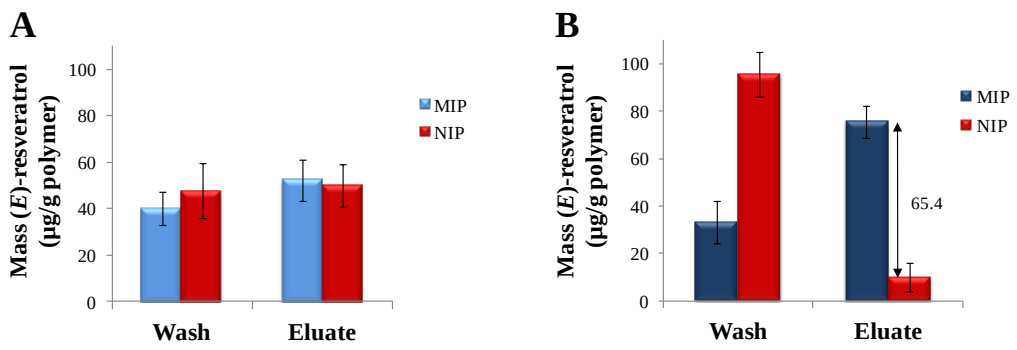

Figure 2.11: The performance of MISPE or NISPE to isolate (*E*)-resveratrol in the wash stages with **(A)** EtOH/H_2O (1:1, v/v) containing 1% (v/v) AcOH or **(B)** EtOH/H_2O (4:1, v/v) containing 1% (v/v) AcOH, prior to elution stages using EtOH/AcOH (9:1, v/v), measured by RP-HPLC. The MIP or NIP (1.0 gram, each) was packed into a large SPE cartridge (2.8 cm in diameter × 13.5 cm in length, sorbent bed height of 0.5 cm). The arrow and number represent the absolute mass difference of bound (*E*)-resveratrol between MIP and NIP. Measurements were determined in duplicate with two replicates (n = 4). Error bars indicate the standard error.

2.3.3.1.2 MISPE cartridge design

The second series of these optimisation experiments involved the modification of the MISPE cartridges. The MIP material (1.0 gram) was packed into a smaller polypropylene SPE cartridge (2.0 cm diameter × 8.7 cm length), which resulted in 2-fold higher sorbent bed of 1.0 cm in height **(Figure 2.12-A)** compared to a large SPE cartridge (2.8 cm diameter × 13.5 cm length) with a sorbent bed of 0.5 cm height **(Figure 2.12-B)**. The same MISPE procedures were implemented based on the previous experiments **(Section 2.3.3.1.1)** in order to compare and evaluate the selectivity and affinity of the MIP against NIP.

The MISPE or NISPE cartridge was loaded with 5 mL of an (*E*)-resveratrol standard solution (0.1 mM, 103.1 µg) using a mixture of EtOH/H_2O (15:85, v/v). The majority of (*E*)-resveratrol was retained in the MIP binding sites after wash steps with 80% (v/v) EtOH in water containing 1% (v/v) AcOH. In contrast, most of the (*E*)-resveratrol was removed from the NISPE cartridge during the wash stages as the non-selective bound materials. The elution steps with 10% (v/v) AcOH in EtOH resulted in 85.0 µg/g polymer of (*E*)-resveratrol to be eluted from the MISPE cartridge. The total recovery of (*E*)-resveratrol from the MISPE cartridge was determined to be 99.5% whilst 99.2% from the NISPE cartridge. The overall performance of the MIP packed into the small SPE cartridge (MIP-NIP = 78.7 µg/g polymer) **(Figure 2.13)** was superior to that of the large SPE cartridge (MIP-NIP = 65.4 µg/g polymer) **(Figure 2.11-B)** with regards to the amount of (*E*)-resveratrol eluted after MISPE and NISPE treatment. The differences in the (*E*)-resveratrol recognition from the same amount of MIP sorbent (1.0 gram) can be attributed to the different heights of the beds. Since the superficial velocities of the fluids are different with the two columns, the residency times will be different. Longer residency times will favour greater retention of the template at the loading/wash stages and kinetically favour higher sample loadings for the narrower columns. The results demonstrated the MIP's ability to retain and ultimately concentrate (*E*)-resveratrol from an aqueous solution *via* an environmentally friendly MISPE protocol.

These two different sizes (large and small design) of MISPE or NISPE cartridges that were packed with the small amount (1.0 gram) of MIP or NIP particles were reused throughout the period of this study which indicated that the MISPE cartridges were robust and could withstand extreme conditions of different solvents and pH, without any apparent loss of binding capacity at room temperature. The reusable cartridge features could be an efficient way to decrease the cost of sample analysis.

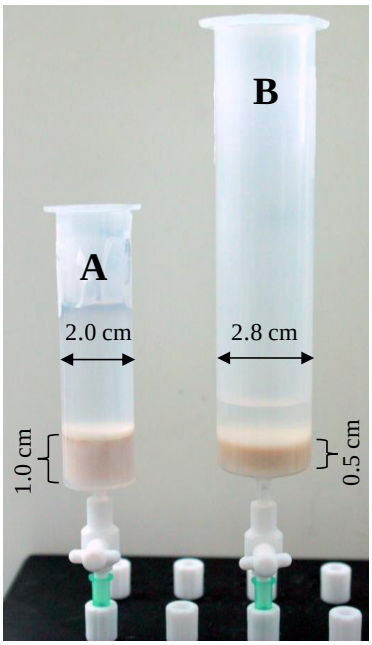

Figure 2.12: **(A)** MIP sorbent bed of 1.0 cm height in the small SPE cartridge (2.0 cm diameter × 8.7 cm length); **(B)** MIP sorbent bed height of 0.5 cm in the large SPE cartridge (2.8 cm diameter × 13.5 cm length). All of the SPE cartridges were packed with 1.0 gram of MIP particles.

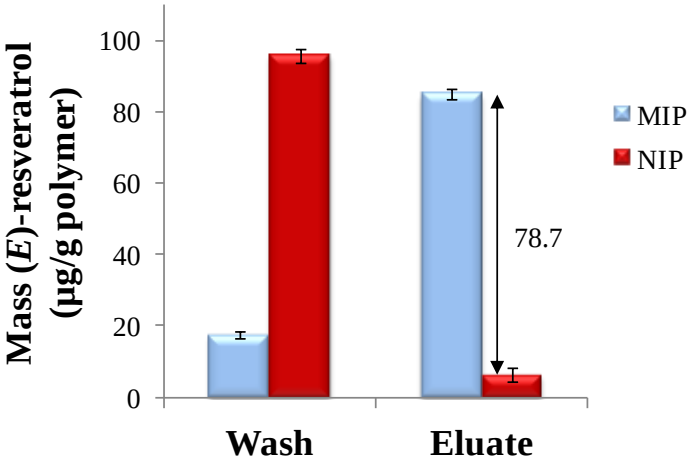

Figure 2.13: The performance of 1.0 gram MISPE or NISPE material packed into the small SPE cartridge (2.0 cm diameter × 8.7 cm length) to selectively uptake (*E*)-resveratrol in the wash stage with EtOH/H_2O (4:1, v/v) containing 1% (v/v) AcOH and elution stage with EtOH/AcOH (9:1, v/v). The arrow and number represent the absolute mass difference of bound (*E*)-resveratrol between MIP and NIP. Measurements were determined in duplicate (n = 2). Error bars indicate the standard error.

2.4 Conclusions

This chapter presents a new method to separate ten standard polyphenols under the application of benign chemicals and tools according to the principle of Green Chemistry, as it employed a mixture of ethanol-water and a low concentration of formic acid at ambient temperature for the RP-HPLC analysis. A down-scale was performed to microLC-MS/MS with minimal solvent usage and waste. LC-ESI-MS/MS was proven to be effective in the negative ionisation mode for the peak identity confirmation of ten important polyphenols. The mass spectrometric identification was demonstrated with the example of (*E*)-resveratrol. The application of a newly developed MIP in SPE format was optimised in terms of size of the SPE cartridge, loading, wash and elution stages with suitable benign solvents for the selective enrichment of (*E*)-resveratrol. The comparison of MIP and control NIP demonstrated the MIP contained effective imprinting sites. This optimised chromatographic microLC separation and MISPE methodology will be applied for the analysis of health-beneficial phenolic compounds from the complex matrices of wine **(Chapter 3)** and grape byproducts **(Chapter 4** and **6)**.

2.5 References

1. Merken, H. M.; Beecher, G. R., Measurement of food flavonoids by high performance liquid chromatography: a review. *J. Agric. Food Chem.* **2000**, *48*, 577-599.
2. Hearn, M. T. W.; Langford, S.; Tuck, K. L.; Harris, S.; Boysen, R. I.; Perchyonok, V. T.; Danylec, B.; Schwarz, L.; Chowdhury, J. Molecularly imprinted polymers. 2010-AU882010085851, 20100129., **2010**.
3. Schwarz, L. J.; Danylec, B.; Harris, S. J.; Boysen, R. I.; Hearn, M. T. W., Preparation of molecularly imprinted polymers for selective recognition of bioactive polyphenol, (*E*)-resveratrol. *J. Chromatogr., A* **2011**, *1218*, 2189-2195.
4. Mane, C.; Souquet, J. M.; Olle, D.; Verries, C.; Veran, F.; Mazerolles, G.; Cheynier, V.; Fulcrand, H., Optimization of simultaneous flavanol, phenolic acid, and anthocyanin extraction from grapes using an experimental design: application to the characterization of Champagne grape varieties. *J. Agric. Food Chem.* **2007**, *55*, 7224-7233.
5. Weingerl, V.; Strlic, M.; Kocar, D., Comparison of methods for determination of polyphenols in wine by HPLC-UV/Vis, LC-MS/MS and spectrophotometry. *Acta Chim. Slov.* **2009**, *56*, 698-703.
6. Gavrilova, V.; Kajdzanoska, M.; Gjamovski, V.; Stefova, M., Separation, characterization and quantification of phenolic compounds in blueberries and red and black currants by HPLC-DAD-ESI-MS^n. *J. Agric. Food Chem.* **2011**, *59*, 4009-4018.
7. Chen, N. N.; Zhao, S. C.; Deng, L. G.; Guo, C. Y.; Mao, J. S.; Zheng, H.; Yang, G. S.; Lu, X.; Aboul Enein, H. Y., Determination of five polyphenols by HPLC-DAD and discrimination of apple varieties. *Chromatographia* **2011**, *73*, 595-598.
8. Snyder, L. R.; Kirkland, J. J.; Glajch, J. L., Practical HPLC method development. *John Wiley & Sons, New York, USA* **1997**, *Second Edition*, p 211.

9. Wang, G.; Cole, R. B., Effects of solvent and counterion on ion pairing and observed charge states of diquaternary ammonium salts in electrospray ionization mass spectrometry. *J. Am. Soc. Mass Spectrom.* **1996**, *7*, 1050-1058.
10. Temesi, D.; Law, B., The effect of LC eluent composition on MS responses using electrospray ionization. *LC-GC* **1999**, *17*, 626-629.
11. Lee, S. T.; Olesik, S. V., Comparison of enhanced fluidity and elevated temperature mobile phases in reversed-phase high-performance liquid chromatography. *Anal. Chem.* **1994**, *66*, 4498-4506.
12. Sun, Y.; Qiao, L.; Ye, X.; Liu, D.; Zhang, X.; Huang, H., The sonodegradation of caffeic acid under ultrasound treatment: relation to stability. *Molecules* **2013**, *18*, 561-573.
13. Borges, M. F. M.; Pinto, M. M. M., Isocratic high-performance liquid chromatography separation of esculetin and *cis-trans* isomers of caffeic acid. *J. Liq. Chromatogr.* **1989**, *12*, 2345-2354.
14. Temerdashev, Z. A.; Frolova, N. A.; Kolychev, I. A., Determination of phenolic compounds in medicinal herbs by reversed-phase HPLC. *J. Anal. Chem.* **2011**, *66*, 407-414.
15. Allan, K. E.; Lenehan, C. E.; Ellis, A. V., UV light stability of cyclodextrin/resveratrol host guest complexes and isomer stability at varying pH. *Aust. J. Chem.* **2009**, *62*, 921-926.
16. Boysen, R. I.; Hearn, M. T. W., Modern methods in natural product chemistry: high-performance chromatography separation methods, in: Comprehensive Natural Products Chemistry II, Chemistry and Biology. *Elsevier, Oxford* **2010**, *9*, 5-49.
17. Stella, L.; De Rosso, M.; Panighel, A.; Dalla Vedova, A.; Flamini, R.; Traldi, P., Collisionally induced fragmentation of $[M-H]^-$ species of resveratrol and piceatannol investigated by deuterium labelling and accurate mass measurements. *Rapid Commun. Mass Spectrom.* **2008**, *22*, 3867-3872.
18. Molinelli, A.; Weiss, R.; Mizaikoff, B., Advanced solid-phase extraction using molecularly imprinted polymers for the determination of quercetin in red wine. *J. Agric. Food Chem.* **2002**, *50*, 1804-1808.
19. Blahova, E.; Lehotay, J.; Skacani, I., The use of molecularly imprinted polymer for selective extraction of (+)-catechin. *J. Liq. Chromatogr. Relat. Technol.* **2004**, *27*, 2715-2731.

Chapter 3

Rapid molecularly imprinted solid-phase extraction for the analysis of resveratrol and other polyphenols from red wine

Abstract

The phytoalexin (*E*)-resveratrol has attracted considerable interest due to its remarkable pharmacological activity and for its potential in the prevention of various human diseases such as cancer and cardiovascular disorders. (*E*)-resveratrol (*trans*-3,5,4'-trihydroxystilbene) occurs in grapes, wines and other grape dietary products. Due to the low concentrations of (*E*)-resveratrol in food and the compositional complexity of food, the isolation of (*E*)-resveratrol normally requires several extraction and separation steps. Thus, the current investigation aimed to develop a new green methodology for the extraction, identification and quantification of (*E*)-resveratrol and structurally related polyphenols from red wine using molecularly imprinted solid-phase extraction (MISPE) coupled with capillary-reversed-phase high-performance liquid chromatography (capRP-HPLC) and tandem mass spectrometry (ESI-MS/MS). Tandem mass spectrometry afforded the identification of the phenolic compounds before and after MISPE treatment thereby generating information on the selectivity of the MIP. This information was then used to refine the MISPE protocol such that recovery of up to 99% (*E*)-resveratrol from an Australian Pinot noir wine sample was achieved. This investigation has demonstrated the application of advanced analytical LC-MS methods for the development of an efficient and reliable MISPE protocol for (*E*)-resveratrol and catechin/epicatechin derivatives for red wine polyphenol analysis. Furthermore, this study provides scope for the development of beverage analysis and enrichment of food compounds with nutraceuticals isolated and concentrated form natural sources.

Table of Contents

3.1 Introduction

The beneficial biological effects on human health from moderate consumption of red wine as typified by the 'French paradox' phenomenon (*1*) had been attributed to its polyphenolic content and their metabolites. Red wine was reported to contain a significant amount of polyphenols including resveratrol, catechin and procyanidin in comparison to white wine (*2*). This is related to the polyphenol contents of red grapes and the length of interaction of the red grape skins and seeds with the must during the fermentation process (*3, 4*). In white wine production, the skins and seeds are removed before fermentation thus resulting in a lower level of polyphenols after extraction (*5*). Amongst the polyphenols present in red wines and grapes, the phytoalexin (*E*)-resveratrol (*trans*-3,4',5-trihydroxystilbene) has attracted considerable interest because of its nutraceutical properties (*6*) in the prevention of various human diseases such as cancer and cardiovascular disorders (*7-9*). The increased awareness of the beneficial impact of (*E*)-resveratrol upon human health and the challenges posed by its low and variable concentrations in highly complex samples has driven the need for the development of a rapid and reliable method for (*E*)-resveratrol analysis in grapes, wine and other dietary sources.

An effective way to address these challenges is with molecularly imprinted polymers (MIPs), which are used for the solid-phase extraction (SPE) of targeted compounds from wine samples prior to analysis. Several applications of such molecularly imprinted solid-phase extractions (MISPE) for the analysis of wines have been developed, *e.g.* to determine off-flavour contaminants including ethylphenol and 2,4,6-trichloroanisole (*10*), and to assess the flavonoids (*11-13*) quercetin and rutin (*13*).

Existing methods for the analysis and detection of (*E*)-resveratrol and other phenolic compounds in plant derived samples (either before or after MISPE pre-concentration) have predominantly employed high-performance liquid chromatography (HPLC) with diode array detection (DAD). This study aims at an enhanced sensitivity and capacity for peak identification through the development of an environmentally friendly aqueous MISPE sample preparation technique in combination with HPLC and electrospray ionisation mass spectrometry (ESI-MS/MS) for the rapid analysis of (*E*)-resveratrol and related polyphenols from a red wine represented herein by an Australian Pinot noir.

3.2 Materials and Methods

3.2.1 Reagents, standards and instrumentation

For reagents, standards and instrumentation conditions, see **Chapter 2 (Section 2.2)**.

3.2.1.1 (E)-Resveratrol calibration curve

The calibration curve for (*E*)-resveratrol was constructed through serial dilution of the (*E*)-resveratrol stock solution with EtOH covering a concentration range of 2.4×10^{-4} - 5.0×10^{-1} mM. The standard curve was calculated by linear regression according to the formula $y = mx + b$, where y is the peak area obtained after RP-HPLC, x is the concentration of (*E*)-resveratrol (mg/L), m is the slope and b is the intersection near to the origin (~0.0). The equation for the resulting calibration curve was $y = 68.8x$ with a correlation factor (R^2) of 0.9. The limit of detection (LOD) (multiplying the standard deviation (SD) by a factor of 3) and the limit of quantitation (LOQ) (10 times the SD) for (*E*)-resveratrol were determined to be 8.9×10^{-3} mg/L and 2.9×10^{-2} mg/L, respectively.

3.2.2 Sample preparation

The Pinot noir red wine (vintage 2012) from the Mornington Peninsula winery (Victoria, Australia) was stored at 4 °C in a 50 mL plastic centrifuge tube and sealed with parafilm. The wine sample in the tube was protected against sunlight using aluminium foil to minimise light-induced isomerisation of resveratrol (*14*). For RP-HPLC or LC-ESI ion trap MS/MS experiments, the red wine sample was centrifuged for 10 min at 4000 rpm at 20 °C and the supernatant used for analysis.

3.2.3 MISPE procedure

The MISPE and NISPE cartridges (2.0 cm diameter × 8.7 cm length) were conditioned (in sequence) with EtOH/AcOH (9:1, v/v), EtOH and EtOH/H_2O (15:85, v/v) (3 × 5 mL), respectively. The red wine supernatant (5 mL) was loaded onto the MISPE or NISPE cartridge, respectively. The MISPE or NISPE cartridge was washed with EtOH/H_2O (9:1, v/v) containing 1% (v/v) AcOH (4 × 5 mL) followed by elution with EtOH/AcOH (9:1, v/v)

(10 × 5 mL). Both cartridges were reconditioned in sequence with H_2O, EtOH and EtOH/H_2O (15:85, v/v) (3 × 5 mL), respectively. In the case of more complex samples, an additional wash step with 0.1 mM NaOH in water was introduced.

3.3 Results and Discussion

Several series of experiments were carried out using different types of red wine samples (vintage 2010 to 2012) including Pinot noir and Shiraz sourced from Victoria, Australia. The main objectives of these experiments were to develop the optimal MISPE procedure with such complex samples like wine in terms of appropriate amount of sample loading, washing solvent and elution solvent compositions. Initially, the MISPE optimisation procedure with wine was performed in a larger cartridge (2.8 cm diameter × 13.5 cm length) which resulted in a lower binding affinity in comparison to the results with a smaller cartridge (2.0 cm diameter × 8.7 cm length), in accordance with the observations made with the resveratrol standard in **Chapter 2 (Section 2.3.3.1.2)**. Due to the substantial amounts of data obtained during the wine analysis, only the relevant results are reported in this chapter.

A previously described MIP (*15, 16*) capable of the pre-concentration of (*E*)-resveratrol from peanut press waste was used for the first time to analyse wine (Australian Pinot noir vintage 2012) *via* an off-line MISPE application. The determination of (*E*)-resveratrol was performed with a Pinot noir, as the grapes of this variety had been reported to contain higher concentrations of (*E*)-resveratrol compared to other varieties (*7*).

3.3.1 Analysis of (*E*)-resveratrol from red wine by RP-HPLC

The supernatant of red wine sample was injected directly into a RP-HPLC system. The peak numbering for the chromatograms obtained from RP-HPLC and LC-ESI ion trap MS/MS was synchronised. (*E*)-Resveratrol **(peak 29)** was identified at a retention time (t_R) of 32.7 min by comparing its characteristic absorbance wavelength spectra and chromatographic retention times with the standard reference **(peak 5)** using RP-HPLC **(Figure 3.1-front)**. The concentration of (*E*)-resveratrol was determined to be 7.8 mg/L in the sample based on a linear (*E*)-resveratrol standard calibration curve, which was consistent with common values in the literature for red wines (*2, 17*). The MISPE treatment exhibited highly selective binding affinity for (*E*)-resveratrol and demonstrated the adsorption of this compound onto the

imprinted binding sites **(Figure 3.1-back)**. Further explanation about the identification of polyphenols in red wine or after treatment by MISPE will be provided later in **Section 3.3.3**.

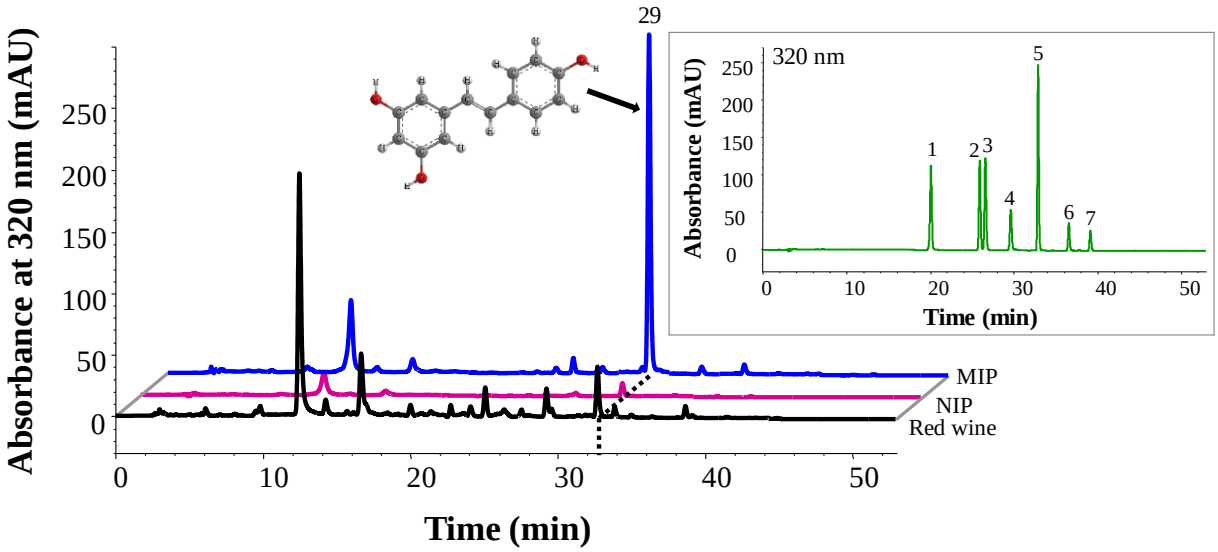

Figure 3.1: RP-HPLC chromatograms recorded at a wavelength of 320 nm for the quantification of (*E*)-resveratrol (t_R = 32.7 min, **peak 29**) in Pinot noir red wine sample (front chromatogram), after MISPE (back chromatogram) and NISPE (middle chromatogram) treatment. Inserted is a RP-HPLC chromatogram of a standard mixture of seven polyphenols (**1**: caffeic acid; **2**: ferulic acid; **3**: *p*-coumaric acid; **4**: rutin; **5**: (*E*)-resveratrol; **6**: morin; **7**: quercetin) at a concentration of 0.1 mM, recorded at 320 nm. The chromatograms were separated on a Zorbax Eclipse XDB C_{18} column (4.6 mm × 150 mm, 5 µm particle size) at 20 °C. LC conditions: eluent A: 10 mM formic acid in water, eluent B: 10 mM formic acid in EtOH/H_2O (4:1, v/v), gradient: 0-2 min to 10% (v/v) B, 2-52 min to 70% (v/v) B, 52-53 min to 10% (v/v) B; flow rate: 0.5 mL/min; 5 µL injection.

3.3.2 MISPE with red wine sample

An Australian Pinot noir red wine sample (5 mL) determined to contain 39.0 µg of (*E*)-resveratrol was MISPE pre-treated with the optimised conditions developed to enhance the analysis of (*E*)-resveratrol, and other similarly structured polyphenol components. After the wine sample was loaded onto the MISPE cartridge, the breakthrough fraction showed the absence of (*E*)-resveratrol, whilst some of the target analyte was observed in the breakthrough from the NISPE cartridge (0.1 µg). The washing step with a mixture of EtOH/ H_2O (4:1, v/v) containing 1% (v/v) AcOH resulted in the near total removal of all components including (*E*)-resveratrol (37.4 µg) from the NISPE control cartridge thus indicating that various non-selectively bound wine components had been displaced. In contrast, a large proportion of (*E*)-resveratrol (82.6%) was retained on the MISPE cartridge presumably due to the

complimentary shape and functionality of the resveratrol imprinted MIP binding sites. Elution of the MISPE cartridge with EtOH/AcOH (9:1, v/v) afforded a significantly greater yield of (*E*)-resveratrol (32.2 µg) in comparison to the NISPE cartridge (1.0 µg) with an imprinting factor (*IF* = MIP eluate/NIP eluate) of 32 and a similarly impressive concentration enrichment up to 32.2 mg/L (in the MISPE eluate) from 7.8 mg/L (on a mass and volume normalized basis). Total recovery of (*E*)-resveratrol MISPE treated wine sample was determined to be 99.7% **(Table 3.1)**. These results were reproducible with further wine samples upon regeneration of the MIP. The binding performance of MISPE and NISPE after washing and elution steps can be seen in **Figure 3.2**.

Table 3.1: The recovered amount of (*E*)-resveratrol (µg) in an Australian Pinot noir red wine after the washing steps (EtOH/H_2O (4:1, v/v) containing 1% (v/v) AcOH) followed by the elution steps (EtOH/AcOH (9:1, v/v) from SPE cartridge packed with 1.0 g of MIP and control NIP, respectively.

		(*E*)-Resveratrol (µg)	
		MISPE	**NISPE**
Untreated sample	Sample loading (1 × 5 mL)	39.0	39.0
	After washing steps (4 × 5 mL)	6.7	37.4
Fractions	After elution steps (10 × 5 mL)	32.2	1.0
	Total amount after washing and elution steps	38.9	38.4
Total recovery (%)		99.7	98.5

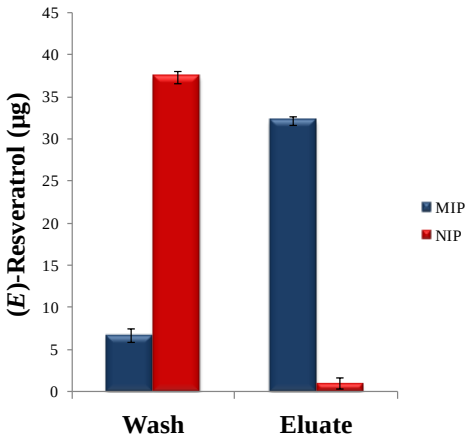

Figure 3.2: Amounts of (*E*)-resveratrol (µg) captured from the Pinot noir red wine sample in wash or elution fractions of MISPE and NISPE cartridges. Measurements were determined in duplicate (n = 2). Error bars indicate the standard error expressed by the formula $Error = \sigma/\sqrt{n}$, where σ is the standard deviation and n is the number of measurements.

3.3.3 Identification of (*E*)-resveratrol as well as other polyphenols from red wine

3.3.3.1 Before MISPE treatment

In total, 33 polyphenols including (*E*)-resveratrol **(peak 29)** with precursor ion $[M-H]^-$ at *m/z* 227.0 have been successfully identified by LC-ESI ion trap MS/MS in the Pinot noir red wine sample prior to MISPE treatment as shown in **Figure 3.3**. The gradient system was specifically chosen for phenolic compounds, and the broad peak in the base peak chromatogram with the retention time between 8 min to 10 min represents weakly retained components. **Table 3.2** displays the most characteristic product ion/(s) based on the *m/z* value observed for each compound obtained by MS/MS fragmentation from the precursor ion $[M-H]^-$ in the wine sample.

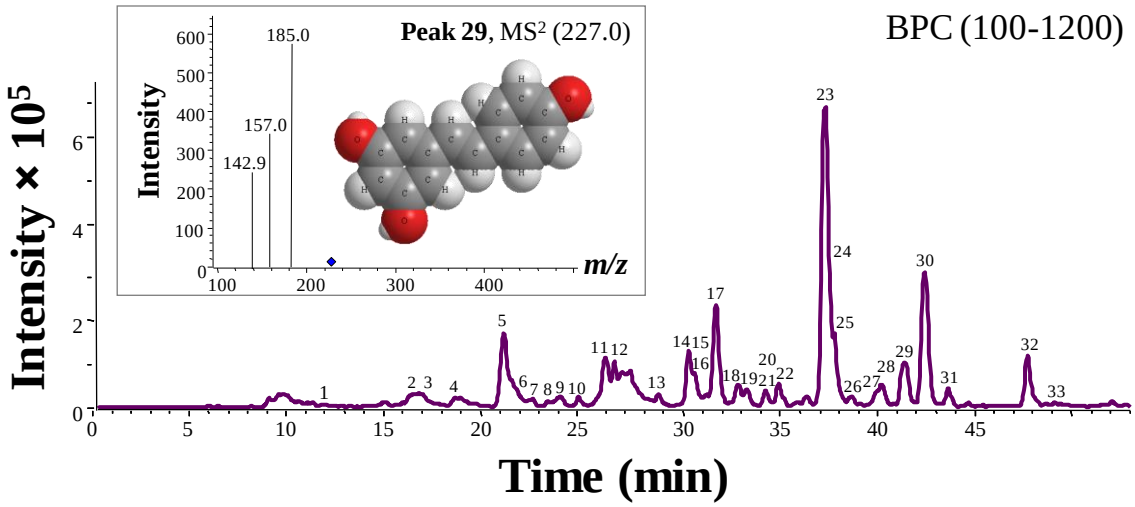

Figure 3.3: Base peak chromatogram (BPC) of a Pinot noir red wine sample in the *m/z* range from 100-1200 in the negative ionisation mode by LC-ESI ion trap MS/MS. (*E*)-Resveratrol **(peak 29)** was eluted at t_R= 41.5 min. Peak identification of compounds **(1)-(33)** are summarised in **Table 3.2**. Inserted is a MS/MS spectrum at *m/z* 227.0 for **peak 29** displaying the fragmentation pattern for (*E*)-resveratrol in the sample. The chromatogram was obtained after RP-HPLC on a Zorbax XDB C_{18} capillary column (0.3 mm × 150 mm, 3.5 µm particle size) at 20 °C. LC conditions: eluent A: 10 mM formic acid in water, eluent B: 10 mM formic acid in EtOH/H_2O (4:1, v/v), gradient: 0-2 min to 10% (v/v) B, 2-52 min to 70% (v/v) B, 52-53 min to 10% (v/v) B; flow rate: 2 µL/min; 0.1 µL injection.

Table 3.2: Characterisation of polyphenols from the Pinot noir red wine analysed in the *m/z* range from 100-1200 using the negative ionisation mode by LC-ESI ion trap MS/MS based on the elution order in **Figure 3.3**.

Peak No.	Compound name	t_R (min)	Precursor ion $[M-H]^-$, *m/z*	Observed product ion(s), *m/z*	Ref. [a]
1	Gallic acid	11.5	169	125	(*18*)
*2	B-type procyanidin	16.3	577	451, 425, 407, 289	(*19*)
3	B-type procyanidin trimer	16.7	865	739, 713, 695, 577, 289	(*20*)
4	Caftaric acid	18.1	311	179	(*21*)
5	(±)-Catechin	20.8	289	245, 205, 179	(*22*)
*6	B-type procyanidin	21.6	577	451, 425, 407, 289	(*19*)
7	*p*-Coumaryl-3-*O*-glucoside	22.5	325	265, 187, 163, 145	(*23*)
8	Coutaric acid	22.9	295	163, 149	(*21*)
9	*p*-Coumaric acid	23.2	163	119	(*21*)
*10	B-type procyanidin	24.5	577	451, 425, 407, 289	(*19*)
11	(±)-Epicatechin	25.8	289	245, 205, 179	(*22*)
*12	B-type procyanidin	26.3	577	451, 425, 407, 289	(*19*)
13	Taxifolin-3-*O*-glucoside	28.9	465	303, 285	(*23*)
14	Myricetin-3-*O*-glucoside	30.3	479	355, 317, 299	(*24*)
15	Epicatechin-3-*O*-gallate	30.8	441	289, 169	(*25*)
16	Syringic acid	31.2	197	182, 153	(*18*)
*17	B-type procyanidin	31.5	577	451, 425, 407, 289	(*19*)
18	(*E*)-Piceid	32.9	389	227	(*26*)
19	Viniferin	33.2	453	359, 265	(*27*)
20	Piceatannol glucoside	34.1	405	243	(*28, 29*)
21	Taxifolin	34.2	303	285, 177, 125	(*30*)
22	Epigallocatechin	35.0	305	179, 125	(*31*)
23	(+)-Astilbin	37.2	449	303, 285, 151	(*32*)
24	Quercetin-3-*O*-glucuronide	37.5	477	301, 179, 151	(*24, 33*)
25	Laricitrin-3-*O*-glucoside	37.6	493	331, 316	(*34, 35*)
26	Epicatechin-ethyl dimer	38.8	605	451, 315, 289, 245, 205	(*36, 37*)
27	Syringetin-3-*O*-glucoside	39.8	507	355, 345	(*24, 35*)
28	(-)-Astilbin	40.1	449	303, 285, 151	(*32*)
29	**(*E*)-Resveratrol**	41.5	227	185, 157, 143	(*28*)
30	(*Z*)-Piceid	42.3	389	227	(*26*)
31	Quercetin-3-*O*-xyloside	43.5	433	301, 287, 179, 151	(*24*)
32	(*Z*)-Resveratrol	47.7	227	185, 157, 143	(*26*)
33	Quercetin	49.1	301	179, 151	(*22, 38*)

* Based on the MS/MS spectra, no further identification was possible;
[a] References which confirm precursor and product ion(s) for the particular compound.

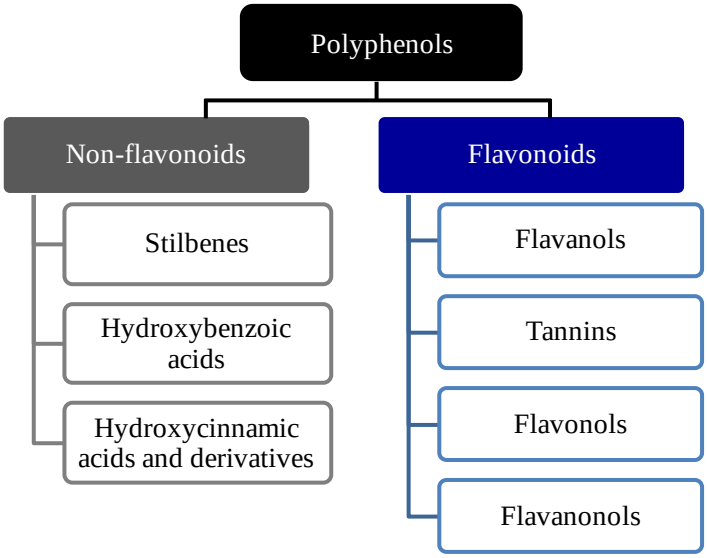

Figure 3.4: Classification of polyphenols in a red wine sample.

Polyphenols in the red wine sample were identified and characterised based on their two main categories, namely the non-flavonoids and flavonoids **(Figure 3.4)**. The non-flavonoid group includes stilbenes, hydroxybenzoic acids as well as hydroxycinnamic acids and derivatives. The flavonoid group represents flavanols, tannins, flavonols and flavanonols.

3.3.3.1.1 Non-flavonoids

i) Stilbenes

The peak identity confirmation of (*E*)-resveratrol **(peak 29**, **Figure 3.3)** at a retention time of 41.5 min was based on the precursor ion $[M-H]^-$ at *m/z* 227.0 and the obtained product ions. During collision-induced dissociation, a product ion at *m/z* 185.0 was generated due to the loss of CHCOH (42 mass units). This product ion underwent fragmentation to give rise to two characteristic product ions at *m/z* 157.0 and 142.9 corresponding to the loss of CO (28 mass units) and C_2H_2O (42 mass units), respectively. The fragmentation characteristic of this compound concurred with data in (*28*), and was verified using an (*E*)-resveratrol reference standard. The longer retention time of about 8 min observed for (*E*)-resveratrol obtained with the microLC-ESI MS system compared to that obtained with the analytical LC system can be primarily attributed to the difference in the gradient delay volumes of the two LC systems. The higher gradient delay volume of the microLC system is the direct result of the different models of autosampler used and the additional tubing required for connecting autosampler and column in the two-stack microLC system compared to the one-stack analytical LC system. In addition, the detection in the microLC system was performed with UV detection and MS detection in series, introducing an additional delay volume between UV detector and MS detector, whilst the detection in the analytical LC system was only performed with UV detection. Since the down-scaling method was performed under

consideration of the respective column dimensions of the analytical and the capillary column, the difference in column void volumes – after adjustment of the flow rates – is accounted for, assuming identical packing density for both sizes of columns. The *cis*-stereoisomer (*Z*)-resveratrol **(peak 32)** was also observed with similar fragmentation behaviour to the (*E*)-isomer but eluted with a longer retention time (47.7 min). It has been suggested that this is due to the proximity of the two phenol rings in the *cis*-configuration resulting in stronger hydrophobic interactions with the C_{18} stationary phase in the chromatographic system (*26, 39*). The occurrence of (*Z*)-resveratrol in the sample might be promoted by photo-isomerisation during the vinification process or bottling of wines (*17*). The resveratrol-3-*O*-glucoside (piceid) for the (*E*)- and (*Z*)-isomers were identified at the retention times of 32.9 min **(peak 18)** and 42.3 min **(peak 30)**, respectively. Both isomers had precursor ions $[M-H]^-$ at *m/z* 389 which fragmented by losing a neutral glucoside moiety $[M-C_6H_{11}O_5]^-$ to generate free resveratrol at *m/z* 227 (*26*). Viniferin, an oligomer of resveratrol, which is present in grape skins, was also identified in the wine sample at a t_R of 33.2 min **(peak 19)**. Although viniferin has not been as extensively investigated as (*E*)-resveratrol, this compound is a bioactive polyphenol with reported pharmacological properties (*40*). Presumably this compound was generated during the fermentation process, and identification was based on the precursor ion $[M-H]^-$ at *m/z* 453. Viniferin underwent fragmentation to generate product ions at *m/z* 359 due to the loss of hydroxybenzene $[M-C_6H_5O-H]^-$, and at *m/z* 265 $[M-(C_6H_5O-H^-)-(C_6H_5O-H)^-]$ (*27*). Piceatannol glucoside (3,4,3',5'-tetrahydroxystilbene glucoside) was identified based on the precursor ion $[M-H]^-$ at *m/z* 405 **(peak 20)**, and this compound fragmented in the ion source by losing a glucoside moiety to form a characteristic product ion at *m/z* 243 (piceatannol) (*28, 29*).

ii) Hydroxybenzoic acids

Gallic **(peak 1)** and syringic **(peak 16)** acids were the main hydroxybenzoic acids identified in the wine sample. The typical loss of $[M-H-44]^-$ corresponding to the carboxylic acid moiety was observed for gallic acid. The fragmentation of syringic acid from the precursor ion $[M-H]^-$ at *m/z* 197 generated *m/z* 182 due to the loss of a CH_3 group $[M-H-15]^-$ (*18*).

iii) Hydroxycinnamic acids and their derivatives

Caftaric **(peak 4)** and coutaric **(peak 8)** acids were identified at the precursor ion $[M-H]^-$ of *m/z* 311 and *m/z* 295, respectively. These compounds fragmented *via* MS/MS experiments to

generate caffeic acid (*m/z* 179) and *p*-coumaric acid (*m/z* 163) due to the cleavage of the ester bond $[M-H-132]^-$ from their molecular structures, respectively (*21*). *p*-Coumaric acid **(peak 9)** was detected based on the presence of the precursor ion $[M-H]^-$ at *m/z* 163. The fragmentation of this compound was characterised by the loss of a CO_2 group $[M-H-44]^-$ (from the carboxylic acid function) to generate a product ion at *m/z* 119 (*21*). **Peak 7** revealed the presence of *p*-coumaryl glucoside at the precursor ion $[M-H]^-$ of *m/z* 325 (*23*). This compound underwent fragmentation to produce several characteristic product ions at *m/z* 265, 187 and 163. The latter signal was assigned as *p*-coumaric acid (*m/z* 163) caused by the breakdown of a glucoside moiety $[M-H-162]^-$.

3.3.3.1.2 Flavonoids

i) Flavanols

The presence of (±)-catechin **(peak 5)** and its stereoisomer (±)-epicatechin **(peak 11)** were confirmed with the precursor ions $[M-H]^-$ at *m/z* 289 (*22*). Both compounds showed the same fragmentation trends with several characteristic product ions at *m/z* 245, 205 and 179. The product ion at *m/z* 245 could be explained by a neutral loss of CO_2 $[M-H-44]^-$ (*41*), or from the loss of CH_2-CHOH-($[M-H-44]^-$) (*42*). The successive fragmentation of this *m/z* 245 ion generated two product ions at *m/z* 205 and 179, due to the elimination of the A-ring and B-ring in the flavanol structure. Although these two isomers were indistinguishable by mass spectrometry, they were identified by their different elution times. The peak identified as (±)-catechin was verified using a commercial reference standard at a retention time of 20.8 min.

Epicatechin-3-*O*-gallate **(peak 15)** was characterised based on the presence of the precursor ion $[M-H]^-$ at *m/z* 441 (*25*). After collision-induced dissociation, the product ions at *m/z* 289 (epicatechin monomer) and *m/z* 169 (gallic acid moiety) were observed resulting from the cleavage of ester bond. Epigallocatechin **(peak 22)** had a precursor ion $[M-H]^-$ at *m/z* 305. This compound was fragmented *via* MS/MS experiments to generate *m/z* 179 and 151, which is consistent with previous data (*31*).

ii) Tannins

Several peaks with the same precursor ions ($[M-H]^-$, *m/z* 577) and similar fragmentation patterns were encountered for the **peaks 2**, **6**, **10**, **12** and **17** at different retention times. They

were identified as epicatechin oligomers, commonly referred to as B-type procyanidins (*19*). A single C_4-C_8 or C_4-C_6 linkage tethers the monomer units together and several isomers exist depending on the α- or β-linkage configuration. The unequivocal identification of the B-type procyanidin isomers in the red wine sample was not possible with LC-MS/MS instrumentation in the absence of reference standards, however the MS/MS fragmentation of the precursor ion yielded several characteristic product ions at *m/z* 451, 425, 407 and 289. The main product ion was observed at *m/z* 451 corresponding to the loss of pyrogallol (126 mass units) from the flavonoid C-ring. Subsequent fragmentations occurred at the B-ring of this compound to generate the product ion at *m/z* 425 due to the loss of 152 mass units. This product ion (*m/z* 425) fragmented to produce *m/z* 407 through the elimination of water (18 mass units). The signal observed at *m/z* 289 characterised the catechin/epicatechin monomer.

In this sample, B-type procyanidin trimer **(peak 3)** was detected based on the precursor ion $[M-H]^-$ at *m/z* 865 (*20*). The MS/MS fragmentation generated several characteristic product ions at *m/z* 739 due to the loss of a pyrogallol unit (126 mass units), *m/z* 713, 695, 577 (procyanidin dimer) and 289 (catechin/epicatechin monomer).

iii) Flavonols

Myricetin-3-*O*-glucoside **(peak 14)** was identified based on the precursor ion $[M-H]^-$ at *m/z* 479 (*24*). This compound underwent fragmentation to yield the main product ion at *m/z* 317, corresponding to the myricetin aglycone due to the cleavage of a glucoside moiety $[M-H-162]^-$. **Peak 24** was characterised as quercetin-3-*O*-glucuronide by having the precursor ion $[M-H]^-$ ion at *m/z* 477 (*24, 33*). This compound was fragmented to generate the quercetin aglycone at *m/z* 301 as a consequence of the neutral loss of a glucuronide moiety (176 mass units). The successive fragmentation of the quercetin aglycone generated product ions at *m/z* 179 and 151. Although the majority of flavonols are found in grapes as *O*-glucosides and *O*-glucuronides with conjugation mainly occurring at the C_3 positions, in wines they exist in the aglycone form, as the glycosides are hydrolysed during fermentation and aging. However, the presence of quercetin-3-*O*-glucuronide in this red wine sample is consistent with findings of Castillo-Munoz *et al. (35),* which suggested this compound might be resistant to acid hydrolysis during wine making. The presence of precursor ion $[M-H]^-$ at *m/z* 433 (*24*) led to the identification of quercetin-3-*O*-xyloside **(peak 31)**. This compound

underwent fragmentation in the ion trap to generate a quercetin aglycone (*m/z* 301) due to the loss of a xyloside moiety $[M-H-132]^-$. **Peak 33** (quercetin) was observed at a longer retention time (49.1 min) in comparison to its corresponding glycosides (*38*). The identification of quercetin with the precursor ion $[M-H]^-$ of *m/z* 301 was validated with its standard reference. After MS/MS fragmentation, the product ions at *m/z* 179 and 151 were formed from the breakage of the heterocyclic C-ring (*22*).

The presence of laricitrin and syringetin glycosides (new types of flavonoids) was reported for the first time in 2007 by Castillo-Munoz and co-workers (*35*). Interestingly, laricitrin-3-*O*-glucoside and syringetin-3-*O*-glucoside appeared in this Pinot noir wine sample. Laricitrin-3-*O*-glucoside **(peak 25)** ($[M-H]^-$, *m/z* 493) showed an intense laricitrin aglycone peak at *m/z* 331 through the elimination of a glucoside moiety $[M-H-162]^-$ (*24, 34, 35*). Laricitrin was only found in red grape and this feature can be useful information for the taxonomic of grape cultivar. **Peak 27** with the precursor ion $[M-H]^-$ of *m/z* 507 (*24, 35*) revealed the presence of syringetin-3-*O*-glucoside which later fragmented to yield a product ion at *m/z* 345 due to the cleavage at the glucosidic-*O*-linkage $[M-H-162]^-$.

iv) Flavanonols

Astilbin found in wine (*43*) is gaining increasing attention since several studies continue to probe mechanisms of absorption, biotransformation and excretion of this dietary polyphenol for human health benefits (*44*). Like stilbenes, astilbin is possibly used by the grape as a phytoalexin for the protection against *Botrytis cinenera* infection (*32*). In this study, astilbin (also known as dihydroquercetin-3-*O*-rhamnoside) and its isomer were identified as **peak 23** and **peak 28**, respectively. These compounds had precursor ions $[M-H]^-$ at *m/z* 449. The loss of a rhamnoside moiety (146 mass units) from the precursor ion resulted in the formation of dihydroquercetin (*m/z* 303). The successive fragmentation occurred at *m/z* 303 by losing a neutral molecule of water (18 mass units) to produce *m/z* 285 (*32*). Taxifolin (dihydroquercetin) was assigned based on *m/z* 303, **peak 21** (*30*). Further fragmentation of this compound generated a product ion at *m/z* 285 due to the loss of water (18 mass units). Taxifolin-3-*O*-glucoside **(peak 13)** was assigned based on the precursor ion $[M-H]^-$ of *m/z* 465 (*23*). This compound showed the prominent characteristic product ions at *m/z* 303 corresponding to taxifolin after losing a unit of a glucose moiety $[M-H-162]^-$ and *m/z* 285, resulting from water elimination. Taxifolin has shown to inhibit ovarian cancer cell

growth (*45*), to have antiproliferative effects on breast cancer and enhances the efficacy of conventional antibiotics (*46*).

3.3.3.2 After MISPE treatment

A further aim of this study was to demonstrate that MISPE can be used to isolate a range of closely related structural analogues to (*E*)-resveratrol, so that this method could be used to rapidly identify other polyphenols in red wine and in other complex media. The separation of a number of polyphenols from MISPE and NISPE eluates, and their identification *via* LC-ESI-MS/MS are shown in **Figure 3.5**.

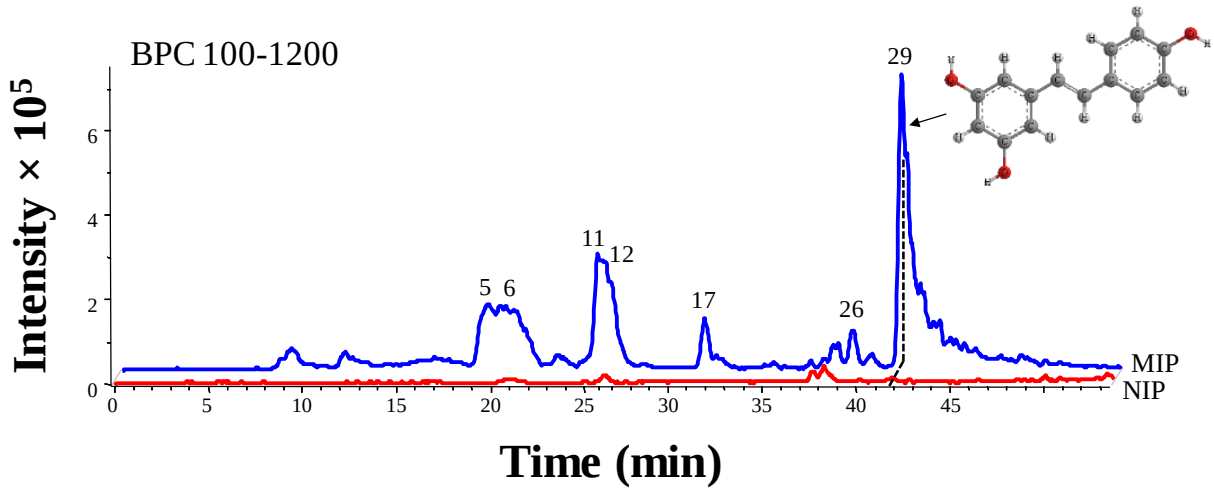

Figure 3.5: Base peak chromatograms (BPC) of a Pinot noir red wine sample when treated using either an (*E*)-resveratrol template MISPE (blue line, back chromatogram) cartridge or the corresponding NISPE (red line, front chromatogram) cartridge. Polyphenolic compound enrichments are summarised in **Table 3.3**. The chromatograms were obtained after RP-HPLC on a Zorbax XDB C_{18} capillary column (0.3 mm × 150 mm, 3.5 µm particle size) in the *m/z* range of 100-1200 using the negative ionisation mode by LC-ESI ion trap MS/MS at 20 °C. LC conditions: eluent A: 10 mM formic acid in water, eluent B: 10 mM formic acid in EtOH/H_2O (4:1, v/v), gradient: 0-2 min to 10% (v/v) B, 2-52 min to 70% (v/v) B, 52-53 min to 10% (v/v) B; flow rate: 2 µL/min; 0.1 µL injection.

As expected, the MISPE treatment resulted in a significantly enhanced concentration of the (*E*)-isomer of resveratrol **(peak 29)** compared to the (*Z*)-isomer **(peak 32)**. The capability of the MIP to selectively enrich (*E*)-resveratrol is strongly influenced by the number and position (*meta* and/or *para*) of hydroxyl-groups in the phenolic aromatic rings. Although (*Z*)-resveratrol has three hydroxyl-groups similar to the template molecule, the *cis*-structural feature is expected to result in steric hindrance. This will affect the interaction of the *meta*- and *para*-positioned hydroxyl-groups with the pyridine functional groups within the polymer

network, thereby leading to a reduced affinity towards the (*Z*)-isomer. The possible binding mechanisms for resveratrol isomers either in (*E*)- or (*Z*)-form are shown in 3-D molecular structures viewed from different angles (**Figure 3.6)**. It shows that precise MIP architectures can selectively recognise (*E*)-resveratrol and at the same time differentiate between the two isomers.

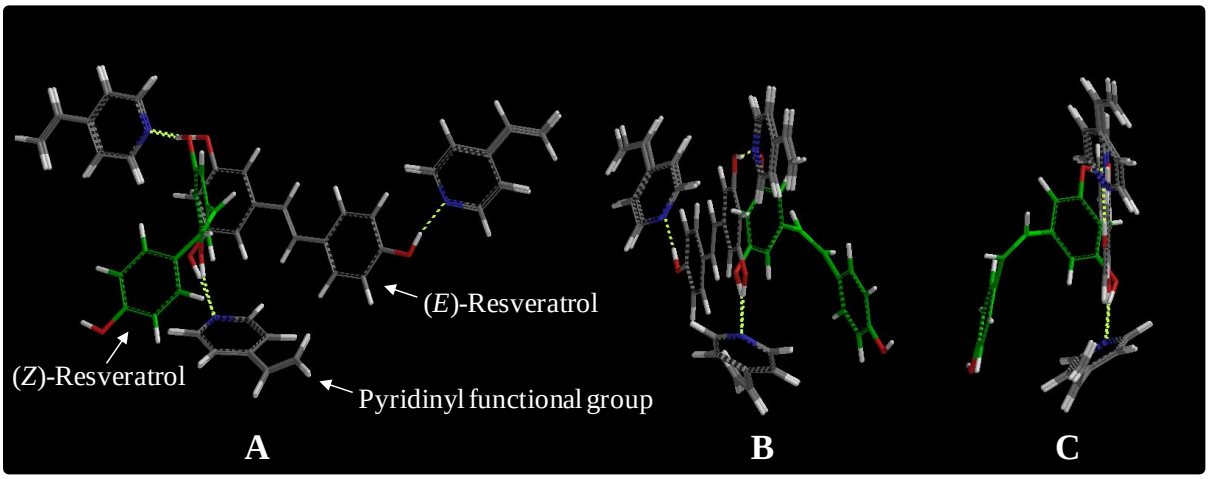

Figure 3.6: The possible binding recognition in 3-D molecular structures of (*E*)-resveratrol (grey) in relation to (*Z*)-resveratrol (green) viewed from **(A)** top angle; **(B)** and **(C)** side angles with pyridinyl functional groups to generate hydrogen bonding interactions. The dashed lines demonstrate OH---N hydrogen bonds. The images were produced using Spartan ′10 for Windows version 1.1.0 software package on a Pentium IV 2.0 GHz.

Several other red wine components were observed in the MISPE eluate. Notable were **peaks 5**, **6**, **11**, **12**, **17** and **26**, that obviously selectively interacted with the MIP stationary phase. These peaks were subsequently identified as both catechin and epicatechin isomers and derivatives thereof **(Figure 3.5**, **Table 3.2** and **Table 3.3)**. Details about the fragmentation characteristics for **peaks 5**, **6**, **11**, **12**, **17** and **29** were previously described in **Section 3.3.3.1**. The presence of catechin **(5)** and its stereoisomer epicatechin **(11)** were confirmed with the precursor ions $[M-H]^-$ at *m/z* 289 (*22*). Out of five B-type procyanidins, which were identified before MISPE treatment, three peaks **(6**, **12** and **17)** have been enriched after MISPE.

Compound **26** is most likely to be the epicatechin-ethyl dimer based on the presence of the precursor ion $[M-H]^-$ at *m/z* 605 (*36*). As described by Saucier *et al.* (*37*), the epicatechin-ethyl dimer is a condensed products of epicatechin with acetaldehyde corresponding to two units of epicatechin linked by an ethyl-bridge. According to He *et al.* *(47)*, acetaldehyde is the major aldehyde found in wine possibly from fermentation

intermediary products. It has been suggested that after the protonation of acetaldehyde in wine, the electrophilic substitution by acetaldehyde on the nucleophilic of C_6 or C_8 position of the A-ring flavanol resulted in the formation of condensation products.

The epicatechin-ethyl dimer underwent MS/MS fragmentation in the ion trap to generate several product ions at *m/z* 451, 315, 289, 245 and 205. The product ion observed at *m/z* 451 is possibly related to the fragmentation mechanism of the dimer. The signal of *m/z* 315 corresponds to a vinyl-catechin adduct due to the instability of the ethyl-bridge of catechin oligomers (*37*). The breakdown fragments of *m/z* 289 observed at *m/z* 245 and 205 were the characteristic fragmentation fingerprint similar to that for catechin/epicatechin.

These results demonstrated the polyphenols derived from catechin/epicatechin monomers possess a high affinity towards the resveratrol binding site in the MIP. The significant enrichment of catechin and epicatechin is of interest due to their roles as tannin precursors for wine sensory qualities. The occurrence of phenolic compounds in the MISPE eluate fraction possessing closely structural related traits to (*E*)-resveratrol may be due to the adoption of a conformation or orientation within the MIP binding sites which facilitates hydrogen bonding interactions of the appropriately positioned polyphenol substituents.

In addition, the overall size and shape of the target analytes appears to be important in generating their selectivity towards the MIP (*48*). For instance, the shape and bulky size of resveratrol glycosides with either (*E*)- or (*Z*)-configuration, as well as the shape of resveratrol oligomers resulted in their low affinity towards the MIP binding sites. The presence of a bulky glycoside unit is likely to prevent any favourable interactions between the phenolic *meta*- and *para*- hydroxyl-groups with the precisely positioned pyridinyl groups around the cavities. Similarly this may be the case for the resveratrol dimer viniferin, where the dimerization through one of the *meta*-positioned hydroxyl-groups creates a bulky group that could conceivably inhibit interactions between the molecules other hydroxyl-groups and the binding cavity. The molecular dimensions of B-type procyanidin are larger than that of (*E*)-resveratrol. This compound can be visualized as being made from two monomers of catechin/epicatechin, and due to their structural similarity and spatial complementarity with the resveratrol template, B-type procyanidins may be oriented in a way that one of the monomer units resides within the cavity. This would enable recognition through the generation of hydrogen bonding interactions with the surrounding pyridinyl-functionalities in the cavities and these interactions could be stabilised through secondary hydrophobic π-π or

Van der Waals interactions. This may explain the recognition of bulkier oligomer components of the Pinot noir red wines by this MIP.

Table 3.3: Polyphenol compounds detected in red wine, after MISPE and NISPE eluates, by LC-ESI-MS/MS with the ion current intensity > 0.5 × 10^5. Highlighted are compounds significantly enriched after MISPE treatment.

Peak No.	Compound name	Red wine	MISPE	NISPE
1	Gallic acid	✓	×	×
*2	B-type procyanidin	✓	*lc*	×
3	B-type procyanidin trimer	✓	×	×
4	Caftaric acid	✓	×	×
5	**(±)-Catechin**	✓	✓	*lc*
***6**	**B-type procyanidin**	✓	✓	*lc*
7	*p*-Coumaryl-3-*O*-glucoside	✓	×	×
8	Coutaric acid	✓	×	×
9	*p*-Coumaric acid	✓	×	×
*10	B-type procyanidin	✓	×	×
11	**(±)-Epicatechin**	✓	✓	*lc*
***12**	**B-type procyanidin**	✓	✓	×
13	Taxifolin-3-*O*-glucoside	✓	×	×
14	Myricetin-3-*O*-glucoside	✓	×	×
15	Epicatechin-3-*O*-gallate	✓	✓	×
16	Syringic acid	✓	×	×
***17**	**B-type procyanidin**	✓	×	×
18	(*E*)-Piceid	✓	×	×
19	Viniferin	✓	×	×
20	Piceatannol glucoside	✓	×	×
21	Taxifolin	✓	×	×
22	Epigallocatechin	✓	×	×
23	(+)-Astilbin	✓	*lc*	*lc*
24	Quercetin-3-*O*-glucuronide	✓	*lc*	*lc*
25	Laricitrin-3-*O*-glucoside	✓	×	×
26	**Epicatechin-ethyl dimer**	✓	*lc*	×
27	Syringetin-3-*O*-glucoside	✓	×	×
28	(-)-Astilbin	✓	×	×
29	**(*E*)-Resveratrol**	✓	✓	×
30	(*Z*)-Piceid	✓	×	×
31	Quercetin-3-*O*-xyloside	✓	×	×
32	(*Z*)-Resveratrol	✓	×	×
33	Quercetin	✓	×	×

* Based on the MS/MS spectra no further identification was possible;
lc Phenolic compound present at low concentration.

3.4 Conclusions

A new protocol for the extraction, detection and enrichment of (*E*)-resveratrol and other polyphenols from red wine was developed using a molecularly imprinted polymer as the stationary phase in an off-line SPE sample pre-treatment procedure. This procedure enabled the enrichment of (*E*)-resveratrol and the improved analysis, by way of significant sample clean up, of several structurally related polyphenols, most notably catechin and epicatechin and their derivatives. This method was established in accordance with the principles of Green Chemistry ensuring a rapid analysis, low energy consumption in the enrichment step, reusable separation polymers, and the use of environmentally benign solvents. Advancing the understanding of the recognition mechanisms and the potential of MIPs tailor-made for health-beneficial multiple phenolic or other targets should facilitate the development of generic MIP protocols for complex matrices of benefit to the food and nutraceuticals industries.

3.5 References

1. Renaud, S.; de Lorgeril, M., Wine, alcohol, platelets, and the French paradox for coronary heart disease. *Lancet* **1992**, *339*, 1523-1526.
2. Belitz, H. D.; Grosch, W.; Schieberle, P., Food Chemistry. *Springer* **2004**, 906-929.
3. Jeandet, P.; Bessis, R.; Gautheron, B., The production of resveratrol (3,5,4'-trihydroxystilbene) by grape berries in different developmental stages. *Am. J. Enol. Vitic.* **1991**, *42*, 41-46.
4. Ector, B. J.; Magee, J. B.; Hegwood, C. P.; Coign, M. J., Resveratrol concentration in muscadine berries, juice, pomace, purees, seeds, and wines. *Am. J. Enol. Vitic.* **1996**, *47*, 57-62.
5. Orea, J. M.; Montero, C.; Jimenez, J. B.; Urena, A. G., Analysis of *trans*-resveratrol by laser desorption coupled with resonant ionization spectrometry. Application to *trans*-resveratrol content in vine leaves and grape skin. *Anal. Chem.* **2001**, *73*, 5921-5929.
6. Bradamante, S.; Barenghi, L.; Villa, A., Cardiovascular protective effects of resveratrol. *Cardiovasc. Drug Rev.* **2004**, *22*, 169-188.
7. Stervbo, U.; Vang, O.; Bonnesen, C., A review of the content of the putative chemopreventive phytoalexin resveratrol in red wine. *Food Chem.* **2006**, *101*, 449-457.
8. Savouret, J. F.; Quesne, M., Resveratrol and cancer: a review. *Biomed. Pharmacother.* **2002**, *56*, 84-87.
9. Udenigwe, C. C.; Ramprasath, V. R.; Aluko, R. E.; Jones, P. J. H., Potential of resveratrol in anti-cancer and anti-inflammatory therapy. *Nutrition Reviews* **2008**, *66*, 445-454.
10. Garde-Cerdan, T.; Zalacain, A.; Lorenzo, C.; Alonso, J. L.; Salinas, M. R., Molecularly imprinted polymer-assisted simple clean-up of 2,4,6-trichloroanisole and ethylphenols from aged red wines. *Am. J. Enol. Vitic.* **2008**, *59*, 396-400.
11. Molinelli, A.; Weiss, R.; Mizaikoff, B., Advanced solid-phase extraction using molecularly imprinted polymers for the determination of quercetin in red wine. *J. Agric. Food Chem.* **2002**, *50*, 1804-1808.

12. Weiss, R.; Molinelli, A.; Jakusch, M.; Mizaikoff, B., Molecular imprinting and solid-phase extraction of flavonoid compounds. *Bioseparation* **2001**, *10*, 379-387.
13. Theodoridis, G.; Lasakova, M.; Skerikova, V.; Tegou, A.; Giantsiou, N.; Jandera, P., Molecular imprinting of natural flavonoid antioxidants: application in solid-phase extraction for the sample pretreatment of natural products prior to HPLC analysis. *J. Sep. Sci.* **2006**, *29*, 2310-2321.
14. Trela, B. C.; Waterhouse, A. L., Resveratrol: Isomeric Molar Absorptivities and Stability. *J. Agric. Food Chem.* **1996**, *44*, 1253-1257.
15. Schwarz, L. J.; Danylec, B.; Harris, S. J.; Boysen, R. I.; Hearn, M. T. W., Preparation of molecularly imprinted polymers for selective recognition of bioactive polyphenol, (*E*)-resveratrol. *J. Chromatogr., A* **2011**, *1218*, 2189-2195.
16. Schwarz, L. J.; Danylec, B.; Yang, Y.; Harris, S. J.; Boysen, R. I.; Hearn, M. T. W., Enrichment of (*E*)-resveratrol from peanut byproduct with molecularly imprinted polymers. *J. Agric. Food Chem.* **2011**, *59*, 3539-3543.
17. Lamuela-Raventos, R. M.; Romero-Perez, A. I.; Waterhouse, A. L.; de la Torre-Boronat, M. C., Direct HPLC analysis of *cis*- and *trans*-resveratrol and piceid isomers in Spanish red *Vitis vinifera* wines. *J. Agric. Food Chem.* **1995**, *43*, 281-283.
18. Kammerer, D.; Claus, A.; Carle, R.; Schieber, A., Polyphenol screening of pomace from red and white grape varieties (*Vitis vinifera* L.) by HPLC-DAD-MS/MS. *J. Agric. Food Chem.* **2004**, *52*, 4360-4367.
19. Sun, W.; Miller, J. M., Tandem mass spectrometry of the B-type procyanidins in wine and B-type dehydrodicatechins in an autoxidation mixture of (+)-catechin and (-)-epicatechin. *J. Mass Spectrom.* **2003**, *38*, 438-446.
20. Callemien, D.; Collin, S., Use of RP-HPLC-ESI(-)-MS/MS to differentiate various proanthocyanidin isomers in lager beer extracts. *J. Am. Soc. Brew. Chem.* **2008**, *66*, 109-115.
21. Maier, T.; Sanzenbacher, S.; Kammerer, D. R.; Berardini, N.; Conrad, J.; Beifuss, U.; Carle, R.; Schieber, A., Isolation of hydroxycinnamoyltartaric acids from grape pomace by high-speed counter-current chromatography. *J. Chromatogr., A* **2006**, *1128*, 61-67.
22. Bravo, M. N.; Silva, S.; Coelho, A. V.; Boas, L. V.; Bronze, M. R., Analysis of phenolic compounds in Muscatel wines produced in Portugal. *Anal. Chim. Acta* **2006**, *563*, 84-92.
23. Pussa, T.; Floren, J.; Kuldkepp, P.; Raal, A., Survey of grapevine *Vitis vinifera* stem polyphenols by liquid chromatography diode array detection tandem mass spectrometry. *J. Agric. Food Chem.* **2006**, *54*, 7488-7494.
24. Castillo-Munoz, N.; Gomez-Alonso, S.; Garcia-Romero, E.; Gomez, M. V.; Velders, A. H.; Hermosin-Gutierrez, I., Flavonol 3-*O*-glycosides series of *Vitis vinifera* cv. Petit Verdot red wine grapes. *J. Agric. Food Chem.* **2009**, *57*, 209-219.
25. Sun, J.; Liang, F.; Yan, B.; Li, P.; Duan, C., Screening non-colored phenolics in red wines using liquid chromatography ultraviolet and mass spectrometry mass spectrometry libraries. *Molecules* **2007**, *12*, 679-693.
26. Careri, M.; Corradini, C.; Elviri, L.; Nicoletti, I.; Zagnoni, I., Liquid chromatography electrospray tandem mass spectrometry of *cis*-resveratrol and *trans*-resveratrol: development, validation, and application of the method to red wine, grape, and winemaking byproducts. *J. Agric. Food Chem.* **2004**, *52*, 6868-6874.
27. Pezet, R.; Perret, C.; Jean-Denis, J. B.; Tabacchi, R.; Gindro, K.; Viret, O., δ-Viniferin, a resveratrol dehydrodimer: one of the major stilbenes synthesized by stressed grapevine leaves. *J. Agric. Food Chem.* **2003**, *51*, 5488-5492.

28. Stella, L.; de Rosso, M.; Panighel, A.; Dalla, V. A.; Flamini, R.; Traldi, P., Collisionally induced fragmentation of $[M-H]^-$ species of resveratrol and piceatannol investigated by deuterium labelling and accurate mass measurements. *Rapid Commun. Mass Spectrom.* **2008**, *22*, 3867-3872.
29. Buiarelli, F.; Coccioli, F.; Jasionowska, R.; Merolle, M.; Terracciano, A., Analysis of some stilbenes in Italian wines by liquid chromatography tandem mass spectrometry. *Rapid Commun. Mass Spectrom.* **2007**, *21*, 2955-2964.
30. Gomez-Romero, M.; Zurek, G.; Schneider, B.; Baessmann, C.; Segura-Carretero, A.; Fernandez-Gutierrez, A., Automated identification of phenolics in plant derived foods by using library search approach. *Food Chem.* **2010**, *124*, 379-386.
31. Miketova, P.; Schram, K. H.; Whitney, J.; Li, M.; Huang, R.; Kerns, E.; Valcic, S.; Timmermann, B. N.; Rourick, R.; Klohr, S., Tandem mass spectrometry studies of green tea catechins. Identification of three minor components in the polyphenolic extract of green tea. *J. Mass Spectrom.* **2000**, *35*, 860-869.
32. Landrault, N.; Larronde, F.; Delaunay, J. C.; Castagnino, C.; Vercauteren, J.; Merillon, J. M.; Gasc, F.; Cros, G.; Teissedre, P. L., Levels of stilbene oligomers and astilbin in French varietal wines and in grapes during noble rot development. *J. Agric. Food Chem.* **2002**, *50*, 2046-2052.
33. Makris, D. P.; Boskou, G.; Andrikopoulos, N. K.; Kefalas, P., Characterisation of certain major polyphenolic antioxidants in grape (*Vitis vinifera* cv. *Roditis*) stems by liquid chromatography mass spectrometry. *Eur. Food Res. Technol.* **2008**, *226*, 1075-1079.
34. Tourino, S.; Fuguet, E.; Jauregui, O.; Saura-Calixto, F.; Cascante, M.; Torres, J. L., High resolution liquid chromatography electrospray ionization time-of-flight mass spectrometry combined with liquid chromatography electrospray ionization tandem mass spectrometry to identify polyphenols from grape antioxidant dietary fiber. *Rapid Commun. Mass Spectrom.* **2008**, *22*, 3489-3500.
35. Castillo-Munoz, N.; Gomez-Alonso, S.; Garcia-Romero, E.; Hermosin-Gutierrez, I., Flavonol profiles of *Vitis vinifera* red grapes and their single cultivar wines. *J. Agric. Food Chem.* **2007**, *55*, 992-1002.
36. Rockenbach, I. I.; Jungfer, E.; Ritter, C.; Santiago-Schuebel, B.; Thiele, B.; Fett, R.; Galensa, R., Characterization of flavan-3-ols in seeds of grape pomace by CE, HPLC-DAD-MS^n and LC-ESI-FTICR-MS. *Food Res. Int.* **2012**, *48*, 848-855.
37. Saucier, C.; Guerra, C.; Pianet, I.; Laguerre, M.; Glories, Y., (+)-Catechin-acetaldehyde condensation products in relation to wine aging. *Phytochemistry* **1997**, *46*, 229-234.
38. La Torre, G. L.; Saitta, M.; Vilasi, F.; Pellican, T.; Dugo, G., Direct determination of phenolic compounds in Sicilian wines by liquid chromatography with PDA and MS detection. *Food Chem.* **2006**, *94*, 640-650.
39. Camont, L.; Cottart, C. H.; Rhayem, Y.; Nivet-Antoine, V.; Djelidi, R.; Collin, F.; Beaudeux, J. L.; Bonnefont-Rousselot, D., Simple spectrophotometric assessment of the *trans*-/*cis*-resveratrol ratio in aqueous solutions. *Anal. Chim. Acta* **2009**, *634*, 121-128.
40. Gonzalez-Sarrias, A.; Gromek, S.; Niesen, D.; Seeram, N. P.; Henry, G. E., Resveratrol oligomers isolated from *Carex* species inhibit growth of human colon tumorigenic cells mediated by cell cycle arrest. *J. Agric. Food Chem.* **2011**, *59*, 8632-8638.
41. Stoggl, W. M.; Huck, C. W.; Bonn, G. K., Structural elucidation of catechin and epicatechin in sorrel leaf extracts using liquid chromatography coupled to diode array-, fluorescence-, and mass spectrometric detection. *J. Sep. Sci.* **2004**, *27*, 524-528.
42. Perez-Magarino, S.; Revilla, I.; Gonzalez-SanJose, M. L.; Beltra, S., Various applications of liquid chromatography mass spectrometry to the analysis of phenolic compounds. *J. Chromatogr., A* **1999**, *847*, 75-81.

43. Baderschneider, B.; Winterhalter, P., Isolation and characterization of novel benzoates, cinnamates, flavonoids and lignans from Riesling wine and screening for antioxidant activity. *J. Agric. Food Chem.* **2001**, *49*, 2788-2798.

44. Closa, D.; Torres, M.; Hotter, G.; Bioque, G.; Leon, O. S.; Gelpi, E.; Rosello-Catafau, J., Prostanoids and free radicals in $C_{14}C$-induced hepatotoxicity in rats: effect of astilbin. *Prostaglandins, Leukotrienes Essent. Fatty Acids* **1997**, *56*, 331-334.

45. Luo, H.; Jiang, B. H.; King, S. M.; Chen, Y. C., Inhibition of cell growth and VEGF expression in ovarian cancer cells by flavonoids. *Nutr. Cancer* **2008**, *60*, 800-809.

46. An, J.; Zuo, G. Y.; Hao, X. Y.; Wang, G. C.; Li, Z. S., Antibacterial and synergy of a flavanonol rhamnoside with antibiotics against clinical isolates of methicillin-resistant *Staphylococcus aureus* (MRSA). *Phytomedicine* **2011**, *18*, 990-993.

47. He, F.; Pan, Q. H.; Shi, Y.; Duan, C. Q., Chemical synthesis of proanthocyanidins *in vitro* and their reactions in aging wines. *Molecules* **2008**, *13*, 3007-3032.

48. Simon, R.; Collins, M. E.; Spivak, D. A., Shape selectivity *versus* functional group pre-organization in molecularly imprinted polymers. *Anal. Chim. Acta* **2007**, *591*, 7-16.

Chapter 4

The use of a molecularly imprinted polymer for the enrichment of resveratrol from grape pressing residues

Abstract

The wine industry produces large amounts of waste materials such as grape marc. The current exploitation of grape marc implies acid recovery and distillation but end-products are then used for animal feedstock or compost, despite some problems associated with animal indigestion and soil mineralisation. However, the grape marc contains a significant amount of polyphenols, fibres and oils which also could be exploited. Thus, new technologies to utilise grape marc as an inexpensive source of bioactives are of potential commercial value. The phytoalexin (*E*)-resveratrol (*trans*-3,4',5-trihydroxystilbene) occurs naturally in grapes and its dietary products and has been associated with the prevention of a wide range of human diseases such as cancer. However, the extraction of (*E*)-resveratrol from grape waste is currently a tedious process. Molecularly imprinted polymers (MIPs) possess synthetic recognition sites that impart predetermined selectivity towards molecular targets. An (*E*)-resveratrol imprinted MIP has been used in this research involving solid-phase extraction (SPE) of (*E*)-resveratrol from grape pressing residues. The efficacies of the MIP to extract (*E*)-resveratrol from extracts of fresh and aged grape pressing residues were determined by reversed-phase liquid chromatography in combination with electrospray ionisation tandem mass spectrometry. The MISPE protocol was intensified until a recovery of 99% (*E*)-resveratrol was achieved. Such MIP-based enrichment methods provide a new, efficient reusable tool and valuable information on polyphenols with health-beneficial potential at different stages of biological waste products. It demonstrated that the incorporation of Green Chemistry methods can create sustainable economic opportunities from new revenue streams.

Table of Contents

4.1 Introduction

Grapes are one of the world's important fruit crops, with an approximate annual production of 60 million metric tons worldwide (*1*). About 80% of the cultivated grapes are used for wine making (*2*). During grape processing, large quantities of grape waste (known as grape marc) which predominantly consists of skins, seeds and sometimes stalks are normally generated. The total amount of grape marc produced worldwide is about 5-9 million metric tonnes per year (*3, 4*).

In 2011, 120,000 tonnes of grape marc were generated by the wine industry in Australia (*5*). Disposal of this complex material is a difficult challenge. Currently, grape marc is processed by specialised companies (*e.g.*, Tarac Technologies, South Australia) to retrieve tartaric acid or is distilled for low-grade alcohol (*5*). The waste generated from this production is mainly transformed into compost. However, because of certain issues, it is difficult to use the grape marc compost generated by small wineries in practical applications. The high K (potassium) and polyphenol levels in grape marc was reported to affect the growth and germination properties of plants (*6*). In some countries, grape marc is used as cattle feed but it is not very digestible because of the presence of large amounts of polyphenolic compounds, especially tannins, which may bind to proteins and thus prevent digestion in the bovine rumen (*7, 8*). Spirits distilled from fermented grape marc are very popular in the Mediterranean region. Several countries produce traditional distilled alcoholic beverages from grape marc, such as the Greek *tsipouro*, Italian *grappa* and Portuguese *bagaceiras*. Grape marc has also been employed in the production of traditional food products such as molasses and vinegar (*9*).

Grape waste is an inexpensive source of polyphenols (flavanols, flavonols and stilbenes), grape seed oil, citric acid, dietary fibre and ethanol (*6, 10*). The phytoalexin (*E*)-resveratrol is being actively investigated nowadays due to its remarkable pharmacological properties and therapeutic potential (*11, 12*). However, despite ample research on the detection of polyphenols in grape marc, very few studies have focussed on the isolation of (*E*)-resveratrol from grape marc because the process is tedious, labour-intensive and requires the use of toxic organic solvents (*13-15*).

Since grape waste is generated on a large scale and is inexpensive and widely available, it can be used commercially to produce a range of valuable products. One of the challenges in the effective use of grape waste is that it is produced seasonally. For continual conversion of

grape waste into nutraceutical products, it is imperative to investigate the content and distribution of bioactive compositions over a given period of grape waste storage.

With the advent of synthetic imprinting technology, the molecularly imprinted polymers in the solid-phase extraction (MISPE) techniques have been used to specifically isolate target molecules from their original matrices. To the best of my knowledge, there is no previous report on the application of MISPE for the determination of (*E*)-resveratrol in grape waste. Therefore, this study aims at the development of a comprehensive selectivity evaluation procedure *via* the application of off-line MISPE to identify and quantify (*E*)-resveratrol and other types of polyphenols derived from red grape pressing residues, in combination with RP-HPLC and LC-ESI ion trap MS/MS. This environmentally friendly investigation has also been used to obtain information on the complete polyphenol composition of grape pressing residues at different stages of waste storage.

4.2 Materials and Methods

4.2.1 Reagents, standards and instrumentation

For reagents, standards and instrumentation involved for grape pressing residues analysis, see **Chapter 2 (Section 2.2)**. An (*E*)-resveratrol calibration curve was constructed using eight different concentrations of an (*E*)-resveratrol standard in a range of 4.1×10^{-3} to 1.0×10^{-1} mM. The equation for the calibration curve was $y = 35.5x$, where y is the peak area obtained after RP-HPLC and x is the concentration of (*E*)-resveratrol (mg/L). The linear calibration curve showed a correlation factor (R^2) of 0.9. The results obtained from this work are expressed by µg/g dry grape pressing residues (on a mass normalised basis). The limit of detection (LOD) of (*E*)-resveratrol was determined to be 1.9×10^{-2} mg/L whilst the limit of quantification (LOQ) was 6.4×10^{-2} mg/L.

4.2.2 Fresh grape pressing residues

The red grapes (*Vitis vinifera* L., cultivar Pinot noir, vintage 2010) were sourced from the Mornington Peninsula vineyard (Victoria, Australia). After the grapes were harvested, they were stored in a cold room at 4 °C for two days before further analysis. Two bunches of grapes were manually de-stemmed followed by crushing using a blender (Kambrook, Victoria, Australia, 500 watt) for three seconds at speed control setting of one in the dark. The

sample was filtered using a 20 µm pore sized glass frit under a moderate vacuum pressure. The remaining solid residue, mainly consisting of partially broken skins and crushed seeds was employed in this work whilst the juice was used in a different series of experiments. The pressing samples were then divided into portions "A" and "B". Portion "A" as illustrated in **Figure 4.1-A**, referred to as fresh grape pressing residues was employed in this chapter.

4.2.3 Aged grape pressing residues

Portion "B" was placed into a glass storage container. The sample was covered with aluminium foil with two small holes to encourage spontaneous fermentation. It is important to note that this fermentation process did not involve any yeast addition to the pressing residues. The sample was then left at room temperature for 51 days in a laboratory and called aged grape pressing residues or portion "B" **(Figure 4.1-B)**.

A **B**

Figure 4.1: **(A)** The portion "A", skins and seeds of fresh grape pressing residues, **(B)** the portion "B", skins and seeds of aged grape pressing residues.

4.2.4 Sample preparations

Portion "A" (fresh grape pressing residues) was quickly freeze-dried and left in the lyophillizer at 0.01 mbar (Labconco, Missouri, USA) for 2 days to remove all moisture. The dried grape pressing residue was ground with mortar and pestle until it became fine powder to improve the extraction efficiency, which allows the solvent to penetrate all components including seed cell walls and extract the polyphenols (*16*).

The powdered sample (5.0 grams) was extracted with a mixture of EtOH/H_2O (1:1, v/v, 30 mL) and left in the dark (60 min) followed by ultrasonication (60 min). The protocol for the extraction of polyphenols from grape waste was employed based on previous studies with some modifications (*17, 18*). The sample was then centrifuged at 3500 rpm at

20 °C for 20 min. The supernatant was transferred to a volumetric flask and made up to 50 mL volume with the extraction solvent (EtOH/H_2O (1:1, v/v)) prior to MISPE treatment. The MISPE analysis was performed using optimised protocols that have been described in **Chapter 2 (Section 2.3.3)**. During sample handling, the extract was constantly protected from light by covering the sample with aluminium foil. Similar sample preparations and extraction protocols were applied to portion "B" with the starting material of 5.0 grams.

4.2.5 MISPE procedure

The MISPE and NISPE cartridges (2.8 cm diameter × 13.5 cm length) were conditioned (in sequence) with EtOH/AcOH (9:1, v/v), EtOH and EtOH/H_2O (15:85, v/v) (3 × 5 mL). The supernatant of grape pressing residues either in fresh or aged state (5 mL) was loaded onto the MISPE or NISPE cartridge, respectively. Each cartridge was washed with EtOH/H_2O (9:1, v/v) containing 1% (v/v) AcOH (4 × 5 mL) followed by elution with EtOH/AcOH (9:1, v/v) (10 × 5 mL). Finally, both cartridges were reconditioned in sequence with H_2O, EtOH and EtOH/H_2O (15:85, v/v) (3 × 5 mL). In the case of more complex samples, an additional wash step with 0.1 mM NaOH in water was introduced.

4.3 Results and Discussion

The analyses of grape pressing residues in these experiments were performed with grapes of the Pinot noir cultivar vintage 2010. In order to determine the dry matter content, the mass before and after lyophilisation was calculated based on the formula in **Equation 4.1**, the dry matter was 52.6% (g/g).

$$\text{Dry matter, \%} = \frac{Weight\ of\ sample\ after\ freeze\text{-}drying\ (g)}{Weight\ of\ sample\ before\ freeze\text{-}drying\ (g)} \times 100\%\ , \qquad \textbf{Equation 4.1}$$

The portion "B" of grape pressing residues was stored for 51 days at room temperature with minimal light and air exposure. After this period, the sample was observed to have some moulds of grey colour and an unpleasant odour. The substance was then subjected to freeze-drying and the dry matter was determined to be 45.3% (g/g) by using **Equation 4.1**. The aged grape pressing residues were expected to have a lower percentage of dry matter content because the sample lost moisture through evaporation and fungal absorption.

4.3.1 Analysis of (*E*)-resveratrol and other polyphenols from grape pressing residues by RP-HPLC and LC-ESI ion trap MS/MS

4.3.1.1 Before MISPE treatment

The fresh and aged grape pressing residue extracts (prior MISPE treatment) were analysed *via* RP-HPLC for the quantifications of (*E*)-resveratrol. The amount of (*E*)-resveratrol in the extract of portion "A" was determined to be 14.3 µg/g dry grape pressing residue whilst 8.7 µg/g dry grape pressing residue was revealed from the extract of portion "B", based on a linear calibration curve of (*E*)-resveratrol standard. There was 39.2% reduction of (*E*)-resveratrol compared to the (*Z*)-isomer during 51 days of storage. With regards to the analysis of (*E*)-resveratrol in grape marc extract, Careri *et al.* (*19*) reported the concentration of this compound to be 6.0 µg/g. In order to extract (*E*)-resveratrol from its complex matrix, the method required 13 hours of extraction using a mixture of MeOH/EtOH (4:1, v/v) with several separation steps prior to analysis by complex instrumentation.

The identification of many polyphenolic compounds in the grape pressing residue samples was credited to the high efficiency of LC-ESI ion trap MS/MS technique. Base peak chromatograms (BPC) in **Figure 4.2** show that at least 32 polyphenolic compounds were detected from the extracts of **(A)** fresh and **(B)** aged grape pressing residues, although some polyphenols were present at low concentrations. The broad peak observed at a retention time between 6 to 9 min in the front of the chromatogram is due to some weakly retained sample components in the reversed-phase C_{18} column, which was specifically chosen for polyphenols analysis. Obviously, the extract from aged grape pressing residues delivered lower levels of polyphenols than the fresh grape pressing extract. The reduction of polyphenol occurrence in the aged extract might be due to the oxidation of polyphenols by phenoloxidase enzymes (*20*) and to the activity of fungi and bacteria.

Figure 4.3 shows a comparison of both extracts depicting the (*E*)-resveratrol profiles *via* extracted ion chromatogram (EIC). It should be noted that the results obtained from LC-ESI ion trap MS/MS, in particular BPC and EIC are not similar. BPC represents the most intensive ions at any time point whilst the EIC reveals the intensity of specific ions. In the fresh grape pressing residue extract, a high peak intensity of resveratrol **(Figure 4.3-A)** was observed with a predominance of the (*E*)-form **(peak 29)**, being about three-fold higher than the intensity of the (*Z*)-isomer **(peak 31)**.

Further investigations studied (*E*)-resveratrol degradation in the aged extract of grape pressing residues. Due to some exposure to oxygen (although at a minimum level) or microbial activity during the ageing process, some of (*E*)-resveratrol **(peak 29)** had been converted to the (*Z*)-isomer as evidenced by the higher peak intensity of **peak 31 (Figure 4.3-B)**. The proportion of (*Z*)-resveratrol was 1.0 to 1.3 in fresh grape pressing residue *versus* that of aged pressing residue extracts. The degradation of (*E*)-resveratrol was previously investigated by Trela and co-workers *(21)* who reported that under a fluorescent light in a laboratory, 86.1% of the (*E*)-resveratrol standard (418 µmol/L) isomerised to (*Z*)-isomer within 60 days.

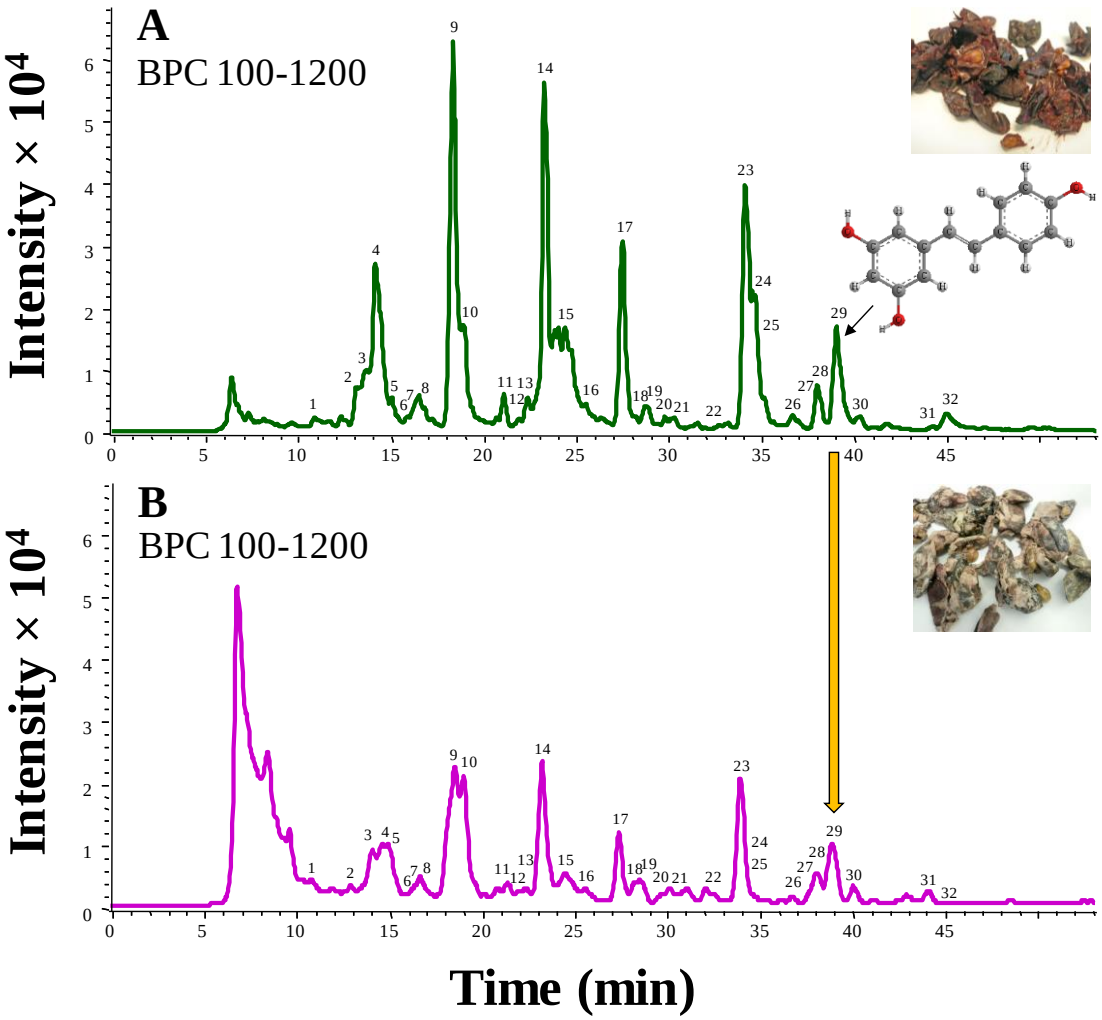

Figure 4.2: Base peak chromatograms (BPC) of **(A)** fresh grape pressing residue extract and **(B)** aged grape pressing residue extract. (*E*)-resveratrol **(peak 29)** eluted at t_R = 38.8 min. The chromatograms were obtained after RP-HPLC separation on a Zorbax XDB C_{18} capillary column (0.3 mm × 150 mm, 3.5 µm particle size) in the *m/z* range of 100-1200 using the negative ionisation mode by LC-ESI ion trap MS/MS at 20 °C. LC conditions: eluent A: 10 mM formic acid in water, eluent B: 10 mM formic acid in EtOH/H_2O (4:1, v/v), gradient: 0-2 min to 10% (v/v) B, 2-52 min to 70% (v/v) B, 52-53 min to 10% (v/v) B; flow rate: 2 µL/min; 0.1 µL injection.

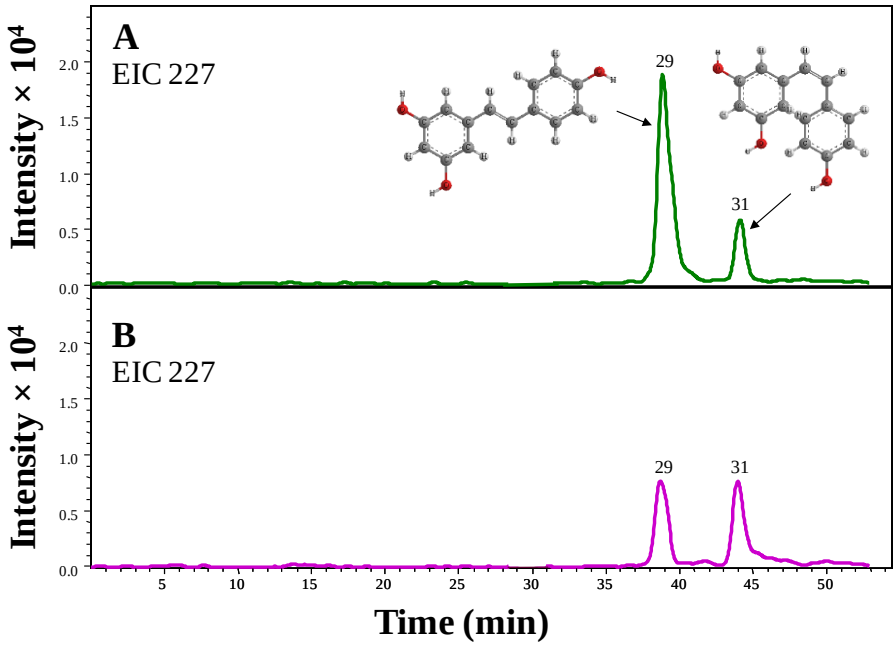

Figure 4.3: Extracted ion chromatograms (EIC) at *m/z* 227 revealed the presence of (*E*)-resveratrol **(peak 29)** eluted at t_R = 38.8 min and (*Z*)-resveratrol **(peak 31)** eluted at t_R = 44.0 min from the extracts of **(A)** fresh and **(B)** aged grape pressing residues. The extracted ion chromatograms were obtained after RP-HPLC separation on a Zorbax XDB C_{18} capillary column (0.3 mm × 150 mm, 3.5 µm particle size) in the *m/z* range of 100-1200 using the negative ionisation mode by LC-ESI ion trap MS/MS at 20 °C. LC conditions: eluent A: 10 mM formic acid in water, eluent B: 10 mM formic acid in EtOH/H_2O (4:1, v/v), gradient: 0-2 min to 10% (v/v) B, 2-52 min to 70% (v/v) B, 52-53 min to 10% (v/v) B; flow rate: 2 µL/min; 0.1 µL injection.

A further objective of this study was to characterise other polyphenolic compounds present in the fresh and aged grape pressing residue extracts. The incentive for the identification of all polyphenols from both extracts was based on some evidences of their association with biological activities and health promoting benefits. The extract from grape marc has been shown to inhibit the activity of metalloproteinases-2 and expressed a significant antiproliferative effect on human colon adenocarcinoma cells (*22*). In a recent investigation, it was demonstrated that the extracts of grape marc had an antioxidative activity and exerted an anti-inflammatory effect in diets which induced obesity (*23*). In addition, the grape marc extracts were shown to selectively inhibit an intestinal α-glucosidase activity and to suppress postprandial hyperglycemia in diabetic mice *(24)*. Shin and co-workers (*25*) claimed that the polyphenolic constituents in red grape marc have the potential to suppress chronic inflammation induced by lipopolysaccaride and galactosamine *in vivo*.

In the present experiments, polyphenolic compounds from grape pressing residue extracts were successfully characterised based on the precursor ions and characteristic product ions by

LC-ESI ion trap MS/MS in the negative ionisation mode **(Table 4.1)**. It should be noted that the numbering system **(1-32)** of the polyphenol peaks in the HPLC and LC-ESI ion trap MS/MS chromatograms from both extracts before MISPE **(Figure 4.2)**, after MISPE and NISPE treatment **(Figure 4.5** and **Figure 4.6)** is corresponding to that in **Table 4.1** and **Table 4.2**.

In comparison with previous studies, this method employing a highly feasible extraction protocol with minimal benign solvent consumption composed of EtOH/H_2O (1:1, v/v). Amico *et al.* (*26*) extracted 100 g of red grape marc under continuous stirring with acidified methanol for 12 hour. The extract was evaporated, followed by defatting with *n*-hexane and subsequent extraction with ethyl acetate prior to analysis by HPLC and LC-ESI-MS/MS. This multi-step sample extraction resulted in the determination of eight compounds of the flavonol group and ten different anthocyanins. Multiple extraction steps for polyphenols screening were also applied by Kammerer and co-workers (*27*), whereby with laborious-intensive procedures, the method identified 27 components of polyphenols including (*E*)-resveratrol and (*E*)-piceid in 5 g of grape pomace sample.

Further explanation about the identification and fragmentation involved for polyphenols in **Table 4.1** are described below. The characterisations of polyphenols in both extracts (before MISPE treatment) were classified based on the non-flavonoids and flavonoids categories.

4.3.1.1.1 Non-flavonoids

i) Stilbenes

Resveratrol was observed as two peaks in the chromatographic profiles from both, fresh and aged grape pressing residue extracts which could be attributed to the (*E*)-**(peak 29)** and (*Z*)-**(peak 31)** isomers of resveratrol. The peak identity of these resveratrol compounds (*m/z* 227) was then confirmed by collision-induced dissociation (CID) to generate a product ion at *m/z* 185 due to the loss of CHCOH (42 mass units). This product ion fragmented in the ion trap to form two product ions at *m/z* 157 and 143 by losing CO (28 mass units) and C_2H_2O (42 mass units), respectively. This fragmentation pattern corroborates the findings of the previous work done by Stella and co-workers (*28*). (*E*)-Resveratrol **(peak 29)** in these experiments was identified at a retention time of 38.8 min, whilst in the red wine sample **(Chapter 3)**, this compound was eluted at 41.3 min by LC-ESI ion trap MS/MS. The variation of the retention times (2.5 min) might be due to these experiments were performed

in 2010 with a used C_{18} capillary column whilst the current results reported in **Chapter 3** were obtained in 2012 with a new C_{18} capillary column (same chemistry and properties as the former column). It should be noted that the preparation of mobile phase might have also influenced the drifting of retention time. However, the variability was not detrimental to these experiments since the retention times of all peak components change proportionally to each other and resolution was preserved. In addition, the retention time of (*E*)-resveratrol (38.8 min) obtained from the microLC system was about 8 min higher in comparison to the retention time obtained from the analytical RP-HPLC system (30.8 min) because of the differences in gradient delay volume of these systems (as explained previously in **Chapter 3 (Section 3.3.3.1.1)**.

In order to confirm the presence of (*E*)-resveratrol in the portions "A" and "B", the (*E*)-resveratrol standard was used. (*Z*)-resveratrol **(peak 31)** was observed at a longer retention time (44.0 min), most likely due to the hydrophobic nature of the *cis*-structural feature on the reversed-phase C_{18} column (*29*). The resveratrol glycosides known as piceid (or polydatin) were assigned based on the precursor ions $[M-H]^-$ at *m/z* 389 in both sample extracts in (*E*)-**(peak 20)** and (*Z*)-**(peak 30)** configurations. These compounds underwent MS/MS fragmentation in the ion trap by losing the glucoside moiety $[M-H-162]^-$ to generate resveratrol (*m/z* 227) (*29*). Due to the high polarity and hydrophilicity of resveratrol glucosides, the (*E*)-piceid and (*Z*)-piceid were observed at earlier retention times (29.7 min and 40.2 min, respectively) in comparison to the isomers of resveratrol aglycone.

ii) Hydroxybenzoic acids

Gallic acid **(peak 1)** was identified with a precursor ion $[M-H]^-$ of *m/z* 169 (*27*). This compound was fragmented to generate a product ion of *m/z* 125 due to the loss of a carboxylic acid moiety $[M-H-44]^-$.

iii) Hydroxycinnamic acid and derivatives

Caftaric acid **(peak 6)** and fertaric acid **(peak 11)** were observed at the precursor ions $[M-H]^-$ of *m/z* 311 and 325, respectively (*30*). These compounds were fragmented in the ion trap by losing the ester bond $[M-H-132]^-$ from their molecular structures to produce caffeic acid and ferulic acid, respectively. Caffeic acid **(peak 7)** with the precursor ion $[M-H]^-$ of *m/z* 179 (*30*), generated a product ion at *m/z* 135 after losing a carboxylic acid moiety $[M-H-44]^-$ during the fragmentation process.

Table 4.1: Polyphenol compounds in extracts of **(A)** fresh grape pressing residue and **(B)** aged grape pressing residue, measured by LC-ESI ion trap MS/MS in the negative ionisation mode.

Peak No.	Retention time, t_R (min)	Compound name	Precursor ion, *m/z*	Observed product ion(s), *m/z*	Ref. [a]	A	B
1	10.4	Gallic acid	169	125	(*27*)	✓	✓
*2	12.8	B-type procyanidin	577	451, 425, 407, 289	(*31*)	✓	✓
3	14.0	B-type procyanidin trimer	865	739, 695, 577, 289	(*32*)	✓	✓
*4	14.2	B-type procyanidin	577	451, 425, 407, 289	(*32*)	✓	✓
*5	15.0	B-type procyanidin	577	451, 425, 407, 289	(*32*)	✓	*lc*
6	15.5	Caftaric acid	311	179, 149	(*30*)	✓	*lc*
7	15.9	Caffeic acid	179	135	(*30*)	✓	✓
*8	16.6	B-type procyanidin	577	451, 425, 407, 289	(*32*)	✓	*lc*
9	18.2	(±)-Catechin	289	245, 205, 179	(*33*)	✓	✓
*10	19.0	B-type procyanidin	577	451, 425, 407, 289	(*32*)	✓	✓
11	21.0	Fertaric acid	325	193	(*30*)	✓	*lc*
12	21.2	B-type procyanidin dimer gallate	729	577, 559, 407, 289	*(32)*	*lc*	*lc*
*13	22.2	B-type procyanidin	577	451, 425, 407, 289	(*32*)	✓	*lc*
14	23.2	(±)-Epicatechin	289	245, 205, 179	(*33*)	✓	✓
15	24.6	Malvidin-3-*O*-glucoside	491	329	(*34*)	✓	*lc*
*16	25.6	B-type procyanidin	577	451, 425, 407, 289	(*32*)	✓	✓
17	27.4	Malvidin-3-*O*-glucoside hydrate	509	491, 347, 329, 355	(*34*)	✓	✓
18	28.1	Epicatechin-3-*O*-gallate	441	289, 169	*(35)*	*lc*	*lc*
*19	28.4	B-type procyanidin	577	451, 425, 407, 289	(*32*)	✓	✓
20	29.7	(*E*)-Piceid	389	227	*(29)*	*lc*	*lc*
21	30.7	Taxifolin	303	285, 179, 125	*(36)*	*lc*	*lc*
22	32.3	A-type procyanidin	621	575, 449, 405, 287	*(37)*	*lc*	*lc*
23	34.0	(+)-Astilbin	449	303, 285	(*38*)	✓	✓
24	34.4	Quercetin-3-*O*-glucuronide	477	301, 179, 151	(*39*)	✓	*lc*
25	34.8	Quercetin-3-*O*-glucoside	463	301, 179, 151	(*39*)	✓	*lc*
26	36.6	(-)-Astilbin	449	303, 285	(*38*)	✓	*lc*
27	37.7	Quercetin-3-*O*-rhamnoside	447	301, 179, 151	(*39*)	✓	✓
28	37.8	Quercetin-3-*O*-xyloside	433	301, 287, 179, 151	(*39*)	✓	✓
29	**38.8**	**(*E*)-Resveratrol**	227	185, 157, 143	(*28*)	✓	✓
30	40.2	(*Z*)-Piceid	389	227	(*29*)	✓	✓
31	44.0	(*Z*)-Resveratrol	227	185, 157	(*29*)	✓	✓
32	45.2	Quercetin	301	179, 151	(*40*)	✓	*lc*

∗ Based on the MS/MS spectra no further identification was possible;
lc Phenolic compound present at low concentration;
[a] References which confirm precursor and product ion(s) for the particular compound.

4.3.1.1.2 Flavonoids

i) Flavanols

(±)-Catechin **(peak 9)** and its stereoisomeric structure, (±)-epicatechin **(peak 14)** were detected at the precursor ions $[M-H]^-$ of *m/z* 289 (*33*). The peak identity of catechin was authenticated with a reference standard. After fragmentation, catechin/epicatechin produced several characteristic product ions at *m/z* 245, 205 and 179 due to the loss of a CO_2 group ($[M-H-44]^-$), elimination of the A-ring and B-ring from the molecular structure, respectively. Epicatechin gallate **(peak 18)** also appeared in the samples. This compound was observed at the precursor ion $[M-H]^-$ of *m/z* 441 (*35*), which later fragmented to yield two distinctive product ions at *m/z* 289 (catechin/epicatechin) and *m/z* 169 (gallic acid).

ii) Tannins

Several tannins in dimeric, dimeric gallate and trimer structures were successfully identified from both extracts **(Figure 4.4)**. According to the polyphenols data in **Table 4.1**, the multiple peaks with the same precursor ions ($[M-H]^-$, *m/z* 577) were encountered for the **peaks 2**, **4**, **5**, **8**, **10**, **13**, **16** and **19** that may correspond to the B-type procyanidin dimeric based on the information of the fragmentation published in the literature (*32, 41*). The characteristic product ions for this compound were identified at *m/z* 451, 425, 407 and 289. According to Callemien and co-workers (*32*), procyanidin dimer deprotonates $[M-H]^-$ to give a precursor ion at *m/z* 577. This compound underwent fragmentation at *m/z* 451 corresponding to the loss of a pyrogallol unit $[M-H-126]^-$ on the C-ring *via* heterocyclic ring fission. The elimination of the B-ring from its molecular structure through a retro-Diels-Alder reaction generated a product ion at *m/z* 425. The *m/z* 407 $[M-H-152-18]^-$ formed due to the water elimination of *m/z* 425, most likely the hydroxyl-group from the C_3 position (*42*). In that study, the catechin/epicatechin monomer was monitored at a signal of *m/z* 289 resulting from quinine methide fission cleavage.

Peak 12 was identified as the B-type procyanidin dimer gallate based on the precursor ion $[M-H]^-$ at *m/z* 729 (*32*) in fresh and aged grape pressing residue extracts. This compound was fragmented to yield a characteristic product ion at *m/z* 577 (B-type procyanidin dimer) due to the loss of a galloyl-group (152 mass units). An interflavan bond cleavage produced a monomer of catechin/epicatehin at *m/z* 289. B-type procyanidin trimer **(peak 3)** was observed in extracts of both types of grape pressing residue by having the precursor ion $[M-H]^-$ at

m/z 865. This compound underwent fragmentation in the ion trap and produced *m/z* 739 due to the loss of a pyrogallol unit $[M-H-126]^-$ through heterocyclic ring fission (*32*), and subsequently cleaved *via* a retro-Diels-Alder reaction to generate two characteristic product ions at *m/z* 713 and 695. Further fragmentation of this compound resulted in product ions at *m/z* 577 (procyanidin dimer) and 289 (monomer catechin/epicatechin). The characteristic product ions of the B-type oligomeric procyanidins (procyanidin dimer, procyanidin dimer gallate and procyanidin trimer) in the present studies were similar with previous investigations done by Callemien *et al.(32)*, suggesting that these compounds might follow the same fragmentation pathways. The fragmentation pattern of procyanidin was also consistent with earlier investigations reported in the literature (*42*). Procyanidins from grape pomace has been reported to inhibit NADPH oxidase activity in human endothelial cells of *in vitro* and *ex vivo* models for therapeutic alternatives for cardiovascular diseases (*43*). Santos-Buelga and co-workers (*44*) found that the low procyanidin oligomers (degree of polymerisation below than four) could be absorbed in the gastrointestinal tract. Procyanidin dimers have been found in human blood after the respondent consumed procyanidins-rich diet (*45*). In the studies performed by Deprez *et al*. (*46*), procyanidin trimers have been shown to be absorbed through the human intestinal cell line Caco-2.

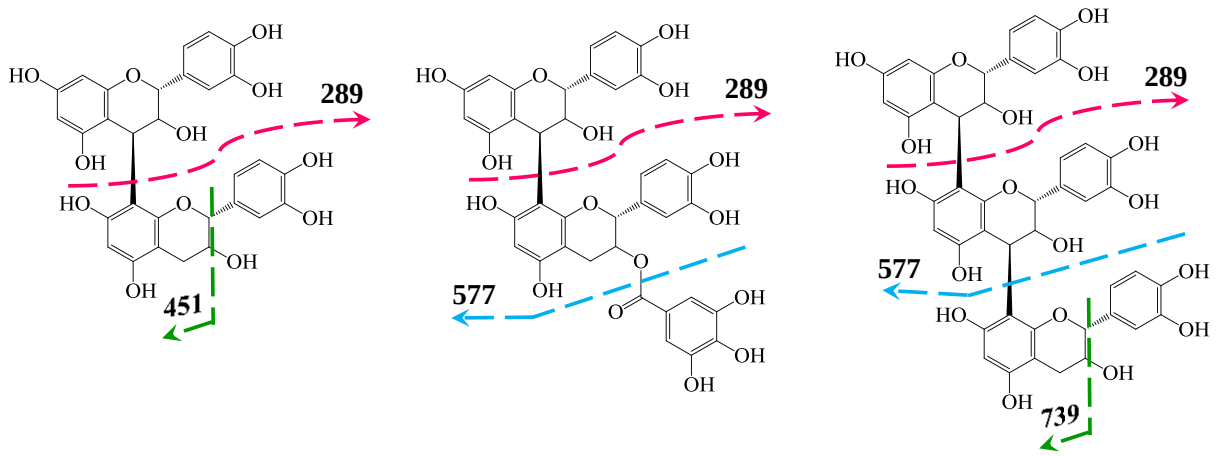

B-type procyanidin dimer ($[M-H]^-$, *m/z* 577)

B-type procyanidin dimer gallate ($[M-H]^-$, *m/z* 729)

B-type procyanidin trimer ($[M-H]^-$, *m/z* 865)

Figure 4.4: Different degrees of polymerisation of tannins (arrows indicating the main fragmentation characteristics) which were identified from the extracts of fresh and aged grape pressing residues as analysed by LC-ESI ion trap MS/MS in the negative ionisation mode.

Peak 22 had low intensities in both samples with the precursor ion of *m/z* 621. This compound might be identified as the A-type procyanidin with a formate adduct $[M+HCOO]^-$, consistent with the reported adduct-free $[M-H]^-$ *m/z* of 575 (*37*) of the A-type procyanidin dimer. The occurrence of formate adducts is possible when formic acid is used as mobile phase additive. The product ions observed at *m/z* 449 and 287 correspond to the characteristic fragmentation pattern of this compound. The A-type procyanidin dimer was claimed to have lower antioxidant activity in comparison to the B-type oligomeric procyanidin (*47*). However, this compound showed a high antiviral activity against the herpes simplex virus and human immunodeficiency virus (*48*). Thus, the identification of the procyanidin oligomers from grape pressing residues in this study provides valuable information for their potential use as nutraceutials.

iii) Flavonols

The majority of flavonols identified in both grape pressing residue extracts were in the form of various types of glycosides. **Peak 24** was characterised as quercetin-3-*O*-glucuronide based on the precursor ion $[M-H]^-$ at *m/z* 477 (*39*). This compound fragmented *via* MS/MS experiments to generate an aglycone quercetin at *m/z* 301 because of the loss of a glucuronide moiety $[M-H-176]^-$. The following fragmentation of quercetin aglycone (*m/z* 301) yielded two characteristic product ions at *m/z* 179 and 151. The presence of a precursor ion $[M-H]^-$ at *m/z* 463 **(peak 25)** led to the identification of quercetin-3-*O*-glucoside (*39*). Due to the loss of a unit glucose $[M-H-162]^-$ during fragmentation, the quercetin aglycone (*m/z* 301) was formed. The identity of quercetin-3-*O*-rhamnoside **(peak 27)** and quercetin-3-*O*-xyloside **(peak 28)** was assigned based on the precursor ion $[M-H]^-$ at *m/z* 447 (*39*) and *m/z* 433 (*39*), respectively. These compounds underwent fragmentation in the ion trap to generate several characteristic product ions of quercetin. The peak at **32** was attributed to quercetin based on the precursor ion $[M-H]^-$ at *m/z* 301 (*40*). Quercetin has anti-inflammatory qualities, and is investigated for a wide range of potential health-benefits including cancer (*49*). Due to the fragmentation within its molecular structure, two distinctive product ions were produced (*m/z* 179 and 151). The fragmentation trend of quercetin from the samples was verified with a commercial standard. An interesting observation from the fragmentation behaviours of all herein studied flavonols was that they produced structurally characterised product ions at *m/z* 179 and 151. This information may be used to narrow the search for unknown compounds in the flavonol category in a biological sample.

iv) Flavanonols

Taxifolin (also known as dihydroquercetin), **peak 21**, was detected at the precursor ion $[M-H]^-$ of *m/z* 303 (*36*), which later fragmented to produce three product ions at *m/z* 285, 179 and 125. (+)-Astilbin **(peak 23)** and its isomer (-)-astilbin **(peak 26)** had precursor ions $[M-H]^-$ at *m/z* 449 (*38*). These compounds underwent fragmentation *via* MS/MS experiments to generate *m/z* 303 (taxifolin) and 285 due to the loss of a rhamnoside moiety (146 mass units) and water (18 mass units), respectively. Taxifolin has shown to inhibit the ovarian cancer cell growth in a dose-dependent way (*50*).

v) Anthocyanins

Peak 15 might be attributed to the presence of malvidin-3-*O*-glucoside based on the precursor ion $[M-2H]^-$ at *m/z* 491 (*34*). The product ion generated at *m/z* 329 after MS/MS fragmentation corresponds to the loss of a glucoside moiety. This is consistent with a report that malvidin-3-*O*-glucoside in the hydrated form was identified in the grape skin extracts with the precursor ion $[M-H]^-$ of *m/z* 509 (*34*) and product ions at *m/z* 491 and 329 due to the loss of water and a glucoside moiety, respectively.

4.3.1.1.3 After MISPE treatment

i) Fresh grape pressing residue extract

The MIP demonstrated its selective binding to (*E*)-resveratrol **(peak 29)** through a higher enrichment of the target analyte than the NIP in eluate fractions. The results obtained from RP-HPLC **(Figure 4.5-insert)** showed the comparison of eluates between the MIP and NIP at the wavelength of 320 nm. The concentration enrichment of (*E*)-resveratrol after MIP eluate was determined to be 4.5 mg/L from the original concentration of 1.5 mg/L in the extract (on a mass and volume normalised basis). The limited suitability of RP-HPLC for identifying the polyphenols present in the extracts led to further analysis by LC-ESI ion trap MS/MS in the negative ionisation mode. The peak identity confirmation (ion current intensity > 0.2×10^5) resulted in 16 phenolic compounds withheld by the MIP and obtained in the eluate as a result of competitive binding **(Figure 4.5)**. As expected, fewer compounds (3 components) were found in the NISPE eluate because most of the non-selective bound material was removed after the washing steps. The summary of polyphenols found after MISPE and NISPE treatment is listed in **Table 4.2**. Besides (*E*)-resveratrol **(peak 29)**, a noticeable phenolic

enrichment can be seen for **peaks 5**, **9**, **10**, **13**, **18**, **19**, **21**, **26** and **32**. Details about the characterisation of these components were described earlier in **Section 4.3.1.1**.

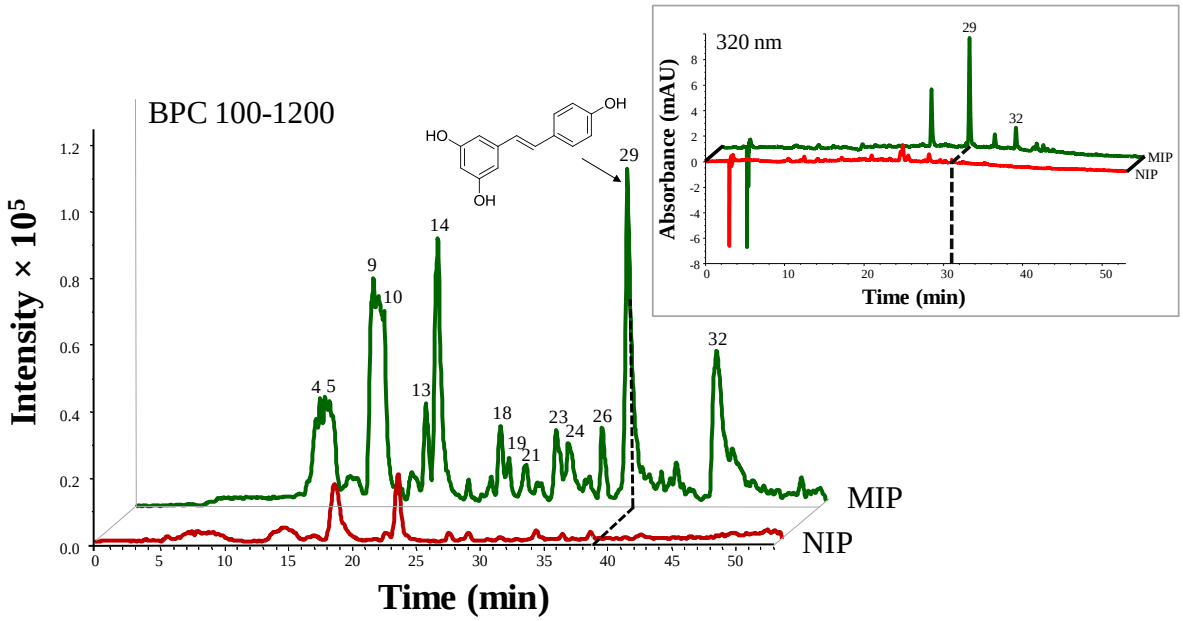

Figure 4.5: Base peak chromatograms (BPC) of eluates after MISPE (green line, back chromatogram) and NISPE (red line, front chromatogram) from extracts of fresh grape pressing residues. (*E*)-resveratrol **(peak 29)** eluted at t_R = 38.8 min. The base peak chromatograms were obtained after RP-HPLC separation on a Zorbax XDB C_{18} capillary column (0.3 mm × 150 mm, 3.5 µm particle size) in the *m/z* range of 100-1200 using the negative ionisation mode by LC-ESI ion trap MS/MS at 20 °C. LC conditions: eluent A: 10 mM formic acid in water, eluent B: 10 mM formic acid in EtOH/H_2O (4:1, v/v), gradient: 0-2 min 10% (v/v) B, 2-52 min to 70% (v/v) B, 52-53 min to 10% (v/v) B; flow rate: 2 µL/min; 0.1 µL injection. Inserted are RP-HPLC chromatograms recorded at a wavelength of 320 nm for the quantification of (*E*)-resveratrol (t_R = 30.8 min, **peak 29**) after MIP (green line, back) and NIP (red line, front) SPE treatment from the fresh grape pressing residue extract. The LC chromatograms were obtained with a Zorbax Eclipse XDB C_{18} column (4.6 mm × 150 mm, 5 µm particle size) at 20 °C. LC conditions: eluent A: 10 mM formic acid in water, eluent B: 10 mM formic acid in EtOH/H_2O (4:1, v/v), gradient: 0-2 min to 10% (v/v) B, 2-52 min to 70% (v/v) B, 52-53 min to 10% (v/v) B; flow rate: 0.5 mL/min; 5 µL injection.

ii) Aged grape pressing residue extract

Likewise, the MIP specifically captured (*E*)-resveratrol **(peak 29)** in contrast to its control polymer (NIP) from the aged grape pressing residue extract **(Figure 4.6)**. From RP-HPLC results **(Figure 4.6-insert)**, the MISPE eluate fraction not only consisted of (*E*)-resveratrol but also several other compounds. The concentration enrichment of (*E*)-resveratrol after MIP eluate was calculated to be 5.5 mg/L from the concentration of 0.9 mg/L in the extract (on a mass and volume normalised basis).

Based on the retention times of the commercial reference standards, (*E*)-resveratrol **(peak 29)** and quercetin **(peak 32)** were identified in the extracts. Although half of the (*E*)-resveratrol had been converted to (*Z*)-isomer, the MISPE technique enabled to pre-concentrate and enrich this compound as well as discriminate the (*E*)-resveratrol due to the size and shape selectivity for this template molecule. By using LC-ESI ion trap MS/MS, the identification of several polyphenols structurally related to (*E*)-resveratrol was achieved from the MISPE eluate. Therefore, eight compounds, in particular **peaks 9**, **10**, **18**, **23**, **24** and **32** with significant enrichment were observed. In contrast, the majority of polyphenols (29 components) was eliminated during the wash steps as the non-selective bound components from NISPE **(Table 4.3)**.

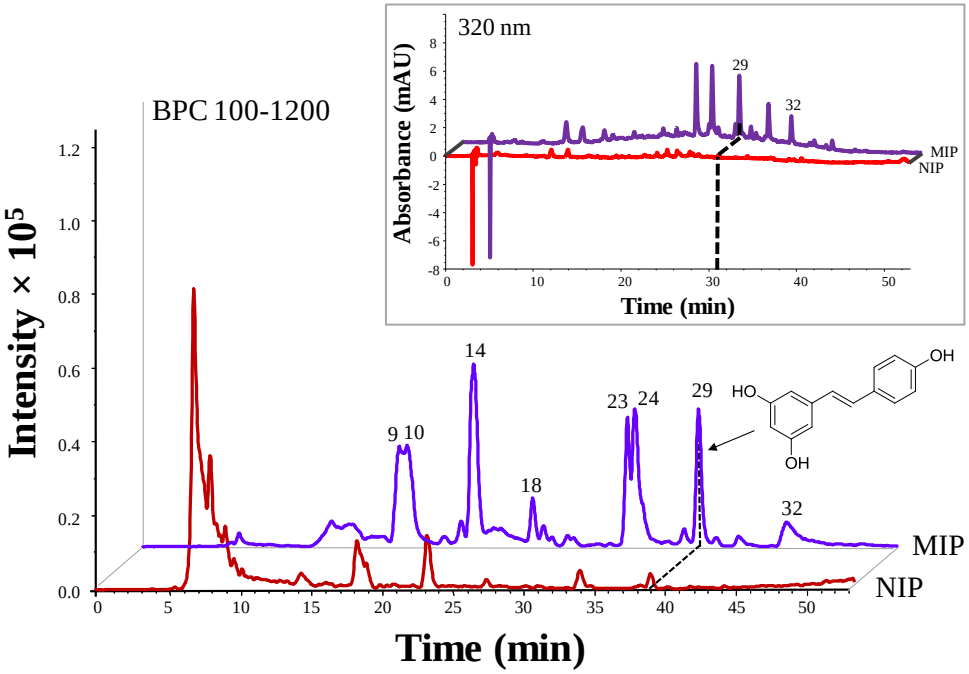

Figure 4.6: Mass chromatograms of eluates after MISPE (purple line, back chromatogram) and NISPE (red line, front chromatogram) from extracts of aged grape pressing residues. (*E*)-resveratrol **(peak 29)** eluted at t_R = 38.8 min. The base peak chromatograms were obtained with RP-HPLC on a Zorbax XDB C_{18} capillary column (0.3 mm × 150 mm, 3.5 µm particle size) in the *m/z* range of 100-1200 using the negative ionisation mode by LC-ESI ion trap MS/MS at 20 °C. LC conditions: eluent A: 10 mM formic acid in water, eluent B: 10 mM formic acid in EtOH/H_2O (4:1, v/v), gradient: 0-2 min 10% (v/v) B, 2-52 min to 70% (v/v) B, 52-53 min to 10% (v/v) B; flow rate: 2 µL/min; 0.1 µL injection. Inserted are RP-HPLC chromatograms recorded at a wavelength of 320 nm for the quantification of (*E*)-resveratrol (t_R = 30.8 min, **peak 29**), after MIP (purple line, back) and NIP (red line, front) SPE treatment from the aged grape pressing residue extract. The chromatograms were obtained with a Zorbax Eclipse XDB C_{18} column (4.6 mm × 150 mm, 5 µm particle size) at 20 °C. LC conditions: eluent A: 10 mM formic acid in water, eluent B: 10 mM formic acid in EtOH/H_2O (4:1, v/v), gradient: 0-2 min to 10% (v/v) B, 2-52 min to 70% (v/v) B, 52-53 min to 10% (v/v) B; flow rate: 0.5 mL/min; 5 µL injection.

Table 4.2: The comparison of polyphenol substances in MISPE and NISPE eluates from extracts of **(A)** fresh and **(B)** aged grape pressing residues detected by LC-ESI ion trap MS/MS with the ion current intensity > 0.2 × 10^5. Highlighted are compounds significantly enriched after MISPE treatment.

			Fresh grape pressing residue extract "A"		**Aged grape pressing residue extract "B"**	
Peak No.	**Retention time, t_R (min)**	**Compound name**	**MISPE**	**NISPE**	**MISPE**	**NISPE**
1	10.4	Gallic acid	×	×	×	×
*2	12.8	B-type procyanidin	✓	×	×	×
3	14.0	B-type procyanidin trimer	×	×	×	×
*4	14.2	B-type procyanidin	✓	×	×	×
***5**	**15.0**	**B-type procyanidin**	✓	×	×	×
6	15.5	Caftaric acid	×	×	×	×
7	15.9	Caffeic acid	×	×	×	×
8	16.6	B-type procyanidin	×	×	×	×
9	**18.2**	**(±)-Catechin**	✓	✓	✓	✓
***10**	**19.0**	**B-type procyanidin**	✓	✓	✓	✓
11	21.0	Fertaric acid	×	×	×	×
12	21.2	B-type procyanidin dimer gallate	×	×	×	×
***13**	**22.2**	**B-type procyanidin**	✓	×	×	×
14	**23.2**	**(±)-Epicatechin**	✓	✓	✓	✓
15	24.6	Malvidin-3-*O*-glucoside	×	×	×	×
16	25.6	B-type procyanidin	×	×	×	×
17	27.4	Malvidin-3-*O*-glucoside hydrate	×	×	✓	×
18	**28.1**	**Epicatechin-3-*O*-gallate**	✓	×	×	×
***19**	**28.4**	**B-type procyanidin**	✓	×	×	×
20	29.7	(*E*)-Piceid	*lc*	×	×	×
21	**30.7**	**Taxifolin**	✓	×	×	×
22	32.3	A-type procyanidin	×	×	×	×
23	**34.0**	**(+)-Astilbin**	✓	×	✓	×
24	**34.4**	**Quercetin-3-*O*-glucuronide**	✓	×	✓	×
25	34.8	Quercetin-3-*O*-glucoside	×	×	×	×
26	**36.6**	**(-)-Astilbin**	✓	×	×	×
27	37.7	Quercetin-3-*O*-rhamnoside	×	×	×	×
28	37.8	Quercetin-3-*O*-xyloside	×	×	×	×
29	**38.8**	**(*E*)-Resveratrol**	✓	×	✓	×
30	40.2	(*Z*)-Piceid	×	×	×	×
31	44.0	(*Z*)-Resveratrol	×	×	×	×
32	**45.2**	**Quercetin**	✓	×	✓	×

* Based on the MS/MS spectra, no further identification was possible;
lc Phenolic compound present at low concentration.

4.3.2 Grape pressing residue extracts analysed with MISPE

4.3.2.1 Fresh grape pressing residue extract

The efficacies of MISPE and NISPE before and after treatment with respect to the selective enrichment of (*E*)-resveratrol from extracts of **(A)** fresh and **(B)** aged grape pressing residues are shown in **Table 4.3**. The extract of fresh grape pressing residue was determined previously by RP-HPLC had 14.3 µg/g (*E*)-resveratrol. The extract (5 mL) was loaded onto the MIP and the NIP cartridges, respectively. The cartridges were washed several times with EtOH/H_2O (4:1, v/v) containing 1% (v/v) AcOH (4 × 5 mL) to remove weakly bound and/or non-specific bound compounds from the MIP or NIP sorbents **(Figure 4.7-A)**. During the wash stages, the majority of the (*E*)-resveratrol (13.9 µg/g dry grape pressing residues) was eluted from the NIP cartridge whereas the MIP cartridge showed some wash-off of the target analyte (5.6 µg/g dry grape pressing residues). The eluting steps with EtOH/AcOH (9:1, v/v) presented a higher binding affinity of (*E*)-resveratrol (8.6 µg/g dry grape pressing residue) eluted from the MIP cartridge in contrast to an insignificant amount eluted from the NIP cartridge (0.2 µg/g dry grape pressing residues). The selectivity recognition for (*E*)-resveratrol approximately was 43-fold based on an imprinting factor obtained from the MIP eluate *versus* NIP eluate due to the imprinting effect of (*E*)-resveratrol. The recovery of (*E*)-resveratrol from the MIP was 99.3%.

4.3.2.1.1 Aged grape pressing residue extract

The extract of aged grape pressing residues (8.7 µg/g dry grape pressing residues, 5 mL) was loaded onto the MISPE or NISPE cartridge. After the wash steps, almost all non-specifically bound (*E*)-resveratrol was eliminated (8.3 µg/g dry grape pressing residues) from the NIP cartridge, whilst only 3.3 µg/g dry grape pressing residues of (*E*)-resveratrol was removed as non-selectively bound component from the MIP **(Figure 4.7-B)**. In the eluting steps, the MIP showed greater binding selectivity for the target analyte as the (*E*)-resveratrol uptake was determined to be 5.3 µg/g dry grape pressing residues compared to 0.3 µg/g dry grape pressing residues from the control NIP. The MIP specifically captured (*E*)-resveratrol about 18-fold (*IF* = MIP eluate/NIP eluate) in the eluate fraction than the NIP, which can be attributed to the (*E*)-resveratrol imprinting effect.

Since nearly half of the (*E*)-resveratrol was converted to the (*Z*)-isomer during the ageing process there was probably a better chance for the compounds structurally related to the target molecule to reside in the binding sites. The high competition of template-like-molecules including epicatechin, astilbin, quercetin glucuronide and quercetin to afford binding recognition presumably resulted in the low imprinting factor of (*E*)-resveratrol from the aged grape pressing extract. The percentage of (*E*)-resveratrol recovery after wash and elution steps from the MIP cartridge was 98.9%. Although the recovery for (*E*)-resveratrol from the NIP cartridge was as the same as the MIP (98.9%), the majority of (*E*)-resveratrol had been removed after the wash steps. For both samples, the use of the NIP led to a quick washout of (*E*)-resveratrol whereas the MIP retained about two-thirds of the target compound, which later could be eluted.

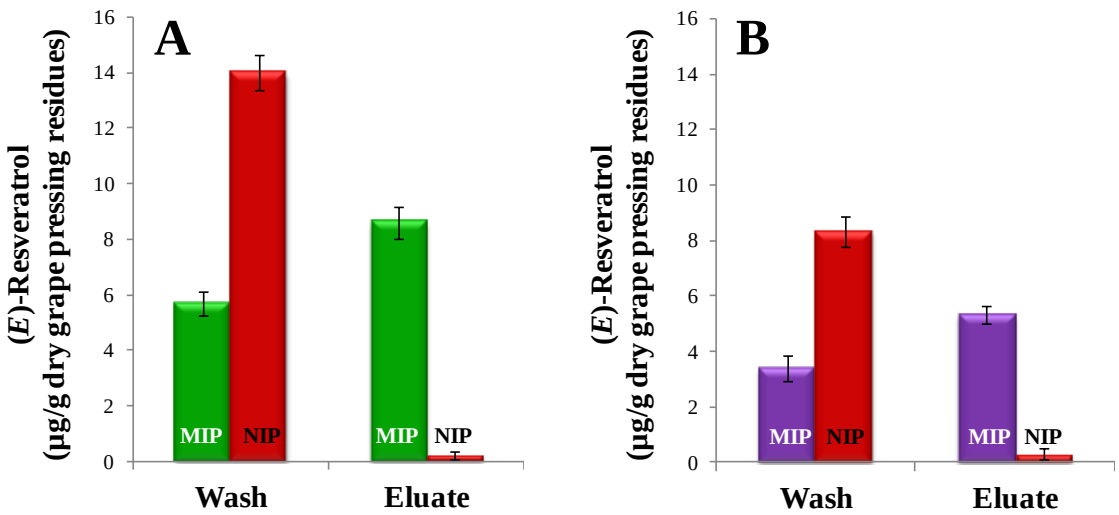

Figure 4.7: The amount of (*E*)-resveratrol (µg/g dry grape pressing residues) in wash and eluate fractions after MISPE and NISPE treatment from extracts of **(A)** fresh and **(B)** aged grape pressing residues. Measurements were determined in duplicate (n = 2). Error bars indicate the standard error expressed by the formula $Error = \sigma/\sqrt{n}$, where σ is the standard deviation and n is the number of measurements.

Table 4.3: Recovery of (*E*)-resveratrol (µg/g dry grape pressing residue) from extracts of **(A)** fresh and **(B)** aged grape pressing residues after MISPE or NISPE treatment.

		(*E*)-resveratrol in "A" (µg/g dry grape pressing residues)		**(*E*)-resveratrol in "B" (µg/g dry grape pressing residues)**	
		MISPE	**NISPE**	**MISPE**	**NISPE**
Untreated sample	Sample loaded contained (*E*)-resveratrol (1 × 5 mL)	14.3	14.3	8.7	8.7
After treatment	Wash steps (4 × 5 mL)	5.6	13.9	3.3	8.3
	Elution steps (10 × 5 mL)	8.6	0.2	5.3	0.3
	Total amount of (*E*)-resveratrol after wash and elution steps	14.2	14.1	8.6	8.6
	Total (*E*)-resveratrol recovery (%)	99.3	98.6	98.9	98.9
	Imprinting factor (*IF* = MIP eluate / NIP eluate)	43		18	

There is a considerable commercial interest in identifying uses of grape wastes in the field of pharmaceuticals and cosmetics. However, before grape wastes can be successfully used to produce commercial products, an understanding of the factors that influence the polyphenol content of the waste is necessary. The present studies provide basic information on the potential effects of storage time and conditions on the composition and distribution of polyphenols in grape wastes. This was investigated by a comparative study of the chromatographic profiles of fresh and aged grape pressing residue extracts. The aged extracts contained lower amounts of polyphenols as a result of the physiological processes involved during ageing. The lengthy storage period for the grape pressing residue resulted in the conversion of (*E*)-resveratrol (nearly 40%) into the (*Z*)-isomer. One of the reasons was probably infestation of the sample by mould. As a result of a decrease in the amount of the (*E*)-resveratrol phytoalexin, the moisture and residual levels of sugars present in the aged sample could possibly have rendered it more susceptible to microbial spoilage during storage. The occurrence of substantial amounts of mould spores intrinsic to this small-scale laboratory sample reflects the real situation of grape waste in storage bins in vineyards before being transported to companies such as Tarac Technologies. Although lower amounts of polyphenols were observed after 51 days of storage, about 60% of (*E*)-resveratrol still remained in the sample. Another factor that affects the conversion of (*E*)-resveratrol into

(*Z*)-form is through photo-isomerisation under light exposure. The occurrence of (*Z*)-resveratrol is less important because it has fewer health benefits than the (*E*)-isomer (*51*).

This is the first time that comprehensive enrichment of (*E*)-resveratrol from grape pressing residues at different stages of waste storage has been performed using a rapid MISPE technique prior to analysis by RP-HPLC and LC-ESI-MS/MS. This methodology has been developed based on a Green Chemistry 'benign by design' concept, and used a mixture of ethanol-water as the main solvent for the extraction, the MISPE protocol, chromatographic analysis and MS detection. In addition, this method had a shorter analysis time and reduced solvent consumption compared with conventional extraction protocols.

In sample cleanup and enrichment, the MIP clearly demonstrated selective recognition towards *(E)*-resveratrol from extracts of two different samples of grape pressing residues. A higher enrichment level of (*E*)-resveratrol was achieved from the fresh sample compared to from the aged sample. The quantification analysis after MISPE, using RP-HPLC revealed significant binding recognition, with recovery of two-thirds of the resveratrol in the MIP eluent. However, about one-third of the target compound was not retained in the MIP sorbent during the wash steps. The rather short interaction time for the target analyte to adsorb properly into the MIP binding sites may have affected the binding retention when a large SPE cartridge (sorbent bed height of only 0.5 cm) was used. It was proposed that due to the inadequate penetration of the target analyte into the pyridinyl-based MIP cavities, the hydroxyl-groups of the aqueous-EtOH washing solvent competed with the hydroxyl-groups of (*E*)-resveratrol to generate hydrogen bonding interactions with the pyridinyl-functionalities, resulting in a lower binding affinity. The results obtained with a large MISPE cartridge in this study showed that binding recognition achieved (about 60%) of *(E)*-resveratrol. In order to increase the amount of *(E)*-resveratrol obtained in the elution steps, and at the same time reduce the non-selective binding in the wash step from the MISPE, a smaller cartridge was recommended for future experiments.

The analysis of MIP properties also revealed cross-reactivity for compounds structurally related to (*E*)-resveratrol. Interestingly, the MIP showed different degrees of binding preference between the procyanidin dimer **(peak 10)**, procyanidin dimer gallate **(peak 12)** and procyanidin trimer **(peak 3)**. Due to the size, shape and chemical functionality of the resveratrol template (imprint) molecule, only the procyanidin dimeric structure can fit into the binding sites because the building block of this compound is made from a

catechin/epicatechin monomer, which exhibits some structural similarities to the imprint molecule. The procyanidin dimer most probably arranged its molecular structure orientation to encourage hydrogen bonding interactions with the pyridinyl functional monomers in the polymer networks. The binding mechanisms of bulky components such as B-type procyanidin dimer were discussed before in **Chapter 3 (Section 3.3.3.2)**. In contrast, the access of very large substrates to binding sites is severely impeded. The work herein demonstrated that the sizes and molecular structures of the procyanidin dimer gallate and procyanidin trimer were not compatible with the MIP cavities hence no binding occurred. This indicates that chemical functionality and spatial complementarity of the imprint molecule strongly influence the binding recognition mechanisms. The inherent selectivity and affinity of the MIP could be used for compound specific as well as group specific recognition in the SPE format (*52*).

4.4 Conclusions

These results provide an efficient, green new method to potentially capture and enrich polyphenols with health-beneficial potential from raw grape marc and other biological waste products and deliver fast information on their concentrations at different stages of waste material processing. This approach may contribute to generate a new perspective for a 'green economy' to benefit the agricultural and nutraceutical industries as well as minimise environmental footprints.

4.5 References

1. FAOSTAT-FAO, Grape production in the world. *Statistical database available online http://www.faostat.fao.org/* **2007**.
2. Ruberto, G.; Renda, A.; Amico, V.; Tringali, C., Volatile components of grape pomaces from different cultivars of *Sicilian Vitis vinifera* L. *Bioresour. Technol.* **2008**, *99*, 260-268.
3. Makris, D. P.; Boskou, G.; Andrikopoulos, N. K., Polyphenolic content and *in vitro* antioxidant characteristics of wine industry and other agri-food solid waste extracts. *J. Food Compos. Anal.* **2007**, *20*, 125-132.
4. Laufenberg, G.; Kunz, B.; Nystroem, M., Transformation of vegetable waste into value added products: (A) the upgrading concept; (B) practical implementations. *Bioresour. Technol.* **2003**, *87*, 167-198.
5. Schwarz, L. J.; Danylec, B.; Harris, S. J.; Boysen, R. I.; Hearn, M. T. W., Preparation of molecularly imprinted polymers for the selective recognition of the bioactive polyphenol, (*E*)-resveratrol. *Journal of Chromatography A* **2011**, *1218*, 2189-2195.
6. Negro, C.; Tommasi, L.; Miceli, A., Phenolic compounds and antioxidant activity from red grape marc extracts. *Bioresour. Technol.* **2003**, *87*, 41-44.

7. Spanghero, M.; Salem, A. Z. M.; Robinson, P. H., Chemical composition including secondary metabolites and rumen fermentability of seeds and pulp of Californian (USA) and Italian grape pomaces. *Anim. Feed Sci. Technol.* **2009**, *152*, 243-255.
8. Sanchez, A.; Ysunza, F.; Beltran Garcia, M. J.; Esqueda, M., Biodegradation of viticulture wastes by Pleurotus: A source of microbial and human food and its potential use in animal feeding. *J. Agric. Food Chem.* **2002**, *50*, 2537-2542.
9. Baydar, N. G.; Ozkan, G.; Cetin, E. S., Characterization of grape seed and pomace oil extracts. *Grasas Aceites (Sevilla, Spain)* **2007**, *58*, 29-33.
10. Torres, J. L.; Varela, B.; Garcia, M. T.; Carilla, J.; Matito, C.; Centelles, J. J.; Cascante, M.; Sort, X.; Bobet, R., Valorization of grape *(Vitis vinifera)* by-products. Antioxidant and biological properties of polyphenolic fractions differing in procyanidin composition and flavonol content. *J. Agric. Food Chem.* **2002**, *50*, 7548-7555.
11. Shrikhande, A. J., Wine by-products with health benefits. *Food Res. Int.* **2000**, *33*, 469-474.
12. Baur, J. A.; Sinclair, D. A., Therapeutic potential of resveratrol: the *in vivo* evidence. *Nat. Rev. Drug Discovery* **2006**, *5*, 493-506.
13. Soleas, G. J.; Goldberg, D. M.; Diamandis, E. P.; Karumanchiri, A.; Yan, J.; Ng, E., A derivatized gas chromatographic mass spectrometric method for the analysis of both isomers of resveratrol in juice and wine. *Am. J. Enol. Vitic.* **1995**, *46*, 346-352.
14. Ju, Z. Y.; Howard, L. R., Effects of solvent and temperature on pressurized liquid extraction of anthocyanins and total phenolics from dried red grape skin. *J. Agric. Food Chem.* **2003**, *51*, 5207-5213.
15. Palenzuela, B.; Arce, L.; Macho, A.; Munoz, E.; Rios, A.; Valcarcel, M., Bioguided extraction of polyphenols from grape marc by using an alternative supercritical fluid extraction method based on a liquid solvent trap. *Anal. Bioanal. Chem.* **2004**, *378*, 2021-2027.
16. Lin, L. Z.; Harnly, J. M., A screening method for the identification of glycosylated flavonoids and other phenolic compounds using a standard analytical approach for all plant materials. *J. Agric. Food Chem.* **2007**, *55*, 1084-1096.
17. Nawaz, H.; Shi, J.; Mittal, G. S.; Kakuda, Y., Extraction of polyphenols from grape seeds and concentration by ultrafiltration. *Sep. Purif. Technol.* **2006**, *48*, 176-181.
18. Makris, D. P.; Boskou, G.; Chiou, A.; Andrikopoulos, N. K., An investigation on factors affecting recovery of antioxidant phenolics and anthocyanins from red grape *(Vitis vinifera* L.*)* pomace employing water/ethanol-based solutions. *Am. J. Food Technol.* **2008**, *3*, 164-173.
19. Careri, M.; Corradini, C.; Elviri, L.; Nicoletti, I.; Zagnoni, I., Direct HPLC analysis of quercetin and *trans*-resveratrol in red wine, grape and winemaking byproducts. *J. Agric. Food Chem.* **2003**, *51*, 5226-5231.
20. Jeandet, P.; Bessis, R.; Gautheron, B., The production of resveratrol (3,5,4'-trihydroxystilbene) by grape berries in different developmental stages. *Am. J. Enol. Vitic.* **1991**, *42*, 41-46.
21. Trela, B. C.; Waterhouse, A. L., Resveratrol: isomeric molar absorptivities and stability. *J. Agric. Food Chem.* **1996**, *44*, 1253-1257.
22. Lazze, M. C.; Pizzala, R.; Gutierrez, P. F. J.; Gaton, G. P.; Antolin, R. J. M.; Fabris, N.; Bianchi, L., Grape waste extract obtained by supercritical fluid extraction contains bioactive antioxidant molecules and induces antiproliferative effects in human colon adenocarcinoma cells. *J. Med. Food* **2009**, *12*, 561-568.
23. Hogan, S.; Canning, C.; Sun, S.; Sun, X.; Zhou, K., Effects of grape pomace antioxidant extract on oxidative stress and inflammation in diet induced obese mice. *J. Agric. Food Chem.* **2010**, *58*, 11250-11256.

24. Hogan, S.; Zhang, L.; Li, J.; Sun, S.; Canning, C.; Zhou, K., Antioxidant rich grape pomace extract suppresses postprandial hyperglycemia in diabetic mice by specifically inhibiting α-glucosidase. *Nutr. Metab.* **2010**, *7*, 71-79.

25. Nishiumi, S.; Mukai, R.; Ichiyanagi, T.; Ashida, H., Suppression of lipopolysaccharide and galactosamine induced hepatic inflammation by red grape pomace. *J. Agric. Food Chem.* **2012**, *60*, 9315-9320.

26. Amico, V.; Chillemi, R.; Mangiafico, S.; Spatafora, C.; Tringali, C., Polyphenol enriched fractions from Sicilian grape pomace: HPLC-DAD analysis and antioxidant activity. *Bioresour. Technol.* **2008**, *99*, 5960-5966.

27. Kammerer, D.; Claus, A.; Carle, R.; Schieber, A., Polyphenol screening of pomace from red and white grape varieties *(Vitis vinifera* L.*)* by HPLC-DAD-MS/MS. *J. Agric. Food Chem.* **2004**, *52*, 4360-4367.

28. Stella, L.; De Rosso, M.; Panighel, A.; Dalla Vedova, A.; Flamini, R.; Traldi, P., Collisionally induced fragmentation of $[M-H]^-$ species of resveratrol and piceatannol investigated by deuterium labelling and accurate mass measurements. *Rapid Commun. Mass Spectrom.* **2008**, *22*, 3867-3872.

29. Careri, M.; Corradini, C.; Elviri, L.; Nicoletti, I.; Zagnoni, I., Liquid chromatography electrospray tandem mass spectrometry of *cis*-resveratrol and *trans*-resveratrol: development, validation and application of the method to red wine, grape and winemaking byproducts. *J. Agric. Food Chem.* **2004**, *52*, 6868-6874.

30. Maier, T.; Sanzenbacher, S.; Kammerer, D. R.; Berardini, N.; Conrad, J.; Beifuss, U.; Carle, R.; Schieber, A., Isolation of hydroxycinnamoyltartaric acids from grape pomace by high-speed counter-current chromatography. *J. Chromatogr., A* **2006**, *1128*, 61-67.

31. Sun, W.; Miller, J. M., Tandem mass spectrometry of the B-type procyanidins in wine and B-type dehydrodicatechins in an autoxidation mixture of (+)-catechin and (-)-epicatechin. *J. Mass Spectrom.* **2003**, *38*, 438-446.

32. Callemien, D.; Collin, S., Use of RP-HPLC-ESI(-)-MS/MS to differentiate various proanthocyanidin isomers in lager beer extracts. *J. Am. Soc. Brew. Chem.* **2008**, *66*, 109-115.

33. Tourino, S.; Fuguet, E.; Jauregui, O.; Saura-Calixto, F.; Cascante, M.; Torres, J. L., High resolution liquid chromatography electrospray ionization time of flight mass spectrometry combined with liquid chromatography electrospray ionization tandem mass spectrometry to identify polyphenols from grape antioxidant dietary fiber. *Rapid Commun. Mass Spectrom.* **2008**, *22*, 3489-3500.

34. Sarni-Manchado, P.; Cheynier, V.; Moutounet, M., Reactions of polyphenoloxidase generated caftaric acid *o*-quinone with malvidin 3-*O*-glucoside. *Phytochemistry* **1997**, *45*, 1365-1369.

35. Sun, J.; Liang, F.; Yan, B.; Li, P.; Duan, C., Screening non-colored phenolics in red wines using liquid chromatography ultraviolet and mass spectrometry mass spectrometry libraries. *Molecules* **2007**, *12*, 679-693.

36. Gomez-Romero, M.; Zurek, G.; Schneider, B.; Baessmann, C.; Segura-Carretero, A.; Fernandez-Gutierrez, A., Automated identification of phenolics in plant derived foods by using library search approach. *Food Chem.* **2010**, *124*, 379-386.

37. Maatta-Riihinen, K. R.; Kahkonen, M. P.; Torronen, A. R.; Heinonen, I. M., Catechins and procyanidins in berries of *Vaccinium* species and their antioxidant activity. *J. Agric. Food Chem.* **2005**, *53*, 8485-8491.

38. Landrault, N.; Larronde, F.; Delaunay, J. C.; Castagnino, C.; Vercauteren, J.; Merillon, J. M.; Gasc, F.; Cros, G.; Teissedre, P. L., Levels of stilbene oligomers and astilbin in French varietal wines and in grapes during noble rot development. *J. Agric. Food Chem.* **2002**, *50*, 2046-2052.

39. Castillo-Munoz, N.; Gomez-Alonso, S.; Garcia-Romero, E.; Gomez, M. V.; Velders, A. H.; Hermosin-Gutierrez, I., Flavonol 3-*O*-glycosides series of *Vitis vinifera* cv. Petit Verdot red wine grapes. *J. Agric. Food Chem.* **2009**, *57*, 209-219.

40. La Torre, G. L.; Saitta, M.; Vilasi, F.; Pellican, T.; Dugo, G., Direct determination of phenolic compounds in Sicilian wines by liquid chromatography with PDA and MS detection. *Food Chem.* **2006**, *94*, 640-650.

41. Bravo, M. N.; Silva, S.; Coelho, A. V.; Boas, L. V.; Bronze, M. R., Analysis of phenolic compounds in Muscatel wines produced in Portugal. *Anal. Chim. Acta* **2006**, *563*, 84-92.

42. Gu, L.; Kelm, M. A.; Hammerstone, J. F.; Zhang, Z.; Beecher, G.; Holden, J.; Haytowitz, D.; Prior, R. L., Liquid chromatographic electrospray ionization mass spectrometric studies of proanthocyanidins in foods. *J. Mass Spectrom.* **2003**, *38*, 1272-1280.

43. Alvarez, E.; Rodino-Janeiro, B. K.; Jerez, M.; Ucieda-Somoza, R.; Nunez, M. J.; Gonzalez-Juanatey, J. R., Procyanidins from grape pomace are suitable inhibitors of human endothelial NADPH oxidase. *J. Cell Biochem.* **2012**, *113*, 1386-1396.

44. Santos-Buelga, C.; Scalbert, A., Proanthocyanidins and tannin-like compounds - nature, occurrence, dietary intake and effects on nutrition and health. *J. Sci. Food Agric.* **2000**, *80*, 1094-1117.

45. Holt, R. R.; Lazarus, S. A.; Sullards, M. C.; Zhu, Q. Y.; Schramm, D. D.; Hammerstone, J. F.; Fraga, C. G.; Schmitz, H. H.; Keen, C. L., Procyanidin dimer B_2 [epicatechin-(4β-8)-epicatechin] in human plasma after the consumption of a flavanol rich cocoa. *Am. J. Clin. Nutr.* **2002**, *76*, 798-804.

46. Deprez, S.; Mila, I.; Huneau, J. F.; Tome, D.; Scalbert, A., Transport of proanthocyanidin dimer, trimer, and polymer across monolayers of human intestinal epithelial Caco-2 cells. *Antioxid. Redox Signaling* **2001**, *3*, 957-967.

47. Kondo, K.; Kurihara, M.; Fukuhara, K.; Tanaka, T.; Suzuki, T.; Miyata, N.; Toyoda, M., Conversion of procyanidin B-type (catechin dimer) to A-type: evidence for abstraction of C-2 hydrogen in catechin during radical oxidation. *Tetrahedron Lett.* **2000**, *41*, 485-488.

48. De Bruyne, T.; Pieters, L.; Witvrouw, M.; De Clercq, E.; Vanden, B. D.; Vlietinck, A. J., Biological evaluation of proanthocyanidin dimers and related polyphenols. *J. Nat. Prod.* **1999**, *62*, 954-958.

49. Murakami, A.; Ashida, H.; Terao, J., Multitargeted cancer prevention by quercetin. *Cancer Lett.* **2008**, *269*, 315-325.

50. Luo, H.; Jiang, B. H.; King, S. M.; Chen, Y. C., Inhibition of cell growth and VEGF expression in ovarian cancer cells by flavonoids. *Nutr. Cancer* **2008**, *60*, 800-809.

51. Basly, J. P.; Marre-Fournier, F.; Le Bail, J. C.; Habrioux, G.; Chulia, A. J., Estrogenic/antiestrogenic and scavenging properties of (*E*)- and (*Z*)-resveratrol. *Life Sci.* **2000**, *66*, 769-777.

52. Sellergren, B.; Editor, Molecularly imprinted polymers: man-made mimics of antibodies and their applications in analytical chemistry. *Tech. Instrum. Anal. Chem.*, **2001**, *23*, p 557.

Chapter 5

Evaluation and characterisation of novel molecularly imprinted polymers for the analysis of sterols in solid-phase extraction

Abstract

Imprinted polymers were synthesized for the recognition of stigmasterol using either the non-covalent or the covalent approach. The synthesised molecularly imprinted polymers (MIPs) were then evaluated *via* static and dynamic batch binding assays. The conventional non-covalent imprinting method resulted in a MIP which did not possess any binding affinity for stigmasterol. In contrast, a novel MIP fabricated through the covalent approach using the post-synthetically cleavable monomer-template composite stigmasteryl-3-*O*-methacrylate showed good recognition of stigmasterol in aqueous media compared to a MIP generated by non-covalent imprinting. The covalently imprinted MIP showed high binding for stigmasterol in comparison to the non-imprinted polymer (NIP). The affinity and selectivity of the MIP towards the target molecule stigmasterol was observed to be driven by hydrogen bonding interactions with the residual carboxyl group derived from the polymer-embedded methacrylate-portion as well as the size and shape complementarities to the binding sites. The MIP was then used in a solid-phase extraction (SPE) format with the aim to selectively bind stigmasterol or structurally related sterols from sterol mixtures. This dynamic binding assay showed the highest imprinting factor *(IF)* of 12 for stigmasterol with 99% recovery in comparison to cholesterol (*IF* = 6) and ergosterol (*IF* = 4). For the quantification and identification of the sterols, a new green separation technique was developed using an environmentally benign mobile phase composed of ethanol-water mixtures and acetic acid as a mobile phase additive.

Table of Contents

5.1 Introduction

Sterols are important components of cell membranes and play a significant role in human health and well-being (*1, 2*). They are present in rapeseed, soya beans, cocoa beans, and other nuts and seeds. Grape seeds, the abundant byproducts of wine making, have been shown to contain sterols (*3*). The utilisation of these waste materials for nutraceutical purposes may become economically interesting. Due to the small amounts of sterols in biological samples, the currently used analytical methods (*4, 5*) are time consuming and require intensive sample preparations. This prompted the development of a new environmentally benign extraction method.

A new way to extract and pre-concentrate specific target sterols such as cholesterol, stigmasterol and β-sitosterol from a complicated matrix is the use of a molecularly imprinted solid-phase extraction (MISPE) technique prior to their analysis by chromatographic methods. However, due to the amphipathic sterol nature with a single hydroxyl-group at the C_3 position and a relatively large size (molecular weight 300-800 g/mol), the design of synthetic, molecular recognition-based polymer networks for sterol compounds is challenging.

In the past, several strategies to improve the MIP technology for sterol analysis had focused either on pre-polymerisation stages by choosing the appropriate functional monomers and stabilising the template-monomer assemblies (*6*) or on post-polymerisation procedures by modifying the distribution of binding sites *via* physical (*7*) or chemical approaches (*8*). Whitcombe *et al.* (*9*) introduced a hybrid covalent/non-covalent approach or "sacrificial spacer" methodology that had been shown to produce a single dissociation constant. The method involved hydrolytically cleaving a covalently bound cholesterol template-monomer which resulted in the formation of non-covalent recognition sites. Zhong and co-workers (*10*) tried to synthesize a cholesterol MIP using the covalent imprinting approach with hydrophilic monomers (2-hydroxyethyl methacrylate) for the application in water-based samples. However, the polymers prepared with that strategy had a low selectivity to cholesterol due to hydrophobic cross linker-monomer interactions.

In previous studies, major emphasis had focussed on the engineering and architectural design of cholesterol MIPs with much fewer papers published on other sterols. **Figure 5.1** shows a breakdown by the percentage of 56 publications related to the types of sterol-template used for MIP synthesis from 1994 to 2012 (data obtained from SciFinder). Various aspects of

cholesterol MIPs (84%) have been investigated including their binding capacity, imprinting effect and mechanism of recognition. Although stigmasterol-templated MIPs have been explored to a very limited extent (11% of all sterol MIP papers), there is no information with respect to their application in water-based media. Therefore, the aim of the present study was to develop a new method for the isolation and analysis of sterols, in particular stigmasterol from water-based extracts from food sources.

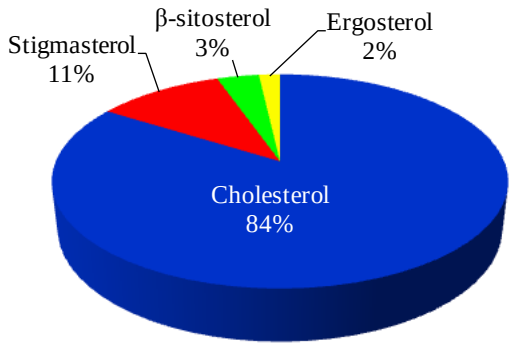

Figure 5.1: Publications related to sterol-templated MIPs from 1994 to 2012 using the search terms "molecularly imprinted polymers", "cholesterol", "stigmasterol", "ergosterol" and "β-sitosterol" in SciFinder (Chemical Abstracts Service, Columbus, Ohio, USA). The non-covalent approach was used in 73.2% and the covalent approach was applied in 26.8% of the investigations.

5.2 Materials and Methods

5.2.1 Reagents

Reagent grade acetic acid (AcOH), formic acid (FA) and hydrochloric acid (HCl) were purchased from Ajax Finechem (Melbourne, Australia). Ethanol (EtOH), acetonitrile (ACN), methanol (MeOH), chloroform ($CHCl_3$) and sodium hydroxide (NaOH) were purchased from Merck (Melbourne, Australia). All solvents used for the MIP preparations and evaluations as well as chromatographic separations were HPLC grade. Water was purified using a water purification system (Pall Corp., Melbourne, Australia) to a resistivity of 18.2 MΩ.cm. For the preparation of MIPs using either the non-covalent or covalent imprinting approach, methacrylic acid (MAA), 4-vinyl pyridine (4-VP), ethyleneglycol dimethacrylate (EGDMA) and 2,2-azobis(2-methylpropionitrile) (AIBN) were purchased from Sigma-Aldrich (Sydney, Australia).

5.2.2 Standards

All commercial standards of sterols including stigmasterol (Sigma, Melbourne, Australia), cholesterol (Aldrich, Melbourne, Australia) and ergosterol (Fluka Chemicals, Melbourne,

Australia) were used in these experiments with purity of ≥ 95%. A series of commercially unavailable stigmasterol analogue standards (stigmasteryl-3-*O*-ferulate, stigmasteryl-3-*O*-(4-acetoxyferulate) and stigmasteryl-3-*O*-acetate) were chemically synthesised by Mr. Basil Danylec in the laboratories of the Centre for Green Chemistry, Monash University, Melbourne, Australia.

5.2.3 Instrumentation

5.2.3.1 RP-HPLC

The analysis of sterol compounds was performed using an Agilent HPLC 1100 series, 80 Hz full spectra ultra fast LC (Agilent Technologies, Waldbronn, Germany) equipped with ChemStation software (B.02.01 SR1), a degasser, a binary gradient pump, an auto-sampler with a 900 µL sample loop, a thermostated column compartment and a diode array detector (DAD). The DAD was set to an acquisition range of 200-600 nm at a spectral acquisition rate of 2 nm scans per step (peak width 0.1 min). Analytical RP-HPLC separations were performed with a double end-capped Zorbax Eclipse XDB C_{18} column (4.6 mm × 150 mm, 5 µm particle size) purchased from Agilent Technologies (Melbourne, Australia) at 23 °C. Simultaneous monitoring of stigmasterol, stigmasterol analogues and cholesterol was performed with an UV-DAD detector at the wavelength of 210 nm whilst ergosterol was recorded at 280 nm. For this work, the best way to prepare the mobile phase was premixing the EtOH with H_2O in a ratio of 9:1 v/v in one bottle and degassing the solution in an ultrasonic bath (Elmasonic, Singen, Germany) for 30 min to prevent bubble formation. The eluent was subsequently delivered isocratically to the RP-HPLC column at the flow rate of 0.5 mL/min and the injection volume was 5 µL. All solutions were filtered through a polypropylene membrane filter of 0.2 µm pore size with a diameter of 47 mm (Pall Corp., Melbourne, Australia). The total run time for the separation of stigmasterol, cholesterol and ergosterol was 25 min whilst the separation for stigmasterol and its analogues was 65 min.

A six-point calibration curve for stigmasterol quantification was prepared by serial dilution of a stigmasterol standard at known concentrations of 0.05 to 0.50 mM in ACN/H_2O (9:1, v/v) and mixed well prior injection into the RP-HPLC system. The same procedures were implemented for the construction of the stigmasterol calibration curve using neat ACN (99.9% purity) as dilution solvent.

5.2.3.2 LC-ESI ion trap MS/MS

Identification of sterols was carried out on an Agilent 1100 Series LC/MSD-SL ion trap mass spectrometer equipped with an Agilent G1607A orthogonal electrospray ionisation (ESI) interface (Agilent Technologies, Palo Alto, California, USA), Agilent 1100 HPLC and an UV-Vis DAD. The reversed-phase HPLC separations of sterol compounds were performed using a double end-capped Zorbax XDB capillary C_{18} column (0.3 mm × 150 mm, 3.5 µm particle size) purchased from Agilent Technologies (Melbourne, Australia) at 23 °C. The experiments were carried out using the same isocratic elution program, which was previously described for the analytical RP-HPLC **(Section 5.2.3.1)** except for varying the injection volume and the flow rate. The column was equilibrated with the eluent for 15 min prior every injection.

The chromatographic conditions of the microLC were established based on a down-scale approach from the analytical LC procedure (see formula in **Chapter 2 - Section 2.3.2**). The flow rate and injection volume of the capillary LC method were determined to be 2 µL/min and 0.1 µL, respectively. The mass detection was performed in the full scan mode in the *m/z* range from 100 to 1000 using the positive ionisation mode. The capillary voltage was set to 3.5 kV. Nitrogen was used as the nebulising gas at a pressure of 10 psi. The drying gas flow rate was set to 5 L/min at 300 °C. The target mass, the compound stability and the trap drive level were set to *m/z* 600, 80% and 100%, respectively. The ion accumulation time was automatically adjusted *via* the Ion Charge Control (ICC) feature of the instrument. The ICC target was 30,000 units and the maximal accumulation time was 300 ms. For MS/MS analysis, helium was used as the gas for collision induced dissociation (CID). The instrument was operated using the "smart fragmentation" mode, which allowed the fragmentation amplitude to be varied from 30-200%. The instrument automatically changed from MS to MS/MS mode when the intensity of a particular ion surpassed the threshold of 10,000 units. Active exclusion was carried out after two spectra for 1 min. The fragmentation amplitude was set to 1.5 V to encourage fragmentation of sterol compounds and the number of precursor ion selection was set to 2. Data acquisition and processing were conducted using the MSD Trap Control software and Agilent ChemStation version 4.2.

5.2.4 MIP preparation with the non-covalent imprinting approach

5.2.4.1 Mini-MIP method

The mini-MIPs made using a stigmasterol-template were prepared in small glass vials (1.5 mL). This screening approach was conducted before the bulk monolith polymerisations were performed. The mini-MIPs experiments were carried out according to the method previously described elsewhere (*11*), however with some modifications. Different types of functional monomers were compared, namely methacrylate acid (MAA), 4-vinylpyridine (4-VP) and N,N′-dimethylacrylamide (DMAMM), all in the presence of a porogen ($CHCl_3$) and a crosslinker EGDMA (ethylene glycol dimethacrylate). The mini-NIPs (non-imprinted polymers) were made using the same procedure as for the MIPs, except the stigmasterol template was omitted.

Overall, six mini-MIPs as well as their control polymers (mini-NIPs) were tested with two different molar ratios of template:monomer:porogen (1:1:5 and 1:10:100). The polymerisation was carried out using the non-covalent self-assembly approach whereby the mixture in each vial was degassed with nitrogen for 5 min, sealed with a screw cap and thermally polymerised at 60 °C for 24 h in a thermostatically controlled water bath (Ratek Instruments, Victoria, Australia). After the polymerisation was complete, evident through the appearance of a white solid disk (50 mg) in the glass vial, the resultant mini-MIP or mini-NIP was crushed in the same glass vial with a small spatula until it became white powder. Subsequently, the stigmasterol template was extracted from the mini-MIP with a mixture of $CHCl_3$/AcOH (9:1, v/v) at room temperature. Stigmasterol release from the MIP was checked periodically and the procedure repeated until no stigmasterol was detected at 210 nm by RP-HPLC.

5.2.4.2 Mini-MIP binding procedure

The performance of the MIP or NIP was evaluated through static binding experiments with stigmasterol standard in $CHCl_3$ (0.1 mM, 1 mL) after the solution was incubated for 18 h at room temperature using a rotary mixer (Ratek Instruments, Victoria, Australia) at 40 rpm. The supernatant obtained from each vial was evaporated until dryness using a vacuum evaporator (Genevac EZ-2, Radiometer Pacific, Melbourne, Australia) operated in the low boiling point mode (30 °C), and redissolved with EtOH prior to analysis by RP-HPLC.

5.2.4.3 Bulk MIP preparation with non-covalent imprinting

MIPs were prepared by the non-covalent imprinting method with stigmasterol (0.1 g, 1 mmol) as template and 4-VP (0.3 g, 10 mmol) as monomer in chloroform (25 mL). The mixture was sonicated for 10 min followed by stirring in an ice bath for 30 min to stabilise the template-monomer interaction. The resulting mixture was purged with nitrogen gas for 10 min prior to the addition of the crosslinker EGDMA (5.0 g, 100 mmol) and the free radical initiator AIBN (0.1 g, 0.4 mmol). The mixture was then polymerised in a thermostatically controlled water bath (Ratek Instruments, Victoria, Australia) at 60 °C for 22 h and was further annealed at 65 °C for another 2 h. The resulting white solid bulk monoliths were dried under vacuum at room temperature overnight to remove $CHCl_3$ traces. Subsequently, the dried polymer was ground using a mortar and pestle and sieved to yield a particle size distribution of 60-90 µm using a sieving apparatus (Retsch, Haan, Germany). The stigmasterol-template molecule was extracted from the MIP by repeated wash, using MeOH/AcOH (9:1, v/v) until the template was no longer detected in the wash solution by RP-HPLC at the wavelength of 210 nm. The MIP particles were then washed in sequence with MeOH and acetone to remove traces of AcOH and dried overnight in a vacuum. The non-imprinted polymer (NIP) was prepared in the same manner as the MIP but without the template. The MIP was subjected to static batch binding procedures in order to evaluate its binding affinity for stigmasterol (target analyte) in comparison to the NIP.

5.2.4.4 Bulk MIP binding procedure

Selectivity studies were conducted for the MIP and the NIP (template:monomer:porogen ratio of 1:10:100) with a stigmasterol standard at different concentrations at the range from 0.5 mM to 10.0 mM in *n*-hexane (1 mL) using a constant amount of polymer particles (20 mg) in sealable Eppendorf tubes. Stigmasterol is soluble up to a concentration of 10.0 mM in *n*-hexane, compared to a maximum concentration of 1.0 mM achievable in polar solvents such as MeOH. The polymers were incubated with the analyte solution and kept at 20 °C on a rotary mixer (Ratek Instruments, Victoria, Australia) at 40 rpm for 12 h. The mixture was centrifuged (Thermo Fisher Scientific, Massachusetts, USA) at 13,000 rpm for 15 minutes to pellet the polymer. The supernatant (100 µL) was evaporated until dryness using a vacuum evaporator (Genevac EZ-2, Radiometer Pacific, Melbourne, Australia), operated in the low

boiling point mode (30 °C). The residue obtained was re-dissolved in EtOH (100 µL) prior to analysis by RP-HPLC with UV-DAD detection at 210 nm.

5.2.5 MIP preparation with the covalent imprinting approach

A novel functionalised stigmasterol-template (stigmasteryl-3-*O*-methacrylate) as shown in **Figure 5.2** was chemically synthesised by Mr. Basil Danylec (Centre for Green Chemistry, Monash University, Melbourne, Australia). This new compound was prepared based on synthetic routes described elsewhere (*12*). The synthesis of the MIP using the covalent approach was performed by Dr. Lachlan Schwarz (Centre for Green Chemistry, Monash University, Melbourne, Australia) according to the following procedure (*12*).

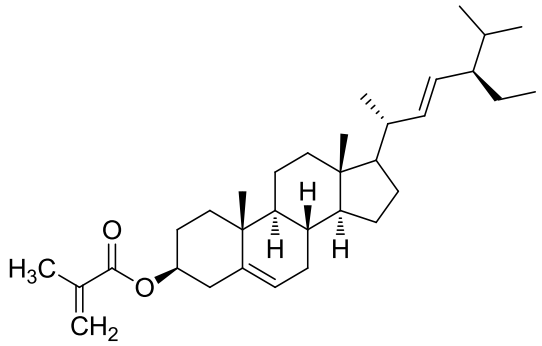

Figure 5.2: Stigmasteryl-3-*O*-methacrylate (cleavable monomer-template composite).

The stigmasteryl-3-*O*-methacrylate (0.5 g, 1 mmol) was mixed with EGDMA (2.0 g, 10 mmol), AIBN (0.1 g, 0.3 mmol) and dissolved in $CHCl_3$ (6 mL) in a thick-walled glass test tube and sealed with a rubber stopper. The mixture was sonicated for 1 min and placed in an ice bath to avoid the start of the polymerisation reaction. Subsequently, the mixture was purged with nitrogen gas for 5 min and then subjected to polymerisation at 60 °C in a thermostatically controlled water bath (Ratek Instruments, Victoria, Australia) for 24 h. After polymerisation, the bulk polymer was crushed and ground using a Retsch RM 200 ball mill (Haan, Germany) followed by a mortar and pestle to obtain finer polymer particles. The ground polymer was refluxed with 1 M NaOH in MeOH for 24 h to cleave the stigmasteryl group template from the MIP and washed with 3.2% (v/v) aqueous HCl to neutralise the basic solution. The resultant polymer was expected to have 'memory cavities' and was sieved using two sieves (Precision Eforming, New York, USA), one with a 90 µm mesh size cut off and then with one of a 30 µm mesh size to produce a particle size in a range of 30-90 µm. In order to allow incorporation of the polymer particles into the SPE cartridge format, particle sizes

below 30 µm were excluded so that no particles could escape through the 20 µm pore sized frit filters of the cartridges. The MIP particles were extensively washed with MeOH to ensure complete template extraction and the wash solution was analysed by RP-HPLC with detection at the absorbance of 210 nm until no trace of stigmasterol was observed. Finally, the polymers were dried overnight under vacuum at room temperature. The preparation of the NIP was performed under the same experimental conditions as the MIP with EGDMA (crosslinker) and porogen ($CHCl_3$), except in the absence of stigmasteryl-methacrylate (cleavable monomer-template composite).

5.2.5.1 MIP surface identification by SEM examination

Scanning electron microscopy was performed on a SEM model 840A (JEOL, Tokyo, Japan) at the Monash Centre for Electron Microscopy (Monash University, Victoria, Australia) to document the surface morphology of the polymers prepared with the covalent imprinting technique. The MIP flake (before grinding, after template removal) was mounted on a stub (sample holder) as shown in **Figure 5.3**. Prior to SEM examination, dust particles were removed from the sample by purging with nitrogen gas. The sample was then coated with AuPt using a sputter coater (Model 208 HR) from Cressington (Watford, England) to minimise the surface charging effect. The same procedure was performed on the non-imprinted polymer (NIP) for comparison. Images were taken at a magnification of 6000 ×, with 30 kV of acceleration voltage, 1×10^{-9} A of probe current and 34 mm working distance.

Figure 5.3: MIP flake on the sample holder for the surface examination by scanning electron microscopy. The size of the flake is 0.5 mm ± 0.1 mm in diameter and the thickness is 0.3 mm ± 0.1 mm.

5.2.5.2 MIP binding site characterisation

5.2.5.2.1 MIP binding protocol

In order to evaluate the effectiveness of the MIP in comparison to the control NIP regardless of their mode of imprinting (non-covalent or covalent), binding site characterisations are

compulsory. The MIPs (after template removal or cleavage of template portion of the polymer-embedded monomer-template composite) were evaluated based on equilibrium batch rebinding experiments with static batch binding followed by dynamic binding assays. The experimental workflow for the characterisation of the binding sites is depicted in **Figure 5.4**. The static batch binding experiments were generally conducted using a constant amount of polymer (*e.g.*, 20 mg in a sealable Eppendorf tube) in a constant-temperature adsorption process (isotherms). The efficacies of the isotherms static batch binding assays (single analyte or multi-cross competitive binding) were measured by the selectivity of the MIP to capture the target molecule in the polymer network in comparison to the NIP. The subsequent dynamic binding assays were performed based on the information obtained from the static binding experiments, for example with respect to the suitability of solvent to bind the target analyte in the MIP cavities.

In this work, dynamic binding studies were performed using an off-line SPE mode. The MIP particles (approximately 200-1000 mg) were packed into the SPE cartridge for further use as molecularly imprinted solid-phase extraction (MISPE) techniques. The dynamic binding experiments conducted using the MISPE technique were required to allow optimisation of loading capacity during wash and elution stages in order to afford a high recovery of the target analyte. In cases where static batch binding assays did not show any promising imprinting effects for a particular MIP system, the dynamic binding assay was not performed.

5.2.5.2.2 Single analyte static binding

The single analyte static batch binding studies for the covalent MIP particles (cleavable monomer-template composite:crosslinker, 1:10) (20 mg) and the NIP particles (no cleavable monomer-template composite:crosslinker, 0:10) (20 mg) were carried out with stigmasterol (0.1 mM) in a mixture of ACN/H_2O (9:1, v/v, 1 mL) or neat ACN (1 mL) at different incubation times (30 min, 2 h or 18 h) in sealable Eppendorf tubes.

The MIP binding study was also extended to various concentrations of stigmasterol (0.1 mM to 0.5 mM) with both solvent systems. The analyte solution was incubated using a rotary mixer (Ratek Instruments, Victoria, Australia) at 40 rpm for 2 h at 20 °C. The mixture was then centrifuged (Thermo Fisher Scientific, Massachusetts, USA) at 13,000 rpm for 15 min to pellet the polymer. The supernatant was directly injected into the RP-HPLC and the stigmasterol signal was detected by UV-DAD at the absorbance of 210 nm. The amount of

stigmasterol bound to the MIP was calculated by subtracting the concentration of stigmasterol analyte in the supernatant from the initial concentration, expressed by µmoles/g polymer.

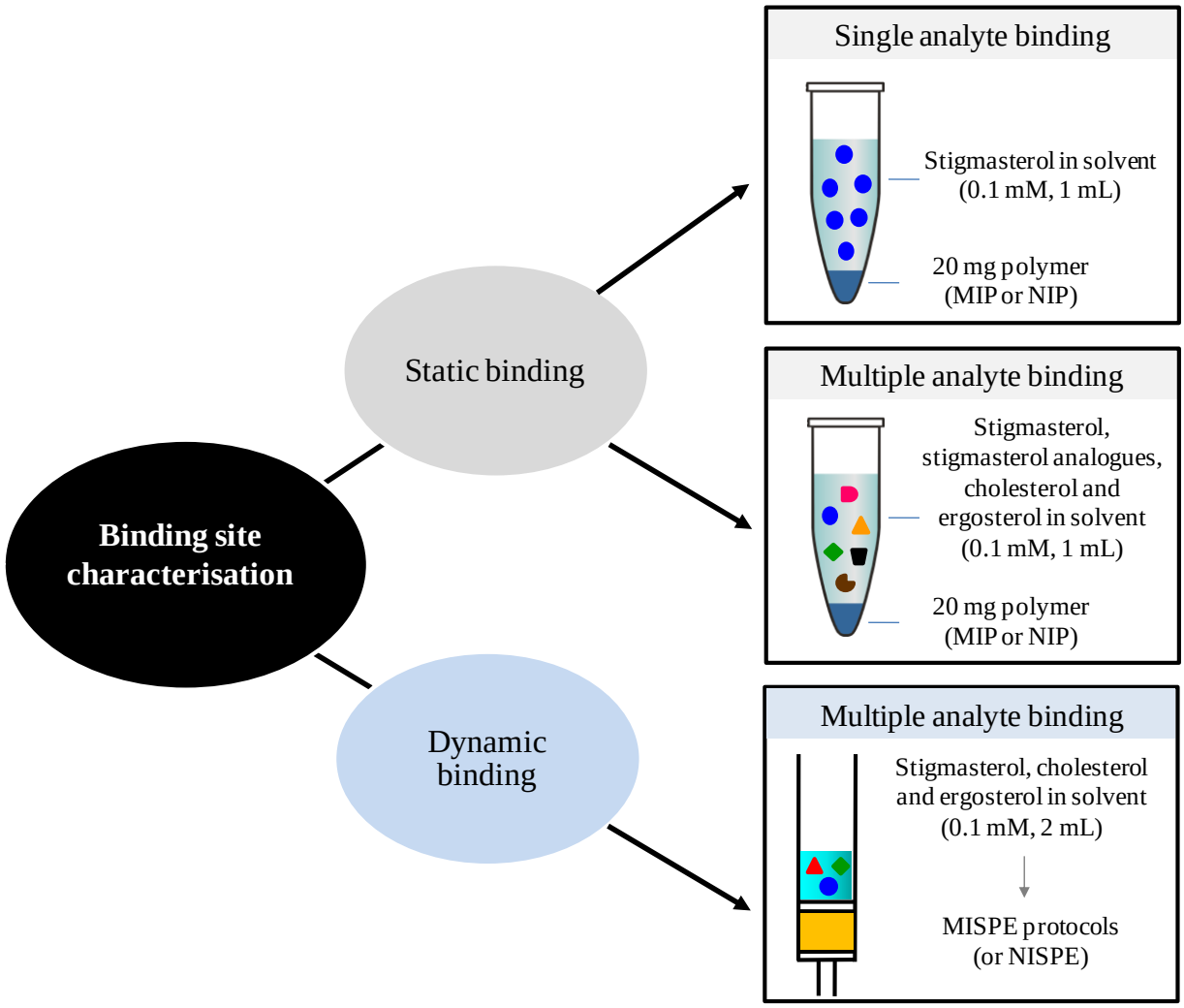

Figure 5.4: Experimental approaches for the evaluation of MIP binding sites *via* static or dynamic binding assays.

5.2.5.2.3 Multiple analyte static binding

A mixture with several sterol analytes namely stigmasterol, stigmasteryl-3-*O*-ferulate, stigmasteryl-3-*O*-(4-acetoxyferulate), stigmasteryl-3-*O*-acetate, cholesterol and ergosterol (0.1 mM for each component) in ACN/H_2O (9:1, v/v, 1 mL) using the MIP or NIP (20 mg) were tested *via* isothermic static binding assays. The polymers were incubated with the six component analytes mixture at 20 °C for 2 h on a rotary mixer (Ratek Instruments, Victoria, Australia) at 40 rpm prior to centrifugation (Thermo Fisher Scientific, Massachusetts, USA) at 13, 000 rpm for 15 min. The supernatant was directly analysed by RP-HPLC at 210 nm for

the detection of stigmasterol, stigmasterol analogues and cholesterol. Ergosterol gave a maximum peak at the absorbance of 280 nm but this compound also can be detected at 210 nm (lower intensity).

5.2.5.2.4 Dynamic binding

The dynamic binding studies for the MIP prepared with the stigmasteryl-methacrylate covalent imprinting approach were conducted in an SPE cartridge **(Figure 5.5)**. The MIP particles (451.1 mg, nominal particle size distribution of 30-90 µm) were slurry packed using 30 mL of ACN into the SPE cartridges which were fitted with polypropylene frits (20 µm pore size). The same packing protocol was performed for the NIP (451.1 mg, nominal particle size distribution of 30-90 µm). The resulting SPE columns were conditioned in sequence using ACN and ACN/H_2O (9:1, v/v) (3 × 2 mL), respectively. A sterol mixture containing stigmasterol, cholesterol and ergosterol at a concentration of 0.1 mM (for each component) in ACN/H_2O (9:1, v/v, 2 mL) was loaded onto the MISPE and NISPE cartridges, respectively. The wash steps were then applied to each cartridge using ACN/H_2O (9:1, v/v) (2 × 2 mL), after which the compounds bound to each cartridge were eluted using EtOH/AcOH (9:1, v/v) (2 × 2 mL). The columns were finally re-conditioned with ACN (3 × 2 mL) for reuse. All fractions were collected by allowing them to drip through under gravity flow (about 4 drops/second) without the application of a vacuum system.

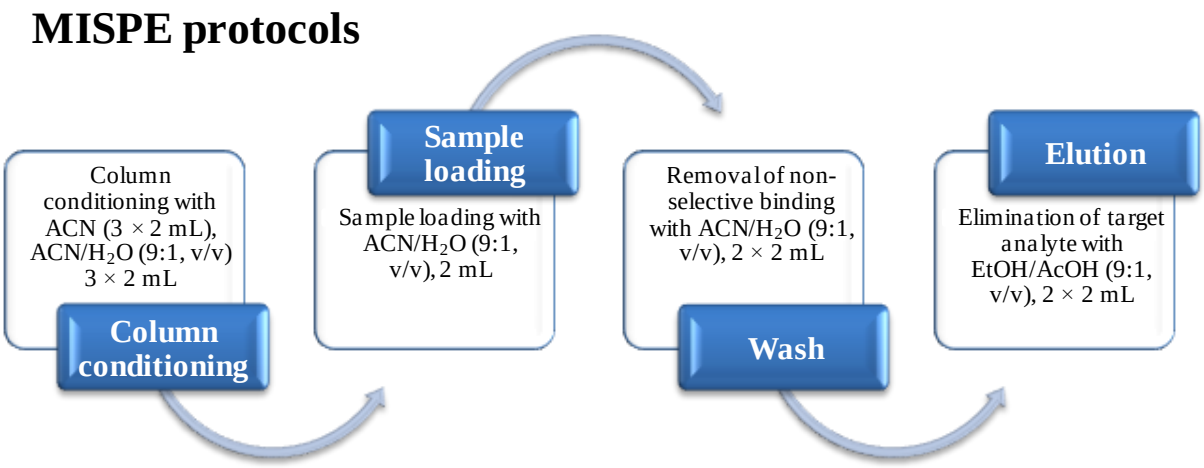

Figure 5.5: MISPE protocols involving column conditioning, sample loading, wash and elution stages for the analysis of a mixture of sterol standards, namely stigmasterol, cholesterol and ergosterol each at a concentration of 0.1 mM.

5.3 Results and Discussion

5.3.1 Optimisation of HPLC chromatographic parameters

Although gas chromatography (GC) is frequently applied for the determination of sterols, this technique requires additional handling procedures including an extra step for sample derivatisation to convert the sterols to trimethylsilyl ethers which typically takes 60 min per reaction (*13*). This approach has been gradually superseded by a liquid chromatography (LC) technique either in the reversed-phase (RP) or normal-phase (NP) mode, which can be performed using a direct injection without sample derivatisation. The latter method however has several shortcomings such as long equilibrium times and involves the usage of hazardous volatile organic solvents (*14*) compared to RP-HPLC. To allow a good separation of sterol components, a double end-capped reversed-phase C_{18} column was selected due to minimised peak tailing (*15*) and operability over a pH range of 2-9.

5.3.1.1 Impact of mobile phase compositions and mobile phase additive on peak width at half height of stigmasterol

During the development of a suitable chromatographic separation method, the most challenging part is to choose an optimal combination of mobile phase and mobile phase additive(s) for the RP-HPLC system and target analytes. A number of publications have addressed how to optimise the solvent system efficiently and various mathematical prediction models have been proposed (*16*). However, these models are sometimes not applicable for the detection of sterols in multi-component samples.

The major issue with sterol components arose with their solubility. The sterols involved in this study were insoluble in water or only partially soluble in polar organic solvents like EtOH, MeOH or ACN. However, these sterols were found to be soluble in polar solvents up to 1.0 mM under 10 min of ultrasonification to enhance the mass transfer rate (*17*) and solvent penetration of the sterol molecules. The sterols used in this work are highly soluble in non-polar solvents such as *n*-hexane, chloroform or toluene.

Three types of mobile phases (ACN, MeOH or EtOH) and mobile phase additives (AcOH or FA) in a range of 0.1% (v/v) to 0.3% (v/v) were employed. The impact of each solvent on sterol separations and the influence of a small amount of acid added were assessed by

RP-HPLC based on the smallest value of peak width at half height ($w_{1/2}$) of stigmasterol in a sterol mixture. The sterol mixture was prepared from stigmasterol, stigmasterol analogues (stigmasteryl-3-*O*-ferulate, stigmasteryl-3-*O*-(4-acetoxyferulate) and stigmasteryl-3-*O*-acetate), cholesterol and ergosterol in aqueous ACN (0.1 mM for each sterol component). Besides the $w_{1/2}$ measurement, the sterol mixture was employed to evaluate the separation performance of those components in different types of mobile phases with a range of mobile phase additive concentrations. The stigmasterol peak was benchmarked for the $w_{1/2}$ measurement due to its consistent symmetrical shape in the chromatogram resulting from every injection.

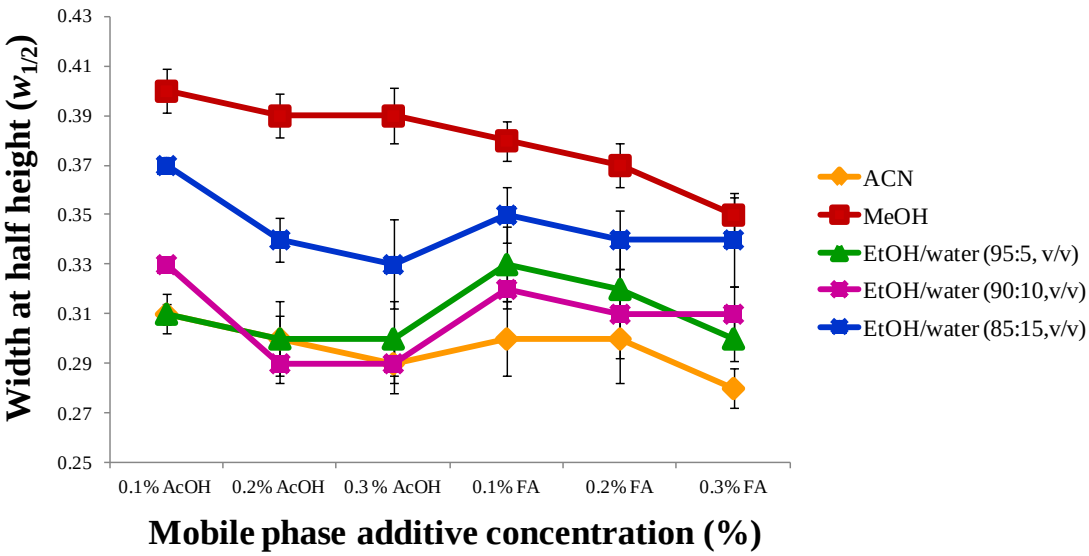

Figure 5.6: Effect of acetic acid and formic acid at different concentrations (0.1% to 0.3%, v/v) with various types of mobile phase compositions (ACN, MeOH, EtOH/H_2O (95:5, v/v), EtOH/H_2O (90:10, v/v) and EtOH/H_2O (85:15, v/v) on peak width at half height, $w_{1/2}$ of stigmasterol in a sterol mixture. LC conditions: isocratic elution, flow rate: 0.5 mL/min, 5 µL injection. Measurements were performed in duplicate (n = 2). Error bars indicate the standard error expressed by the formula $Error = \sigma/\sqrt{n}$, where σ is the standard deviation and n is the number of measurements.

A combination of ACN with 0.3% (v/v) FA gave the lowest value of $w_{1/2}$ (0.28), which led to a better peak shape **(Figure 5.6)**. Despite ACN showing a good result, this solvent was not chosen in order to support a sustainable practice in accordance with the principles of Green Chemistry. When MeOH was applied, the highest values of $w_{1/2}$ (0.35 - 0.40) were observed which reflect broad peaks of sterols regardless of mobile phase additive concentration. Unlike ACN and MeOH, EtOH is more viscous (1.14 mPa·s at 20 °C), hence needs to be mixed with a small proportion of H_2O in a range of 5% (v/v) to 15% (v/v) to minimise high back pressure

in HPLC. The addition of water to the EtOH helped to provide a baseline separation with good resolution (in the case of 5%, v/v and 10%, v/v water content) for all the sterols contained in the mixture. However, when more water was used (15%, v/v water) with EtOH as organic mobile phase modifier, broader peaks of stigmasterol were observed in the chromatogram at all concentrations of acids with higher values of $w_{1/2}$ (0.33 - 0.37). This might be due to the hydrophobic interactions between the dissolved sterols and the immobilised C_{18} ligands in the reversed-phase column. With EtOH/H_2O (95:5, v/v) containing 0.2% - 0.3% (v/v) AcOH, the lowest $w_{1/2}$ was determined to be 0.30. Interestingly, at a concentration of 0.2% - 0.3% (v/v) AcOH, a combination of EtOH/H_2O (90:10, v/v) resulted in a lower value of $w_{1/2}$ (0.29). Thus, EtOH/H_2O (90:10, v/v) with 0.2% (v/v) AcOH was selected as an ideal, environmentally friendly combination of organic mobile phase modifier and mobile phase additive. Based on the optimised chromatographic parameters, this is the first time stigmasterol and structurally related sterols were simultaneously separated using green solvents consisting of EtOH/H_2O and AcOH with isocratic elution by RP-HPLC **(Figure 5.7)**.

5.3.2 Detection method for stigmasterol by LC-MS/MS

Due to the non-polar nature of sterols, LC-MS with atmospheric pressure chemical ionisation (APCI) (*18*) has been reported for the analysis of these compounds, whilst less work has been done using an electrospray ionisation (ESI) technique. In this study, stigmasterol was successfully identified with LC-ESI ion trap MS/MS at the fragmentation amplitude of 1.5 V in the positive ionisation mode using a reversed-phase C_{18} capillary column **(Figure 5.8)**. A higher voltage (1.5 V) was required for sterol experiments in comparison to the polyphenol analysis (1.0 V) to encourage the ionisation process due to the sterol's chemical properties and size of the molecules. The chromatographic parameters of LC-MS/MS were established *via* a down-scaled method from an analytical HPLC column to micro-capillary column dimensions. This approach was implemented to reduce the time of method development and to minimise waste generation.

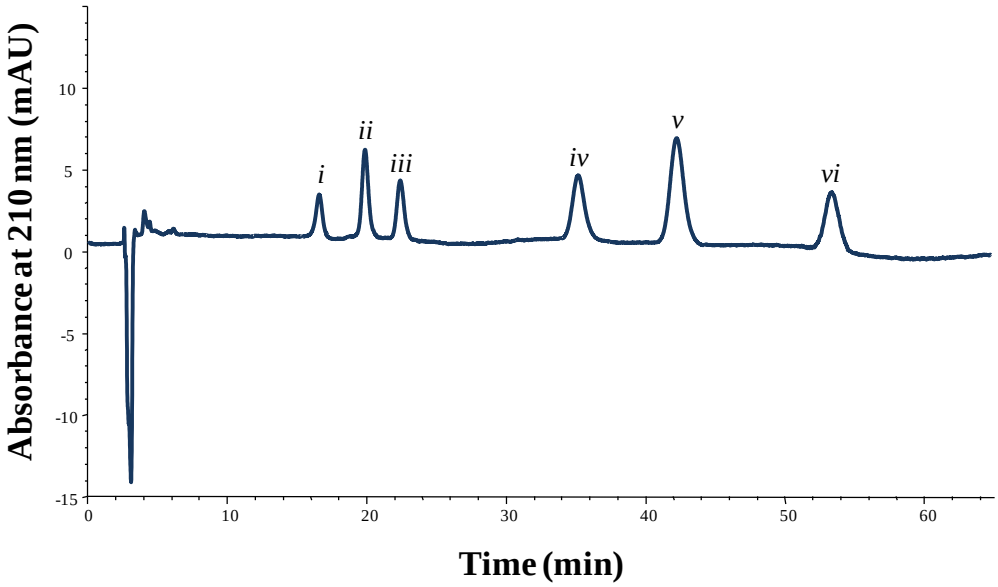

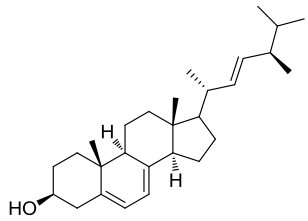

i: ergosterol

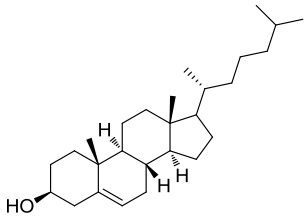

ii: cholesterol

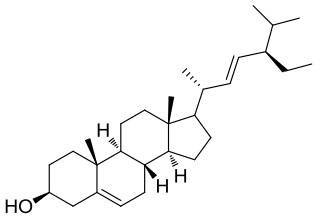

iii: stigmasterol

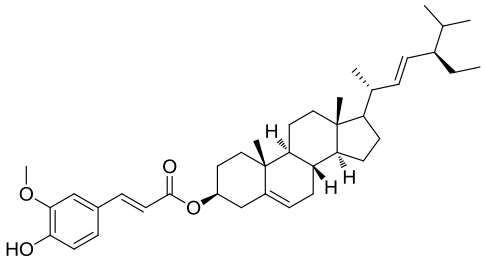

iv: stigmasteryl-3-*O*-ferulate

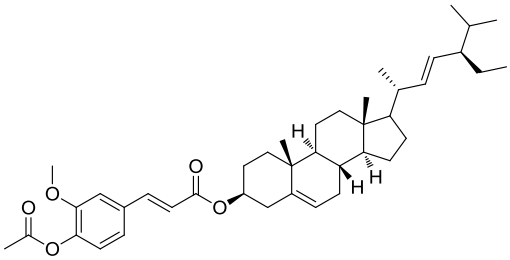

v: stigmasteryl-3-*O*-(4-acetoxyferulate)

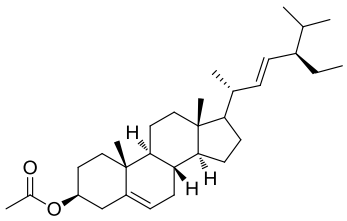

vi: stigmasteryl-3-*O*-acetate

Figure 5.7: RP-HPLC chromatograms of a mixture of six sterol standards at a concentration of 0.1 mM (for each sterol component) labelled as ***(i)-(vi)***, obtained with a Zorbax Eclipse XDB C_{18} column (4.6 mm × 150 mm, 5 µm particle size) at 23 °C using isocratic elution. The eluent was EtOH/H_2O (9:1, v/v) with 0.2% (v/v) AcOH; flow rate: 0.5 mL/min; 5 µL injection. The chromatograms were recorded at 210 nm using an UV-DAD detector.

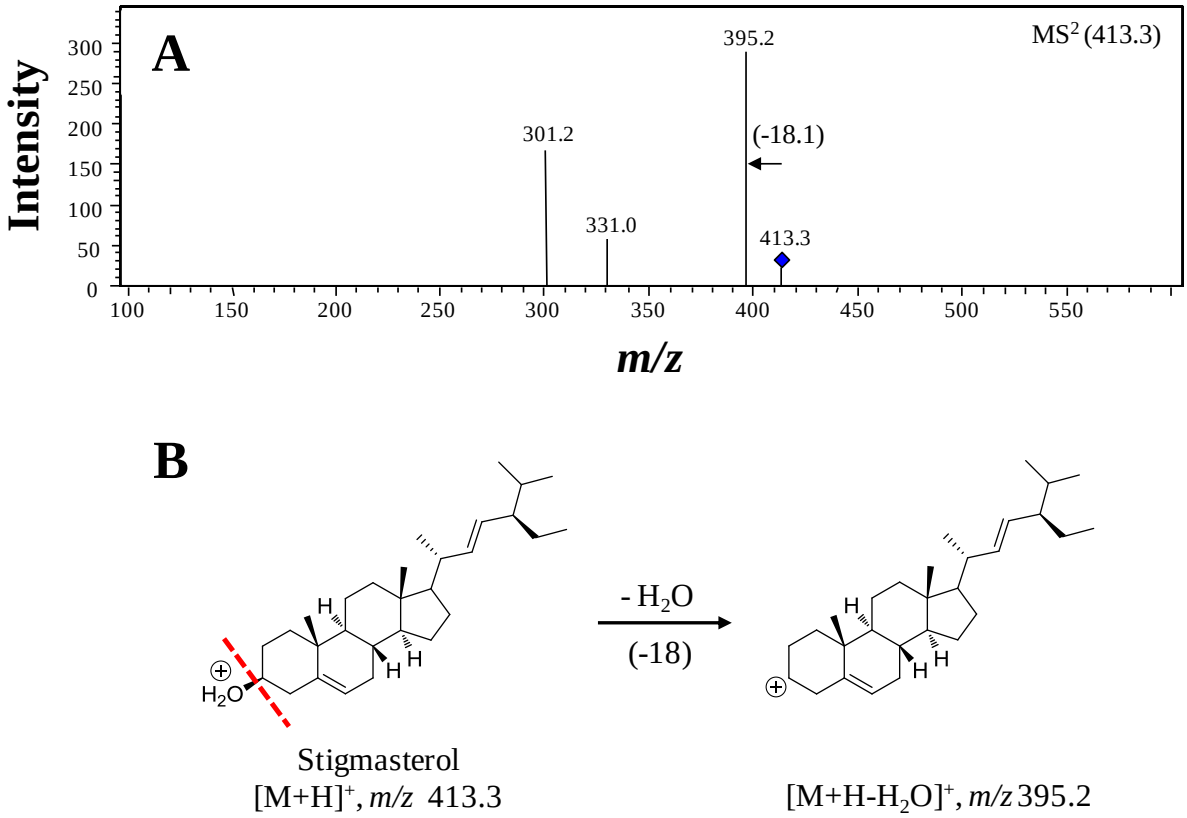

Figure 5.8: **(A)** The MS/MS spectrum of a stigmasterol standard (95% purity) at a concentration of 0.2 mM with ACN in the positive ionisation mode at fragmentation amplitude of 1.5 V. **(B)** The precursor ion $[M+H]^+$ of stigmasterol at *m/z* 413.3 underwent fragmentation to yield a product ion at *m/z* 395.2 after the neutral loss of water (18 mass units). The diamond (♦) symbol shows the position of the residual precursor ion.

5.3.3 Stigmasterol binding to a non-covalently imprinted MIP

5.3.3.1 Efficacy of mini-MIPs

In the non-covalent imprinting approach, the complementary intermolecular interactions between a template and polymer-embedded functional monomers are amongst the important factors for attaining molecular recognition for the MIP. In order to select the best method for the production of a sterol MIP, a series of mini-scale format MIPs and NIPs was prepared. The performance of the mini-MIP was evaluated based on the highest amount of stigmasterol bound to the imprinted polymer in comparison to its control. The small scale MIP was evaluated using the static single analyte binding studies with $CHCl_3$. Chloroform was selected as a binding solvent based on (i) the high solubility of the template in this solvent and (ii) solvent matching with the porogen used during polymerisation. It was expected that when

using the same type of porogen as a binding solvent, stigmasterol could interact selectively with the polymer system during the rebinding process. With regards to the cross-linker selection, EGDMA was chosen for the polymerisation process based on several positive outcomes from previous investigations. Whitcombe *et al.* (*9*) reported that EGDMA showed higher binding capacities in comparison to DVB, irrespective of the imprinting method or the nature of the template. In another study (*19*), EGDMA-based polymers demonstrated superior performance in terms of separation factors obtained with chiral stationary phases in comparison to DVB-based polymeric materials. Therefore, EGDMA was employed as a cross-linking agent and the polymerisation was performed thermally using AIBN as initiator in all cases of the present investigation.

As shown in **Figure 5.9**, the MIP prepared with 4-VP (stigmasterol:4-VP:$CHCl_3$) at a ratio of 1:10:100 proved to be a suitable functional monomer with the ability to specifically bind stigmasterol (MIP-NIP = 0.3 µmoles/g polymer) when rebinding absorption was performed in $CHCl_3$. The MIP made using the functional monomer MAA in a ratio of 1:1:5 (stigmasterol:MAA:$CHCl_3$) was observed to generate very little recognition whilst the MIP made from the monomer DMAAM failed to reveal any affinity towards stigmasterol. The outcomes from these studies were used as a guideline to provide a basis for the preparation of a stigmasterol MIP at a larger scale.

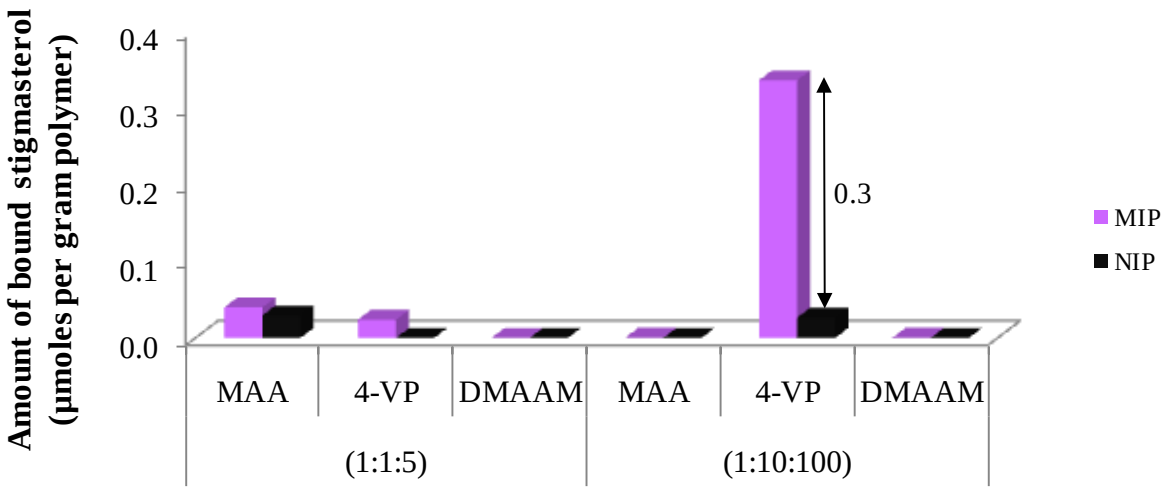

Figure 5.9: Amount of bound stigmasterol detected in mini-MIPs or mini-NIPs after 18 h incubation with chloroform (0.1 mM, 1 mL) using two different template:monomer:porogen molar ratios (1:1:5 and 1:10:100) with MAA, 4-VP or DMAAM. The arrow and number represent the difference of the amount of stigmasterol bound by the MIP *vs.* the NIP.

5.3.3.2 Stigmasterol binding to a non-covalently imprinted MIP

In this case, the low polarity of the stigmasterol-template makes the selection of the complementary functional group very difficult. Due to the fact that the acidic functional monomer (MAA) can be used to produce a cholesterol MIP with high selectivity (*20*), the first attempt was to synthesise a stigmasterol MIP using the non-covalent approach by thermal polymerisation in a molar ratio of 1:1:5 (stigmasterol:MAA:EGDMA). The resultant MIP was unsuccessful to capture stigmasterol in EtOH probably due to the hydroxyl-group in EtOH competing with the hydroxyl-group from stigmasterol which weakens the formation of hydrogen bonding of the compounds with the functional monomer. In another experiment, the MIP was capable to bind appreciable amounts of stigmasterol when a mixture of *n*-hexane:ethyl acetate (4:1, v/v) was used, however there was no imprinting effect. The low template-monomer ratios (1:1) might have reduced the number of binding sites for high affinity recognition due to the insufficient amount of functional groups and less efficient mass transfer in the high density polymer (*21*). Since MAA failed to bind stigmasterol, other monomer combinations needed to be incorporated with the template.

The second effort to prepare the stigmasterol MIP with the basic functional monomer (4-VP) was inspired by the positive results obtained from the mini-MIP experiments **(Section 5.3.3.1)**. Hwang *et al.* (*22*) compared the functional monomer strength between MAA and 4-VP to facilitate interaction with cholesterol using the MIP prepared from the non-covalent approach. That study concluded that the 4-VP generated stronger interaction with hydroxyl-groups from the cholesterol molecule which increased the retention factor, compared to MAA as functional monomer. Therefore, in the present work, the synthesis of a MIP on a larger scale at a ratio of 1:10:100 (stigmasterol:4-VP:$CHCl_3$) was performed. After removal of the template by solvent extraction, the resultant MIP was subjected to single analyte static batch binding experiments with 0.1 mM of stigmasterol standard solution using various types of solvents including EtOH, MeOH, ACN, *n*-hexane or $CHCl_3$. The results showed that in the presence of polar solvents, stigmasterol did not bind, whilst with *n*-hexane or $CHCl_3$ this compound was held within the binding sites of the MIP. Thus, single analyte batch binding experiments at different concentrations of stigmasterol in a range from 0.5 mM to 10.0 mM were performed with *n*-hexane as a binding solvent, being less toxic/hazardous than $CHCl_3$. The concentrations of bound stigmasterol after MIP or NIP treatment in the static binding experiments are shown in **Figure 5.10**. Although the MIP bound stigmasterol at

different concentrations, the NIP exhibited similar performance, which resulted in a poor imprinting effect.

The failure of the stigmasterol MIP made by the non-covalent imprinting to selectively recognise the template molecule might be due to several factors. Although the synthesis of bulk MIP was completely adapted from the procedure of the stigmasterol mini-MIP recipe, the mini-scale polymer preparation made in a glass vial was probably not completely crushed into small particles. Due to the size heterogeneity of the resultant MIP, the stigmasterol-template might not have been released properly or may have still been partially entrapped within the polymeric matrix, even after extensive clean-up, therefore having led to inaccurate quantification results. Another factor that may have influenced the ineffectiveness of the MIP might have been caused by the thermal imprinting process. As the MIP's activity is based on an entropically driven association between the functional monomers and the template, an exothermic polymerisation reaction at 60 °C and the subsequent rise of the temperature to 65 °C may have inherently changed the equilibrium between the template and functional monomer. Since there is only one terminal hydroxyl-group at the C_3 position in the stigmasterol molecule to engage in a hydrogen bonding interaction, photo-polymerisation (by UV-light) at low temperature (usually 4 °C) may be more favourable to stabilise the template-monomer pre-organisation for maximizing the imprint recognition (*20*).

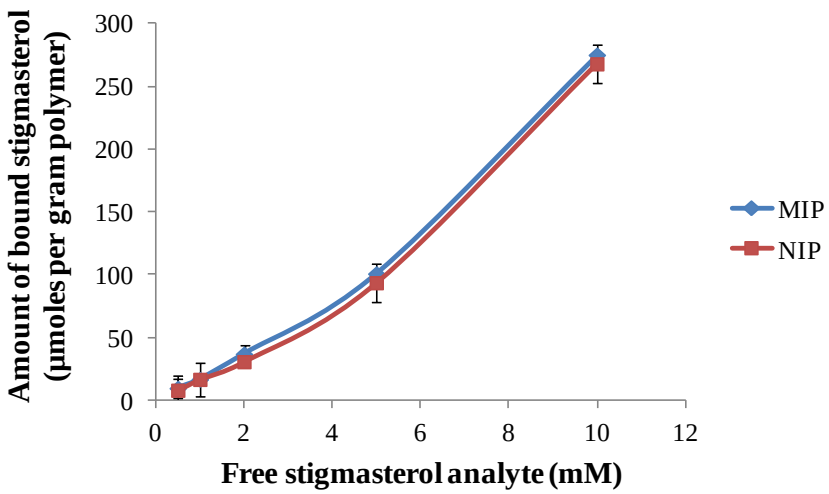

Figure 5.10: Static binding isotherms of stigmasterol at different concentrations (0.5 mM to 10.0 mM) in *n*-hexane (1 mL) using MIP particles (20 mg) prepared by the non-covalent approach in comparison to the NIP for 12 h incubation time. The MIP was prepared with stigmasterol (template), 4-vinylpyridine (functional monomer) and chloroform (porogen) in a ratio of 1:10:100 in the presence of ethylene glycol dimethacrylate (crosslinker). Measurements were determined in duplicate with two replicates (n = 4). Error bars indicate the standard error.

5.3.4 Stigmasterol binding to a semi-covalently imprinted MIP

In the semi-covalent imprinting, two variations of approach can be distinguished; (i) the template and functional monomer are connected directly or (ii) the template and functional monomer are connected using a spacer group. Whitcombe *et al.* (*9*) used cholesteryl (4-vinylphenyl) carbonate as a covalently bound template monomer for the polymerisation. The cleavage of carbonate esters released cholesterol and CO_2 to form the non-covalent recognition sites. The successful results exemplified by the synthesis of cholesterol imprinted bulk polymers with the covalent/semi-covalent strategies in that study have provoked this work to imprint a monomer functionalised stigmasterol using a similar approach. Stigmasterol was selected as a target due to the rigidity of the steroid ring system and because it is a representative of a class of phytosterols which possess significant health-beneficial qualities.

From an extensive search of the scientific literature, to the best of my knowledge this is the first time a stigmasterol MIP has been prepared with stigmasteryl-3-*O*-methacrylate, whereby the stigmasteryl-functionality is covalently bound to the functional monomer methacrylic acid at the outset to yield the desired cleavable monomer-template composite. This imprinting approach was carried out without the application of a sacrificial spacer as this was thought to give a more “exact” recognition cavity. The use of cleavable monomer-template composite during the polymerisation step should result in higher binding capacities, more homogeneous binding sites and much better binding site integrity because this approach is far more stable and defined than the non-covalently imprinted MIP.

In this work, the MIP was synthesised by thermal polymerisation at 60 °C for 24 hours. The imprinting process involved a slow, equilibrium-driven process which allowed interactions between the functionalised monomer-template compound and the crosslinker (EGDMA) in the presence of a porogen ($CHCl_3$). The template-portion of stigmasteryl-3-*O*-methacrylate was removed from the resultant polymers *via* base hydrolysis (chemical cleavage) followed by washing with 3.2% (v/v) aqueous acetic acid. This removal of the template-portion of the cleavable stigmasteryl-3-*O*-methacrylate resulted in a residual carboxylic acid group in the binding site intended to interact with the stigmasterol-target through hydrogen bonding formation. To ensure a complete removal of the stigmasterol from the polymer network extensive washing was carried out with the absence of stigmasterol in the wash fraction confirmed with RP-HPLC with detection at 210 nm.

This mixed-mode protocol involved a stable (yet cleavable) and stoichiometric composite compound in the covalent imprinting as the synthesis part and the fast guest binding (rapid kinetic binding of the target analyte) in the non-covalent imprinting as the application part. A schematic representation of cavity formation, template removal and binding events for the recognition strategies of stigmasterol (target analyte) in the polymer networks is shown in **Figure 5.11**. With regards to the selectivity evaluation of the MIP, the non-imprinted polymer (NIP), acting as a control, was synthesised with the crosslinker (EGDMA) and the porogen ($CHCl_3$), in the absence of the cleavable monomer-template composite (stigmasteryl-3-*O*-methacrylate). The preparation of the NIP was based on the method introduced by Whitcombe and co-workers (*9*), without the use of any functional monomer such as methacrylic acid in the polymerisation mixture.

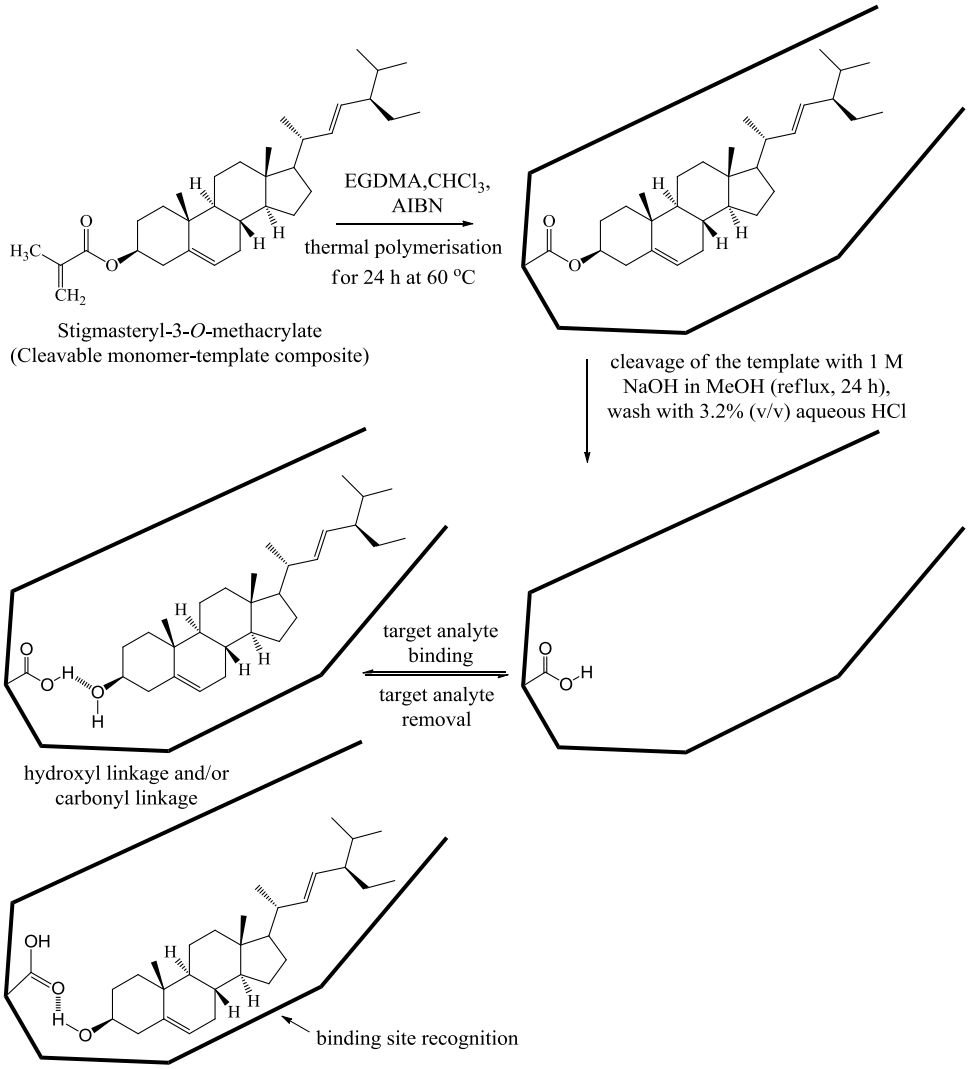

Figure 5.11: Schematic representation of molecularly imprinted polymer prepared by the covalent approach with stigmasteryl-3-*O*-methacrylate (cleavable monomer-template composite) and stigmasterol binding options.

5.3.4.1 Surface examination of the stigmasterol MIP and NIP

In order to examine the structure and surface morphology of the produced MIP (before template removal by chemical cleavage, without grinding) and the corresponding NIP polymer, scanning electron microscopy (SEM) was used. As depicted in **Figure 5.12**, the imprinted polymer had a more uniform and smooth surface than the NIP. Since the only difference between the MIP and NIP formulations was the presence or absence of the monomer-template composite during polymerisation, it can be presumed that the monomer-template composite is accountable for the surface variations (*23*).

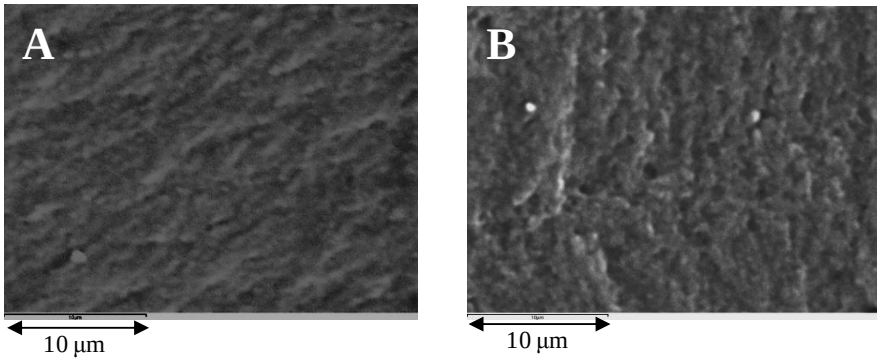

Figure 5.12: SEM micrographs of **(A)** the MIP synthesized using a cleavable monomer-template composite (stigmasteryl-3-*O*-methacrylate) and crosslinker (EGDMA) at a 1:10 ratio with the porogen (chloroform) using the covalent imprinting approach (image captured before template removal). **(B)** NIP prepared with crosslinker (EGDMA) and porogen ($CHCl_3$), under the same experimental conditions as the MIP in the absence of the cleavable monomer-template composite. The SEM images were captured at magnification of 6000 ×, 30 kV of acceleration voltage, 1×10^{-9} A of probe current and 34 mm working distance.

5.3.4.2 Static binding

5.3.4.2.1 Incubation binding time

For the MIPs based on molecular recognition, in these host-guest binding interactions fast adsorption-desorption kinetics are important. To investigate the equilibrium time, that is to estimate how long the polymer system takes to reach the binding equilibrium, studies of the isotherms of static batch binding were performed. The measurements for stigmasterol recognitions (at a concentration of 0.1 mM) were conducted using a covalently imprinted MIP or NIP (20 mg each) with two different binding solvent systems consisting of ACN (1 mL) or ACN/H_2O (9:1, v/v, 1 mL) at different incubation times (30 min, 2 h or 18 h).

As shown in **Figure 5.13**, the amount of specifically bound stigmasterol (MIP-NIP) was higher when ACN/H_2O (9:1, v/v) was used as a binding solvent for all incubation times than that when neat ACN was used. The highest amount of specifically bound stigmasterol was observed with ACN/H_2O (9:1, v/v) at 2 h incubation time (MIP-NIP = 1.3 µmoles/g polymer) compared to 18 h (MIP-NIP = 1.2 µmoles/g polymer) and 30 min (MIP-NIP = 1.1 µmoles/g polymer). It was concluded that 2 h incubation in a mixture of ACN/H_2O (9:1, v/v) is an effective equilibrium time to allow the target analyte to diffuse to the specific binding sites. This method was implemented for the evaluation of single analyte binding site characteristics at different concentrations and multiple cross-reactivity binding studies.

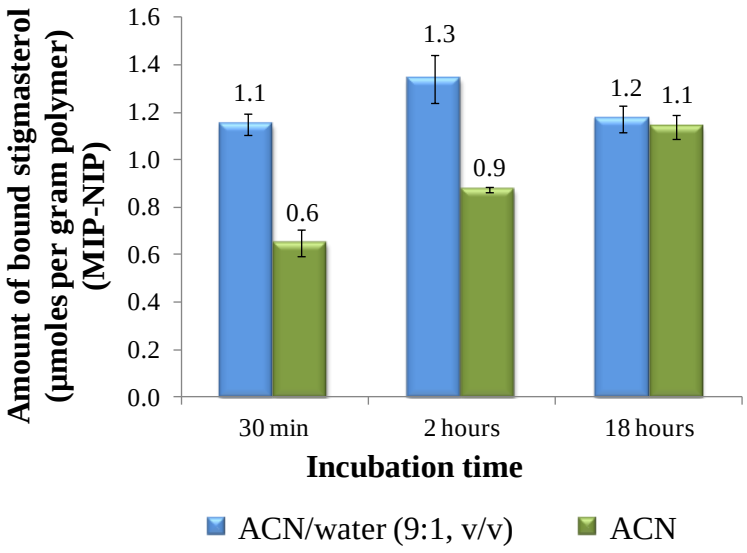

Figure 5.13: Specific binding performance (MIP-NIP) of stigmasterol (0.1 mM, 1 mL) at different incubation times with two different binding solvents under static binding conditions. Measurements were made in duplicate (*n* = 2). Error bars indicate the standard error.

5.3.4.2.2 Stigmasterol binding at different concentrations of binding solvent

The solvent effect on the specific recognition properties of the imprinted polymer (20 mg) was initially investigated through single analyte static equilibrium batch binding assays for the stigmasterol-target (0.1 mM) using polar and non-polar solvents including EtOH, *n*-hexane and ACN (1 mL, respectively). The MIP showed no recognition towards stigmasterol when EtOH was used as a rebinding solvent, possibly due to the competition between the hydroxyl-group of EtOH with the target analyte. The MIP displayed a high affinity towards stigmasterol in the presence of *n*-hexane, however there was no apparent

imprinting effect, as the NIP showed a similar amount of stigmasterol uptake. In contrast, the MIP demonstrated the ability to capture stigmasterol in ACN, possibly due to the hydrogen bonding interactions. Although the MIP displayed an imprinting effect in neat ACN, it was anticipated that these binding interactions may be improved upon by the introduction of water in the binding environment based on the results reported by Puoci *et al.* (*20*). They optimised the binding protocol of the non-covalent MIP (prepared with a photo-polymerisation procedure) in the SPE format towards cholesterol from cheese products using ACN with different proportions of water (ACN:H_2O (10:0 (v/v), 9:1 (v/v), 8:2 (v/v) and 7:3 (v/v)). The results showed that the best binding was achieved with a combination of ACN/H_2O (7:3, v/v).

In the present investigation, the single analyte static binding assays were performed for the recognition of stigmasterol (0.1 mM) with the MIP prepared *via* the semi-covalent imprinting technique using different combinations of ACN:H_2O (9:1 (v/v), 8:2 (v/v) and 7:3 (v/v)). The selective uptake of stigmasterol (MIP - NIP) showed that a combination of ACN/H_2O (9:1, v/v) gave a pronounced imprinting effect. In comparison, the use of ACN/H_2O (8:2, v/v) and ACN/H_2O (7:3, v/v) led to an increase of hydrophobically driven non-specific binding, which was similarly observed previously with a nicotine-imprinted MIP in ACN-aqueous media (*24*).

The isotherm batch binding studies were performed with stigmasterol at different concentrations (0.05 mM to 0.50 mM) in 1 mL of ACN/H_2O (9:1, v/v) or neat ACN (1 mL) using MIP or NIP (20 mg particles) at 2 h incubation time. **Figure 5.14** show the comparisons of stigmasterol bound to the MIP or NIP in these two different binding solvent systems across all concentrations. The MIP clearly showed a two-fold higher binding capability for stigmasterol with ACN/H_2O (9:1, v/v) compared to using neat ACN under similar experimental conditions. The concentrations of unbound stigmasterol in ACN/H_2O (9:1, v/v) were calculated based on the linear calibration curve. The equation for the resulting calibration curve was $y = 1131.5x$ with a correlation factor (R^2) of 0.9. The unbound concentrations of stigmasterol in ACN were determined from the linear calibration curve, $y = 804.5x$ with a correlation factor (R^2) of 0.9. Subtraction of this value from the initial total analyte concentration gave the amount of bound analyte which was then expressed as µmoles/g polymer.

This investigation demonstrated the solvent effect between neat ACN and ACN/H_2O (9:1, v/v) solutions on the selectivity of the recognition sites. The different

physico-chemical properties of these two solvent systems may considerably influence the specific binding of the target analyte to the MIP. Binding recognition of stigmasterol in ACN primarily is governed by the intermolecular hydrogen bond interaction between the hydroxyl-group of the target analyte and the residual carboxylic functionality in the imprinted binding sites. However in ACN/H_2O (9:1,v/v), the hydrophobic nature of the EGDMA-based-MIP and stigmasterol's structural backbone may be exploited, as the introduction of a small proportion of water (10%, v/v) into the binding environment may enable the formation of ancillary hydrophobic interactions. Therefore, stigmasterol was herein found to possess a greater affinity to the MIP when water was present, with respect to the amount bound in ACN alone. These results indicate the importance of the nature of the solvent in the MIP performance.

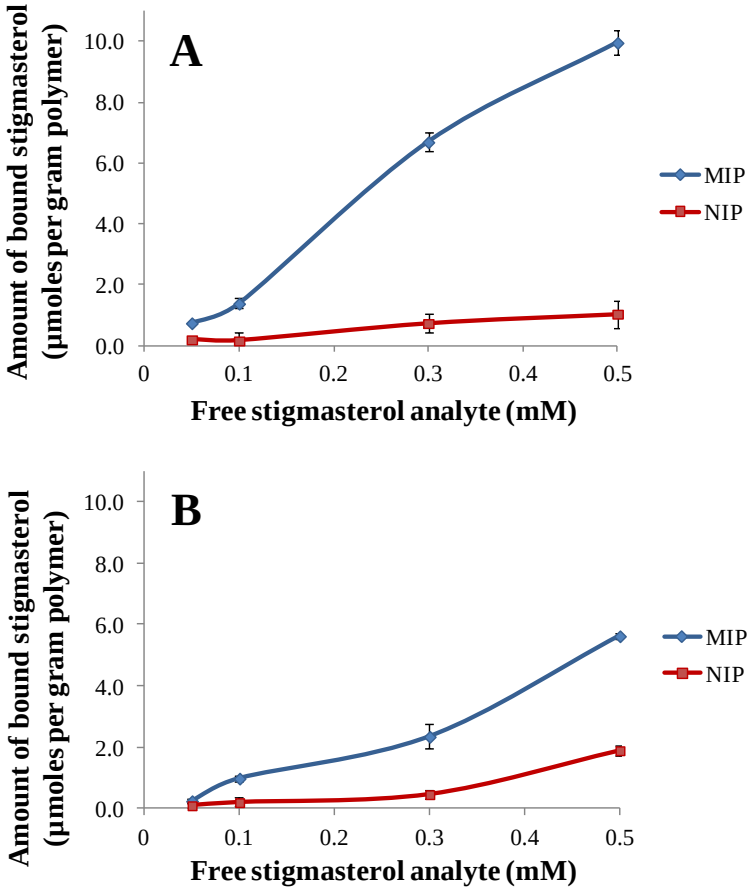

Figure 5.14: Static binding isotherms of stigmasterol at different concentrations (0.05 mM to 0.50 mM) using MIP (20 mg) prepared by covalent approach in comparison to the NIP (20 mg) with **(A)** ACN/H_2O (9:1, v/v, 1 mL) or **(B)** ACN (1 mL) for an incubation time of 2 h. Measurements were determined in duplicate with two replicates (n = 4). Error bars indicate the standard error.

5.3.4.3 Static cross-reactivity binding study

This research presents the first example of a static binding evaluation of the novel stigmasterol MIP with a standard mixture of six sterols. Such experiments are often limited by the availability of the stigmasterol analogues, which must be chemically synthesised if they are not commercially available. In this work, a mixture containing stigmasterol, stigmasteryl-3-*O*-ferulate, stigmasteryl-3-*O*-(4-acetoxyferulate), stigmasteryl-3-*O*-acetate, cholesterol and ergosterol (0.1 mM for each component) in ACN/H_2O (9:1, v/v, 1 mL) was incubated with the MIP or NIP particles (20 mg), respectively, in a sealed Eppendorf tube.

The performance of the MIP *versus* NIP with respect to the binding selectivity for the sterols from the standard mixture is shown in **Figure 5.15**. The stigmasterol-target exhibited the highest amount of stigmasterol bound to the MIP (1.6 µmoles/g polymer) in comparison to the NIP (0.2 µmoles/g polymer) due to the imprinting effect. A higher amount of stigmasterol (molecular weight 412.7 g/mol) was retained on the MIP compared to the NIP (MIP-NIP = 1.4 µmoles/g polymer) which might have been due to a combination of hydrogen bonding and electrostatic interactions between the target analyte and the residual carboxylic acid group in the binding site. The MIP also demonstrated a significant binding selectivity for cholesterol (MIP-NIP = 1.1 µmoles/g polymer) and ergosterol (MIP-NIP = 1.0 µmoles/g polymer) because they possess some similarities in the backbone molecular structures to the stigmasterol-target. Thus, the resulting MIPs behave towards the free sterol molecules according to the particular chemistry of the stigmasterol binding site, which was capable of binding stigmasterol, cholesterol and ergosterol.

Unexpectedly, strong binding affinities of stigmasteryl-3-*O*-ferulate were observed for both the MIP (2.3 µmoles/g polymer) and the NIP (1.5 µmoles/g polymer), which resulted in a low binding selectivity (MIP-NIP = 0.8 µmoles/g polymer). A possible explanation for this may be associated with the acidity of the stigmasteryl-3-*O*-ferulate in comparison to the free sterols due to the presence of the aromatic hydroxyl-group in the ferulate moiety. This hydroxyl-group which can behave as either a hydrogen bond acceptor or hydrogen bond donor could interact with the residual carboxylic acid (hydrogen bond donor or/and hydrogen bond acceptor) in the MIP cavities, thereby governing hydrogen bond interactions. This hypothesis was supported by the lower amount of bound stigmasteryl-3-*O*-(4acetoxyferulate) when the hydroxyl-group of the phenol in stigmasteryl-3-*O*-ferulate was replaced by an acetate in the stigmasteryl-3-*O*-(4-acetoxyferulate). In addition, the abundance of

π-electrons within the conjugated cinnamate ester in the stigmasteryl-3-*O*-ferulate could stabilise the intermolecular recognition through secondary hydrophobic electrostatic interactions. The fact that the corresponding NIP also displayed high binding suggests that substantial non-selective binding interactions occurred between the ester functionalities of polyEGDMA and stigmasteryl-3-*O*-ferulate. Moreover, the bulky size of stigmasteryl-3-*O*-ferulate (molecular weight 588.9 g/mol) may have had a significant impact leading to a lower binding selectivity due to size exclusion effects. This finding is in agreement with the study performed by Simon *et al. (25)* who demonstrated compounds larger than the target molecule showed a lower selectivity in the MIP recognition process explained by a steric exclusion, reducing the binding sites uptake.

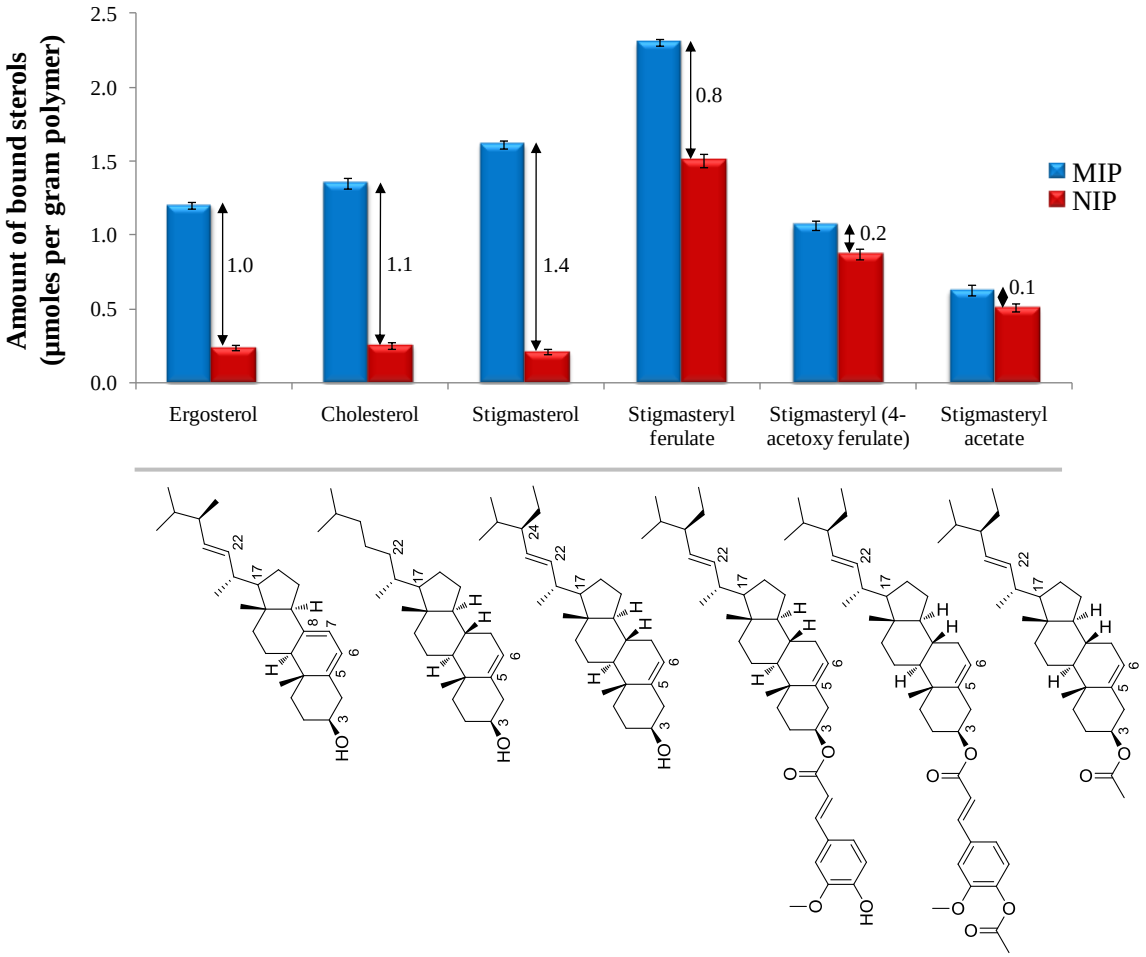

Figure 5.15: Amounts of bound sterols in a sterol mixture solution containing stigmasterol, stigmasterol analogues, cholesterol and ergosterol (0.1 mM for each component) in ACN/H_2O (9:1, v/v, 1 mL) with MIP (prepared by semi-covalent imprinting style) or NIP (20 mg, respectively) using the isotherm static batch binding protocol. The arrows and numbers represent the difference of amount of stigmasterol bound by the MIP *vs*. the NIP. Measurements were determined in duplicate with two replicates (n = 4). Error bars indicate the standard error.

In comparison, stigmasteryl-3-*O*-(4-acetoxyferulate) (MIP-NIP = 0.2 µmoles/g polymer) and stigmasteryl-3-*O*-acetate (MIP-NIP = 0.1 µmoles/g polymer) resulted in an even lower uptake by the MIP. The hydrogen bond site at the C_3 position in both molecules is blocked by a 4-acetoxyferulate moiety and acetyl group, respectively, therefore they cannot form hydrogen bonding with the carboxylic acid functionality in the imprinted cavities. The stigmasteryl-3-*O*-(4-acetoxyferulate) and stigmasteryl-3-*O*-acetate showed the similar binding magnitudes for the NIPs which were notably less than that observed for the stigmasteryl-3-*O*-ferulate, presumably due to the later ability to interact with the ester functionalities of the cross-linker *via* the acid phenolic group.

These studies demonstrated the importance of the hydroxyl functionality in the target analyte and/or target analogues for the formation of selective hydrogen bond interactions with the residual carboxylic acid in the imprinted cavities. In addition, the size and shape of the analytes influenced the binding recognition mechanism of the MIP.

5.3.4.4 Dynamic binding

To the best of my knowledge, this is the first time dynamic binding studies were performed with a stigmasterol MIP prepared by covalent imprinting. The aim was to assess the selectivity of the recognition sites with several structurally related compounds in comparison to the NIP *via* a MISPE technique. For this study, a mixture of sterols containing stigmasterol, cholesterol and ergosterol at a concentration of 0.1 mM (for each component) in ACN/H_2O (9:1, v/v, 2 mL) was loaded onto MIP or NIP cartridges followed by gravity elution. Due to the low solubility of sterols in aqueous-ACN media, the concentration of each sterol in the mixtures loaded onto the MIP or NIP cartridge must be in a range of 0.05 mM to 0.50 mM, *i.e.*, the concentration must be $\leq$ 0.5 mM. Moreover, an increase of H_2O content above 20% (v/v) with ACN as loading solvent results in a precipitation of the target sterols within the polymer matrix.

The second stage of the MISPE process involved several wash steps with the same solvent combination as used in the loading stage, whereby ACN/H_2O (9:1, v/v) proved to be an appropriate combination to remove the majority of the non-selectively bound compounds. The amount of bound stigmasterol, cholesterol and ergosterol in wash and elution stages after MISPE and NISPE can be seen in **Figure 5.16** and **Table 5.1**. The majority of the non-selectively bound material eliminated from the NIP cartridge in the wash stage was

observed for **(A)** stigmasterol, **(B)** cholesterol and **(C)** ergosterol. This competitive dynamic binding resulted in 37.41% (43.1 µg/g polymer) loss of stigmasterol during the wash steps, whilst 40.03% (39.2 µg/g polymer) loss of cholesterol was observed, and 49.4% (49.2 µg/g polymer) of ergosterol was diminished after the wash stages. This phenomenon was expected in the wash stages due to the fact that only one terminal of hydroxyl-group was present in the stigmasterol molecule at the β-position of C_3 to generate hydrogen bonding interactions. Because of the very limited number of potential interaction sites in the tested sterol structures and the use of a wash solvent containing aqueous-ACN, the propensity for target binding in the wash step was reduced.

The target analytes were then removed from the MISPE cartridge during the elution stage *via* a disruption of the hydrogen bonding with EtOH/AcOH (9:1, v/v). Due to the 'memory' of the binding sites to recognise molecules with dimensions of the stigmasterol-target, the MIP had captured 71.3 µg/g polymer of stigmasterol which was obtained in the eluate fraction, compared to 5.9 µg/g polymer of the target molecule eluted from the NIP, with the highest selectivity (MIP-NIP = 65.4 µg/g polymer and highest imprinting factor (12) amongst the tested sterols present in the mixture. The binding of structurally related sterols in the MIP was determined to be 57.9 µg/g polymer for cholesterol (with a lower selectivity of MIP-NIP = 47.6 µg/g polymer) whilst for ergosterol it was 50.4 µg/g polymer (and the lowest selectivity of MIP-NIP = 36.9 µg/g polymer).

The sterols involved in these experiments possess the same backbone structures except for ergosterol, which has an additional double bond at the C_7-C_8 in the B-ring. The most obvious structural differences between stigmasterol, cholesterol and ergosterol are the double bonds at C_{22} and the alkyl chain at the position of C_{24} **(Figure 5.16-D)**. Since cholesterol displayed the closest structural similarity to the target molecule, the binding recognition for cholesterol was slightly higher than that for ergosterol. Since the highest binding selectivity was obtained for stigmasterol, it can be assumed that the side chain of stigmasterol enhances the fidelity of the recognition sites of the imprinted polymer for this compound. This demonstrated the potential of MIP polymers to have binding site attributes which possess the ability to 'memorise' small structural differences amongst sterols. The recoveries of the tested sterols in the mixture containing stigmasterol, cholesterol and ergosterol are shown in **Table 5.1**.

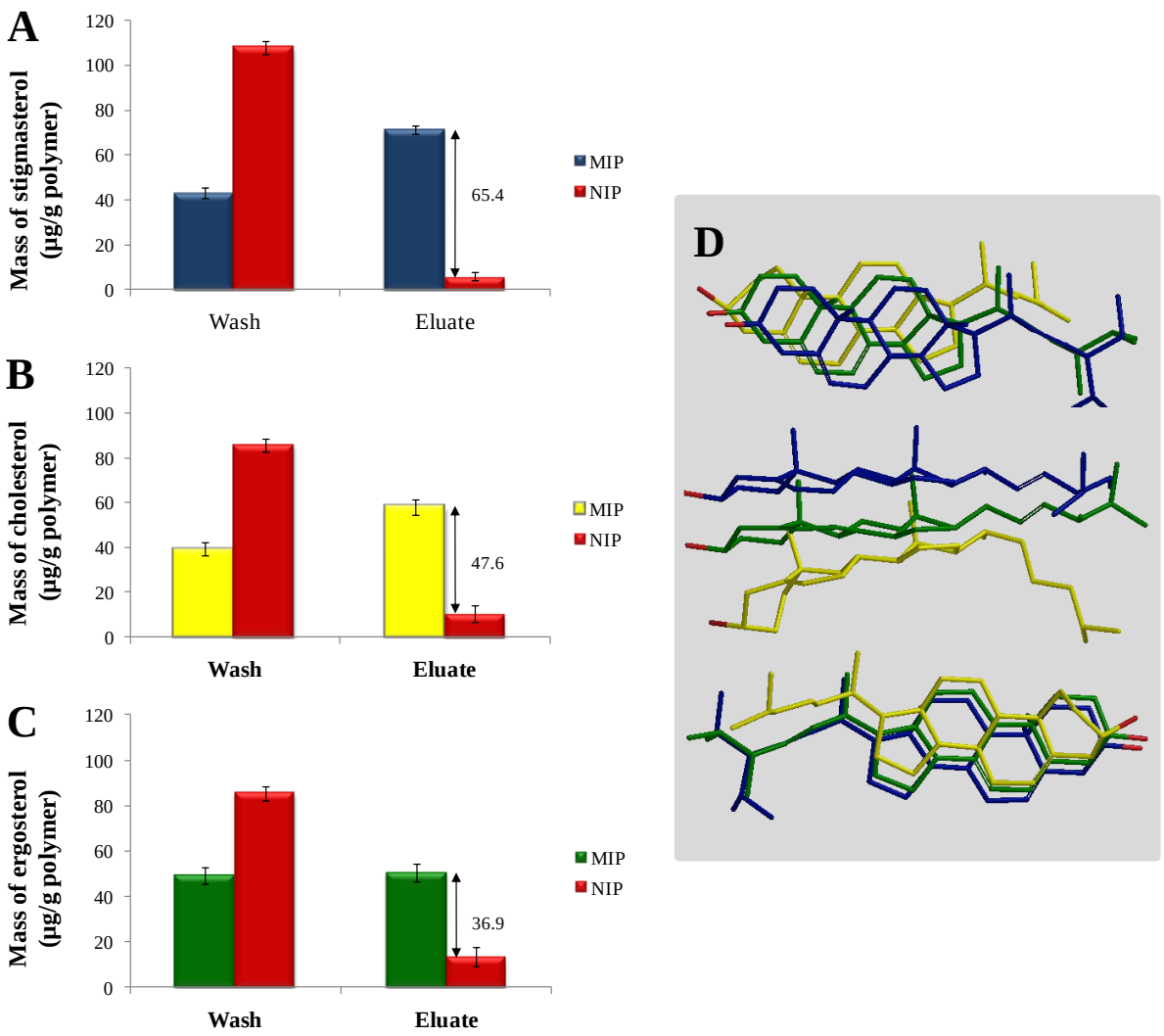

Figure 5.16: Amounts of sterols bound out of a mixture of sterol standards (0.1 mM in ACN/H_2O (9:1, v/v)) containing **(A)** stigmasterol, **(B)** cholesterol and **(C)** ergosterol (µg/g polymer) in wash and eluate fractions after MISPE and NISPE. The arrows and numbers represent the absolute mass difference of bound sterols between the MIP and the NIP. Measurements were determined in duplicate (n =2). Error bars indicate the standard error. **(D)** Structure overlays of stigmasterol (blue), cholesterol (yellow) and ergosterol (green) in 3D-view at different angles. The images were produced using Spartan ′10 for Windows version 1.1.0 software package on a Pentium IV 2.0 GHz.

Table 5.1: The amounts (µg/g polymer) of **(A)** stigmasterol, **(B)** cholesterol and **(C)** ergosterol in a mixture of sterols after wash and elution fractions obtained from MISPE or NISPE cartridges.

MISPE/NISPE procedure	(A) Stigmasterol (µg/g polymer)		(B) Cholesterol (µg/g polymer)		(C) Ergosterol (µg/g polymer)	
	MIP	NIP	MIP	NIP	MIP	NIP
Sample loading (1 × 2 mL)	115.1	115.1	97.8	97.8	100.6	100.6
Wash fraction (2 × 2 mL)	43.1	108.2	39.2	85.7	49.2	85.4
Eluate fraction (3 × 2 mL)	71.3	5.9	57.9	10.3	50.4	13.5
Total sterol in wash and eluate fraction	114.4	114.1	97.1	96.0	99.6	98.9
Total recovery (%)	99.4	99.1	99.3	98.2	99.0	98.3
Selectivity = MIP eluate - NIP eluate	65.4		47.6		36.9	
Imprinting factor, *IF*= MIP eluate / NIP eluate	12		6		4	

5.4 Conclusions

The main aim of this research was to prepare MIPs for the selective binding of stigmasterol either based on the non-covalent or covalent three-dimensional imprinting methods and to optimise stigmasterol recognition when on its own or in the presence of other structurally related sterols. The characterisation of the generated binding sites within polymer matrix was achieved through static batch absorption binding and dynamic binding assays. Although the MIP prepared by the non-covalent method was easy to produce, it led to low stigmasterol selectivity of MIP *versus* NIP in polar or non-polar solvents, as observed from the mini-MIPs experiments with very little specific recognition of the target analyte (MIP-NIP = 0.3 µmoles/g polymer) bound to the MIP.

In contrast, the novel MIP fabricated through the covalent approach showed good recognition abilities towards stigmasterol when a mixture of sterol standards containing stigmasterol analogues, cholesterol and ergosterol was used with aqueous-ACN in static multiple analyte batch binding experiments, which resulted in 1.6 µmoles/g polymer of target analyte retained in the polymer binding sites. The MIP imprinted to recognise the target molecule stigmasterol was assessed for cross-reactivity dynamic binding towards the stigmasterol, cholesterol and ergosterol. The MIP was capable of interacting with these sterol molecules of biological

relevance *via* hydrogen bonding due to the similar size and backbone structure, however the binding sites showed better recognition for its original stigmasterol-target in comparison to the other sterols. Since cholesterol and ergosterol have a close structural resemblance to stigmasterol, one additional positive outcome of this investigation is that the MIP could be utilised as a multi-purpose extraction medium to enrich/purify these sterols. Instead of having a MIP designed to capture an individual compound, this MIP can be used for the detection of several sterols not only from plants but also animal and fungi derived sources, for various types of applications. From a clinical point of view, cholesterol plays a major role in human health and a high blood cholesterol level is an easily monitored risk factor for cardiovascular disease and stroke (*26*). Therefore, the detection of cholesterol in human blood is very important area to prevent the formation of those diseases. Several studies have demonstrated that ergosterol and its peroxidation products may contribute to potential human health-benefits with potent pharmacological activities including reducing pain related to inflammation, reducing the incidence of cardiovascular diseases, acting as an antioxidant, antimicrobial and anti-tumour substance (*27*, *28*).

In multiple-analyte competitive static binding assays, the specificity of the MIP binding sites tested with the stigmasterol analogues were evaluated. The stigmasteryl-3-*O*-ferulate showed high binding affinity to the MIP as well as the NIP, which resulted in a low binding selectivity. This observation may be explained by the aromatic hydroxyl-group of the ferulate moiety that could interact with the carboxylic acid functionality in the imprinted cavities thereby governing hydrogen bond interactions. The high amount of this compound bound to the MIP was also observed for the corresponding NIP suggesting that substantial non-selective binding interactions between the ester functionalities of the cross-linker and acid phenolic group in the stigmasteryl-3-*O*-ferulate molecular structure have occurred. Moreover, the bulky size of stigmasteryl-3-*O*-ferulate would appear to be a contributing factor for the low recognition due to size exclusion effects. In contrast, the absence of hydroxyl-groups in the stigmasteryl-3-*O*-(4-acetoxyferulate) and stigmasteryl-3-*O*-acetate revealed a significant impact upon the low binding selectivity of these compounds in the MIP *versus* NIP experiments, respectively. The MIP was also used for dynamic recognition binding studies whereby the MISPE protocols were tailored to provide specific recognition properties by optimising the sample loading, wash and elution conditions. Both, static and dynamic binding assays showed two main synergistic effects, (i) hydrogen bonding interactions between the hydroxyl-substituent of sterol molecules and the residual

carboxyl group derived from the polymer-embedded methacrylate-portion of the monomer-template composite in the binding sites of the polymer networks and (ii) the effects of size and shape of the analytes with respect to that of the template imprint.

These results have shown that the effort to synthesise the MIP by a covalent approach is worthwhile and that the herein demonstrated successful new approaches for binding site characterisation, selectivity optimisation and performance monitoring of this new sterol sensitive MIP in SPE format will lead to further developments in MIP technology. Moreover, chromatographic optimisations using green separation techniques were elaborated. The new stigmasterol MIP allowed a simultaneous capture of ergosterol and cholesterol but discriminated against large sterol molecules in complex mixtures. The methods developed will in subsequent studies be applied to the analysis of sterols from agricultural byproducts in **Chapter 6**.

5.5 References

1. Moreau, R. A.; Whitaker, B. D.; Hicks, K. B., Phytosterols, phytostanols, and their conjugates in foods: structural diversity, quantitative analysis, and health promoting uses. *Prog. Lipid Res.* **2002**, *41*, 457-500.
2. Awad, A. B.; Downie, A.; Fink, C. S.; Kim, U., Dietary phytosterol inhibits the growth and metastasis of MDA-MB-231 human breast cancer cells grown in SCID mice. *Anticancer Res.* **2000**, *20*, 821-824.
3. Crews, C.; Hough, P.; Godward, J.; Brereton, P.; Lees, M.; Guiet, S.; Winkelmann, W., Quantitation of the main constituents of some authentic grape seed oils of different origin. *J. Agric. Food Chem.* **2006**, *54*, 6261-6265.
4. Fialkov, A. B.; Steiner, U.; Lehotay, S. J.; Amirav, A., Sensitivity and noise in GC-MS: Achieving low limits of detection for difficult analytes. *Int. J. Mass Spectrom.* **2007**, *260*, 31-48.
5. Ryu, H. K.; Jung, B. H.; Kim, K. M.; Yoo, E. A.; Woo, J. T.; Chung, B. C., Determination of cholesterol in human hair using gas chromatography mass spectrometry. *Biomed. Chromatogr.* **2006**, *20*, 999-1003.
6. Sellergren, B., *Molecularly imprinted polymers: man-made mimics of antibodies and their applications in analytical chemistry Tech. Instrum. Anal. Chem.*: 2001; Vol. 23, p 557.
7. Chen, Y.; Kele, M.; Sajonz, P.; Sellergren, B.; Guiochon, G., Influence of thermal annealing on the thermodynamic and mass transfer ninetic properties of *D*- and *L*-phenylalanine anilide on imprinted polymeric stationary phases. *Anal. Chem.* **1999**, *71*, 928-938.
8. Kirsch, N.; Alexander, C.; Lubke, M.; Whitcombe, M. J.; Vulfson, E. N., Enhancement of selectivity of imprinted polymers *via* post-imprinting modification of recognition sites. *Polymer* **2000**, *41*, 5583-5590.
9. Whitcombe, M. J.; Rodriguez, M. E.; Villar, P.; Vulfson, E. N., A new method for the introduction of recognition site functionality into polymers prepared by molecular imprinting: synthesis and characterization of polymeric receptors for cholesterol. *J. Am. Chem. Soc.* **1995**, *117*, 7105-7111.
10. Zhong, N.; Byun, H. S.; Bittman, R., Hydrophilic cholesterol binding molecular imprinted polymers. *Tetrahedron Lett.* **2001**, *42*, 1839-1841.

11. Lanza, F.; Sellergren, B., Method for synthesis and screening of large groups of molecularly imprinted polymers. *Anal. Chem.* **1999**, *71*, 2092-2096.
12. Schwarz, J. L.; Leung, K. Y. B.; Danylec, B.; Harris, J. S.; Hearn, T. W. M., Phytosterol recognition *via* rationally designed molecularly imprinted polymers. *Unpublished results* **2012**.
13. Zhang, X.; Cambrai, A.; Miesch, M.; Roussi, S.; Raul, F.; Aoude-Werner, D.; Marchioni, E., Separation of Δ5- and Δ7-phytosterols by adsorption chromatography and semipreparative reversed-phase high performance liquid chromatography for quantitative analysis of phytosterols in foods. *J. Agric. Food Chem.* **2006**, *54*, 1196-1202.
14. Careri, M.; Elviri, L.; Mangia, A., Liquid chromatography UV determination and liquid chromatography atmospheric pressure chemical ionization mass spectrometric characterization of sitosterol and stigmasterol in soybean oil. *J. Chromatogr., A* **2001**, *935*, 249-257.
15. www.chem.agilent.com, What are the possible causes of peak tailing in reversed-phase HPLC?
16. Borman, P. J.; Chatfield, M. J.; Damjanov, I.; Jackson, P., Design and analysis of method equivalence studies. *Anal. Chem.* **2009**, *81*, 9849-9857.
17. Wang, L.; Weller, C. L., Recent advances in extraction of nutraceuticals from plants. *Trends Food Sci. Technol.* **2006**, *17*, 300-312.
18. Lerma-Garcia, M. J.; Simo-Alfonso, E. F.; Mendez, A.; Lliberia, J. L.; Herrero-Martinez, J. M., Classification of extra virgin olive oils according to their genetic variety using linear discriminant analysis of sterol profiles established by ultra performance liquid chromatography with mass spectrometry detection. *Food Res. Int.* **2011**, *44*, 103-108.
19. Wulff, G.; Vietmeier, J.; Poll, H. G., Enzyme-analog built polymers. Influence of the nature of the crosslinking agent on the performance of imprinted polymers in racemic resolution. *Makromol. Chem.* **1987**, *188*, 731-740.
20. Puoci, F.; Curcio, M.; Cirillo, G.; Iemma, F.; Spizzirri, U. G.; Picci, N., Molecularly imprinted solid-phase extraction for cholesterol determination in cheese products. *Food Chem.* **2007**, *106*, 836-842.
21. Chassaing, C.; Stokes, J.; Venn, R. F.; Lanza, F.; Sellergren, B.; Holmberg, A.; Berggren, C., Molecularly imprinted polymers for the determination of a pharmaceutical development compound in plasma using 96-well MISPE technology. *J. Chromatogr., B: Anal. Technol. Biomed. Life Sci.* **2004**, *804*, 71-81.
22. Hwang, C. C.; Lee, W. C., Chromatographic characteristics of cholesterol imprinted polymers prepared by covalent and non-covalent imprinting methods. *J. Chromatogr., A* **2002**, *962*, 69-78.
23. Yu, L.; Yun, Y.; Zhang, W.; Wang, L., Preparation, recognition characteristics and properties for quercetin molecularly imprinted polymers. *Desalin. Water Treat.* **2011**, *34*, 309-314.
24. Horemans, F.; Weustenraed, A.; Spivak, D.; Cleij, T. J., Towards water compatible MIPs for sensing in aqueous media. *J. Mol. Recognit.* **2012**, *25*, 344-351.
25. Simon, R.; Collins, M. E.; Spivak, D. A., Shape selectivity versus functional group pre-organization in molecularly imprinted polymers. *Anal. Chim. Acta* **2007**, *591*, 7-16.
26. Tabas, I., Cholesterol in health and disease. *J. Clin. Invest.* **2002**, *110*, 583-590.
27. Zhang, Y.; Mills, G. L.; Nair, M. G., Cyclooxygenase inhibitory and antioxidant compounds from the mycelia of the edible mushroom *Grifola frondosa*. *J Agric. Food Chem.* **2002**, *50*, 7581-7585.
28. Yasukawa, K.; Aoki, T.; Takido, M.; Ikekawa, T.; Saito, H.; Matsuzawa, T., Inhibitory effects of ergosterol isolated from the edible mushroom *Hypsizigus marmoreus* on TPA-induced inflammatory ear edema and tumor promotion in mice. *Phytother. Res.* **1994**, *8*, 10-13.

Chapter 6

Extraction and analysis of polyphenols and phytosterols from grape byproducts

Abstract

The use of grape byproducts as natural health-beneficial antioxidant as substitutes for synthetic antioxidants is a cost effective and environmentally sustainable strategy with immense potential for the future.

Isolation of bioactives from grape byproducts can be achieved with molecularly imprinted polymers (MIPs). The MIP incorporated in the SPE format provided significant advantages to extract and enrich (*E*)-resveratrol from grape skin and seed extracts. The MISPE had shown its functionality as an efficient cleanup reusable tool to discard the unwanted endogenous compounds from the complex sample extract. Due to the structural similarity and spatial complementarity to the target compound, the MIP was also able to bind quercetin glucuronide (from grape skins) and epicatechin gallate (from grape seeds). The high recoveries of more than 99% of (*E*)-resveratrol for both waste extracts were achieved with a high imprinting factor. For the phytosterol analysis, a novel MIP prepared by the covalent approach was capable of recognising stigmasterol in aqueous media derived from unsaponified grape seeds with an imprinting factor of 12 and a satisfactory recovery of 96% after MISPE treatment.

The application of RPLC-ESI ion trap MS/MS for the identification of numerous non-binding compounds and binding target compound as well structurally related compounds in the flow-through and eluate fractions of two MISPE led to insights into the physical and chemical interaction of the MIPs with their target analytes and with molecules that can be eliminated.

This chapter introduced a new method to enrich the health-beneficial resveratrol, procyanidin and epicatechin as well as stigmasterol and campesteryl glycoside from one grape skin and seed feedstock with green chemistry methods.

The application of MISPE for the selective enrichment of health-beneficial compounds from agricultural waste materials provides a new, efficient, cost-effective and sustainable approach to natural resource utilisation as demonstrated for the successive capture of (*E*)-resveratrol (from grape skins and seeds) and stigmasterol (from grape seed).

Table of Contents

6.1 Introduction

Increasing knowledge of the health promoting properties of antioxidants in everyday foods, has led grape byproducts to be considered as a new revenue stream for incorporation in a 'green economy'. The global wine industry is producing a large volume of waste. The main winery byproducts are generated during de-stemming (stems), and grape crushing and pressing (skins and seeds). The accumulation of substantial amounts of grape byproducts (about 5-9 million tonnes worldwide) has the potential to create an industrial waste problem (*1*). Grape byproducts have been used for the generation of tartaric acid and the production of compost. To extract health-beneficial compounds would be an alternative use, providing new sources of income with a positive impact on the environment. Grape pressings contain valuable amounts of bioactive health-beneficial phenolic and sterol substances. However, far too little attention has been paid to the analysis of skins and seeds compared with research concerning wine (*2*).

Grape skins have been associated with appreciable amount of polyphenols, in particular flavonols, anthocyanins (*3*) and resveratrol. The grape seeds have been reported to contain 40% fiber, 16% oil, 11% protein, 7% phenolic compounds and less than 6% of sterols (*4*). In contrast to grape skins, grape seeds contain the phenolic procyanidins, which are flavan-3-ol derivatives. Oligomeric and polymeric procyanidins in grape seeds possess a broad spectrum of therapeutic properties and are one of the most potent natural antioxidants. Catechin/epicatechin are the major antioxidative phenolic components of grape seeds (*3*). Resveratrol has been shown to be present in grape seeds (*5*) and has important *in vitro* and *in vivo* anticancer properties (*6, 7*).

The phytosterols such as β-sitosterol, campesterol and stigmasterol have also been obtained from grape seed oil (*8*). The polyphenol and phytosterol compositions in grape byproducts depend on the cultivar, climatic condition, geographical origin and degree of grape maturity (*8, 9*).

It is an on-going challenge to develop low cost, rapid and efficient analytical methods for the determination of bioactive compounds from plants for use in the food, pharmaceutical and cosmetic industries. An elegant approach to the rapid isolation of specific target compounds from complex samples can be achieved using molecularly imprinted polymers (MIPs). The incorporation of MIPs in the solid-phase extraction (SPE) format, known as MISPE, has been

used widely to facilitate difficult chemical separations (*10, 11*). In this thesis, the exploitation of the molecular recognition properties of the imprinted polymers and the sample pretreatment was shown to be of crucial importance for the selective enrichment and cleanup of polyphenols. The previous studies focussed on the development and optimisation of an (*E*)-resveratrol-templated MIP, as presented in **Chapter 2**. Several successful applications of (*E*)-resveratrol MIPs using different types of complex samples derived from grapes have been demonstrated in **Chapter 3** and **Chapter 4**. In **Chapter 5**, a MIP for grape derived sterols was developed. In the present chapter, the extraction of polyphenols from the skins or seeds of grapes and an enrichment of (*E*)-resveratrol using a (*E*)-resveratrol-templated MIP is described. Furthermore, the solid residue of the grape seed polyphenol extraction process is reused to extract sterols and the enrichment of stigmasterol is attempted using a stigmasterol-templated MIP. To the best of my knowledge, this is the first time the same source of grape waste has been used for the successive extraction and analysis of polyphenols and phytosterols, moreover using green analytical methodologies.

6.2 Materials and Methods

6.2.1 Reagents and standards

6.2.1.1 (E)-Resveratrol and other polyphenol analysis

For reagents and standards, see **Chapter 2 (Section 2.2)**.

6.2.1.2 Special precautions

All laboratory procedures involving the manipulations of (*E*)-resveratrol containing samples were performed in dim light to avoid photochemical isomerisation of (*E*)-resveratrol to (*Z*)-resveratrol.

6.2.1.2.1 Standard calibration curve of (E)-resveratrol

i) Grape skins analysis

The calibration curve for (*E*)-resveratrol quantification was constructed from a serial dilution of the (*E*)-resveratrol standard with EtOH at a concentration between 1.3×10^{-4} mM and 5.0×10^{-1} mM. The standard curve was calculated by linear regression according to the

formula $y = mx + b$, where y is the peak area obtained after RP-HPLC, x is the concentration of (*E*)-resveratrol (mg/L), m is the slope and b is the intersection near to the origin (~0.0). The equation for the resulting calibration curve was $y = 68.8x$ with a correlation factor (R^2) of 0.9. The limit of detection (LOD) (multiplying the standard deviation (SD) by a factor of 3) and the limit of quantitation (LOQ) (10 times the SD) for (*E*)-resveratrol were determined to be 1.3×10^{-2} mg/L and 4.4×10^{-2} mg/L, respectively.

ii) Grape seeds analysis

For the calibration, a set of (*E*)-resveratrol standards between concentrations from 1.3×10^{-4} mM to 5.0×10^{-1} mM prepared with EtOH was used. The linear regression equation for the standard curve, $y = 77.1x$ with a correlation coefficient (R^2) of 0.9 was obtained by plotting the concentration (mg/L) of the (*E*)-resveratrol standard against the peak area. The limit of detection (LOD) and limit of quantification (LOQ) was determined to be 1.1×10^{-2} µg/L and 3.7×10^{-2} mg/L, respectively.

6.2.1.3 Stigmasterol and phytosterol analysis

For reagents and standards see **Chapter 5 (Section 5.2)**.

6.2.1.3.1 Standard calibration curve of stigmasterol

Standard solutions of stigmasterol was prepared in a serial dilution of concentrations in a range from 1.6×10^{-2} mM to 5.0×10^{-1} mM in ACN/H_2O (9:1, v/v) to obtain a linear calibration curve with the regression equation of $y = 950.1x$, where y is the peak area obtained after RP-HPLC, x is the concentration of stigmasterol (mM), m is the slope and b is the intersection near to the origin (~0.0). The correlation factor (R^2) of the resulting calibration curve is 0.9. The limit of detection (LOD) and limit of quantification (LOQ) was determined to be 1.2×10^{-3} mM and 3.9×10^{-3} mM, respectively.

6.2.2 RP-HPLC and LC-ESI ion trap method

6.2.2.1 Polyphenol analysis

For the separation of polyphenols from the extracts of grape skins and seeds, eluent A (10 mM of formic acid in water) and eluent B (10 mM formic acid in EtOH/H_2O (4:1, v/v)) were used. The LC gradient: 0-2 min to 10% (v/v) B, 2-52 min to 70% (v/v) B, 52-53 min to

10% (v/v) B. The details about the chromatographic parameters are described in **Chapter 2 (Section 2.2.3)**.

6.2.2.2 Phytosterol analysis

The phytosterol analysis was performed using isocratic elution with EtOH/H_2O (9:1, v/v) consisting of 0.2% (v/v) AcOH in the separations performed with the analytical LC system. The analysis of stigmasterol with the microLC system was performed with isocratic elution, with eluent A consisting 0.2% (v/v) AcOH in water (3%, v/v) and eluent B containing 0.2% (v/v) AcOH in EtOH (99.9 purity) (97%, v/v) were employed. For additional instrumentation conditions, see the **Chapter 5 (Section 5.2.3)**.

6.2.3 Sample preparations

Two bunches of fresh Pinot noir grapes (181.0 g) sourced from the Mornington Peninsula (Victoria, Australia) were used in this work. The grapevines were manually de-stemmed prior to being crushed and pressed by a hand press. The juice (96.5 g) liberated during the pressing was discarded whilst the skins and seeds of the grapes were manually separated for further analysis.

6.2.3.1 Grape skins extraction for polyphenols analysis

The grape skins (49.6 g) were lyophilised in a freeze-dryer (Labconco, Missouri, USA) at 0.01 mbar for two days in order to determine the dry matter content. The dried skins were ground with mortar and pestle in the dark. The powdered grape skins (5.0 g) were extracted with a mixture of EtOH/H_2O (1:1, v/v, 30 mL) in a round-bottom flask. The sample mixture was stirred using a magnetic stirrer (IKA RCT Basic, Staufen, Germany) at a speed of two (40 rpm) and left in the dark for 30 min prior to ultrasonication (Elmasonic, Singen, Germany) for 30 min. The mixture was centrifuged (Eppendorf AG Centrifuge 581OR, Hamburg, Germany) for 10 min at 4000 rpm at 20 °C. The supernatant was transferred into a volumetric flask and diluted with the extraction solvent to 50 mL. An aliquot of the extract was directly injected into the RP-HPLC system and the LC-ESI ion trap MS/MS system, and loaded onto MISPE and NISPE cartridges. The injection and the MISPE protocol were performed in duplicate (n = 2).

6.2.3.2 Grape seeds extraction for polyphenol analysis

The grape seeds (19.6 g) were quickly freeze-dried in the lyophiliser (Labconco, Missouri, USA) at 0.01 mbar for two days. The sample (5.0 g) was crushed using a blender (Kambrook, Victoria, Australia) at a speed control setting of one for one min with the extraction solvent containing a mixture of EtOH/H_2O (1:1, v/v, 30 mL). The sample mixture was left in the dark for 30 min and stirred using a magnetic stirrer (IKA RCT Basic, Staufen, Germany) at a speed of two (40 rpm) in a round-bottom flask. The mixture was centrifuged (Eppendorf AG Centrifuge 581OR, Hamburg, Germany) for 10 min at 4000 rpm at 20 °C. The supernatant was transferred into a volumetric flask and diluted to the mark (50 mL) with the extraction solvent. An aliquot of the extract was injected into the RP-HPLC system and the LC-ESI-MS/MS system, and loaded onto MISPE and NISPE cartridges. The injection and the MISPE protocol were carried out in duplicate (n = 2).

6.2.3.3 Grape seeds extraction for phytosterols analysis

The pellet remaining after the centrifugation during the polyphenols analysis was transferred into a glass sintered filter. A vacuum was used to remove the residual solvents and then the sample was dried in a vacuum oven for 1 hour. A saponification procedure was employed based on an established method (ISO 3596-2) with some minor modifications. The sample (5.0 g) was refluxed with 1 M ethanolic potassium hydroxide (50 mL) at 115 °C for 2 h in a round-bottom flask. After 50 mL of distilled water was added, the sample was filtered prior to the extraction with three portions of *n*-hexane (3 × 15 mL) in a separatory funnel. The combined *n*-hexane fractions were washed with distilled water (2 × 50 mL) until neutral according to a pH indicator paper. The *n*-hexane mixture was dried with anhydrous sodium sulphate and filtered using Whatman No. 1 filter paper. The *n*-hexane fraction was evaporated to dryness under reduced pressure using a rotary evaporator (Buchi Rotavapor R-215, Flawil, Switzerland). The removal of the *n*-hexane solvent yielded an unsaponifiable residue and this portion was re-dissolved in 10 mL of ACN/H_2O (9:1, v/v). An aliquot of this extract was injected into RP-HPLC and LC-ESI ion trap MS/MS, as well as loaded onto MISPE and NISPE cartridges. The experimental flow to isolate (*E*)-resveratrol and stigmasterol from this grape seed extract is shown in **Figure 6.1**.

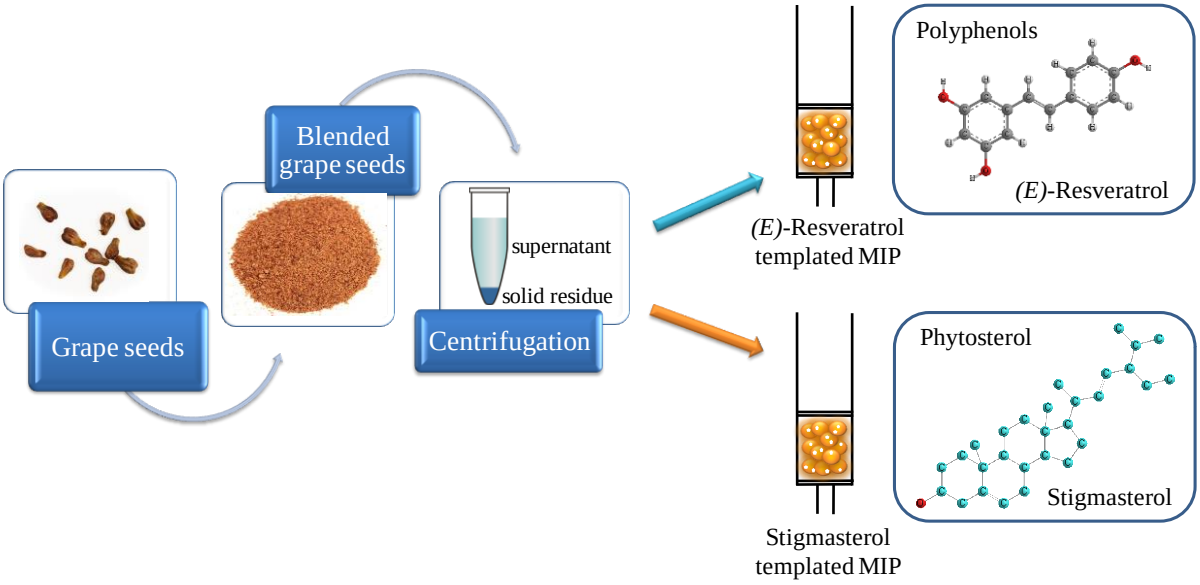

Figure 6.1: Experimental workflow for the extraction of (*E*)-resveratrol and stigmasterol from a single source of grape seeds.

6.2.4 MISPE protocol for (*E*)-resveratrol analysis

The MISPE and NISPE cartridges (2.0 cm diameter × 8.7 cm length) were conditioned (in sequence) with EtOH/AcOH (9:1, v/v), EtOH and EtOH/H_2O (15:85, v/v) (3 × 5 mL), respectively. The supernatant of skins or seeds of grapes (5 mL) was loaded onto the MISPE or NISPE cartridge, respectively. The MISPE or NISPE cartridge was washed with EtOH/H_2O (9:1, v/v) containing 1% (v/v) AcOH (4 × 5 mL) followed by elution with EtOH/AcOH (9:1, v/v) (10 × 5 mL). Finally, both cartridges were reconditioned in sequence with H_2O, EtOH and EtOH/H_2O (15:85, v/v) (3 × 5 mL), respectively. In the case of more complex samples, an additional wash step with 0.1 mM NaOH in water was introduced.

6.2.5 MISPE protocol for stigmasterol analysis

The MISPE and NISPE cartridges (2.0 cm diameter × 8.7 cm length) were conditioned with ACN and ACN/H_2O (9:1, v/v) (2 × 2 mL), respectively. The supernatant of unsaponified grape seed (2 mL) was loaded onto the MISPE or NISPE cartridge, respectively. The MISPE or NISPE cartridge was washed with ACN/H_2O (9:1, v/v) containing 1% (v/v) AcOH (4 × 2 mL) followed by elution with EtOH/AcOH (9:1, v/v) (5 × 2 mL). Both cartridges were finally reconditioned in sequence with H_2O, ACN and ACN/H_2O (9:1, v/v) (3 × 2 mL).

6.3 Results and Discussion

6.3.1 Grape skin extract for polyphenols analysis

The Pinot noir fresh grape pressings resulted in 27.4% (g/g) of skins based on fresh weight. The grape skins were subjected to fast freeze-drying and 30.5% (g/g) of dry matter content was determined based on the mass before and after drying. This procedure avoided the growth of bacterial or any other microbiological agents that could lead to the degradation of the target molecules.

The dried grape skin was extracted with a mixture of benign solvents containing EtOH/H_2O (1:1, v/v). The selection of ethanol as an organic solvent was based on the fact that this solvent, when mixed with water, improves the solubility of phenolic components (*12*). The supernatant obtained after centrifugation was injected directly into the RP-HPLC or LC-ESI-MS/MS system. The chromatographic conditions for both analytical instruments were selected based on the optimised methods developed in **Chapter 2 (Section 2.2.3)**.

6.3.1.1 Analysis of (E)-resveratrol and other polyphenols from grape skin before and after MISPE treatment by RP-HPLC

The separation of polyphenols in the extract of grape skins was achieved with a double endcapped C_{18}-column in order to minimise peak tailing. Based on a linear calibration curve of (*E*)-resveratrol standard, this compound **(peak 18)** was determined to be 31.4 µg/g dry extract with a retention time (t_R) of 33.5 min **(Figure 6.2)**, which is consistent with the value obtained by previous research. In that study (*13*), (*E*)-resveratrol content derived from various types of red and white grape skins were determined in a range of 11.1 µg/g to 123.0 µg/g dry matter due to the differences in variety, climate and phytosanitary conditions. A recent study showed that a higher concentration of (*E*)-resveratrol was found in the skins of Cabernet Sauvignon (12.4 µg/g) in comparison to the Pais cultivar (1.0 µg/g) (*14*). This study was in accordance with an earlier investigation performed by Okuda and co-workers *(15)*, who reported that the amounts of (*E*)-resveratrol in the grape skins varied considerably depending on the grape cultivar. With respect to the pharmacological properties, (*E*)-resveratrol has been shown to possess a wide array of health-beneficial effects with respect to various diseases such as cardiovascular disease, cancer, diabetes and neurodegenerative disorders (*16*).

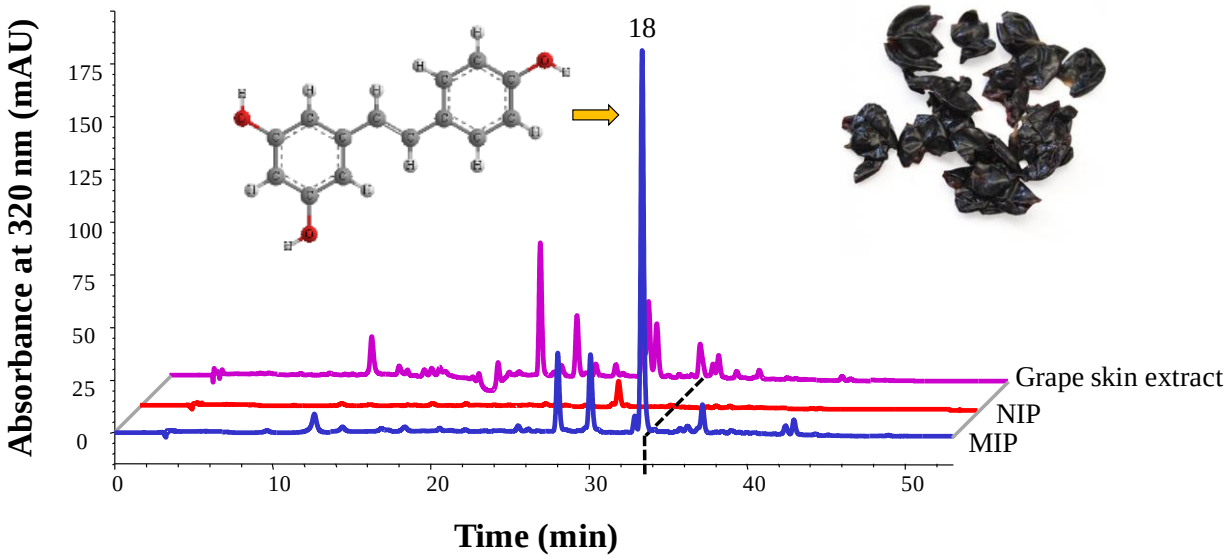

Figure 6.2: RP-HPLC chromatograms recorded at a wavelength of 320 nm for the quantification of (*E*)-resveratrol (t_R = 33.5 min, **peak 18**) in the grape skin (insert) extract (purple line, back chromatogram), after MIP (blue line, front chromatogram) and after NIP (red line, middle chromatogram) SPE treatment. The LC chromatograms were obtained with a Zorbax Eclipse XDB C_{18} column (4.6 mm × 150 mm, 5 µm particle size) at 20 °C. LC conditions: eluent A: 10 mM formic acid in water, eluent B: 10 mM formic acid in EtOH/H_2O (4:1, v/v), gradient: 0-2 min to 10% (v/v) B, 2-52 min to 70% (v/v) B, 52-53 min to 10% (v/v) B; flow rate: 0.5 mL/min; 5 µL injection.

In order to isolate (*E*)-resveratrol from the grape skin extract, MISPE was employed as well as NISPE (which acted as a control). The RP-HPLC elution profiles obtained from MISPE or NISPE can be seen in **Figure 6.2**. MISPE could be successfully used to enrich (*E*)-resveratrol in relation to other components present in the complex grape skin extract. The concentration enrichment of (*E*)-resveratrol after MIP eluate was determined to be 18.3 mg/L from the original concentration of 4.0 mg/L in the extract (on a mass and volume normalized basis). In addition, MISPE had shown its utility as an efficient cleanup tool with only few other components appearing after the elution from the MIP. The phenolic compounds present in the extract were comprehensively identified by LC-ESI-MS/MS, which is described later in **Section 6.3.1.2**. It should be noted that the peak numbering system of the chromatograms obtained from the analytical RP-HPLC is synchronised with the chromatographic profile generated by micro RP-HPLC-ESI ion trap MS/MS.

6.3.1.2 Identification of polyphenols from grape skin extract before and after MISPE treatment by LC-ESI ion trap MS/MS

Identification and characterisation of (*E*)-resveratrol and other polyphenols in grape skin extract was carried out by LC-ESI ion trap MS/MS at the *m/z* range of 100-1200 in the negative ionisation mode. In total, at least 24 phenolic components were identified in the extract prior to MISPE treatment as shown in **Figure 6.3-A**. The broad peak at a retention time between 8.5 min to 12 min in the chromatogram revealed unretained compounds in the gradient elution mode specifically chosen for polyphenols analysis. The detected polyphenols in the grape skin extract are enumerated in **Table 6.1** and are further discussed in the next section.

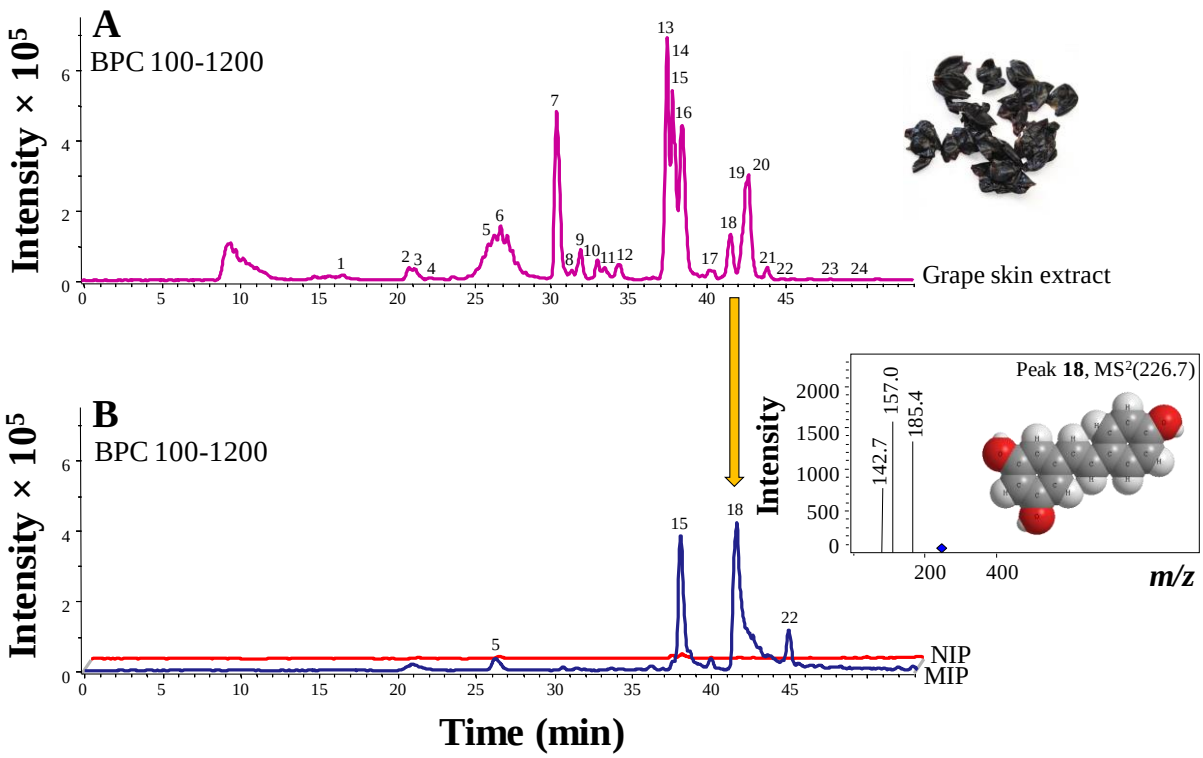

Figure 6.3: Base peak chromatogram (BPC) of **(A)** grape skin extract and **(B)** MISPE (blue line, front chromatogram) and NISPE (red line, back chromatogram) eluates from grape skin extract. Inserted is a mass spectrum of (*E*)-resveratrol with the characteristic product ions. (*E*)-resveratrol **(peak 18)** eluted at t_R = 41.5 min. The base peak chromatograms were obtained after RP-HPLC separation on a Zorbax XDB C_{18} capillary column (0.3 mm × 150 mm, 3.5 µm particle size) in the *m/z* range of 100-1200 using the negative ionisation mode by ESI ion trap MS/MS at 20 °C. LC conditions: eluent A: 10 mM formic acid in water, eluent B: 10 mM formic acid in EtOH/H_2O (4:1, v/v), gradient: 0-2 min to 10% (v/v) B, 2-52 min to 70% (v/v) B, 52-53 min to 10% (v/v) B; flow rate: 2 µL/min; 0.1 µL injection.

Table 6.1: Identifications and characterisations of polyphenols from grape skin extract before and after MISPE and NISPE treatment by LC-ESI ion trap MS/MS at the *m/z* range of 100-1200 in the negative ionisation mode. Bold entries represent significant enrichment of phenolic compounds above the ion current intensity of 0.5×10^5.

Peak No.	Compound name	t_R (min)	Precursor ion $[M-H]^-$, *m/z*	Product ion(s), *m/z*	Grape skin extract	MIP	NIP
*1	B-type procyanidin	16.5	577	451, 425, 407, 289	✓	×	×
2	(±)-Catechin	20.8	289	245, 205, 179	✓	✓	✓
*3	B-type procyanidin	21.6	577	451, 425, 407, 289	✓	✓	✓
4	*p*-Coumaryl glucoside	22.3	325	265, 235, 187, 163, 145	✓	×	×
5	**(±)-Epicatechin**	25.9	289	245, 205, 179	✓	✓	✓
*6	B-type procyanidin	26.6	577	451, 425, 407, 289	✓	×	×
7	Myricetin-3-*O*-glucoside	30.2	479	355, 317, 299, 163	✓	×	×
8	Epicatechin-3-*O*-gallate	31.0	441	289, 205, 169, 125	✓	×	×
*9	B-type procyanidin	31.6	577	451, 425, 407, 289	✓	×	×
10	(*E*)-Piceid	32.8	389	227	✓	×	×
11	Viniferin	33.2	453	359, 265	✓	×	×
12	Piceatannol glucoside	34.1	405	345, 243, 225, 215	✓	×	×
13	(+)-Astilbin	37.2	449	303, 285, 151	✓	×	×
14	Quercetin-3-*O*-rutinoside	37.4	609	301, 179, 151, 107	✓	×	×
15	**Quercetin-3-*O*-glucuronide**	37.6	477	301, 179, 151	✓	✓	×
16	Quercetin-3-*O*-glucoside	38.3	463	301, 179, 151	✓	×	×
17	(-)-Astilbin	40.0	449	303, 285, 151	✓	×	×
18	**(*E*)-Resveratrol**	41.5	227	185, 157, 143	✓	✓	×
19	Kaempherol-3-*O*-glucoside	42.2	447	327, 285, 255	✓	×	×
20	(*Z*)-Piceid	42.5	389	227	✓	×	×
21	Quercetin-3-*O*-xyloside	43.5	433	301, 287, 269, 179, 151	✓	×	×
22	**Dimer adduct of catechin-methyl-5-furfuraldehyde**	44.8	671	653, 429, 411, 287, 259, 245	*lc*	✓	×
23	(*Z*)-Resveratrol	47.8	227	185, 157, 143	✓	×	×
24	Quercetin	49.5	301	179, 151	✓	×	×

* Based on the MS/MS spectra, no further identification was possible;
lc Phenolic compound present at low concentration.

6.3.1.2.1 Identification of polyphenols before MISPE treatment

i) Stilbenes

Several compounds of stilbenes were detected in the extract of grape skins. Resveratrol in (*E*)-**(peak 18)** and (*Z*)-**(peak 23)** forms were identified based on the precursor ions $[M-H]^-$ at *m/z* 227, respectively. These compounds had identical characteristic product ions (*m/z* 185, 157 and 143) but dissimilar retention times (*17*). With the assistance of the (*E*)-resveratrol reference standard, the peak identity and elution profile of the (*E*)-isomer was verified. (*E*)-Resveratrol was observed at a retention time of 41.5 min whilst its stereoisomer eluted at a longer retention time (47.8 min) due to the higher hydrophobicity of (*Z*)-resveratrol in the reversed-phase system. The retention time of (*E*)-resveratrol (41.5 min) obtained from the microLC system was about 8 min higher in comparison to the retention time obtained from the analytical RP-HPLC system due the differences in gradient delay volume of these systems. A more detailed explanation is given in **Chapter 3 (Section 3.3.3.1.1)**. Resveratrol glucosides, known as piceid/polydatin were observed at the retention time of 32.8 min **(peak 10)** and 42.5 min **(peak 20)** corresponding to the (*E*)- and (*Z*)-isomers, respectively. Due to the differences in polarity, the glucosides of resveratrol eluted earlier than resveratrol aglycone. Piceids were identified based on the precursor ion $[M-H]^-$ at *m/z* 389 which underwent fragmentation to generate free resveratrol (*m/z* 227) by losing a unit of glucoside moiety (*18*). A resveratrol oligomer, viniferin **(peak 11)**, was present in the sample with a precursor ion $[M-H]^-$ at *m/z* 453. This compound fragmented v*ia* MS/MS experiments to give two distinctive product ions at *m/z* 359 and 265 (*19*). **Peak 12** was attributed to piceatannol glucoside based on the precursor ion $[M-H]^-$ at *m/z* 405. This compound was fragmented in the MS ion source to generate several characteristic product ions at *m/z* 345, 243 (piceatannol aglycone), 225 and 215 (*20*).

ii) Hydroxycinnamic derivatives

Peak 4 was characterised as *p*-coumaryl glucoside based on the precursor ion $[M-H]^-$ at *m/z* 325. This compound was fragmented to generate some characteristic product ions at *m/z* 265, 235, 187, 163 (*p*-coumaric acid) and 145 (*21*). From this identification, only one compound of the hydroxycinnamic derivative category was identified in the grape skin extract. No hydroxybenzoic acid was detected.

iii) Flavanols

Catechin **(peak 2)** and epicatechin **(peak 5)** were assigned on the basis of their molecular ions $[M-H]^-$ at *m/z* 289. The characteristic product ions (*m/z* 245, 205 and 179) released after collision induced dissociation in the MS/MS experiment confirmed the presence of these compounds in the extract. The fragmentation pattern of catechin/epicatechin are very similar with the one reported in a previous publication (*22*). A (±)-catechin commercial standard was used to verify the identity of catechin, which was observed at a retention time of 20.8 min in comparison to epicatechin (t_R = 25.9 min). **Peak 8** was identified as epicatechin gallate based on the precursor ion $[M-H]^-$ at *m/z* 441 which fragmented to generate *m/z* 289 (epicatechin), 205, 169 and 125 (*23*).

iv) Tannins

The detection of several compounds at different retention times with the similar precursor ions $[M-H]^-$ at *m/z* 577 were monitored. The B-type procyanidins **(peaks 1**, **3**, **6** and **9)** were characterised based on several characteristic product ions at *m/z* 451, 425, 407 and 289 (catechin/epicatechin).

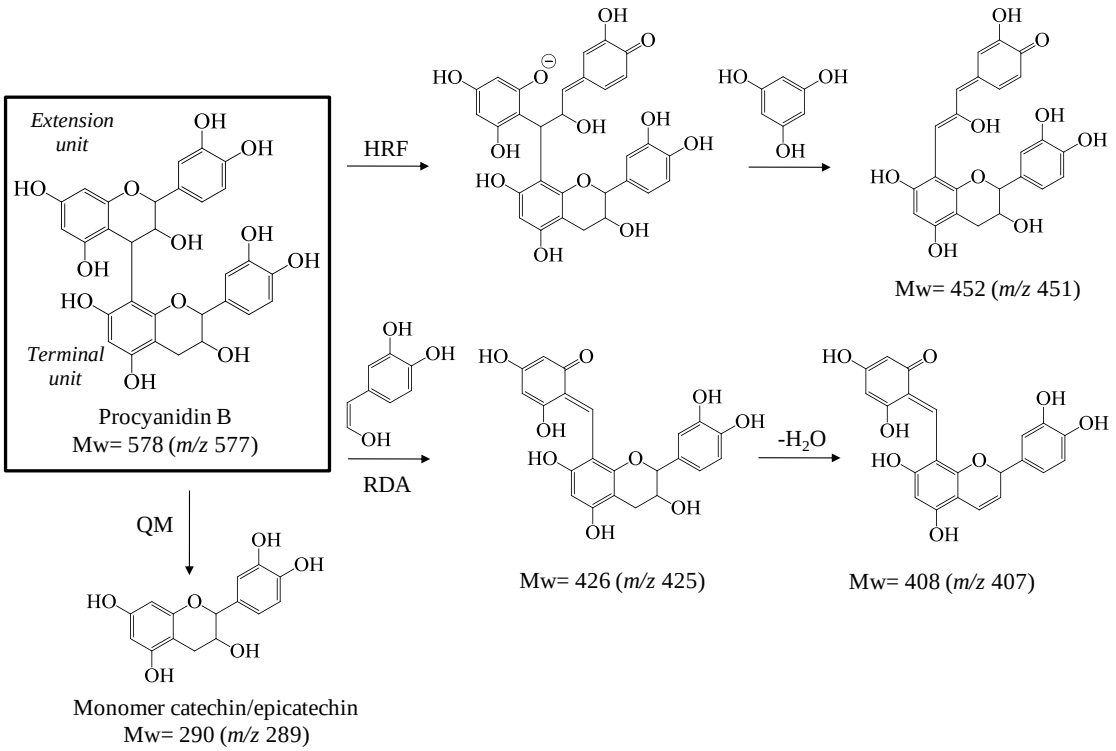

Figure 6.4: The fragment ions of B-type procyanidin from grape skin extract, measured by LC-ESI ion trap MS/MS in the negative ionisation mode. HRF= heterocyclic ring fission; RDA = retro-Diels-Alder reaction; QM= quinine methide fission cleavage.

The fragmentation trend of the current investigation was in accordance with previous studies. Therefore, the fragmentation pattern of procyanidin in this study presumably followed a similar pathway as the one suggested by Callemien and co-workers **(Figure 6.4)** (*24*). A procyanidin dimer is comprised of an extension and a terminal unit. The fragmentation pathway of procyanidin could begin either at the extension or terminal unit *via* retro-Diels-Alder (RDA) and heterocyclic ring fission (HRF) mechanisms. It has been suggested that the fragmentation within the extension unit generates product ions with a large π-π hyperconjugated system (*25*).

v) Flavonols

Peak 7 with the precursor ion $[M-H]^-$ at *m/z* 479 was attributed to myricetin-3-*O*-glucoside. This compound fragmented to yield the main product ion at *m/z* 317 (myricetin aglycone) by losing a glucoside moiety $[M-H-162]^-$ (*26*). Kaempherol-3-*O*-glucoside **(peak 19)** was observed with the precursor ion $[M-H]^-$ at *m/z* 447 (*26*), which fragmented in the ion trap to generate several distinctive product ions at *m/z* 327, 285 (kaempherol aglycone) and 255.

A number of quercetin-based derivatives were detected with different types of glycosides attached to the core structure. The fingerprint fragmentation of quercetin derivatives in these investigations revealed several characteristic product ions at *m/z* 301 (quercetin), 179 and 151. Quercetin-3-*O*-glucuronide **(peak 15)** was identified at a retention time of 37.6 min with the precursor ion $[M-H]^-$ at *m/z* 477 (*26*). This compound fragmented to generate quercetin aglycone (*m/z* 301) by losing a glucuronide moiety $[M-176-H]^-$. The precursor ion $[M-H]^-$ at *m/z* 463 revealed the occurrence of quercetin-3-*O*-glucoside **(peak 16)** in the extract (*26*). The loss of a glucoside moiety $[M-162-H]^-$ from the pseudomolecular ion led to the formation of quercetin aglycone at *m/z* 301. Quercetin-3-*O*-xyloside **(peak 21)** was detected based on the precursor ion $[M-H]^-$ at *m/z* 433 (*26*) with a retention time of 43.5 min. This compound fragmented to generate *m/z* 301 (quercetin).

The identification of rutin, amongst the complex molecular structures in this extract was confirmed by mass spectral analysis which included MS^2 to MS^4 fragmentation **(Figure 6.5)**. Rutin, also known as quercetin-3-*O*-rutinoside **(peak 14)** revealed the precursor ion $[M-H]^-$ at *m/z* 609 (*26*). MS^3 and MS^4 fragmentations were useful in confirming the molecular structure. Based on the fragmentation behaviour of rutin through MS^n spectra, a plausible pathway of rutin in the negative ionisation mode was proposed **(Figure 6.6)**. The MS^2 experiments

resulted in the cleavage of rhamnosyl-glucoside moiety from the precursor ion of *m/z* 609.3 yielded a quercetin aglycone at *m/z* 300.8. During MS^3 analysis, the successive fragmentation of *m/z* 300.8 formed product ions at *m/z* 178.7 and 150.7. When the product ion at *m/z* 178.7 was subjected to MS^4 analysis, *m/z* 150.7 was produced due to the loss of 28.0 mass units. In a similar MS^4 experiment, the signal at *m/z* 150.7 fragmented to generate *m/z* 106.8 because of the loss of a CO_2 molecule (43.9 mass units).

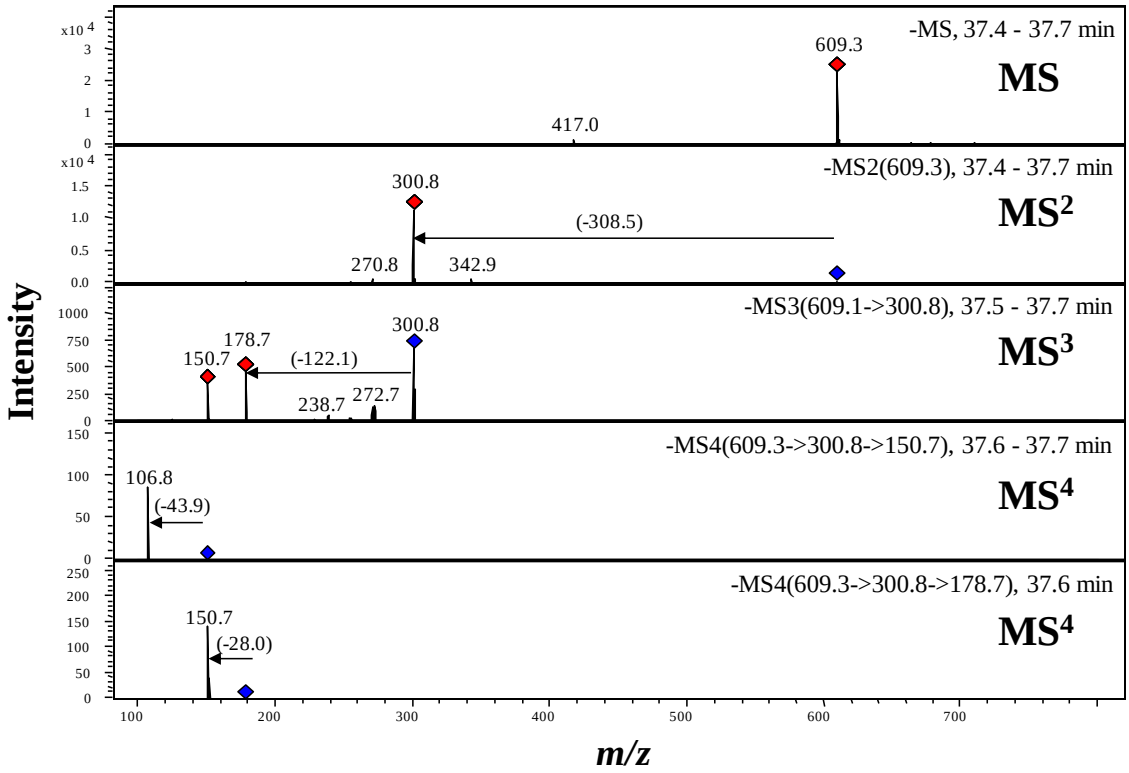

Figure 6.5: Fragmentation of rutin with MS^n analysis (*n* = 2 to 4, sequential MS fragmentation events) in the negative ionisation mode. The diamond (♦) symbol shows the position of the residual precursor ion.

Quercetin **(peak 24)** was identified at a retention time of 49.5 min by having a precursor ion $[M-H]^-$ at *m/z* 301 (*27*). This compound fragmented to generate several characteristic product ions at *m/z* 179 and 151. It was expected that the hydrophobicity of the quercetin aglycone results in a longer retention time than its glycoside compounds. Epidemiological studies claimed that quercetin has powerful antioxidant activity because of its phenolic hydroxyl groups, in particular the catechol group in the B-ring (*28*).

The results showed that the flavonol derivatives were the dominant compounds in the skin extract (before MISPE treatment). The occurrences of myricetin glucoside **(7)**, quercetin rutinoside **(14)**, quercetin glucuronide **(15)** quercetin glucoside **(16)** and kaempherol

glucoside **(19)** at high ion current intensity can be seen in **Figure 6.3-A**. The present findings are consistent with the work of Kammerer *et al*. (*13*), who reported that the flavonol glycosides are the major phenolic compounds in the skins of grape pomace. It has been suggested that the production of these compounds in grape skins functions as screening to protect the tissues from UV-damage (*29*, *30*).

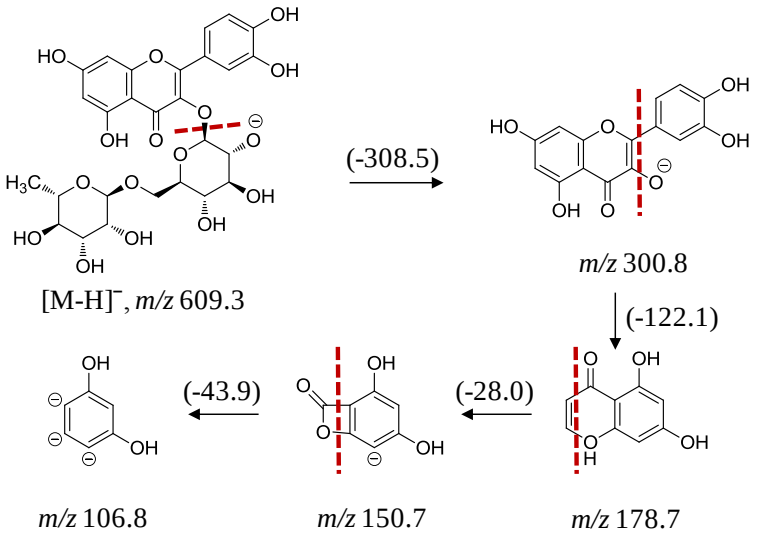

Figure 6.6: The plausible fragmentation pathway of rutin.

vi) Flavanonols

Astilbins (dihydroquercetin rhamnoside, *m/z* 449) were identified at the position of **peaks 13** and **17** with the retention time of 37.2 min and 40.0 min, respectively. These compounds had precursor ions which fragmented to produce the main characteristic product ions at *m/z* 303 and 285 due to the loss of a rhamnoside moiety $[(M-C_6H_{10}O_4)-H]^-$ to generate taxifolin (dihydroquercetin) and a further fragment through the neutral loss of water (18 mass units), respectively (*31*).

6.3.1.2.2 Identification of polyphenols after MISPE treatment

The MISPE and NISPE treatment enabled to remove the non-selectively bound compounds to isolate (*E*)-resveratrol **(peak 18)** from its original complex mixture **(Figure 6.3-B)**. The MIP showed its binding affinity and selectivity towards (*E*)-resveratrol whilst an insignificant small peak was observed from the control NISPE eluate.

Interestingly, the majority of flavonol glycosides **(peaks 7**, **14** and **16)** which were observed before the treatment at high ion current intensity (above 4.0×10^5), were diminished after

MISPE with the exception of **peak 15**. Quercetin glucuronide **(peak 15)** was recorded in the chromatogram with a high intensity due to the competitive binding although relatively large in size in comparison to the target molecule. The quercetin-core structure possesses structural similarity and spatial complementarity to the (*E*)-resveratrol-template, therefore this compound could somehow position itself to reside within the cavities through the formation of hydrogen bonds *via* aromatic intermolecular O-H--N interactions. The binding affinity for quercetin glucuronide with this MIP might be due to the availability of at least two hydroxyl-groups in the *meta* and/or *para* positions on its aromatic rings. The isolation of quercetin glucuronide is of interest because this compound has been described as a highly bioactive substance with antioxidant activity (*32*).

Several other phenolic components were detected at low concentrations and resembled in their structural features the target molecule including a dimer adduct of catechin-methyl-5-furfuraldehyde **(peak 22)** and epicatechin **(peak 5)**. The identification and fragmentation of **peaks 5** and **15** (after MISPE treatment) were described previously in **Section 6.3.1.2.1** and **Table 6.1**. **Peak 22** might be identified as a dimer adduct of catechin-methyl-5-furfuraldehyde (two catechin units bridged by methyl-5-furfuryl groups) based on the precursor ion $[M-H]^-$ at *m/z* 671 (*33*). This compound fragmented *via* MS/MS experiments to generate several product ions at *m/z* 653 (due to the loss of water), 429, 341, 287, 259 and 245. The three latter product ions were possibly related to the characteristic fragmentation pattern of catechin-monomer.

6.3.1.3 Efficacy of MISPE method for grape skin extracts

The grape skin extract (5 mL) was loaded onto the MISPE or the NISPE cartridge, respectively. In order to evaluate the selectivity of the imprinted binding sites in the MIP, a comparison with the control NIP was investigated. As shown in **Table 6.2**, the percolation of EtOH/H_2O (4:1, v/v) containing 1% (v/v) AcOH (4 × 5 mL) had the desired effect as wash solvent, being able to remove 29.8 µg/g (94.9%) of (*E*)-resveratrol from the NISPE cartridge. The elution steps with 10% (v/v) AcOH in EtOH enabled to disrupt the selective interactions of (*E*)-resveratrol (28.7 µg/g) with the MIP sorbent compared to an insignificant amount (0.4 µg/g) of the target analyte being eluted from the NIP sorbent. The imprinting factor of 72 was determined based on the eluate fractions of MIP *versus* NIP. The recovery of (*E*)-resveratrol after MISPE was 99.4% whilst 96.2% from NISPE cartridge. The performance of the MIP in comparison to the NIP in the SPE cartridge is shown in **Figure 6.7**.

In these investigations, the same MIP which was previously employed for the extraction of (*E*)-resveratrol from peanut press waste, red wine and grape pressing residues was reused for the analysis of grape skins and grape seeds. Although the MIP was reused many times (more than 20 times) with those samples, these materials retained their integrity to capture (*E*)-resveratrol with high selectivity and high recovery (in most cases more than 99% recoveries of (*E*)-resveratrol was achieved). This feature highlighted the key benefits of incorporation of MIPs in the SPE format as a reusable tool for the selective enrichment of beneficial-health target components from various complex matrices. In contrast to a previous MIP study performed by Theodoridis and co-workers (*34*), where the recovery of caffeine was diminished if more than four consecutive extractions of blood plasma were performed in the same cartridge, because the accumulation of matrix components was thought to have blocked the active sites of the polymer and to have altered its recognition properties.

Table 6.2: The amount of (*E*)-resveratrol (µg/g) from grape skin extract after MISPE and NISPE treatments. Wash steps were performed with a mixture of EtOH/H_2O (4:1, v/v) containing 1% (v/v) AcOH followed by elution steps with 10% (v/v) AcOH in EtOH.

		(*E*)-Resveratrol (µg/g)	
		MISPE	**NISPE**
Before treatment	Sample loading (1 × 5 mL)	31.4	31.4
After treatment	Wash steps (4 × 5 mL)	2.5	29.8
	Elution steps (10 × 5 mL)	28.7	0.4
	Total wash and elution	31.2	30.2
Total recovery (%)		99.4	96.2
Imprinting factor, (*IF* = MIP eluate/NIP eluate)		72	

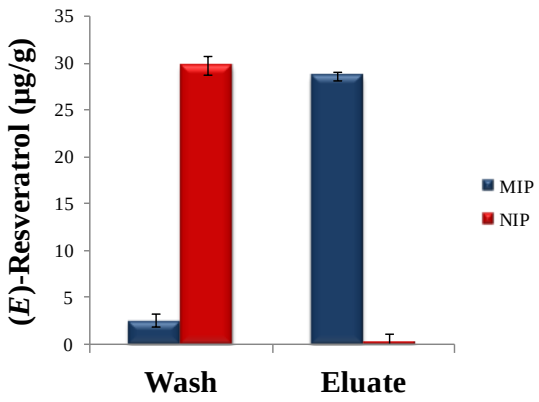

Figure 6.7: The comparison of (*E*)-resveratrol (µg/g) in grape skin extract obtained from wash and elution fractions after MISPE *versus* NISPE treatment. Measurements were performed in duplicate (n = 2). Error bars indicate the standard error expressed by the formula $Error = \sigma/\sqrt{n}$, where σ is the standard deviation and n is the number of measurements.

6.3.2 Grape seed extract for polyphenols analysis

The Pinot noir grape preparation resulted in 10.8% (g/g) grape seed based on fresh weight. These seeds were freeze-dried to remove the moisture. The dry matter content of grape seeds was determined to be 48.3% (g/g) on the basis of relative mass before and after lyophilisation. This value is in agreement with previous publications which have reported that grape seeds constituent about 38 - 52% of dry matter content. This study showed that the percentage of dry matter content of grape seeds is higher than that of the skins. This is explained by the larger amount of water in the cells of skins compared to those of seeds.

6.3.2.1 Analysis of (E)-resveratrol and other polyphenols from grape seed extract before and after MISPE by RP-HPLC

The supernatant of the grape seed extract was injected into the RP-HPLC system and (*E*)-resveratrol **(peak 15)** eluted at a retention time of 32.7 min **(Figure 6.8)**. The amount of (*E*)-resveratrol was determined to be 11.4 µg/g dry extract based on a linear calibration curve of (*E*)-resveratrol standard. In a previous investigation, Sun *et al.* (*35*) reported that in Castelão grape seeds (*E*)-resveratrol was determined to be 5.8 mg/kg dry seed.

In the present study, a higher amount of (*E*)-resveratrol was observed in grape skin (31.4 µg/g) than in seed (11.4 µg/g) extracts. Resveratrol is produced more in the epidermal cells of grape berry skin (*36*) to protect the grapes from abiotic stresses such as fungal infections and excess UV-exposure which is not needed to such a degree in the seeds, in the inner part of the grape.

The RP-HPLC chromatographic profiles of grape seed extract before and after MISPE and NISPE treatment are depicted in **Figure 6.8**. The differences of (*E*)-resveratrol retention time (0.8 min) between the grape skin (33.5 min) and seed extracts (32.7 min) is likely due to the fact that the mobile phase preparations and sample injections were performed on seven different days. For the grape seed extract analysis, (*E*)-resveratrol was assigned as **peak 15** whilst this compound was labelled as **peak 18** in the grape skin extract analysis (**Section 6.3.1.1)**.

Despite a successful determination of (*E*)-resveratrol in the grape seed extract, a poor baseline separation was observed for components of the grape seed extract before MISPE treatment. The remarkable advantage of MISPE for rapid sample cleanup and to sequester

(*E*)-resveratrol can be seen in **Figure 6.8**. The reduction of matrix interferences as well as improvement of the resolution allowed to correctly quantify (*E*)-resveratrol in the sample. The application of the MIP in SPE format resulted in the concentration enrichment of (*E*)-resveratrol up to 6.5 mg/L (in the MISPE eluate) from 1.4 mg/L (on a mass and volume normalized basis). In a comparison to the MISPE binding affinity, the control NISPE cartridge showed negligible recognition of the target analyte.

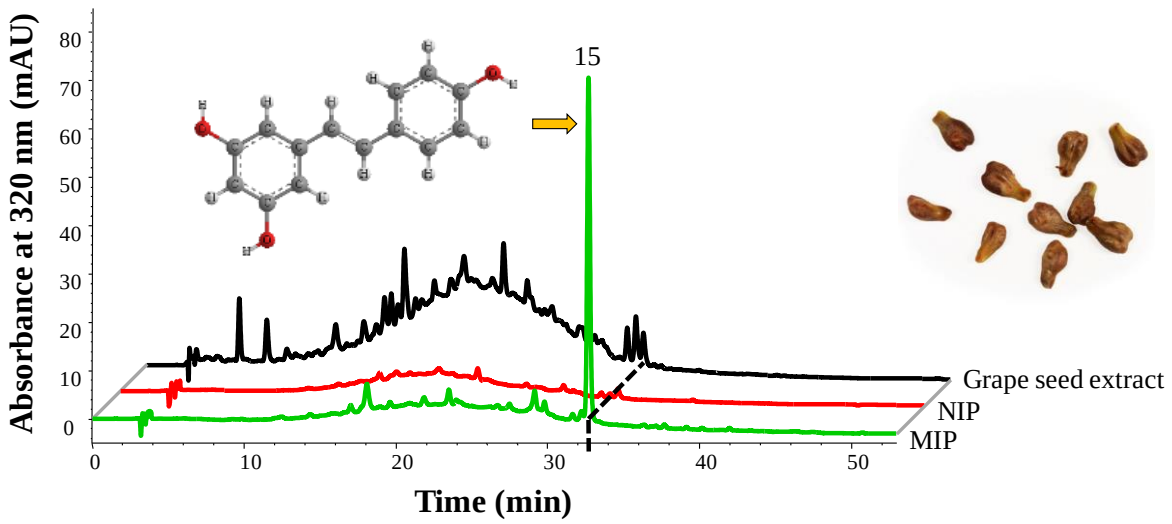

Figure 6.8: RP-HPLC chromatograms recorded at a wavelength of 320 nm for the quantification of (*E*)-resveratrol (t_R = 32.7 min, **peak 15**) in the grape seed extract (black line, back chromatogram), after MIP (green line, front chromatogram) and after NIP (red line, middle chromatogram) SPE treatment. The LC chromatograms were obtained with a Zorbax Eclipse XDB C_{18} column (4.6 mm × 150 mm, 5 µm particle size) at 20 °C. LC conditions: eluent A: 10 mM formic acid in water, eluent B: 10 mM formic acid in EtOH/H_2O (4:1, v/v), gradient: 0-2 min to 10% (v/v) B, 2-52 min to 70% (v/v) B, 52-53 min to 10% (v/v) B; flow rate: 0.5 mL/min; 5 µL injection.

6.3.2.2 Identification of polyphenols from grape seed extract before and after MISPE treatment by LC-ESI ion trap MS/MS

6.3.2.2.1 Analysis of seed polyphenols before MISPE treatment

In the negative ionisation mode, at least 18 phenolic seed compounds were successfully identified by LC-ESI ion trap MS/MS as depicted in **Figure 6.9-A**. The identification and characterisation of the majority of polyphenols present in grape seed extract was described earlier in **Section 6.3.1.2**. This section focuses on the comparison of polyphenolic contents in both skin and seed extracts. The information of polyphenolic substances in grape seed extract

including compound name, retention time, precursor ion, product ion(s) prior and after MISPE and NISPE treatment is presented in **Table 6.3**.

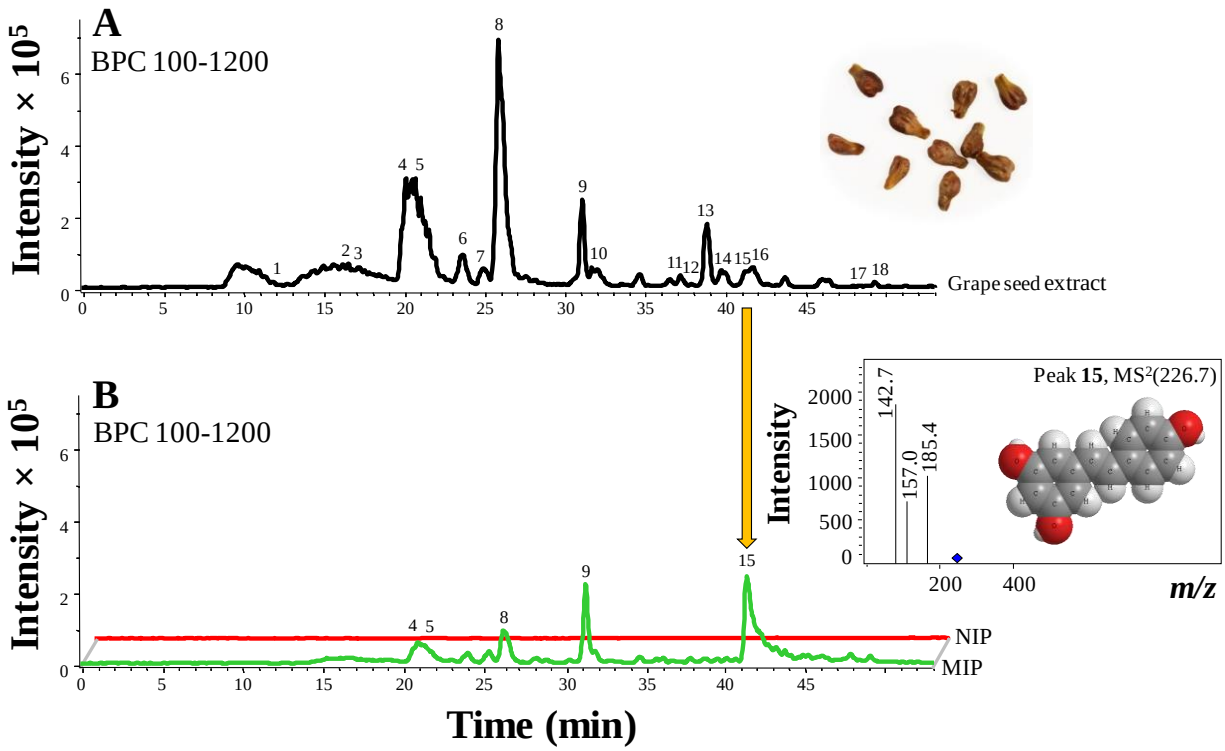

Figure 6.9: Base peak chromatogram (BPC) of **(A)** grape seed extract and **(B)** MISPE (green line, front chromatogram) and NISPE (red line, back chromatogram) eluates from grape seed extract. Inserted is a mass spectrum of (*E*)-resveratrol with the characteristic product ions. (*E*)-resveratrol **(peak 15)** eluted at t_R = 41.5 min. The base peak chromatograms were obtained after RP-HPLC separation on a Zorbax XDB C_{18} capillary column (0.3 mm × 150 mm, 3.5 µm particle size) in the *m/z* range of 100-1200 using the negative ionisation mode by LC-ESI ion trap MS/MS at 20 °C. LC conditions: eluent A: 10 mM formic acid in water, eluent B: 10 mM formic acid in EtOH/H_2O (4:1, v/v), gradient: 0-2 min to 10% (v/v) B, 2-52 min to 70% (v/v) B, 52-53 min to 10% (v/v) B; flow rate: 2 µL/min; 0.1 µL injection.

Table 6.3: Identification and characterisation of polyphenols from grape seed extract before and after MISPE and NISPE treatment. Bold entries represent significant enrichment of phenolic compounds above the ion current intensity of 0.5×10^5.

Peak No.	Compound name	t_R (min)	Precursor ion $[M-H]^-$, *m/z*	Product ion(s), *m/z*	Grape seed extract	MIP	NIP
1	Gallic acid	12.0	169	125	✓	×	×
*2	B-type procyanidin	16.2	577	451, 425, 407, 289	✓	*lc*	✓
3	B-type procyanidin trimer	16.9	865	847, 739, 695, 577	✓	×	×
4	**(±)-Catechin**	20.7	289	245, 205, 179	✓	✓	×
***5**	**B-type procyanidin**	21.6	577	451, 425, 407, 289	✓	✓	✓
6	B-type procyanidin dimer gallate	23.7	729	652, 577, 355, 289, 245	✓	×	×
*7	B-type procyanidin	24.7	577	451, 425, 407, 289	✓	✓	×
8	**(±)-Epicatechin**	25.9	289	245, 205, 179	✓	✓	×
9	**Epicatechin-3-*O*-gallate**	31.0	441	289, 205, 169, 125	✓	✓	×
*10	B-type procyanidin	31.5	577	451, 425, 407, 289	✓	✓	×
11	B-type procyanidin tetramer	31.9	1017	865, 729, 557, 451, 425, 407, 289	✓	×	×
12	(+)-Astilbin	37.2	449	303, 285, 151	✓	×	×
13	Quercetin-3-*O*-glucuronide	37.8	477	301, 179, 151	✓	×	×
14	Epicatechin-ethyl dimer	38.8	605	451, 315, 289, 245, 205	✓	×	×
15	**(*E*)-Resveratrol**	41.5	227	185, 157, 143	✓	✓	×
16	(*Z*)-Piceid	42.7	389	227	✓	×	×
17	(*Z*)-Resveratrol	48.1	227	185, 157, 143	✓	×	×
18	Quercetin	49.2	301	179, 151	✓	×	×

* Based on the MS/MS spectra, no further identification was possible;
lc Phenolic compound present at low concentration.

This study determined the distributions of (*E*)-resveratrol and other polyphenols in different parts of grapes. In this investigation, (*E*)-resveratrol from grape seed extract was assigned as **peak 15** based on the presence of a precursor ion $[M-H]^-$ at *m/z* 227 by LC-ESI ion trap MS/MS in the negative ionisation mode. (*E*)-resveratrol fragmented to generate several distinctive product ions at *m/z* 185, 157 and 143. The details related to the fragmentation of

(*E*)-resveratrol were described previously in **Chapter 2 (Section 2.3.2.3)**. (*E*)-resveratrol was identified at 41.5 min with the micro-LC-MS/MS system and detected at a retention time of 32.7 min with the analytical RP-HPLC. This retention time difference of 8.8 min is due to the differences of the gradient delay volumes of both instruments and the additional delay volume between UV detector and MS detector in the microLC-MS/MS system.

Figure 6.9-A and **Table 6.3** show that the flavanols and tannins were the major bioactive constituents in the grape seed extract based on the ion current intensity. The presence of catechin **(peak 4)** and its stereoisomer epicatechin **(peak 8)** were identified with the precursor ion $[M-H]^-$ at *m/z* 289. Epicatechin-3-*O*-gallate **(peak 9)** at a retention time of 31.0 min was assigned based on the precursor ion $[M-H]^-$ at *m/z* 441. **Peak 14** was detected at the precursor ion $[M-H]^-$ of *m/z* 605, most probably attributed to the epicatechin-ethyl dimer, whereby two units of epicatechin are linked by an ethyl-bridge (*22*). This compound fragmented to generate several characteristic product ions at *m/z* 451, 315, 289, 245 and 205. The product ion of *m/z* 451 possibly corresponded with a RDA fragmentation of the dimer (*22*) whilst *m/z* 315 might be due to a vinyl-catechin adduct (*37*). The signal at *m/z* 289, 245 and 205 showed the distinctive product ions belong to the catechin/epicatechin monomer. The prevalence of flavanols in the grape seeds is in agreement with the findings of Kammerer *et al.* (*13*) in grape pomace who reported that the seeds contained a high amount of flavanols. This is also in accord with the observations performed by Mane *et al.* (*38*) who found that the Pinot noir grape seeds consisted of a higher amount of flavanols than the grape skins. Several studies also claimed that the flavanols (catechin/epicatechin) are located in the skins and seeds of the grapes however the latter comprised higher concentrations of flavanols (*39-41*). A comparative study of the flavanols localisation across different grape cultivars was published by Thorngate *et al.* (*42*), who reported that the Pinot noir seeds contained higher amounts of flavanols than the seeds from a Cabernet Sauvignon cultivar.

Various B-type procyanidins were detected having a different degree of polymerisation including the B-type dimer **(peaks 2**, **5**, **7** and **10)**, dimer gallate **(peak 6)**, trimer **(peak 3)** and tetramer **(peak 11)** with the precursor ions $[M-H]^-$ at *m/z* 577, 729, 865 and 1017, respectively. The procyanidin tetramer (*m/z* 1017) underwent fragmentation in the ion trap to generate the procyanidin trimer (*m/z* 865) followed by the production of procyanidin dimer gallate at *m/z* 729. This product ion further fragmented to yield *m/z* 577 (procyanidin dimer) due to the loss of a galloyl group (152 mass unit). Further fragmentation occurred at *m/z* 451

corresponding to the loss of a pyrogallol unit $[M-H-126]^-$ on the C-ring. The product ion at *m/z* 425 is generated through the elimination of the B-ring followed by the generation of a product ion of *m/z* 407 due to the loss of water. An interflavan bond cleavage produced a monomer of catechin/epicatechin at *m/z* 289. The high occurrences of procyanidin oligomers in the seed extract corroborate the findings by Prieur and co-workers (*43*).

The clinical data has shown that procyanidin B_1 is amongst the most important radical scavenger in grape seed extract (*44*). In a recent investigation, Terra *et al.* (*45*) reported that the daily intake of grape seed procyanidin extract helps to inhibit inflammation associated with obesity. In addition, Feringa *et al.* (*46*) demonstrated that the high amounts of procyanidins in grape seed extract provide a beneficial effect on the cardiovascular system.

6.3.2.2.2 Analysis of polyphenols after MISPE treatment

The use of MISPE for the pretreatment of (*E*)-resveratrol from complex grape seed extract prior to chromatographic analysis was demonstrated. **Figure 6.9-B** shows that the MIP had a strong affinity for (*E*)-resveratrol **(peak 15)** based on the analysis of the MISPE eluate in comparison to the NISPE eluate. The MISPE method improved the resolution of **peak 15** and at the same time allowed to discriminate **peak 16** (resveratrol glucoside). The large reductions of intensity for **peaks 4**, **5** and **8** were also observed after MISPE, with the exception of **peak 9**. **Peak 9** (epicatechin gallate) was in high binding competition to (*E*)-resveratrol, which was observed in the BPC chromatogram after MISPE eluate. However, there was no apparent enrichment of epicatechin gallate as the ion current intensity remained below 30,000 (before and after MISPE). The binding by the MIP of epicatechin gallate might be related to the high concentrations of epicatechin-based compounds in grape seed extracts which may compete with the target molecule for pyridinyl-functionalities in the imprinted sites. Since the epicatechin monomer is structurally related to (*E*)-resveratrol, epicatechin gallate (derivative) can also potentially bind to the cavities in the polymer network. Presumably, the hydrogen bonding interactions between the positively charged 4-VP (the functional monomers in the cavities) and the delocalised π-electron system of the aromatic flavonoid rings, as well as hydrophobic interactions with the aromatic ring system are the main responsible factors for the binding recognition of epicatechin gallate by the MIP (suggestion of binding recognition is shown in **Figure 6.10**). The binding affinity for the procyanidins (two units of catechin/epicatechin monomer) was explained earlier in **Chapter 3 (Section 3.3.3.2)**.

With respect to the bioactivity of flavanols in grape seeds, Silva *et al. (47)* reported that epicatechin gallate from grape seeds, including catechin monomers are potent scavengers of superoxide radical and hydroxyl radicals in aqueous models. According to Ugartondo and co-workers (*48*), the flavanol compounds with a gallate group exhibited higher antioxidant activity than those without the gallate group, as the hydroxyl-group of the galloyl moieties plays an important role in inhibiting and scavenging radicals. Recent investigations showed that the highest antioxidant activity amongst various varieties was determined from Pinot noir grape seeds (*3*).

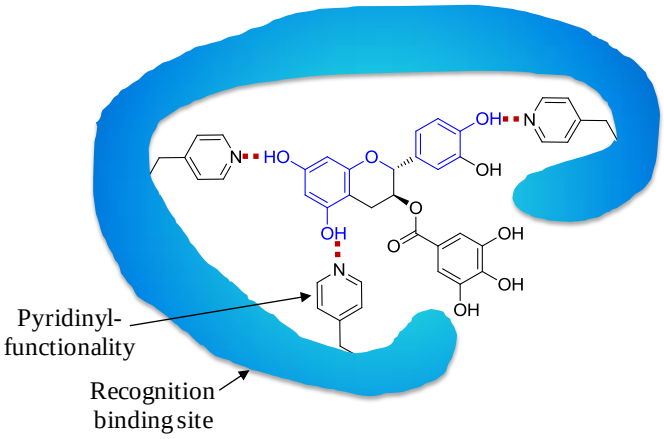

Figure 6.10: The plausible binding recognition of epicatechin gallate with pyridinyl-functionalities in the binding site of an (*E*)-resveratrol imprinted MIP, demonstrating the possibility of OH---N hydrogen bonding (dashed lines). Blue lines resemble the (*E*)-resveratrol structure within epicatechin gallate.

6.3.2.3 Efficacy of the (E)-resveratrol-templated MIP for grape seed extract

In this experiment, 5 mL of grape skin extract was loaded onto a MISPE and a NISPE cartridge, respectively. Both cartridges (2.0 cm diameter × 8.7 cm length) were washed with a mixture of EtOH/H_2O (4:1, v/v) containing 1% (v/v) AcOH (4 × 5 mL) in order to remove the non-selectively bound components. The application of wash solvents enabled the removal of majority of the (*E*)-resveratrol approximately 10.8 µg/g (94.7%), from the NISPE cartridge **(Table 6.4)**. In contrast, the MIP was capable of holding a significant amount of (*E*)-resveratrol (10.4 µg/g), although there was a small amount of the target molecule (0.9 µg/g) eluted from the MIP cartridge during the wash stages. As expected, the MIP exhibited a greater selectivity for (*E*)-resveratrol compared to the NIP. The majority of the

target compound was desorbed from the MIP sorbent after elution with EtOH/AcOH (9:1, v/v) due to the interruption of hydrogen bonding interactions between the hydroxyl-groups from (*E*)-resveratrol and the basic site of pyridinyl-functionalities. The imprinting effect expressed as an imprinting factor, whereby the binding of MIP *versus* NIP in eluate fractions was assessed, was 26. The recovery of (*E*)-resveratrol after MISPE was determined to be 99.1%. The performance of MIP and NIP in SPE cartridges to capture (*E*)-resveratrol from seed extracts is depicted in **Figure 6.11**.

Table 6.4: The amount of (*E*)-resveratrol (µg/g) in different fractions of wash and elution from grape seed extract after MISPE and NISPE treatment.

		(*E*)-Resveratrol (µg/g)	
		MISPE	**NISPE**
Before treatment	Sample loading (1 × 5 mL)	11.4	11.4
After treatment	Wash steps (4 × 5 mL)	0.9	10.8
	Elution steps (10 × 5 mL)	10.4	0.4
	Total wash and elution	11.2	11.2
Total recovery (%)		99.1	98.2
Imprinting factor (*IF*= MIP eluate/NIP eluate)		26	

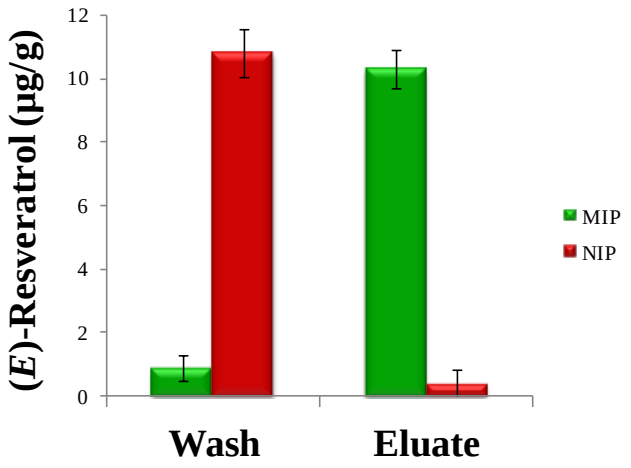

Figure 6.11: The comparison of (*E*)-resveratrol in grape seed extract after wash with EtOH/H_2O (4:1, v/v) containing 1% (v/v) AcOH followed by elution with EtOH/AcOH (9:1, v/v) from MISPE and NISPE cartridges. Measurements were performed in duplicate (n = 2). Error bars indicate the standard error.

6.3.3 Phytosterols analysis in grape seed extract

6.3.3.1 Method optimisation for sample extraction

The analysis of phytosterols in complex matrices is a difficult task and requires reliable analytical techniques for the extraction, isolation and quantitative assays (*49*). Plant-derived sterols in oil seeds can be isolated by solvent extraction followed by saponification and chromatographic separation (*50*). Recent research has shown that phytosterols can be isolated from sunflower seeds by solvent extraction with *n*-hexane followed by a mixture of chloroform-methanol (*51*). The usage of chloroform-based solvent mixtures enables to extract sterols, but the use of carcinogenic chlorinated solvents that can cause pollution problems and difficulties in industrial hygiene was not preferable. To find an optimal procedure for sterol extraction, a series of optimisation steps involving *n*-hexane extraction or saponification (hot or cold approach) was carried out using 1.0 g of pelleted grape seed extract obtained after polyphenol extractions.

6.3.3.2 Grape seed extraction by n-hexane

The grape seed extract pellet (1.0 g) was mixed with *n*-hexane (3 × 5 mL) and sonicated for 30 min. The evaporation of *n*-hexane resulted in 7.8% (g/g) grape seed oil. This value is consistent with a previous study, which has reported about 6-20% of oil extracted from grape seeds (*8*). However, this oil is incompatible with the RP-HPLC system as many hydrophobic substances such as triglycerides are present in the sample (*52*).

The oil fraction (80 mg) was further extracted with ACN (1 mL) and sonicated for 30 min. The mixture was centrifuged at 10,000 rpm at 20 °C for 10 min. The supernatant (upper part containing the ACN layer) was evaporated to dryness and redissolved in ACN (50 µL) prior to injection into RP-HPLC. The results obtained were insignificant due to the very little amounts of stigmasterol that could be determined after RP-HPLC separation although the supernatants were concentrated up to 20-fold.

6.3.3.3 Grape seed extraction with saponification method

One way to extract phytosterols from the original matrix (either in oil or crude extract form) is a combination of saponification and chromatographic fractionation and separation. The saponification method has two main purposes; (i) to remove the dominant triacylglycerols and other acyl lipids from the crude lipid extract by converting them into water-soluble

compounds and (ii) to hydrolyse ester bonds in conjugated phytosterols. By saponification, the triacylglycerols are converted to water-soluble compounds that can easily be excluded by extraction with a combination of water and organic solvent.

Most of the sterol extraction methods described in the literature employed alkaline saponification (1 M ethanolic KOH/NaOH) rather than acid hydrolysis (6 M HCl) (*50*, *53*). Acid hydrolysis is not preferable for the detection of Δ^7-phytosterols (*e.g.*, Δ^7-stigmasterol) because it causes decompostion or isomerisation of these compounds after a short time of acidic hydrolysis (*54*). Alkaline saponifications can be done either at room temperature (cold saponification) or at elevated temperatures (hot saponification). The unsaponifiable matter content is expressed as a percentage by mass of the sample (before and after saponification reaction), as shown in **Equation 6.1**.

$$\text{Unsaponifiable matter content (\%)} = \frac{Mass\ after\ saponification\ (g)}{Mass\ before\ saponification\ (g)} \times 100\%, \qquad \textbf{Equation 6.1}$$

6.3.3.3.1 Cold saponification

The first series of experiments involved cold saponification at room temperature of grape the seed pellet (1.0 g) with 1 M of ethanolic KOH solution (10 mL) at different reactions times (5 h, 12 h and 18 h). The results for a 5 h and 12 h reaction were unsuccessful. When the saponified fraction was extracted with *n*-hexane (without rigorous shaking), a thick emulsion formed. It was very hard to distinguish and separate the *n*-hexane layer from that emulsion in a separatory funnel. In order to prevent the formation of an emulsion, sodium chloride was added but unfortunately without success. Surprisingly, a longer saponification time (18 h) resulted in 4.1% (g/g) of unsaponifiable matter without any emulsion disturbance. Therefore, it was concluded that a cold saponification method requires a longer period of time to complete the reaction.

6.3.3.3.2 Hot saponification

Hot saponification involved refluxes of the grape seed extract pellet (1.0 g) at 115 °C for 1 h, 2 h or 18 h with 1 M ethanolic KOH solution (10 mL). The unsaponifiable matter content at 1 h, 2 h and 18 h reaction time was determined to be 3.8% (g/g), 4.3% (g/g) and 4.4% (g/g), respectively. The comparative results of cold and hot saponification methods shown as the percentage of unsaponified matter were proportional to the reaction time **(Figure 6.12)**.

However, the difference of unsaponified matter content is very small (0.2%, g/g) between cold saponification (18 h) and hot saponification (2 h). Interestingly, hot saponification at 2 h and 18 h resulted in almost similar percentage of unsaponified matter with a variation of 0.1% (g/g). This result indicated that an 18 h reaction is not necessary when using high temperature alkaline hydrolysis method. Therefore, hot saponification at 2 h was considered the optimal extraction method to extract sterols with regard to the percentage of yield and involved a lower energy consumption compared to 18 h of cold or hot saponification.

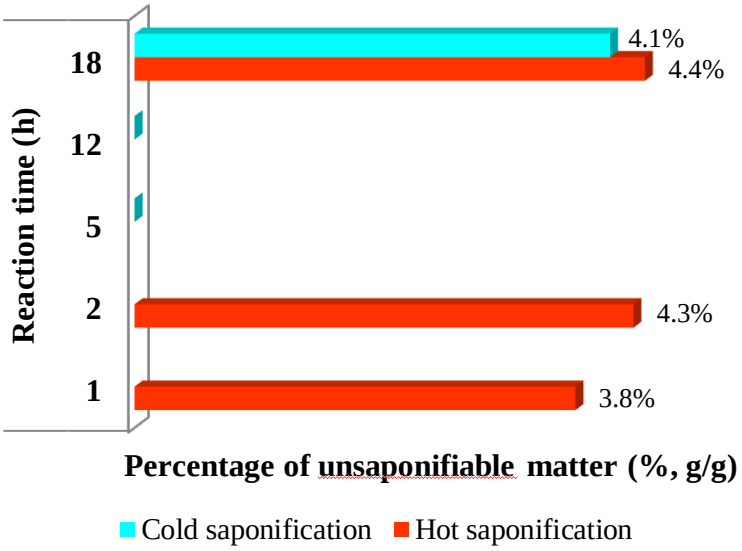

Figure 6.12: The percentage of unsaponifiable matter (%, g/g) after cold and hot saponification in different reaction times. (cold saponification: 5 h, 12 h and 18 h; hot saponification: 1 h, 2 h and 18 h).

6.3.3.4 Determination of stigmasterol before and after MISPE by RP-HPLC

The MIP was previously shown to have binding affinity towards stigmasterol in a standard mixture containing stigmasterol analogues, cholesterol and ergosterol with ACN/H_2O (9:1, v/v) during static batch binding as well as dynamic binding experiments **(Chapter 5-Section 5.3.4)**. Several attempts were undertaken to bind stigmasterol with *n*-hexane in static batch binding, however none of the experiments were successful. Despite some binding of stigmasterol in *n*-hexane system by the MIP, the NIP control also gave similar results, which ultimately reduced the imprinting effect and selectivity. Therefore, a direct loading of the MIP of grape seed oil in *n*-hexane is impossible. For these reasons, the grape seed residues were saponified in order to produce an unsaponified fraction. This

unsaponified matter was redissolved in a mixture of ACN/H_2O (9:1, v/v) to make this portion well suited for the analysis with MISPE and reversed-phase LC.

The analyses of phytosterols usually have been conducted using the normal-phase separation. By contrast, fewer studies analysed sterols by RP-HPLC. In a previous investigation, Careri *et al.* (*55*) reported that the separation of β-sitosterol and stigmasterol in the normal-phase mode with a CN stationary phase using a mixture of heptane and *n*-propanol as mobile phase was unsuccessful. The second stage of separation in that study was performed using reversed-phase chromatography with a mixture of MeOH, H_2O and ACN as mobile phase. A good peak resolution was observed due to the hydrophobic interaction between the lipophilic backbone of the sterol analytes and the C_{18} stationary phase.

Based on the optimised chromatographic parameters of the RP-HPLC method which was previously developed in **Chapter 5 (Section 5.3.1)**, an isocratic elution was the method of choice in this study for the analysis of sterols due to its obvious methodological simplicity. The separation of stigmasterol in a complex sample was conducted using a mixture of EtOH/H_2O (9:1, v/v) containing 0.2% (v/v) AcOH as a benign mobile phase.

The chromatogram of the unsaponified matter showed the occurrence of stigmasterol **(peak 5)** at a retention time of 20.3 min at the absorbance of 210 nm **(Figure 6.13-A)**. Based on a linear calibration curve of stigmasterol, the amount of this compound was determined to be 18.2 µg/g dry extract. The MISPE treatment selectively extracted stigmasterol from the unsaponified fraction as presented in **Figure 6.13-B**. An impressive cleanup of MIP was observed for the compound eluting with a retention time of 6.3 min (obtained by RP-HPLC) in the unsaponified extract whereby the peak nearly completely disappeared after the extraction. The reduction of peak height was also observed at a retention time of 9.7 min and 11.3 min after MISPE as obtained with subsequent chromatographic separation by RP-HPLC. Therefore, the MISPE technique can be considered as a very attractive cleanup method for discarding undesirable endogenous compounds which complicate the extraction of the compound of interest in the sample.

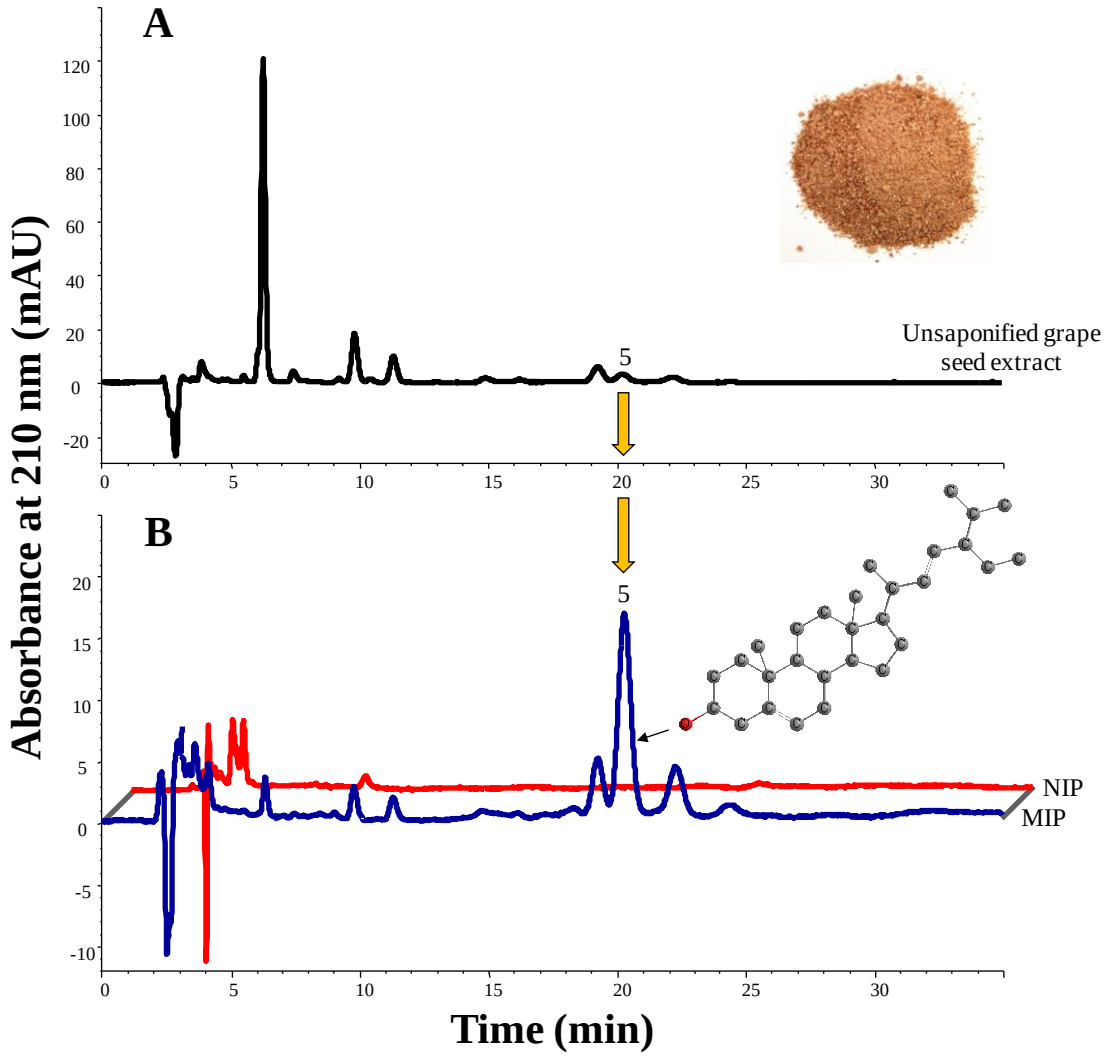

Figure 6.13: RP-HPLC chromatograms recorded at a wavelength of 210 nm for the quantification of stigmasterol (t_R = 20.3 min, **peak 5**) in **(A)** unsaponified grape seed extract and **(B)** concentrated unsaponified grape seed elutions after MISPE (blue line, front chromatogram) and after NISPE (red line, back chromatogram) treatments. The LC chromatograms were obtained with a Zorbax Eclipse XDB C_{18} column (4.6 mm × 150 mm, 5 µm particle size) at 23 °C using isocratic elution. The eluent was EtOH/H_2O (9:1 v/v) with 0.2% (v/v) AcOH; flow rate: 0.5 mL/min; 5 µL injection.

6.3.3.5 Quantification of stigmasterol before and after MISPE treatment

This section focuses on the loading, wash and elution solvents, which allows gaining insight into the binding mechanism of the MIP *versus* NIP. The unsaponified grape seed extract in a mixture of ACN/H_2O (9:1, v/v, 2 mL) was loaded onto the MISPE or NISPE cartridge and allowed to pass through the sorbent bed by gravity. In order to remove the non-selectively bound material whilst keeping the compound of interest retained on the sorbent, wash steps

were applied with ACN/H_2O (9:1, v/v) as previously described in **Chapter 5 (Section 5.2.5.2.4)**. However, when the wash solvent was applied, only a small amount of stigmasterol eluted from the NISPE cartridge.

In contrast, the application of ACN/H_2O (9:1, v/v) containing 1% (v/v) AcOH (4 × 2 mL) resulted in the removal of the majority of stigmasterol (16.4 µg/g) from the NISPE cartridge **Table 6.5**. This indicates that an acid is required to elute the non-selectively bound material from the control polymer when dealing with a complex sample rather than a mixture of sterol standards. In this case, the target stigmasterol (13.1 µg/g) remained trapped in the polymer whilst only a small portion of the target analyte non-selectively bound to the MIP was eluted (4.4 µg/g) after the wash stages. The elution of the stigmasterol-target with EtOH/AcOH (9:1, v/v) was expected due to the disturbance of the hydrogen bonding and hydrophobic interactions in the binding sites. The recovery of stigmasterol from MISPE was determined to be 96.2%. The overall performance of MIP *versus* NIP to capture the target stigmasterol in wash and elution steps can be seen in **Figure 6.14**. This investigation demonstrated the use of MIP to preconcentrate and selectively extract stigmasterol-target from a grape seed residue extract in an ACN-aqueous matrix with an imprinting factor of 12.

Table 6.5: Recoveries of stigmasterol (µg/g) from unsaponified grape seed extract after MIP and NIP in SPE cartridges. The wash steps were performed with a mixture of ACN/H_2O (9:1, v/v) containing 1% (v/v) AcOH and elution stages with EtOH/AcOH (9:1, v/v).

		Stigmasterol (µg/g)	
		MISPE	**NISPE**
Before treatment	Sample loading (1 × 2 mL)	18.2	18.2
After treatment	Wash steps (4 × 2 mL)	4.4	16.4
	Elution steps (5 × 2 mL)	13.1	1.1
	Total wash and elution	17.5	17.5
Total recovery (%)		96.2	96.2
Imprinting factor (*IF*= MIP eluate/NIP eluate)		12	

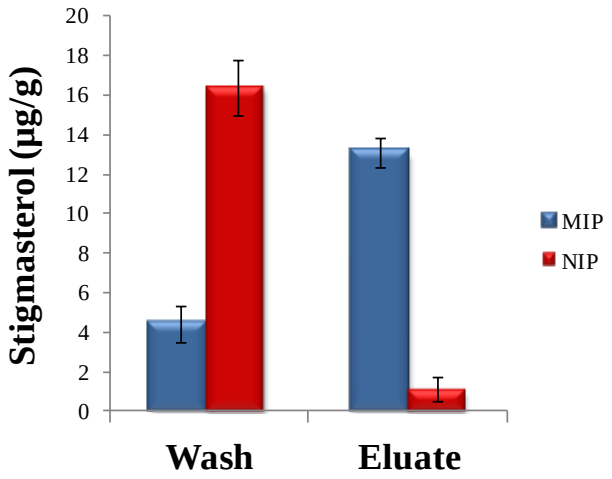

Figure 6.14: Comparison of stigmasterol (µg/g) in unsaponified grape seed extract after wash and elution steps from MISPE and NISPE cartridges. Measurements were performed in duplicate (n = 2). Error bars indicate the standard error.

6.3.3.6 Analysis of stigmasterol before and after MISPE treatment by LC-ESI ion trap MS/MS

The peak identity confirmation of the target compound was performed by LC-ESI ion trap MS/MS in the positive ionisation mode in the *m/z* range from 100-1000 based on the developed method **(Chapter 5-Section 5.3.2)**. Instead of premixing the mobile phase consisting EtOH/H_2O (90:10, v/v) with 0.2% (v/v) AcOH at 23 °C as described in **Section 5.3.2**, the chromatographic parameters for the separation of stigmasterol in the unsaponified complex extract have undergone some alterations with respect to the mobile phase composition and column temperature in order to assist the ionisation process. Two separate mobile phases containing 0.2% (v/v) AcOH in water (eluent A) and 0.2% (v/v) AcOH in EtOH (eluent B) with the eluent composition of EtOH/H_2O (93:7, v/v) were employed. In addition, a high column temperature of 30 °C was applied. The chromatographic profiles obtained from the separation were evaluated based on the peak resolution of stigmasterol.

The base peak chromatogram **(Figure 6.15-A)** showed at least eight components were detected in the unsaponified grape seed extract**.** Stigmasterol **(peak 5)** was identified based on the precursor ion $[M+H]^+$ of *m/z* 413.4. This compound was fragmented through MS/MS experiments in the ion trap to generate a product ion *m/z* 395.5 (due to the neutral loss of a molecule of water). The occurrence of stigmasterol in this sample was verified using the reference standard.

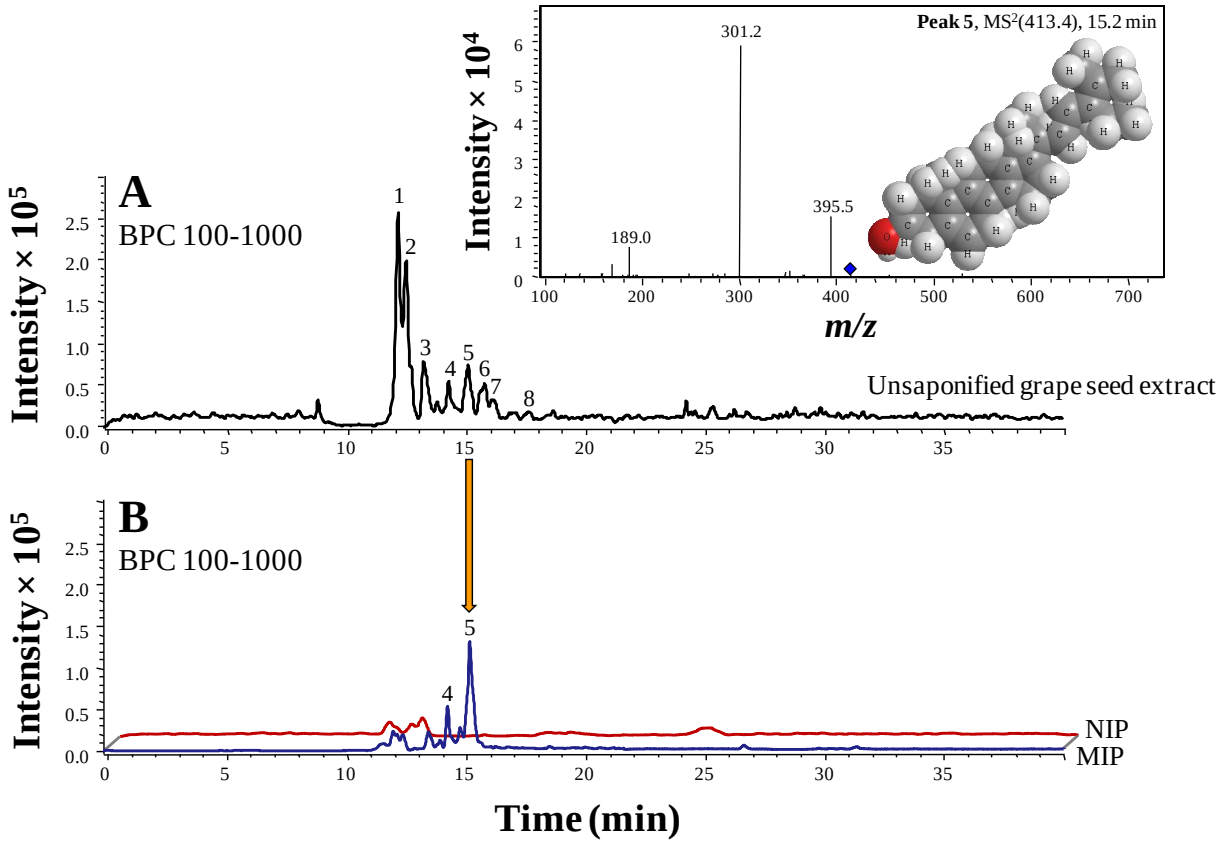

Figure 6.15: Base peak chromatogram (BPC) of **(A)** unsaponified grape seed extract and **(B)** unsaponified grape seed eluates after MISPE (blue line, front chromatogram) and NISPE (red line, back chromatogram) treatments. Inserted is a mass spectrum of stigmasterol with the characteristic product ions. Stigmasterol **(peak 5)** eluted at t_R = 15.2 min. The base peak chromatograms were obtained after RP-HPLC separation on a Zorbax XDB C_{18} capillary column (0.3 mm × 150 mm, 3.5 µm particle size) in the *m/z* range of 100-1000 using the positive ionisation mode by LC-ESI ion trap MS/MS at 30 °C. LC conditions: isocratic; eluent A: 0.2% acetic acid in water (7%, v/v), eluent B: 0.2% acetic acid in EtOH (93%, v/v); flow rate: 2 µL/min; 0.1 µL injection.

The shorter retention time of about 15.2 min observed for stigmasterol obtained with the microLC-ESI MS system compared to that of 20.3 min obtained with the analytical LC system can be primarily attributed to the difference in the composition of the mobile phase employed in the two LC separations. The microLC separations were performed with a mobile phase consisting of EtOH/H_2O (93:7, v/v) whilst for the analytical LC separations a mobile phase consisting of EtOH/H_2O (90:10, v/v) was used. Moreover, the reduction of 5.1 min of the retention time can be attributed to the higher temperature of 30 °C employed in the microLC separations compared to the 23 °C used in the analytical LC system. It should be noted that in contrast to the downscaling of the gradient elution method for (*E*)-resveratrol,

the difference of gradient delay volumes of the two LC systems has no bearing here, since isocratic methods were employed for the separation. Nevertheless, since the detection in the microLC system was performed with UV followed by MS in contrast to the analytical LC system were only UV detection was performed, the contribution of the delay volume between UV detector and MS detector has to be also considered.

Several other compounds were also observed from the unsaponified grape seed extract (before MISPE treatment). The details about the precursor ion and product ions of the compounds present in the sample are listed in **Table 6.6**. The precursor ion $[M+Na]^+$ at *m/z* 677 might be attributed to the presence of β-sitostanol palmitate **(peak 2)** (*56*). This compound underwent fragmentation through MS/MS experiments to generate a product ion at *m/z* 399 (β-sitostanol moiety). **Peak 3** was presumably assigned as Δ^5-avenasterol derivative based on the precursor ion $[M+H]^+$ at *m/z* 647. This compound was fragmented to generate several product ions at *m/z* 610, 497, 413 (avenasterol), 378, 374, 271. The latter signal (*m/z* 271) corresponding to the characteristic product ion of Δ^5-avenasterol (*57*). Meanwhile, the precursor ion $[M+H]^+$ at *m/z* 413 and product ions at *m/z* 395 $[M+H-H_2O]^+$, 299 and 271 were indicative of an Δ^5-avenasterol structure **(peak 8)** (*57*). According to Rozenberg *et al*. (*57*), stigmasterol, Δ^5-avenasterol and Δ^7-avenasterol possess the same molecular mass, however the MS^2 analysis allowed the differentiation of those compounds. With the assistance of a stigmasterol standard in the present study, the elution position and fragmentation fingerprint of stigmasterol in the sample was distinguished from avenasterol. Crews and co-workers (*8*) reported that Δ^5-avenasterol was determined from grape seed oil in a range of 0.3-4.5%.

Campesteryl glucoside **(peak 4)** might be identified in this sample based on the precursor ion $[M+H]^+$ of *m/z* 563, which later underwent fragmentation in the ion trap to produce a distinctive product ion at *m/z* 383 (campesteryl moeity) (*57*). Although the grape seed residue was saponified with 1 M ethanolic potassium hydroxide, the steryl glucoside can still be detected in the unsaponifiable extract. It has been suggested that the ether linkage between the sterol hydroxyl-group and the sugar moiety in the steryl glycosides is not hydrolysed under alkaline conditions (*58*). Cholesteryl arachidonate **(peak 6)** most probably assigned based on the precursor ion $[M+Na]^+$ at *m/z* 697 (*56*). This steryl fatty acid ester fragmented to generate several product ions including the cholesteryl moiety at *m/z* 369. **Peak 7** might be characterised as stigmadiene with the precursor ion $[M+H]^+$ at *m/z* 411. The cleavage of C=O from stigmadiene molecular structure gave a product ion at *m/z* 395 (stigmasteryl moiety).

The high fidelity of the MIP binding sites in comparison to the NIP to capture stigmasterol **(peak 5)** is depicted in **Figure 6.15-B**. Interestingly, the MIP showed a selective binding recognition towards the stigmasterol-target and enabled discrimination of an Δ^5-avenasterol and its derivative. The Δ^5-avenasterol possesses a very similar molecular configuration to stigmasterol except it has a double bond at the C_{24} position in the side chain. On the other hand, the MIP allowed capturing campesteryl glucoside, probably due to the competitive binding although this compound is relatively large in size compared to the target molecule. The reason for this might be the hydroxyl-groups in campesteryl glucoside encouraged the formation of hydrogen bond and hydrophobic interactions with the residual carboxylic acid in the MIP cavities.

Table 6.6: Identification of sterols and other components present in the unsaponified grape seed extract before and after MISPE and NISPE treatment using LC-ESI ion trap MS/MS in the positive ionisation mode in the *m/z* range of 100-1000. Bold entries represent significant enrichment of sterol compounds above the ion current intensity of 0.3×10^5.

Peak No.	t_R (min)	Compound name	Precursor ion, *m/z*	Product ion(s), *m/z*	Unsaponified grape seed extract	MIP	NIP
1	12.3	Unidentified compound	345	326, 300, 282, 265	✓	×	×
2	12.6	β-sitostanol palmitate	677	630, 551, 419, 399, 339, 303	✓	×	×
3	13.4	Δ^5-Avenasterol derivative	647	610, 497, 413, 378, 374, 271	✓	×	×
4	**14.4**	**Campesteryl glucoside**	**563**	**544, 526, 383, 235, 157**	✓	✓	×
5	**15.2**	**Stigmasterol**	**413**	**395, 393, 301, 297, 283, 255, 189**	✓	✓	×
6	15.8	Cholesteryl arachidonate	697	680, 650, 593, 423, 369, 368	✓	×	×
7	16.2	Stigmadiene	411	395, 315, 301, 189, 151	✓	×	×
8	17.8	Δ^5-Avenasterol	413	395, 331, 301, 299, 271, 147	✓	×	×

6.4 Conclusions

One path to tackle the reduction of environmental footprint in food production is the manufacture of nutraceuticals based on the biology-inspired methods utilising agricultural waste resources. The grape byproducts of wine making, in particular skins and seeds, have a high concentration of health-beneficial polyphenolic compounds and valuable bioactive sterols making extraction profitable. The results presented in this study demonstrated the potential of novel methods for polyphenols and phytosterols screening and enrichment.

This chapter introduced new methods to enrich the health-beneficial resveratrol, procyanidin and epicatechin as well as stigmasterol and campesteryl glycoside from one grape skin and seed feedstock with green chemistry methods realized in the grape extraction methods and the syntheses, and application of novel MISPE materials.

The application of LC-ESI ion trap MS/MS for the identification of numerous non-binding compounds and binding target compound as well structurally related compounds in the flow-through and eluate fractions of two MISPE led to insights into the physical and chemical interaction of the MIPs with their target analytes and with molecules that can be eliminated.

The application of MISPE technique for the selective enrichment of health-beneficial compounds from agricultural waste materials provides a new, efficient, cost-effective and sustainable approach to natural resource utilisation forming the basis of green economic opportunities from new revenue streams.

6.5 References

1. Schieber, A.; Stintzing, F. C.; Carle, R., By-products of plant food processing as a source of functional compounds - recent developments. *Trends Food Sci. Technol.* **2002**, *12*, 401-413.
2. Makris, D. P.; Boskou, G.; Andrikopoulos, N. K., Polyphenolic content and *in vitro* antioxidant characteristics of wine industry and other agri-food solid waste extracts. *J. Food Compos. Anal.* **2007**, *20*, 125-132.
3. Rockenbach, I. I.; Gonzaga, L. V.; Rizelio, V. M.; Goncalves, A. E. d. S. S.; Genovese, M. I.; Fett, R., Phenolic compounds and antioxidant activity of seed and skin extracts of red grape (*Vitis vinifera* and *Vitis labrusca*) pomace from Brazilian winemaking. *Food Res. Int.* **2011**, *44*, 897-901.
4. Campos, L., M. A. S.; Leimann, F. V.; Pedrosa, R. C.; Ferreira, S. R. S., Free radical scavenging of grape pomace extracts from Cabernet Sauvingnon (*Vitis vinifera*). *Bioresour Technol* **2008**, *99*, 8413-8420.

5. Ector, B. J.; Magee, J. B.; Hegwood, C. P.; Coign, M. J., Resveratrol concentration in muscadine berries, juice, pomace, purees, seeds, and wines. *Am. J. Enol. Vitic.* **1996**, *47*, 57-62.
6. Hudson, T. S.; Hartle, D. K.; Hursting, S. D.; Nunez, N. P.; Wang, T. T. Y.; Young, H. A.; Arany, P.; Green, J. E., Inhibition of prostate cancer growth by muscadine grape skin extract and resveratrol through distinct mechanisms. *Cancer Res.* **2007**, *67*, 8396-8405.
7. Zhou, K.; Raffoul, J. J., Potential anticancer properties of grape antioxidants. *J. Oncol.* **2012**, 803294-803302.
8. Crews, C.; Hough, P.; Godward, J.; Brereton, P.; Lees, M.; Guiet, S.; Winkelmann, W., Quantitation of the main constituents of some authentic grape seed oils of different origin. *J. Agric. Food Chem.* **2006**, *54*, 6261-6265.
9. Kennedy, J. A.; Matthews, M. A.; Waterhouse, A. L., Changes in grape seed polyphenols during fruit ripening. *Phytochemistry* **2000**, *55*, 77-85.
10. Xu, X.; Zhu, L.; Chen, L., Separation and screening of compounds of biological origin using molecularly imprinted polymers. *J. Chromatogr. B* **2004**, *804*, 61-69.
11. Torres, J. J.; Gsponer, N.; Ramirez, C. L.; Vera, D. M. A.; Montejano, H. A.; Chesta, C. A., Experimental and theoretical studies on the enantioselectivity of molecularly imprinted polymers prepared with a chiral functional monomer. *J. Chromatogr., A* **2012**, *1266*, 24-33.
12. Canals, R.; Llaudy, M. C.; Valls, J.; Canals, J. M.; Zamora, F., Influence of ethanol concentration on the extraction of color and phenolic compounds from the skin and seeds of Tempranillo grapes at different stages of ripening. *J. Agric. Food Chem.* **2005**, *53*, 4019-4025.
13. Kammerer, D.; Claus, A.; Carle, R.; Schieber, A., Polyphenol screening of pomace from red and white grape varieties *(Vitis vinifera* L.*)* by HPLC-DAD-MS/MS. *J. Agric. Food Chem.* **2004**, *52*, 4360-4367.
14. Lutz, M.; Cajas, Y.; Henriquez, C., Phenolics content and antioxidant capacity of Chilean grapes cv. Pais and Cabernet Sauvignon. *CyTA--J. Food* **2012**, *10*, 251-257.
15. Okuda, T.; Yokotsuka, K., *Trans*-resveratrol concentrations in berry skins and wines from grapes grown in Japan. *Am. J. Enol. Vitic.* **1996**, *47*, 93-99.
16. Yu, W.; Fu, Y. C.; Wang, W., Cellular and molecular effects of resveratrol in health and disease. *J. Cell. Biochem.* **2012**, *113*, 752-759.
17. Stella, L.; de Rosso, M.; Panighel, A.; Dalla, V. A.; Flamini, R.; Traldi, P., Collisionally induced fragmentation of $[M-H]^-$ species of resveratrol and piceatannol investigated by deuterium labelling and accurate mass measurements. *Rapid Commun. Mass Spectrom.* **2008**, *22*, 3867-3872.
18. Careri, M.; Corradini, C.; Elviri, L.; Nicoletti, I.; Zagnoni, I., Liquid chromatography-electrospray tandem mass spectrometry of *cis*-resveratrol and *trans*-resveratrol: development, validation, and application of the method to red wine, grape, and winemaking by-products. *J. Agric. Food Chem.* **2004**, *52*, 6868-6874.
19. Pezet, R.; Perret, C.; Jean-Denis, J. B.; Tabacchi, R.; Gindro, K.; Viret, O., δ-Viniferin, a resveratrol dehydrodimer: one of the major stilbenes synthesized by stressed grapevine leaves. *J. Agric. Food Chem.* **2003**, *51*, 5488-5492.
20. Buiarelli, F.; Coccioli, F.; Jasionowska, R.; Merolle, M.; Terracciano, A., Analysis of some stilbenes in Italian wines by liquid chromatography/tandem mass spectrometry. *Rapid Commun. Mass Spectrom.* **2007**, *21*, 2955-2964.
21. Tourino, S.; Fuguet, E.; Jauregui, O.; Saura-Calixto, F.; Cascante, M.; Torres, J. L., High resolution liquid chromatography electrospray ionization time of flight mass spectrometry combined with liquid chromatography electrospray ionization tandem mass spectrometry to identify polyphenols from grape antioxidant dietary fiber. *Rapid Commun. Mass Spectrom.* **2008**, *22*, 3489-3500.

22. Rockenbach, I. I.; Jungfer, E.; Ritter, C.; Santiago-Schuebel, B.; Thiele, B.; Fett, R.; Galensa, R., Characterization of flavan-3-ols in seeds of grape pomace by CE, HPLC-DAD-MS^n and LC-ESI-FTICR-MS. *Food Res. Int.* **2012**, *48*, 848-855.
23. Sun, J.; Liang, F.; Yan, B.; Li, P.; Duan, C., Screening non-colored phenolics in red wines using liquid chromatography ultraviolet and mass spectrometry mass spectrometry libraries. *Molecules* **2007**, *12*, 679-693.
24. Callemien, D.; Collin, S., Use of RP-HPLC-ESI(-)-MS/MS to differentiate various proanthocyanidin isomers in lager beer extracts. *J. Am. Soc. Brew. Chem.* **2008**, *66*, 109-115.
25. Gu, L.; Kelm, M. A.; Hammerstone, J. F.; Zhang, Z.; Beecher, G.; Holden, J.; Haytowitz, D.; Prior, R. L., Liquid chromatographic/electrospray ionization mass spectrometric studies of proanthocyanidins in foods. *J. Mass Spectrom.* **2003**, *38*, 1272-1280.
26. Castillo-Munoz, N.; Gomez-Alonso, S.; Garcia-Romero, E.; Gomez, M. V.; Velders, A. H.; Hermosin-Gutierrez, I., Flavonol 3-*O*-glycosides series of *Vitis vinifera* Cv. *Petit verdot* red wine grapes. *J. Agric. Food Chem.* **2009**, *57*, 209-219.
27. Bravo, M. N.; Silva, S.; Coelho, A. V.; Boas, L. V.; Bronze, M. R., Analysis of phenolic compounds in Muscatel wines produced in Portugal. *Anal. Chim. Acta* **2006**, *563*, 84-92.
28. Bors, W.; Michel, C.; Saran, M., Flavonoid antioxidants: rate constants for reactions with oxygen radicals. *Methods Enzymol* **1994**, *234*, 420-429.
29. Price, S. F.; Breen, P. J.; Valladao, M.; Watson, B. T., Cluster sun exposure and quercetin in Pinot noir grapes and wine. *Am. J. Enol. Vitic.* **1995**, *46*, 187-194.
30. Haselgrove, L.; Botting, D.; van Heeswijck, R.; Hoj, P. B.; Dry, P. R.; Ford, C.; Iland, P. G., Canopy microclimate and berry composition: The effect of bunch exposure on the phenolic composition of *Vitis vinifera* L cv. Shiraz grape berries. *Aust. J. Grape Wine Res.* **2000**, *6*, 141-149.
31. Landrault, N.; Larronde, F.; Delaunay, J. C.; Castagnino, C.; Vercauteren, J.; Merillon, J. M.; Gasc, F.; Cros, G.; Teissedre, P. L., Levels of stilbene oligomers and astilbin in French varietal wines and in grapes during noble rot development. *J. Agric. Food Chem.* **2002**, *50*, 2046-2052.
32. Terao, J.; Murota, K.; Kawai, Y., Conjugated quercetin glucuronides as bioactive metabolites and precursors of aglycone *in vivo*. *Food Funct.* **2011**, *2*, 11-17.
33. Nonier, B. M. F.; Vivas, N.; Absalon, C.; Vitry, C.; Fouquet, E.; Vivas De, G. N., Structural diversity of nucleophilic adducts from flavanols and oak wood aldehydes. *Food Chem.* **2007**, *107*, 1494-1505.
34. Theodoridis, G.; Manesiotis, P., Selective solid-phase extraction sorbent for caffeine made by molecular imprinting. *J. Chromatogr. A* **2002**, *948*, 163-169.
35. Sun, B.; Ribes, A. M.; Leandro, M. C.; Belchior, A. P.; Spranger, M. I., Stilbenes: Quantitative extraction from grape skins, contribution of grape solids to wine and variation during wine maturation. *Anal. Chim. Acta* **2006**, *563*, 382-390.
36. Jeandet, P.; Bessis, R.; Maume, B. F.; Meunier, P.; Peyron, D.; Trollat, P., Effect of enological practices on the resveratrol isomer content of wine. *J. Agric. Food Chem.* **1995**, *43*, 316-319.
37. Saucier, C.; Guerra, C.; Pianet, I.; Laguerre, M.; Glories, Y., (+)-Catechin-acetaldehyde condensation products in relation to wine aging. *Phytochemistry* **1997**, *46*, 229-234.
38. Mane, C.; Souquet, J. M.; Olle, D.; Verries, C.; Veran, F.; Mazerolles, G.; Cheynier, V.; Fulcrand, H., Optimization of simultaneous flavanol, phenolic acid, and anthocyanin extraction from grapes using an experimental design: application to the characterization of Champagne grape varieties. *J. Agric. Food Chem.* **2007**, *55*, 7224-7233.
39. Gonzalez-Manzano, S.; Rivas-Gonzalo, J. C.; Santos-Buelga, C., Extraction of flavan-3-ols from grape seed and skin into wine using simulated maceration. *Anal. Chim. Acta* **2004**, *513*, 283-289.

40. Revilla, E.; Ryan, J. M., Analysis of several phenolic compounds with potential antioxidant properties in grape extracts and wines by high-performance liquid chromatography-photodiode array detection without sample preparation. *J. Chromatogr. A* **2000**, *881*, 461-469.
41. Rodriguez, M. R.; Romero, P. R.; Chacon, V. J. L.; Martinez, G. J.; Garcia, R. E., Phenolic compounds in skins and seeds of ten grape *Vitis vinifera* varieties grown in a warm climate. *J. Food Compos. Anal.* **2006**, *19*, 687-693.
42. Thorngate, J. H.; Singleton, V. L., Localization of procyanidins in grape seeds. *Am. J. Enol. Vitic.* **1994**, *45*, 259-262.
43. Prieur, C.; Rigaud, J.; Cheynier, V.; Moutounet, M., Oligomeric and polymeric procyanidins from grape seeds. *Phytochemistry* **1994**, *36*, 781-784.
44. Guendez, R.; Kallithraka, S.; Makris, D. P.; Kefalas, P., Determination of low molecular weight polyphenolic constituents in grape (*Vitis vinifera* sp.) seed extracts: correlation with antiradical activity. *Food Chem.* **2004**, *89*, 1-9.
45. Terra, X.; Pallares, V.; Ardevol, A.; Blade, C.; Fernandez-Larrea, J.; Pujadas, G.; Salvado, J.; Arola, L.; Blay, M., Modulatory effect of grape seed procyanidins on local and systemic inflammation in diet induced obesity rats. *J. Nutr. Biochem.* **2011**, *22*, 380-387.
46. Feringa, H. H. H.; Laskey, D. A.; Dickson, J. E.; Coleman, C. I., The effect of grape seed extract on cardiovascular risk markers: a meta-analysis of randomized controlled trials. *J. Am. Diet Assoc.* **2011**, *111*, 1173-1181.
47. Da Silva, J. M. R.; Darmon, N.; Fernandez, Y.; Mitjavila, S., Oxygen free radical scavenger capacity in aqueous models of different procyanidins from grape seeds. *J. Agric. Food Chem.* **1991**, *39*, 1549-1552.
48. Ugartondo, V.; Mitjans, M.; Lozano, C.; Torres, J. L.; Vinardell, M. P., Comparative study of the cytotoxicity induced by antioxidant epicatechin conjugates obtained from grape. *J. Agric. Food Chem.* **2006**, *54*, 6945-6950.
49. Maeorg, E.; Laaniste, P.; Joudu, J.; Maeorg, U., Some important aspects of sterol analysis of vegetable oils. *Proc. Est. Acad. Sci., Chem.* **2007**, *56*, 59-66.
50. Abidi, S. L., Chromatographic analysis of plant sterols in foods and vegetable oils. *J. Chromatogr., A* **2001**, *935*, 173-201.
51. Aguirre, M. R.; Ruiz-Mendez, M. V.; Velasco, L.; Dobarganes, M. C., Free sterols and steryl glycosides in sunflower seeds with high phytosterol contents. *Eur. J. Lipid Sci. Technol.* **2012**, *114*, 1212-1216.
52. Rezanka, T.; Mares, P., Determination of plant triacylglycerols using capillary gas chromatography, high-performance liquid chromatography and mass spectrometry. *J. Chromatogr.* **1991**, *542*, 145-159.
53. Shin, E. C.; Pegg, R. B.; Phillips, R. D.; Eitenmiller, R. R., Commercial peanut (*Arachis hypogaea* L.) cultivars in the United States: phytosterol composition. *J. Agric. Food Chem.* **2010**, *58*, 9137-9146.
54. Breinholder, P.; Mosca, L.; Lindner, W., Concept of sequential analysis of free and conjugated phytosterols in different plant matrices. *J. Chromatogr. B Analyt. Technol. Biomed. Life Sci.* **2002**, *777*, 67-82.
55. Careri, M.; Elviri, L.; Mangia, A., Liquid chromatography UV determination and liquid chromatography atmospheric pressure chemical ionization mass spectrometric characterization of sitosterol and stigmasterol in soybean oil. *J. Chromatogr., A* **2001**, *935*, 249-257.
56. Caboni, M. F.; Iafelice, G.; Pelillo, M.; Marconi, E., Analysis of fatty acid steryl esters in tetraploid and hexaploid wheats: identification and comparison between chromatographic methods. *J. Agric. Food Chem.* **2005**, *53*, 7465-7472.

57. Rozenberg, R.; Ruibal-Mendieta, N. L.; Petitjean, G.; Cani, P.; Delacroix, D. L.; Delzenne, N. M.; Meurens, M.; Quetin-Leclercq, J.; Habib-Jiwan, J. L., Phytosterol analysis and characterization in spelt (*Triticum aestivum* ssp. *spelta* L.) and wheat (*T. aestivum* L.) lipids by LC/APCI-MS. *J. Cereal Sci.* **2003**, *38*, 189-197.

58. Toivo, J.; Lampi, A. M.; Aalto, S.; Piironen, V., Factors affecting sample preparation in the gas chromatographic determination of plant sterols in whole wheat flour. *Food Chem.* **1999**, *68*, 239-245.

Chapter 7

Conclusions and possible future investigations

Table of Contents

7.1 Conclusions

Phytochemicals, including polyphenols and phytosterols, are widely recognised as functional components of food and beverages products, and stand alone supplementals. These compounds are extensively researched and reviewed for their roles in protecting humans from degenerative and cardiovascular diseases. Although some of these substances can be synthesized, their capture from natural sources is more common and generally better accepted in the market.

The extraction of polyphenols and phytosterols from natural sources has proven to be an extremely difficult analytical challenge due to the complexity of the numerous chemicals in natural extracts. The material used in this thesis was chosen to be grape pressings, an abundant byproduct of the wine industry that is currently under-utilised, as only tartaric acid and alcohol are retrieved before it is used for compost.

In this thesis, a need for a new, efficient and environmentally benign method for the separation of the extremely health-beneficial (*E*)-resveratrol and stigmasterol from the same form grape waste has been addressed.

The chosen route to separate and enrich these compounds from a complex natural matrix was the use of novel molecularly imprinted polymers (MIPs) in a solid-phase extraction (SPE) format.

In contrast to some rare existing MISPE separations of polyphenols from natural substances, the method developed in this thesis allowed not only the highly efficient separation of the target compound (*E*)-resveratrol and its enrichment, but also the concomitant capture of other health-beneficial polyphenols. Also the herein presented MIP was much more extensively characterised with respect to its selectivity and efficiency.

A thorough selectivity evaluation of the recognition sites in the MIPs of this thesis was performed in batch-binding and dynamic binding experiments using the templates and synthesised template analogues with a non-imprinted polymer as control, on the basis of the quantitative information derived from LC-MS.

For these evaluations systematic investigations of the optimal separation and detection of polyphenols with suitable mobile phases, mobile phase additive concentrations and column temperatures were presented under consideration of Green Chemistry principles, whereby a

mixture of ethanol-water with 10 mM formic acid and a reversed-phase C_{18} column operated at room temperature proved successful and benign. To reduce the time for method development, the optimised analytical method was down-scaled to micro LC-ESI ion trap MS/MS. This method afforded better resolution and sensitivity for the simultaneous separation of polyphenol mixtures in the negative ionisation mode compared with the positive ionisation mode.

The characterisation of the (*E*)-resveratrol imprinted MIP was initially through the isolation of this target molecule from an Australian Pinot noir wine. The RP-HPLC analysis of the red wine resulted in 33 phenolic compounds to be identified. The capability of the MIP to recognise its resveratrol template in such a complex wine sample was demonstrated through a high binding affinity of (*E*)-resveratrol in the cavities of the MIP with an imprinting factor of 32. The recovery of (*E*)-resveratrol after MISPE treatment was 99.7%. The retention mechanism of phenolic substances in the MIP was considered to be largely dependent upon the numbers and positions of the hydroxyl groups of the analytes, to perform hydrogen bonding interactions with the pyridinyl-functionalities of the crosslinked monomers in the imprinted sites. This study also showed that the size and shape complementarity of the template molecule influenced the binding recognition in the polymer network. As hoped for, the MISPE treatment resulted in a significantly enhanced enrichment of the (*E*)-isomer of resveratrol compared to the (*Z*)-isomer. The capability of the MIP to selectively enrich (*E*)-resveratrol is held to be strongly influenced by the number and position (*meta* and/or *para*) of hydroxyl-groups in their phenolic aromatic rings. Although (*Z*)-resveratrol has three hydroxyl-groups similar to the template molecule, the *cis*-structural feature is expected to result in steric hindrance. As a result of several structural similarities and geometric complementarities, catechin, epicatechin and their derivatives were also retained after the MISPE treatment. This may serve as a basis for the development of protocols for the concomitant capture of health-beneficial phenolics from complex matrices in the food and nutraceuticals industries.

When grape pressings were used as a substrate, it was of interest to investigate the polyphenolic distribution at different stages of waste storage. It was found that a long period of storage (51 days) resulted in nearly 40% reduction of (*E*)-resveratrol compared to that in fresh grape pressing residues.

The MIP was shown capable of the isolation and enrichment of (*E*)-resveratrol from fresh and aged grape pressings. Despite the fungal infection of the aged grape pressings, the MIP retained its integrity with respect to extracting (*E*)-resveratrol from the sample, with an imprinting factor of 18. The MISPE protocol for fresh grape pressing extracts was intensified until a recovery of 99% (*E*)-resveratrol was achieved. The MIP enabled the discrimination of (*Z*)-resveratrol and showed cross-reactivity binding for template-like-molecules, most notably for catechin/ epicatechin, B-type procyanidin, (+)-astilbin, quercetin glucuronide and quercetin. These results provide an efficient, green new method to potentially capture and enrich polyphenols with health-beneficial properties from agricultural waste streams and, in conjunction with LC deliver information on their concentrations at different stages of waste material processing. The MIP was found to be reusable, robust and able to withstand treatment with a range of different pH values and solvents, which will be important for the extension of the use of MISPE techniques to other types of bioanalytical applications.

These results may contribute to generate a new tool for reuse and recycling of valuable components from waste material in the agricultural and nutraceutical industries possessing a benign environmental footprint.

The use of MIP materials in the analysis of sterols had several challenges still unsolved, especially in isolating the sterol target analytes from complex mixtures. The studies that have been done were often complicated and time-consuming procedures that used copious amount of environmentally problematic chemicals. In addition, published MISPE methods were not able to collect other compounds or assess the efficiency of the binding of the target of interest in one step. Thus, the present study provided a novel design of stigmasterol imprinted polymers in the SPE format in conjunction with the latest modern LC techniques for the quantification and characterisation of the target compound and its analogues from grape seed extracts.

Several challenges arose during the isolation of the sterol target analytes from the complex mixture of grape extracts. Stigmasterol is amphipathic, has a single hydroxyl group in the molecular structure, and is relatively large, making the design of synthetic recognition-based polymer networks very difficult. In previous studies, major emphasis had focussed on the engineering and architectural design of cholesterol MIPs however, the polymers had a low selectivity to cholesterol due to hydrophobic cross linker-monomer interactions.

The MIP prepared for stigmasterol with non-covalent imprinting failed to capture stigmasterol standards in various solvent systems. In contrast, as shown with static batch binding the MIP synthesised with the covalent approach, showed high fidelity recognition of stigmasterol, although some retention was also observed for cholesterol and ergosterol because of the structural similarities and spatial complementarity to the target molecule. Further dynamic binding experiments were carried out in order to obtain an optimal sample loading, washing and elution conditions for the MISPE protocol with a mixture of stigmasterol, cholesterol and ergosterol standards. The MISPE method showed significant binding recognition towards stigmasterol in acetonitrile-water system with an imprinting factor of 12, and 99.4% of stigmasterol was recovered after MIP extraction. All binding evaluations were also performed with non-imprinted polymers.

A static cross reactivity binding study presented an evaluation of the novel stigmasterol MIP with a standard mixture of six sterols. Such experiments are often limited by the availability of the stigmasterol analogues, however for the present study they had been chemically synthesised at the Centre for Green Chemistry. The new stigmasterol MIP allowed also a simultaneous capture of ergosterol and cholesterol but discriminated against several large sterol molecules according to the particular shape and chemistry of the stigmasterol binding site. The study demonstrated the importance of the hydroxyl functionality in the target analyte and/or target analogues for the formation of selective hydrogen bond interactions with the residual carboxylic acid in the imprinted cavities. In addition, the size and shape of the analytes influenced their binding or rejection in the MIP.

The binding of structurally closely related sterols was further determined in a dynamic binding study. Capture from the originally applied amounts was 71.3 µg/g polymer for stigmasterol, 57.9 µg/g polymer for cholesterol and 50.4 µg/g polymer for ergosterol. The most obvious structural differences between stigmasterol, cholesterol and ergosterol are the double bonds at C_{22} and the alkyl chain at the position of C_{24}. In addition, ergosterol has an additional double bond in the B-ring at the C_7 position. Since cholesterol displayed the closest structure to the target molecule, the binding recognition for cholesterol was slightly higher than that for ergosterol. Since the highest binding selectivity was obtained for stigmasterol, it can be assumed that the side chain of stigmasterol enhances the fidelity of the recognition sites of the imprinted polymer

for this compound. This demonstrated that the binding sites in the MIP possess the ability to 'memorise' the small structural difference of its target molecule.

During the development of a suitable chromatographic separation method to determine the sterols, the most challenging part is to choose an optimal combination of mobile phase and mobile phase additive. A number of publications have addressed how to optimise the solvent system efficiently and various mathematical prediction models have been proposed. However, these models are sometimes not applicable for the detection of sterols in multi-component samples. This study has elaborated the design of a chromatographic method based on environmentally friendly ethanol-water containing 0.2% (v/v) acetic acid using an isocratic elution mode to resolve stigmasterol, stigmasterol analogues, cholesterol and ergosterol. This is the first time stigmasterol and structurally related sterols were simultaneously separated and LC-MS/MS has been successfully used to prove the method's efficiency. The use of green solvents and micro capillary systems points the way to greener analysis methods in other fields of application. This new method can be used for binding site characterisation, selectivity optimisation and monitoring of the performance of MIPs intended for SPE to capture nutraceuticals from complex waste samples, and will contribute to further development in imprinting technology.

Finally a new method to enrich the health-beneficial resveratrol, procyanidin and epicatechin as well as stigmasterol and campesteryl glycoside from one single grape pressing feedstock with two MIPs and green chemistry methods was elaborated.

To this end the compositions of polyphenols in grape skins and seeds have been separately investigated. The results showed that the amount of (*E*)-resveratrol was higher in the grape skin extract than in the seed extract which was expected due to its fungal defence and UV-filter function. The isolation of (*E*)-resveratrol using MISPE resulted in 99% recovery of the target compound in both extracts. The MISPE treatment showed a significant binding affinity for (*E*)-resveratrol and additionally allowed the binding of quercetin glucuronide from grape skin extract. The appropriate geometric positioning of quercetin glucuronide to afford hydrogen bonding interactions, electron delocalisation in the aromatic rings of the flavonoids and hydrophobic interactions would be the factors that explain the retention mechanism of quercetin

glucuronide in the imprinted cavities. Several other phenolic components detected at low concentrations resemble in their structural configuration the target molecule including a dimer adduct of catechin-methyl-5-furfuraldehyde and epicatechin. Catechin and quercetin are also health-beneficial substances worth capturing from waste streams.

In this study, comprehensive extraction of grape seeds to isolate and enrich both, (*E*)-resveratrol and stigmasterol using MISPE applications has provided a new perspective on waste reuse. The (*E*)-resveratrol MIP also enabled the binding of catechin, procyanidin, epicatechin and epicatechin gallate.

The solid residue of the grape seed extract from the polyphenol extraction was used and hot saponified for the analysis of stigmasterol in the non saponified part with the sigmasterol MIP. A 96% recovery of the target analyte was obtained. The MIP also bound campesteryl glycoside probably due to the hydroxyl-groups which encouraged the formation of hydrogen bond and hydrophobic interactions with the residual carboxylic acid in the MIP cavities.

The grape byproducts of wine making, in particular skins and seeds, have a high concentration of health-beneficial polyphenolic compounds and valuable bioactive sterols making extraction profitable. The results presented in this study demonstrated the potential of novel methods for polyphenols and phytosterols screening and enrichment.

The application of LC-ESI ion trap MS/MS for the identification of numerous non-binding and binding target compounds as well structurally related substances in the flow-through and eluate fractions of two MISPE led to insights into the physical and chemical interaction of the MIPs with their target and companion analytes and with molecules that can be eliminated.

7.2 Possible future investigations

The application of MISPE techniques for the selective enrichment of health-beneficial compounds from agricultural waste materials can potentially provide a new, efficient, cost-effective and sustainable approach to natural resource utilisation forming the basis of green economic opportunities from new revenue streams.

This research has also opened up avenues for the deeper elucidation of imprinting chemistries and molecular recognition mechanisms in the field of MISPE using high-end mass spectrometry methods.

Future development of this research can exploit the economic potential and simple applicability of the methods for other agricultural waste products containing valuable nutraceutical compounds.

From the same waste product a wide range of health-beneficial compounds can be targeted simultaneously as demonstrated herein for a wide array of polyphenols and phytosterols.

As has been demonstrated, green extraction and analysis methods can be developed in future for very complex feedstocks from natural sources.

A future development of novel devices based on MIP technology for the capture and identification of health-beneficial substances from natural sources may open opportunities for accessible, affordable nutraceuticals for better health and well-being. Further research will be aimed at developing new MIP-based-sensors with high sensitivity and rapid response times for the selective detection of bioactive polyphenols and phytosterols. Despite considerable improvements in the field of imprinting technology with various types of new polymers, imprinting formats and applications have been achieved, significant challenges regarding the mechanisms underlying the imprinting technique remain to be solved and many opportunities for these applications are still not fully exploited.